

Baryons as Three Flavor Solitons

Herbert Weigel[†]

Institute for Theoretical Physics
Tübingen University
Auf der Morgenstelle 14
D-72076 Tübingen

To appear in Int. J. Mod. Phys. A

[†] Supported by a Habilitanden-Scholarship of the Deutschen Forschungsgemeinschaft (DFG).

Abstract

The description of baryons as soliton solutions of effective meson theories for three flavor (up, down, strange) degrees of freedom is reviewed and the phenomenological implications are illuminated. In the collective approach the soliton configuration is equipped with baryon quantum numbers by canonical quantization of the coordinates describing the flavor orientation. The baryon spectrum resulting from exact diagonalization of the collective Hamiltonian is discussed. The prediction of static properties such as the baryon magnetic moments and the Cabibbo matrix elements for semi-leptonic hyperon decays are explored with regard to the influence of flavor symmetry breaking. In particular, the role of strange degrees of freedom in the nucleon is investigated for both the vector and axial-vector current matrix elements. The latter are discussed extensively within in the context of the *proton spin puzzle*. The influence of flavor symmetry breaking on the shape of the soliton is examined and observed to cause significant deviations from flavor covariant predictions on the baryon magnetic moments. Short range effects are incorporated by a chiral invariant inclusion of vector meson fields. These extensions are necessary to properly describe the singlet axial-vector current and the neutron proton mass difference. The effects of the vector meson excitations on baryon properties are also considered. The bound state description of hyperons and its generalization to baryons containing a heavy quark are illustrated. In the case of the Skyrme model a comparison is performed between the collective quantization scheme and bound state approach. Finally, the Nambu–Jona–Lasinio model is employed to demonstrate that hyperons can be described as solitons in a microscopic theory of the quark flavor dynamics. This is explained for both the collective and the bound state approaches to strangeness.

Contents

1 Introduction and Motivation	4
1.1 The Soliton Picture	5
1.2 The Proton Spin Puzzle	7
1.3 Strangeness in the Nucleon	8
2 The Collective Approach to the SU(3) Skyrme Model	9
2.1 The Skyrme Model	9
2.2 The SU(3) Extension of the Skyrme Lagrangian	11
2.3 Quantization of the Collective Coordinates	15
2.4 Spectrum and Form Factors	19
2.5 Further Developments	31
3 Symmetry Breaking and the Size of the Skyrmion	33
3.1 The “Slow–Rotator” Approach	34
3.2 Radial Excitations	38
4 Inclusion of Vector Mesons	44
4.1 The Vector Meson Lagrangian	44
4.2 Baryon Masses	47
4.3 Static Properties	51
4.4 Two Component Approach to the Proton Spin Puzzle	55
5 The Bound State Approach	58
5.1 Small Fluctuations off the Soliton and the Kaon Bound State	59
5.2 Remarks on Meson Baryon Scattering	66
5.3 Comparison: Collective Approach versus Bound State Approach	68
5.4 Baryons with a Heavy Quark	70
6 Explicit Quark Degrees of Freedom: The NJL Model	72
6.1 The NJL Soliton	72
6.2 The Collective Approach to the NJL Model	78
6.3 Baryon Masses in the Bound State Approach	83
7 Concluding Remarks	87
Appendix A	89
Appendix B	94
Appendix C	98
Appendix D	100

1 Introduction and Motivation

It is well established that the theory of Quantum Chromodynamics (QCD) properly accounts for the strong interaction processes of hadrons [1, 2]. In this theory hadrons are considered as complicated composites of quarks and gluons. The interaction of these fields is described within the framework of a non-abelian gauge theory, the gauge group being color $SU(3)$. The quark fields are represented in the fundamental representation while the gluons, which are the gauge bosons mediating the interaction, reside in the adjoint representation. Although we are still lacking a rigorous proof, the confinement hypothesis is commonly accepted, which states that only color singlet objects are observable. These singlet states represent the physical hadrons.

The solution to the renormalization group equation tells us that the QCD coupling decreases with increasing momentum transfer (asymptotic freedom). In this energy region QCD can therefore be treated within perturbation theory. The predictions, which result from these analyses of QCD, agree favorably with the experimental data obtained *e.g.* in deep inelastic scattering (DIS) processes. However, the behavior of the solution to the renormalization group equation unfortunately prohibits the application of perturbative techniques in the low-energy region. It is therefore mandatory to consider models which can be deduced or at least motivated from QCD in order to describe the low-energy properties of hadrons.

One such model is the description of baryons as solitons, the so-called Skyrme approach. This method emphasizes the role of spontaneously broken chiral symmetry and treats the baryons as collective excitations of meson fields. In particular, the knowledge of the physics of the low-lying mesons provides an exhaustive amount of (almost) parameter free predictions on properties of baryons. As an additional advantage over many other models the soliton description represents a means for studying various aspects (spectrum, electromagnetic and axial form factors, meson-baryon scattering, baryon-baryon interaction, etc.) within a unique framework without making any further assumptions. Before explaining the Skyrme approach in detail, it is appropriate to straighten up a few misconceptions about this description. The Skyrme approach has frequently been criticized as being too crude. This criticism is based on the fact that the original Skyrme model, which only contains pseudoscalar degrees of freedom, yields incorrect predictions on several baryon observables. As will become apparent during the course of this report (see chapter 4) many of these problems are linked to the feature that the pseudoscalar fields contain the long-range physics only. A suitable extension of the model to account for short-range effects as well, provides an appealing solution to these problems. A prominent example is the influence of the vector meson fields on the strong interaction piece of the neutron-proton mass difference and the axial singlet current matrix element which both exactly vanish in the pseudoscalar model. A further common criticism concerns the too large predictions for the absolute values of the baryon masses. This problem has recently been solved by the proper treatment of the quantum corrections to the soliton mass. Except for one application in the baryon number two sector (see section 2.5) this topic, however, will not be addressed in the present article.

There exist a couple of other review articles on the soliton picture for baryons [3, 4, 5, 6]. However, these reviews are mainly limited to the two flavor version of the Skyrme approach. If at all, these articles contain only general aspects of the treatment of strange degrees of freedom. In particular, within the Skyrme approach a detailed survey of neither the influence of flavor symmetry breaking on baryon properties nor on the effects of strange quarks in the nucleon are available. It is the main goal of the present article to fill this gap. For this purpose several treatments of flavor symmetry breaking in the baryon sector will be introduced and

critically compared. In various aspects a detailed discussion must be beyond the scope of this article. However, it is intended to provide a background, which should enable the interested reader to consult the original literature.

1.1 The Soliton Picture

For the purpose of modeling QCD, ideas originally proposed by t' Hooft [7] and later pursued by Witten [8] have turned out to be very fruitful. In these examinations QCD has been generalized from the physical value for the numbers of colors $N_C = 3$ to an arbitrary value. Subsequently its inverse ($1/N_C$) has been treated as an effective expansion parameter. It was recognized that in the limit $N_C \rightarrow \infty$ only a special class of Feynman diagrams survived. These are the planar diagrams with quark loops only at the edges. Applying crossing symmetry and unitarity, as well as assuming confinement, Witten showed [8] that QCD is equivalent to an effective theory of weakly interacting mesons (and glueballs). In this context weakly refers to the fact that an effective four-meson vertex scales like $1/N_C$. Consequently a major goal of phenomenological studies is the construction of effective meson theories. Such approaches are guided by requiring the symmetries of QCD for the meson Lagrangian.

In the case of arbitrary N_C a color singlet baryon consists of N_C quarks. As a result it is obvious that the properties of a single quark cause the masses of baryons to be of the order N_C . Furthermore it can be shown that those contributions to the masses, which are due to the exchange of gluons, are of this order as well. Since the baryons are color singlet states their wave-functions are completely anti-symmetric in the color degrees of freedom of the quarks. As a consequence of the Pauli Principle the wave-function must be symmetric in all other quantum numbers. This allows the quarks to reside in S -wave states causing the mean square radius of baryons to be of the order N_C^0 in the limit of large numbers of colors^a. Obviously the masses of baryons scale like the inverse of the coupling constant of the effective meson theory associated with QCD while the extension of the baryons is essentially independent of this coupling constant. From these analogies Witten argued [8] that baryons emerged as the soliton solutions in the effective meson theory. The solitons are the solutions to the (static) classical Euler-Lagrange equations and may be considered as mappings from coordinate space to the configuration space of the mesons. The latter is commonly given by flavor $SU(2)$ or $SU(3)$ in the cases of two (up, down) or three (up, down, strange) flavors. From a topological point of view these mappings are characterized by the so-called winding number which determines the number of coverings of the configuration space when the coordinate space is passed through exactly once. Solitons with different winding numbers are topologically distinct meaning that there exists no continuous deformation connecting solitons of different winding numbers. Witten conjectured that this winding number be identified with the baryon number. Later on we will see that this identification can be justified once the effective meson theory for three flavors is properly constructed. Witten furthermore analyzed the N_C behavior of other baryon observables as *e.g.* the scattering amplitudes of baryon-baryon and meson-baryon interactions. These were all found to comply with the picture that baryons emerge as the solitons of the effective meson theory to which QCD is equivalent.

As a matter of fact such a topological soliton was already constructed by Skyrme [9] before the notion of quarks and gluons was invented. However, it was just the above mentioned considerations, which enabled the Skyrme model to be established within the context of QCD.

^aThis is in contrast to an atom. In that case the wave-function needs to be anti-symmetric in the spatial quantum numbers and hence the radius increases with the number of electrons.

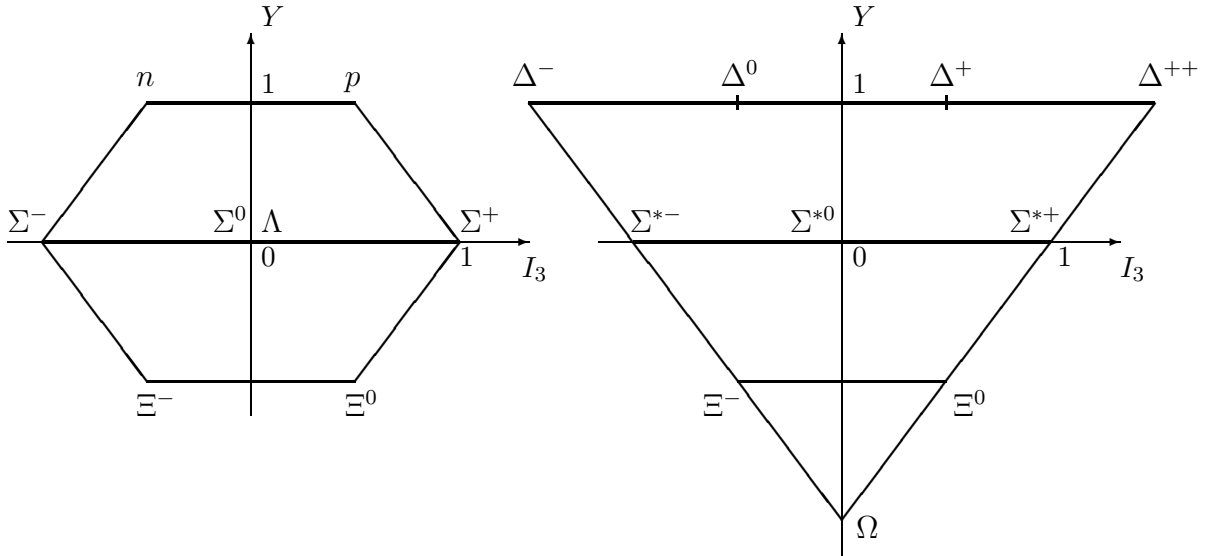


Figure 1.1: The low-lying baryons in the octet (left) and decouplet (right) representations of flavor $SU(3)$. These baryons are characterized by their isospin-projection (I_3) and hypercharge (Y) quantum numbers.

Subsequent to the first application of this model to investigate observables of the nucleon and Δ resonance by Adkins, Nappi and Witten [10] the Skyrme model became a major subject of interest. The Skyrme model contains as fundamental mesonic degrees of freedom only the isovector of the pseudo-scalar pions. As these are by far the lightest (135MeV) mesons their importance at low energies is obvious. The fact that these mesons are the “would-be” Goldstone bosons of the spontaneous breaking of chiral symmetry provides another reason to consider them as the most relevant ingredients. The first results of the examinations within the Skyrme model are reviewed [3, 4]. Later the Skyrme model was extended (and improved) to also contain the light vector mesons $\rho(770)$ and $\omega(783)$ (for a review see ref [5]). All extensions have been performed such that they satisfy the symmetries of QCD. Besides Poincaré invariance the chiral symmetry (see eqs (2.2) and (2.18)) and its spontaneous breaking represents a guiding principle for extending the Skyrme model. Such approaches not only allow one to study static properties of the nucleon but also dynamics as *e.g.* exhibited in pion-nucleon scattering [6]. It will be the primary purpose of this review article to provide a survey on progress achieved in the three flavor generalization of Skyrme type models, this includes those models which contain strange vector mesons as well.

The major focus of these three flavor soliton models is on the description of the low-lying $J^\pi = \frac{1}{2}^+$ and $\frac{3}{2}^+$ baryons. These objects of interest are displayed in figure 1.1 in form of the popular representations of flavor $SU(3)$. The baryons $p, n, \dots, \Delta^-, \dots, \Omega$ are shown as states in the octet and decouplet representations. Later we will see that higher dimensional representations of $SU(3)$ are as well relevant for the low-lying baryons.

The first study within a given model, of course, concerns the spectrum of the baryons. Here the mass splittings between the baryons shown in figure 1.1 will represent the main issue. For a long time it was believed that soliton models considerably overestimated the absolute masses of these baryons. However, recently significant progress has been made by including the quantum corrections associated with meson loops in the background of the soliton [11, 12, 13, 14, 15]. Adopting a regularization scheme motivated by the chiral expansion [16] indeed reproduces the experimental values for the absolute masses reasonably well [12, 15]. Since these corrections affect all baryons approximately equally the consideration of mass differences appears to be

a suitable measure in the semi-classical treatment. In the next step static properties are explored. Although these models are formulated in terms of meson fields it is nevertheless possible to study the quark structure of baryons. The natural question arises, how to identify quark operators within a theory within such a model. Obviously that can only be done for objects which are bilinear in the quark fields. For operators which are related to symmetry currents this is straightforward since imitating the symmetries of QCD within the meson theory directly allows one to identify the currents. Phrased otherwise, advantage is taken of the fact that the effective meson theory imitates the Ward identities of QCD. For operators which do not exhibit this feature one commonly refers back to simplified models of the quark flavor dynamics like the Nambu–Jona–Lasino (NJL) model [17]. In contrast to QCD such models can exactly be converted into meson theories [18, 19]. This also provides the quark bilinears in terms of the meson fields. We will make extensive use of such identifications.

Rather than providing a detailed description of the contents of this article it is more appropriate to qualitatively describe some of the major applications of these three flavor soliton models for recent, present or up-coming experiments. The main part of the review article will serve to make these discussions quantitative. The relation to these experiments will in addition reveal the relevance of “fine-tuned” three flavor soliton models for understanding the structure of the low-lying baryons.

1.2 The Proton Spin Puzzle

The analysis [20] of data obtained in the EMC experiments [21] scattering polarized muons off polarized protons has led to extensive activities on investigating the nucleon matrix elements of axial current. In this analysis the separate contributions of the up, down and strange degrees of freedom to the axial current have been disentangled yielding two surprising results. At first sight, the singlet combination turned out to be compatible with zero. This is counter-intuitive because in the non-relativistic quark model [22] this quantity is identical to twice the spin carried by the quarks and hence should be close to unity. In contrast to the non-relativistic quark model it was soon realized that the Skyrme model indeed predicted an identically vanishing matrix element of the axial singlet in nucleon states [20]. This observation caused a renewed interest in soliton models. Second, it turned out that the strange quarks contributed a significant amount to the axial current of the nucleon, about 30% of the down quarks. In a naïve valence quark picture of the baryon this quantity would identically vanish because strange degrees of freedom are ignored. One major input into the analyses of the various contributions to the axial current has been the assumption of flavor $SU(3)$ symmetry which permits to relate nucleon matrix elements of axial current to strangeness changing matrix elements of the axial current. The latter can be measured in semi-leptonic hyperon decays like $\Lambda \rightarrow pe^- \bar{\nu}_e$ [23]. Again the $SU(3)$ Skyrme model reasonably reproduced this result when the three flavor symmetry was assumed as well [20]. However, it was soon realized [24] that waving this assumption could significantly reduce the strange contribution to the axial current, but the singlet matrix element turned out to be quite insensitive with respect to flavor symmetry breaking [25]. Hence, even a sizable breaking of flavor symmetry does not lead to a matrix element of the singlet axial current which is close to unity as naïvely expected. The interested reader may peek ahead to figure 2.2 where this feature is illustrated.

As the precision of the experiments improved it became clear that the matrix element of the axial singlet current indeed is significantly smaller than unity although different from zero. In addition refining the soliton models by *e.g.* incorporating vector mesons or explicit quarks

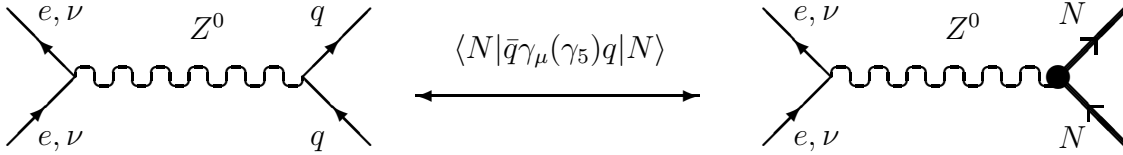


Figure 1.2: The matrix element $\langle N | \bar{q} \gamma_\mu (\gamma_5) q | N \rangle$ relates the electro-weak interaction of the nucleon to the elementary processes of the quarks.

yields also a non-vanishing matrix element [25, 26]. The review of these investigations will constitute a major part of the present article. Special emphasis will be placed on the role of flavor symmetry breaking and the strange degrees of freedom. To further elaborate these issues it will also be interesting to study the related problem of semi-leptonic hyperon decays because for these processes the concept of $SU(3)$ symmetry is well established [27]. It has turned out that indeed a large flavor symmetry breaking occurs for the baryon wave-functions without contradicting the phenomenology of the semi-leptonic hyperon decays. Although this has recently also been understood in the context of extended quark models [28, 29] the three flavor soliton models provide unique frameworks to study these issues comprehensively.

1.3 Strangeness in the Nucleon

We have just observed in the discussion of the axial current that the generalization of soliton models to flavor $SU(3)$ encourages one to study effects of strange degrees of freedom in the nucleon. As explained above this generalization makes possible the investigation of matrix elements of various other strange quark operators. Let us consider two prominent examples. The first one concerns the matrix element of the strange scalar operator in the nucleon $\langle N | \bar{s} s | N \rangle$. Adopting, for the sake of argument, the naïve valence quark picture this quantity is zero. With this assumption one may relate the pion nucleon sigma term $\sigma_{\pi N}$, which is defined via the double commutator of the axial generator with the Hamiltonian, to the spectrum of the low-lying $\frac{1}{2}^+$ baryons [30]. This yields $\sigma_{\pi N} \approx 35 \text{MeV}$. On the other hand $\sigma_{\pi N}$ can be extracted from the isospin symmetric part of the πN scattering amplitude resulting in $\sigma_{\pi N} \approx 45 \text{MeV}$ [31]. Although these analyses are somewhat model dependent this discrepancy can only be resolved when accepting that $\langle N | \bar{s} s | N \rangle$ is non-negligible. The second example refers to the matrix element of the strange vector current $\langle N | \bar{s} \gamma_\mu s | N \rangle$. This quantity is of special interest in the context of electro-weak processes where neutral gauge bosons are exchanged. In the context of the standard model these bosons couple to the quarks and further, the couplings to various quark flavors is completely determined in terms of the parameters of the standard model. In order to describe the electro-weak interaction of the nucleon we require information about the behavior of the quarks inside the nucleon. It is exactly this information, which is contained in the matrix element $\langle N | \bar{q} \gamma_\mu (\gamma_5) q | N \rangle$ where q stands for any quark flavor, see figure 1.2. The axial piece (γ_5) has already been mentioned in the context of the proton spin puzzle. It is obvious that $q = u, d$ play the dominant role but according to the above discussion one expects also the strange vector current matrix element $\langle N | \bar{s} \gamma_\mu s | N \rangle$ to be non-negligible. In the original studies of electroweak processes, this matrix

element was set to zero. This permitted one to consider reactions like $eN \rightarrow eN$ via Z^0 -exchange as precision measurements for the parameters of the standard model, especially the Weinberg angle [32] (left arrow in figure 1.2). In the meantime DIS experiments have provided such precise data for these parameters^b that one may turn around this argument and try to extract a reliable value for $\langle N|\bar{s}\gamma_\mu s|N\rangle$ from $eN \rightarrow eN$ or $\nu N \rightarrow \nu N$ (right arrow in figure 1.2). Quite a few such experiments are scheduled for the near future (or are already taking data). An extensive survey on these experiments may *e.g.* be found in refs [34, 35]. There have already been several attempts to estimate $\langle N|\bar{s}\gamma_\mu s|N\rangle$. The first one was carried out in ref [36] performing a three-pole vector meson fit to dispersion relations [37]. The effect of $\phi - \omega$ mixing has also been investigated in the framework of vector meson dominance [38]. This picture has even been combined [39] with the kaon loop calculation of ref [34]. The study of the matrix element $\langle N|\bar{s}\gamma_\mu s|N\rangle$ in various three flavor soliton models will be reviewed in the present article. Such computations have been performed in the Skyrme model [38], the Skyrme model with vector mesons [40] and the NJL soliton approach [41]. Although these explorations will be discussed in detail later it is appropriate to mention that incorporating flavor symmetry breaking into the nucleon wave-function reduces the effect of strangeness. This feature has already shown up in the discussion of the axial current and can easily be understood qualitatively since without symmetry breaking in the baryon wave-function virtual strange and non-strange quark-antiquark pairs are equally probable. However, this feature is almost the only one which all these $SU(3)$ soliton models have in common concerning their predictions for $\langle N|\bar{s}\gamma_\mu s|N\rangle$. Therefore the data accumulated in the experiments measuring this quantity might also serve to discriminate between these models.

As already indicated, this review article will primarily be concerned with topics related to questions raised in the preceding discussions. The corresponding predictions obtained in different effective theories will be discussed in chapters 2, 4 and 6. Different approaches to include strange degrees of freedom in soliton models will be explained in chapters 2, 3 and 5. In particular, a comparison of these treatments may be found in section 5.3. Furthermore a number of other interesting applications of three flavor soliton models will at least briefly be exemplified.

2 The Collective Approach to the $SU(3)$ Skyrme Model

2.1 The Skyrme Model

Before presenting the details of the three flavor model it is appropriate to discuss general aspects of the soliton solution in the Skyrme model. These are most conveniently presented in the framework of the two flavor reduction. The starting point for many of these effective meson theories is the non-linear σ model. At low energies one expects the most important part of an effective theory to only include the lightest mesons (*i.e.* pions). In order to incorporate these features, chiral symmetry is realized by adopting the non-linear representation of the pion fields $\boldsymbol{\pi}(x)$

$$U(x) = \exp\left(\frac{i}{f_\pi}\boldsymbol{\tau} \cdot \boldsymbol{\pi}(x)\right), \quad (2.1)$$

^bFor a discussion see *e.g.* chapter 26 of ref [33].

where the isovector $\boldsymbol{\tau}$ contains the Pauli matrices. The physical interpretation of the constant \tilde{f}_π will be explained shortly. The matrix $U(x)$ is commonly referred to as the chiral field. The chiral transformations are parametrized by the constant matrices L and R via

$$U(x) \longrightarrow LU(x)R^\dagger. \quad (2.2)$$

Chiral invariance is then manifested by the symmetry of the Lagrangian under this transformation^a. The fact that the vacuum configuration ($\boldsymbol{\pi} = 0$, *i.e.* $U = 1$) is only invariant under the coset $L = R$ reflects the spontaneous breaking of chiral symmetry. In terms of $U(x)$ the non-linear σ model is defined by the Lagrangian

$$\mathcal{L}_{nl\sigma} = \frac{\tilde{f}_\pi^2}{4} \text{tr} \left(\partial_\mu U \partial^\mu U^\dagger \right). \quad (2.3)$$

It is straightforward to construct the Noether currents associated with the symmetry transformation (2.2). The vector and axial-vector currents (V_μ and A_μ) correspond to $R = L$ and $R^\dagger = L$, respectively. These currents may most conveniently be presented by introducing $\alpha_\mu = \partial_\mu U U^\dagger$ and $\beta_\mu = U^\dagger \partial_\mu U$

$$V_\mu^a = -i \frac{\tilde{f}_\pi^2}{2} \text{tr} \left[\frac{\boldsymbol{\tau}^a}{2} (\alpha_\mu - \beta_\mu) \right] = \epsilon_{abc} \pi_b \partial_\mu \pi_c + \dots, \quad (2.4)$$

$$A_\mu^a = -i \frac{\tilde{f}_\pi^2}{2} \text{tr} \left[\frac{\boldsymbol{\tau}^a}{2} (\alpha_\mu + \beta_\mu) \right] = \tilde{f}_\pi \partial_\mu \pi_a + \dots, \quad (2.5)$$

where an expansion in terms of derivatives of the pion fields is indicated. In the framework of the electroweak theory the matrix element of A_μ^a between the vacuum and a state containing one pion of momentum p_μ

$$\langle 0 | A_\mu^a(x) | \pi^b(p) \rangle = i \delta^{ab} p_\mu \tilde{f}_\pi e^{ipx} \quad (2.6)$$

enters the decay width for $\pi \rightarrow \mu \bar{\nu}_\mu$. Its measurement then determines the pion decay constant^b $f_\pi \approx \tilde{f}_\pi = 93 \text{MeV}$ [33].

Simple scaling arguments $U(t, \mathbf{r}) \rightarrow U(t, \lambda \mathbf{r})$ [42] show that the model Lagrangian (2.3) does not possess stable soliton solutions which minimize the energy functional. For that reason Skyrme [9] added a term which is of fourth order in the derivatives

$$\mathcal{L}_{Sk} = \frac{1}{32e^2} \text{tr} ([\alpha_\mu, \alpha_\nu] [\alpha^\mu, \alpha^\nu]) \quad (2.7)$$

but nevertheless only quadratic in the time derivative. This feature will be advantageous for quantizing the theory canonically. The parameter e remains undetermined at the moment. The Lagrangian (2.7) may also be motivated as the remnant of the ρ -meson exchange in the limit $m_\rho \rightarrow \infty$ [43].

Static soliton configurations $U(\mathbf{r})$ represent mappings $U : \mathbb{R}^3 \rightarrow SU(2)$. Demanding the soliton to possess a finite energy requires the boundary condition $U(\mathbf{r}) \xrightarrow{r \rightarrow \infty} 1$. This identifies

^aThe relation of (2.2) to the transformation properties of left- and right-handed quark fields will be explained in chapter 6. See also section 2.2.

^bIn the three flavor model the physical pion decay constant will not exactly be identical to \tilde{f}_π .

all points at spatial infinity and thus compactifies the three-dimensional space to a sphere S^3 . Consequently

$$U : S^3 \rightarrow S^3, \quad (2.8)$$

since $SU(2)$ is equivalent to a three-dimensional sphere. The mappings (2.8) are characterized by the integer winding number

$$\nu[U] = \int d^3x B^0(x) \quad \text{with} \quad B^\mu(x) = \frac{1}{24\pi^2} \epsilon^{\mu\nu\rho\sigma} \text{tr}(\alpha_\nu \alpha_\rho \alpha_\sigma), \quad (2.9)$$

which gives the number of complete coverings of the target space ($SU(2)$) when the configuration space (\mathbb{R}^3) is passed through exactly once. $B^\mu(x)$ is referred to as the topological or winding number current and is conserved independently of the dynamics. As already mentioned in the introduction, it is the main feature of soliton models for baryons to identify the topological current with the baryon number current. Hence we are interested in configurations with $\nu[U] = B = 1$.

In order to construct a soliton solution with unit winding number Skyrme proposed to adopt the static hedgehog *ansatz* [44]

$$U_0(\mathbf{r}) = \exp(i\boldsymbol{\tau} \cdot \hat{\mathbf{r}}F(r)) \quad (2.10)$$

which defines the chiral angle $F(r)$. This *ansatz* possesses the famous grand spin symmetry, *i.e.* it is invariant under the combined spin-isospin transformation generated by $\mathbf{G} = \mathbf{j} + \boldsymbol{\tau}/2$, where \mathbf{j} is the spin operator. Substitution of the *ansatz* (2.10) into the Lagrangian $\mathcal{L}_{nl\sigma} + \mathcal{L}_{Sk}$ provides the static energy functional

$$E[F] = \frac{2\pi f_\pi}{e} \int_0^\infty dx \left\{ (x^2 F'^2 + 2\sin^2 F) + \sin^2 F \left(2F'^2 + \frac{\sin^2 F}{x^2} \right) \right\} \quad (2.11)$$

where a prime indicates a derivative with respect to the dimensionless coordinate $x = ef_\pi r$. Imposing $F(\infty)=0$ and noting that $\nu[U_0] = (F(0) - F(\infty))/\pi$ leads to the boundary condition $F(0) = \pi$. The corresponding solution, which minimizes (2.11), is displayed in figure 2.1. The energy obtained by substituting this solution into (2.11) is found to be $E = 23.2\pi f_\pi/e$ [10]. Up to now only massless pions have been considered. The inclusion of a pion mass term will be discussed together with the mass terms of the pseudo-scalar mesons in the $SU(3)$ extension.

2.2 The $SU(3)$ Extension of the Skyrme Lagrangian

For the inclusion of strange degrees of freedom the chiral field U is elevated from a 2×2 to a 3×3 unitary unimodular matrix, which in addition to the pions, contains the kaons and the octet component of the η . These fields are most conveniently incorporated in the framework of the so-called *Eightfold Way*

$$\Phi = \sum_{a=1}^8 \frac{\phi^a}{f_a} \lambda^a = \begin{pmatrix} \frac{1}{\sqrt{2}} \frac{\pi^0}{f_\pi} + \frac{1}{\sqrt{6}} \frac{\eta_8}{f_\eta} & \frac{\pi^+}{f_\pi} & \frac{K^+}{f_K} \\ \frac{\pi^-}{f_\pi} & -\frac{1}{\sqrt{2}} \frac{\pi^0}{f_\pi} + \frac{1}{\sqrt{6}} \frac{\eta_8}{f_\eta} & \frac{K^0}{f_K} \\ \frac{K^-}{f_K} & \frac{\bar{K}^0}{f_K} & -\frac{2}{\sqrt{6}} \frac{\eta_8}{f_\eta} \end{pmatrix}, \quad (2.12)$$

where λ^a denote the Gell-Mann matrices. The $SU(3)$ chiral field is then defined as

$$U(x) = \exp(i\Phi). \quad (2.13)$$

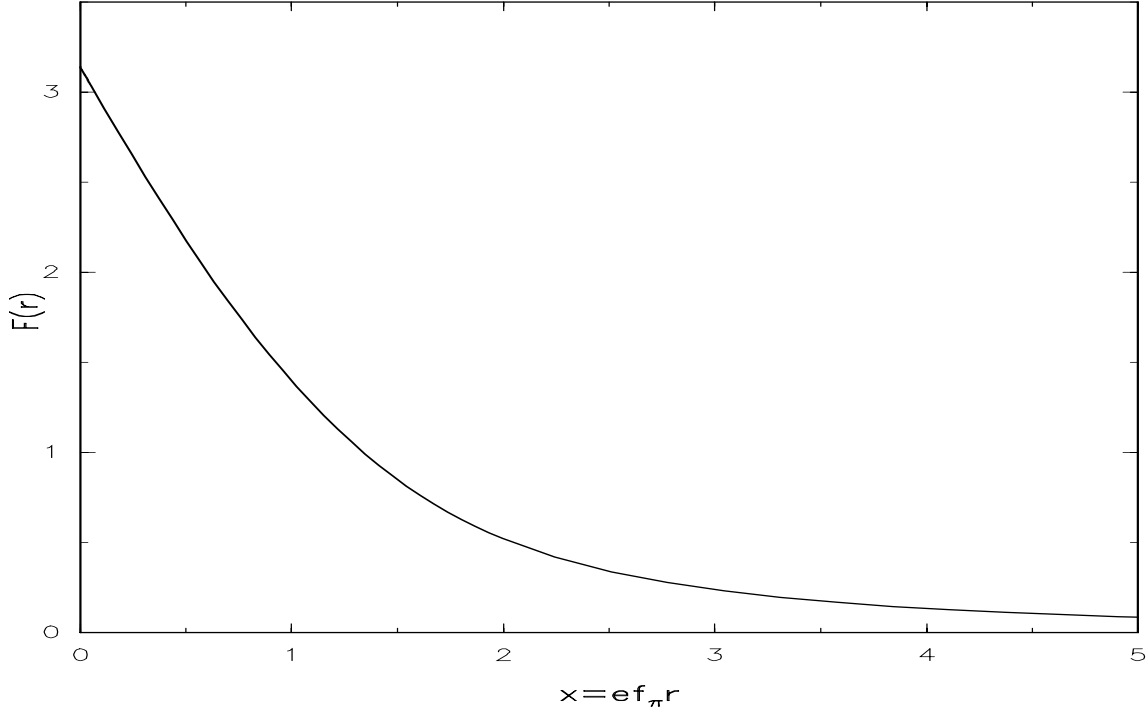


Figure 2.1: The radial dependence of the chiral angle which minimizes (2.11).

In eq (2.12) care has been taken of the different decay constants. These decay constants are defined via the gradient expansion of the axial–vector current analogous to (2.5)

$$A_\mu^a = f_a \partial_\mu \phi^a + \dots, \quad (a = 1, \dots, 8), \quad (2.14)$$

i.e., $f_{1,2,3} = f_\pi = 93\text{MeV}$, $f_{4,\dots,7} = f_K = 113\text{MeV}$ and $f_8 = f_\eta = 78 - 94\text{MeV}$. These data are obtained from the leptonic decays of the pseudo–scalar mesons [33]. Since the η_8 meson is of no special importance for the soliton calculations^c and f_η is not that well known, henceforth the approximation $f_\eta = f_\pi$ will be adopted.

The difference in the decay constants reflects a feature of flavor symmetry breaking. Let us now construct the appropriate symmetry breaking terms systematically from the QCD mass term in the case of three flavors

$$\mathcal{L}_{\text{QCD}}^{\text{mass}} = -m_u \bar{u}u - m_d \bar{d}d - m_s \bar{s}s = -\hat{m} \bar{q} \mathcal{M} q, \quad q = \begin{pmatrix} u \\ d \\ s \end{pmatrix}, \quad (2.15)$$

with $\hat{m} = (m_u + m_d)/2$. The mass matrix is parametrized as [45]

$$\mathcal{M} = y\lambda^3 + T + xS, \quad (2.16)$$

where $T = \text{diag}(1, 1, 0)$ and $S = \text{diag}(0, 0, 1)$ are the projectors on the non–strange and strange subspaces, respectively. Furthermore x and y are the quark mass ratios

$$x = \frac{m_s}{\hat{m}}, \quad y = \frac{1}{2} \frac{m_u - m_d}{\hat{m}}. \quad (2.17)$$

^cThere is one exception from this statement which will be discussed in section 4.4.

The mass term (2.15) is not invariant under the chiral transformation

$$q_L \rightarrow Lq_L, \quad q_R \rightarrow Rq_R, \quad q_{R,L} = \frac{1}{2}(1 \pm \gamma_5)q \quad (2.18)$$

but rather the matrix $q\bar{q} = q_L\bar{q}_R + q_R\bar{q}_L$ transforms like the representation $(\mathbf{3}, \mathbf{3}^*) + \text{h.c.}$ of (L, R) . The symmetry breaking terms of the meson Lagrangian are required to imitate this transformation behavior under prospect of (2.2). A minimal set of symmetry breaking terms is added to the chirally symmetric Lagrangian discussed above. In order to allow for different meson masses and decay constants two additional terms are needed

$$\mathcal{L}_{\text{SB}} = \text{tr} \left\{ \mathcal{M} \left[-\beta' \left(\partial_\mu U \partial^\mu U^\dagger U + U^\dagger \partial_\mu U \partial^\mu U^\dagger \right) + \delta' \left(U + U^\dagger - 2 \right) \right] \right\}. \quad (2.19)$$

The phase conventions have been chosen such that \mathcal{M} is self-adjoint. In general this may not be possible, see *e.g.* eq (2.85). In that case one has to substitute $\text{tr}\{\mathcal{M}(U + U^\dagger)\} \rightarrow \text{tr}\{\mathcal{M}U + U^\dagger\mathcal{M}^\dagger\}$, etc. .

For the moment it is appropriate to assume the isospin limit $y = 0$. The new parameters $(x, \beta'$ and $\delta')$ are determined from the masses and decay constants of the pseudo-scalar mesons [46]

$$m_\pi^2 = \frac{4\delta'}{f_\pi^2}, \quad m_K^2 = \frac{2(1+x)\delta'}{f_K^2} \quad \text{and} \quad \left(\frac{f_K}{f_\pi} \right)^2 = 1 + 4\beta' \frac{1-x}{f_\pi^2}. \quad (2.20)$$

It has already been remarked that \tilde{f}_π in eq (2.3) is not exactly identical to the physical pion decay constant $f_\pi = 93\text{MeV}$, rather $f_\pi^2 = \tilde{f}_\pi^2 - 8\beta'$. Substitution of the experimental data [33] yields [47]

$$\beta' = -2.64 \times 10^{-5} \text{GeV}^2, \quad \delta' = 4.15 \times 10^{-5} \text{GeV}^4 \quad \text{and} \quad x = 37.3. \quad (2.21)$$

Obviously the difference between \tilde{f}_π and f_π is only minor and for convenience we will henceforth omit this distinction. It is also noteworthy that due to the inclusion of different decay constants in the present prediction for the quark mass ratio, x is considerably larger than the value (25.0 ± 2.5) of ref [48]. Further, it should also be noted that additional symmetry breaking terms might be introduced because $\mathcal{M}^{\dagger-1} \det \mathcal{M}^\dagger$ transforms under chiral $SU(3)_L \times SU(3)_R$ in the same way as \mathcal{M} [49]. These terms, however, will not be considered here because the minimal set (2.19) adequately describes the mesonic data.

Now all ingredients necessary to describe the pseudo-scalar mesons properly have been presented in eqs (2.3, 2.7, 2.19). However, as compared to QCD (or nature) this Lagrangian has still a superfluous symmetry. It is straightforward to verify that the above presented pieces of the effective meson Lagrangian are separately invariant under the transformations $U \leftrightarrow U^\dagger$ and $\mathbf{r} \leftrightarrow -\mathbf{r}$. The pseudo-scalar character of the low-lying mesons requires the effective theory to be invariant only when these two transformations are combined. Unfortunately in four space time dimensions no local term can be added such that the separate symmetry is lost. Witten argued [50] however, that a suitable term can be added to the equations of motion

$$\frac{f_\pi^2}{2} \partial_\mu \alpha^\mu + \dots + 5\lambda \epsilon_{\mu\nu\rho\sigma} \alpha^\mu \alpha^\nu \alpha^\rho \alpha^\sigma = 0, \quad (2.22)$$

where the dots refer to the contributions from \mathcal{L}_{S_k} and \mathcal{L}_{SB} . This equation of motion is only invariant under the combined transformation $U \leftrightarrow U^\dagger$ and $\mathbf{r} \leftrightarrow -\mathbf{r}$. Within the context

of the action, this term can be obtained by adding a totally antisymmetric object on a five dimensional manifold M_5 and using Stoke's theorem. The important point is that the boundary of M_5 is the real Minkowski space *i.e.* $\partial M_5 = M_4$. From the path-integral formulation one requires that the action may only change by a multiple of 2π when going from M_5 to its complement, which has the identical boundary. Therefore $n = 240i\pi^2\lambda$ must be integer. This actually is completely analogous to Dirac's quantization of a magnetic monopole [51]. In the next step Witten included the photon fields in a gauge invariant way [50, 52]. This generates a vertex for the decay $\pi^0 \rightarrow \gamma\gamma$

$$\frac{-n}{96\pi^2 f_\pi} \pi^0 \epsilon_{\mu\nu\rho\sigma} F^{\mu\nu} F^{\rho\sigma},$$

where $F^{\mu\nu}$ is the field strength tensor of the photon field. Comparison with the triangle anomaly [53] brings into the game the number of colors $n = N_C$. The same result can be obtained from considering the process $\gamma \rightarrow \pi^+ \pi^0 \pi^-$. The Wess-Zumino term is now completely determined^d

$$\Gamma_{\text{WZ}} = -\frac{iN_C}{240\pi^2} \int_{M_5} (\alpha)^5. \quad (2.23)$$

It should be remarked that as Γ_{WZ} is a five-form it vanishes in the case of two flavors since the maximal number of generators is only four ($\mathbf{1}, \boldsymbol{\tau}$). The complete effective action of the pseudo-scalar mesons for flavor $SU(3)$ is finally given by

$$\Gamma = \int d^4x (\mathcal{L}_{nl\sigma} + \mathcal{L}_{Sk} + \mathcal{L}_{\text{SB}}) + \Gamma_{\text{WZ}}. \quad (2.24)$$

The Wess-Zumino term (2.23) exhibits one more important feature. It provides the only contribution to the Noether current associated with the $U_V(1)$ symmetry $L = R = \exp(i\epsilon\mathbf{1})$ (2.2). This current is, of course, nothing but the baryon number current, which indeed is recognized to be identical to the winding number current B_μ defined in eq (2.9). Obviously the sign of the Wess-Zumino term is fixed by these arguments. The opposite sign of Γ_{WZ} causes the boundary condition $F(0) = -\pi$. Glancing at eq (2.11) we see that the substitution $F(r) \rightarrow -F(r)$ leaves the energy invariant. As a matter of fact the model can consistently be formulated with this opposite sign of the chiral angle.

The first step towards describing baryons in the three flavor model consists of constructing the classical soliton. Although various embeddings of the hedgehog (2.10) within the $SU(3)$ matrix U are possible demanding a minimal static energy fixes it to

$$U_0(\mathbf{r}) = \begin{pmatrix} \exp(i\boldsymbol{\tau} \cdot \hat{\mathbf{r}}F(r)) & | & 0 \\ \hline 0 & 0 & | & 1 \end{pmatrix}. \quad (2.25)$$

Other embeddings yield larger energies as a consequence of the symmetry breaking terms. Hence as compared to the two flavor model the classical mass acquires only a minor correction associated with the β' and δ' terms

$$E_{\text{cl}} = 4\pi \int_0^\infty dr \left\{ \left[\frac{f_\pi^2}{2} + 4\beta'(1 - \cos F) \right] (r^2 F'^2 + 2\sin^2 F) + \frac{\sin^2 F}{2e^2} \left(2F'^2 + \frac{\sin^2 F}{r^2} \right) + 4\delta' r^2 (1 - \cos F) \right\}. \quad (2.26)$$

^dWe use the notation of differential forms $\alpha = \alpha^\mu dx_\mu$.

The chiral angle $F(r)$ is again determined as the solution to the Euler–Lagrange equations extremizing (2.26) subject to the boundary conditions $F(0) = \pi$ and $F(\infty) = 0$. The resulting profile is comparable to the one shown in figure 2.1.

2.3 Quantization of the Collective Coordinates

It can easily be verified that the static field configuration (2.25) does not yield states of good spin and/or flavor because U_0 does not commute with the corresponding generators, $\mathbf{r} \times \boldsymbol{\partial}$ and $\lambda^a/2$. States with good spin and isospin quantum numbers are generated by the well–known cranking procedure [54].

The generators for the flavor transformations and spatial rotations are constructed as Noether charges

$$\mathcal{Q}^a = \int d^3r \left\{ \frac{\partial \mathcal{L}}{\partial \dot{U}} (\delta^a U) + \text{h.c.} \right\}, \quad (2.27)$$

associated with the field configuration which solves the full Euler–Lagrange equations. The infinitesimal form of the symmetry transformation is denoted by $\delta^a U$. It is therefore obvious that time–dependent solutions are required, not only static solutions. Unfortunately no such time–dependent solution is known at present and approximations have to be imposed. Ignoring (for the time being) symmetry breaking effects one recognizes that the energy remains unchanged by global rotations of the hedgehog solution (2.25) in flavor and coordinate spaces. Hence, as a first step a reasonable approximation to the time–dependent solutions is presumably given by assuming these transformations to vary in time,

$$U(\mathbf{r}, t) = \tilde{A}(t)U_0 \left(R^{-1}(t)\mathbf{r} \right) \tilde{A}^\dagger(t) = A(t)U_0(\mathbf{r}) A^\dagger(t). \quad (2.28)$$

Later more elaborate *ansätze* for the time–dependent configuration will be introduced. In eq (2.28) the hedgehog symmetry of U_0 has been employed to express the spatial rotation as a flavor transformation. The $SU(3)$ matrix A is referred to as the collective rotation and contains collective coordinates. It may conveniently be parametrized in terms of eight ‘‘Euler angles’’, *cf.* eq (A.1). The time–dependence of A is measured by eight angular velocities Ω_a , which are defined via

$$A^\dagger(t) \frac{dA(t)}{dt} = \frac{i}{2} \sum_{a=1}^8 \lambda^a \Omega_a. \quad (2.29)$$

It is easy to verify that the angular velocities are invariant under global left transformations $A(t) \rightarrow LA(t)$ while under global right transformations $A(t) \rightarrow A(t)R^\dagger$ they behave like a member of the adjoint representation

$$\Omega_a \rightarrow \sum_{b=1}^8 D_{ab}(R) \Omega_b, \quad D_{ab}(R) = \frac{1}{2} \text{tr} \left(\lambda^a R \lambda^b R^\dagger \right). \quad (2.30)$$

The 8×8 rotation matrix $D_{ab}(A)$ behaves like a vector under both left– and right transformations

$$D_{ab}(A) \rightarrow \sum_{a',b'=1}^8 D_{aa'}(L^\dagger) D_{a'b'}(A) D_{b'b}(R^\dagger). \quad (2.31)$$

For that reason $D_{ab}(A)$ is frequently called the adjoint representation of the rotation A . The combination $\Omega'_a = D_{ab}(A)\Omega_b$ obviously transforms like a left vector $\Omega'_a \rightarrow D_{ab}(L^\dagger)\Omega'_b$.

In general the Lagrange function of the collective coordinates (the so-called collective Lagrangian) contains all combinations of $D_{ab}(A)$ and Ω_a which are consistent with the effective meson action as *e.g.* (2.24). From the *ansatz* (2.28) we infer that the flavor rotations correspond to the left transformation (L) of A . The flavor symmetric part of the action can therefore only contribute terms to the collective Lagrangian with all left indices saturated, *e.g.* $\Omega'_a\Omega'_a = \Omega_a\Omega_a$. On the other hand the flavor symmetry breaking term (2.19) transforms like the eighth component of a flavor vector^e. Hence it contributes terms of the structure $\Omega'_8 = D_{8b}(A)\Omega_b$. In order to gain restrictions of the right indices one recognizes that the spatial rotations may be identified with the “isospin-subset” of the right transformation (R) as a consequence of the hedgehog symmetry. The symmetry under spatial rotations thus permits contributions which separately saturate the subsets^f $i = 1, 2, 3$, $\alpha = 4, \dots, 7$ and $b = 8$ as *e.g.* $\Omega_i\Omega_i = \boldsymbol{\Omega} \cdot \boldsymbol{\Omega}$ or $D_{8\alpha}(A)\Omega_\alpha$. The latter, of course, stems from a term which breaks the flavor symmetry. Employing these arguments it is straightforward to verify that up to quadratic order in both the time derivatives and symmetry breaking the general form of the collective Lagrangian is given by

$$\begin{aligned}
L(A, \Omega_a) = & -E + \frac{1}{2}\alpha^2 \sum_{i=1}^3 \Omega_i^2 + \frac{1}{2}\beta^2 \sum_{\alpha=4}^7 \Omega_\alpha^2 - \frac{N_C B}{2\sqrt{3}}\Omega_8 + \alpha_1 \sum_{i=1}^3 D_{8i}\Omega_i + \beta_1 \sum_{\alpha=4}^7 D_{8\alpha}\Omega_\alpha \\
& - \frac{1}{2}\gamma(1 - D_{88}) - \frac{1}{2}\gamma_S(1 - D_{88}^2) - \frac{1}{2}\gamma_T \sum_{i=1}^3 D_{8i}D_{8i} - \frac{1}{2}\gamma_{TS} \sum_{\alpha=4}^7 D_{8\alpha}D_{8\alpha}. \quad (2.32)
\end{aligned}$$

Here $D_{ab} = D_{ab}(A)$ is implied. The coefficients $\alpha^2, \dots, \gamma_{TS}$ are functionals of the soliton profile(s) and hence are model dependent. It is the main objective of the various models to determine these coefficients. The quantities α^2 and β^2 denote the moments of inertia for rotations in coordinate space and flavor rotations in direction of the strange degrees of freedom, respectively. From symmetry arguments one might have also expected a term proportional to Ω_8^2 . Such a contribution, however, is absent because the hedgehog configuration (2.25) commutes with λ_8 . An expression of the form $D_{88}\Omega_8$ does not appear because of the same reason. Nevertheless a term linear in Ω_8 has shown up. It is a surface term which arises when applying Stoke’s theorem to the Wess–Zumino term (2.23) and its coefficient is uniquely related to the baryon number B . Shortly we will see that this term provides an important restriction on the allowed baryon states. It should be remarked that the quantities involving the coefficients γ_S , γ_T and γ_{TS} only appear when terms of the order \mathcal{M}^2 are included in the meson Lagrangian.

In order to quantize this “classical” theory we require the operators for spin and flavor from eq (2.27). As a consequence of the hedgehog structure the infinitesimal change under spatial rotations can be written as a derivative with respect to $\boldsymbol{\Omega}$

$$[\mathbf{r} \times \boldsymbol{\partial}, U(\mathbf{r}, t)] = \frac{\partial \dot{U}(\mathbf{r}, t)}{\partial \boldsymbol{\Omega}}. \quad (2.33)$$

Upon substitution of this relation into the defining equation (2.27) one observes for the spin operator $\mathbf{J} = \partial L(A, \Omega_a)/\partial \boldsymbol{\Omega}$. The quantization now proceeds along the lines of an $SU(3)$

^eThe isospin breaking, which is omitted here corresponds to the third component of a flavor vector.

^fFrom now on a vector will always refer to the first three components.

rigid top by generalizing this result to the right generators

$$R_a = -\frac{\partial L}{\partial \Omega_a} = \begin{cases} -(\alpha^2 \Omega_a + \alpha_1 D_{8a}) = -J_a, & a=1,2,3 \\ -(\beta^2 \Omega_a + \beta_1 D_{8a}), & a=4,\dots,7 \\ \frac{N_C B}{2\sqrt{3}}, & a=8 \end{cases} \quad (2.34)$$

The quantization prescription then demands the commutation relation $[R_a, R_b] = -if_{abc}R_c$ with f_{abc} being the antisymmetric structure constants of $SU(3)$. Of course, the identification of $\partial L(A, \Omega_a)/\partial \Omega$ as the right generators is consistent with the transformation behavior of a vector (2.30). The explicit forms of these generators in terms of an ‘‘Euler–angle’’ parametrization of A is presented in appendix A.

The generator R_8 is linearly connected to the so–called right hypercharge $Y_R = 2R_8/\sqrt{3} = 1$ for $B = 1$ and $N_C = 3$. In analogy to the Gell–Mann Nishijima relation [55, 56] a right charge

$$Q_R = -J_3 + \frac{Y_R}{2} \quad (2.35)$$

may be defined for the right generators. Completing the analogy we note that the eigenvalues of Q_R are $0, \pm 1/3, \pm 2/3, \pm 1, \dots$. Hence for $Y_R = 1$ the relation (2.35) can only be fulfilled when the eigenvalue of J_3 is half–integer. This yields the important conclusion that the $SU(3)$ model describes fermions. This is *a priori* not expected since the starting point has been an effective model of bosons. Arguing from a path–integral point of view Witten has even shown that these solitons describe fermions when N_C is odd and bosons when N_C is even [50]. This, of course, is expected from considering baryons as being composed of N_C quarks. It should be stressed that this result could only be gained by generalizing the Skyrme model to $SU(3)$ since in $SU(2)$ the Wess–Zumino term (2.23) vanishes. We therefore conclude that the proper incorporation of the anomaly structure of QCD leads to the desired spin–statistics relation.

The left generators, which are defined by the rotation $L_a = D_{ab}R_b$, satisfy the commutation relations $[L_a, L_b] = if_{abc}L_c$. They provide the isospin, $I_i = L_i$ ($i = 1, 2, 3$) and hypercharge, $Y = 2L_8/\sqrt{3}$ operators.

Finally the collective Hamiltonian is conventionally obtained as the Legendre transformation $H = -\sum_{a=1}^8 R_a \Omega_a - L$

$$\begin{aligned} H(A, R_a) &= E + \frac{1}{2} \left[\frac{1}{\alpha^2} - \frac{1}{\beta^2} \right] \mathbf{J}^2 + \frac{1}{2\beta^2} C_2(SU(3)) - \frac{3}{8\beta^2} \\ &+ \frac{\alpha_1}{2\alpha^2} \sum_{i=1}^3 D_{8i} (2R_i + \alpha_1 D_{8i}) + \frac{\beta_1}{2\beta^2} \sum_{\alpha=4}^7 D_{8\alpha} (2R_\alpha + \beta_1 D_{8\alpha}) + \frac{1}{2} \gamma (1 - D_{88}) \\ &+ \frac{1}{2} \gamma_S (1 - D_{88}^2) + \frac{1}{2} \gamma_T \sum_{i=1}^3 D_{8i} D_{8i} + \frac{1}{2} \gamma_{TS} \sum_{\alpha=4}^7 D_{8\alpha} D_{8\alpha} \end{aligned} \quad (2.36)$$

for $B = 1$ and $N_C = 3$. The constraint $R_8 = \frac{\sqrt{3}}{2}$, which yielded the spin–statistics relation, commutes with H permitting one to substitute this value. The term involving $\sum_{\alpha=4}^7 R_\alpha^2$ has been expressed by introducing the quadratic Casimir operator of $SU(3)$, $C_2(SU(3)) = \sum_{a=1}^8 R_a^2$. The standard $SU(3)$ representations are eigenstates of $C_2(SU(3))$ with eigenvalues μ . For the representations displayed in figure 1.1 one finds $\mu(\mathbf{8}) = 3$ and $\mu(\mathbf{10}) = 3$. The eigenstates of $H(A, R_a)$ have to satisfy an additional condition. This arises from the hedgehog structure of the static field configuration. The eigenstates of the flavor symmetric part of

$H(A, R_a)$ are $SU(3)$ representations constituting the basis for diagonalizing the whole Hamiltonian. As outlined in appendix A, the allowed $SU(3)$ representations must contain at least one state which has identical spin and isospin [57], like the nucleon or the Δ resonance.

Under flavor transformations the symmetry breaking parts linear in \mathcal{M} behave like the eighth component of an octet [58] as can be seen from $[L_a, D_{8b}] = if_{8ac}D_{cb}$. Hence the Gell-Mann Okubo mass formulae [59, 60]

$$2(M_N + M_{\Xi}) = M_{\Sigma} + 3M_{\Lambda} \quad (2.37)$$

$$M_{\Omega} - M_{\Xi^*} = M_{\Xi^*} - M_{\Sigma^*} = M_{\Sigma^*} - M_{\Delta} \quad (2.38)$$

will automatically hold at first order. Eqs (2.38) are referred to as the equal spacing relation for the $\frac{3}{2}^+$ baryons. However, there is no guarantee that calculations at leading order in symmetry breaking are reliable and indeed higher order terms may play a significant role. To investigate these one first notes that the symmetry breaking parts mix various $SU(3)$ representations, while they are diagonal in the physical quantum numbers of the baryons like spin and flavor. As an example a matrix element of the nucleon in the octet (**8**) and anti-decuplet ($\overline{\mathbf{10}}$) reads $\langle N, \mathbf{8} | D_{88} | N \overline{\mathbf{10}} \rangle = \sqrt{5}/10$. Such matrix elements can be computed by means of $SU(3)$ Clebsch–Gordon coefficients [61, 24]. Up to third order in the perturbation expansion only the $SU(3)$ representations **8**, $\overline{\mathbf{10}}$ and **27** contribute for the $\frac{1}{2}^+$ baryons. As an example the shifts in energy, which are associated with the dominant symmetry breaking term, are given by [24]

$$\begin{aligned} \delta M_N &= \frac{1}{2\beta^2} \left\{ -0.3\gamma\beta^2 - 0.0287(\gamma\beta^2)^2 + 0.0006(\gamma\beta^2)^3 + \dots \right\} \\ \delta M_{\Lambda} &= \frac{1}{2\beta^2} \left\{ -0.1\gamma\beta^2 - 0.0180(\gamma\beta^2)^2 - 0.0003(\gamma\beta^2)^3 + \dots \right\} \\ \delta M_{\Sigma} &= \frac{1}{2\beta^2} \left\{ 0.1\gamma\beta^2 - 0.0247(\gamma\beta^2)^2 + 0.0002(\gamma\beta^2)^3 + \dots \right\} \\ \delta M_{\Xi} &= \frac{1}{2\beta^2} \left\{ 0.2\gamma\beta^2 - 0.0120(\gamma\beta^2)^2 - 0.0006(\gamma\beta^2)^3 + \dots \right\} . \end{aligned} \quad (2.39)$$

The leading order obviously satisfies (2.37). Since the second order correction to the ground states is always negative the deviation from (2.37) remains moderate at this order. Apparently the series converges sufficiently fast because the products of Clebsch–Gordon coefficients are always significantly smaller than unity. There is one more important fact that can be extracted from the expansion (2.37). Obviously the effective symmetry breaking parameter is the product $\gamma\beta^2$ rather than only the coefficient γ . This can easily be understood because the probability for rotations into strange directions not only depends on the repulsive potential (measured by γ) but also the inertia parameter. This feature can also be observed when considering the expansion of the nucleon wave-function in terms of $SU(3)$ representations

$$|N\rangle = |N, \mathbf{8}\rangle + 0.0745\gamma\beta^2 |N, \overline{\mathbf{10}}\rangle + 0.0490\gamma\beta^2 |N, \mathbf{27}\rangle \dots \quad (2.40)$$

As in eq (2.37) the coefficients are computed from $SU(3)$ Clebsch–Gordon coefficients [61]. These admixtures of higher dimensional $SU(3)$ representations can be interpreted as additional quark–antiquark excitations in the nucleon.

In appendix A it is indicated how the collective Hamiltonian (2.36) can be diagonalized exactly by adopting an ‘‘Euler-angle’’ parametrization of A (A.1). Upon canonical quantization

of these ‘‘Euler-angle’’ the generators R_a become differential operators (A.7) and the eigenvalue problem $H\Psi = \epsilon\Psi$ turns into coupled partial differential equations. Fortunately the symmetry breaking terms acquire quite simple forms as *e.g.* $1 - D_{88} = \frac{3}{2}\sin^2\nu$. The angle ν interpolates between strange and non-strange directions^g, *cf.* eq (A.1). Therefore the partial differential equations simplify considerably to a set of ordinary coupled differential equations in the angle ν when an appropriate parametrization for the baryon wave function is adopted (A.8). This finally yields the mass formula

$$M_B = E + \frac{1}{2} \left(\frac{1}{\alpha^2} - \frac{1}{\beta^2} \right) J(J+1) - \frac{3}{8\beta^2} + \frac{1}{2\beta^2} \epsilon_{\text{SB}} , \quad (2.41)$$

where J denotes the spin of the baryon B and ϵ_{SB} is the eigenvalue of

$$\begin{aligned} C_2 + \beta^2\gamma(1 - D_{88}) + \beta^2\gamma_S(1 - D_{88}^2) + \beta^2\gamma_T \sum_{i=1}^3 D_{8i}D_{8i} + \beta^2\gamma_{TS} \sum_{\alpha=4}^7 D_{8\alpha}D_{8\alpha} \\ + \beta^2\frac{\alpha_1}{\alpha^2} \sum_{i=1}^3 D_{8i}(2R_i + \alpha_1 D_{8i}) + \beta_1 \sum_{\alpha=4}^7 D_{8\alpha}(2R_\alpha + \beta_1 D_{8\alpha}) . \end{aligned} \quad (2.42)$$

In ref [24] it has been shown for the simplest case where only the term proportional to γ is included, that the perturbative expansion up to third order deviates from the exact result by a negligible amount even for large values of $\gamma\beta^2$.

In the literature the exact diagonalization using the ‘‘Euler-angle’’ parametrization is known as the Yabu–Ando approach [62] to three flavor soliton models. In their original approach only the simplest symmetry breaking term ($\gamma(1 - D_{88})$) had been considered because it is the only one appearing in the Skyrme model of pseudo-scalar as will be seen in the proceeding section. Later this treatment was extended to include all types of symmetry breaking terms listed in eq (2.42). These terms come into the game when vector mesons [40] or explicit quark degrees of freedom [63, 64] are included. These models will be discussed in chapters 4 and 6, respectively. Of course, the quality of such approaches is as good as the approximation (2.28) to the exact time-dependent solution to the Euler–Lagrange equations, which should be reasonable for small symmetry breaking. In chapter 5 an approach will be introduced which starts from considering flavor symmetry to be large by not treating the kaon fields being collective excitations of the hedgehog but rather as small amplitude fluctuations in the background of the soliton. *A posteriori* the comparison of both treatments should permit the justification of at least one of them.

2.4 Spectrum and Form Factors

We now return to the special form of the $SU(3)$ Skyrme model defined in eq (2.24). In that case the collective Lagrangian (2.32) simplifies considerably since the coefficients α_1 , β_1 , γ_S , γ_T and γ_{TS} vanish. Substituting the *ansatz* (2.28) gives the moment of inertia for rotations in coordinate space

$$\alpha^2 = \frac{8\pi}{3} \int dr r^2 \sin^2 F \left\{ f_\pi^2 + \frac{1}{e^2} \left[F'^2 + \frac{\sin^2 F}{r^2} \right] + 8\beta'(1 - \cos F) \right\} , \quad (2.43)$$

^gThe angle ν will henceforth be denoted as strangeness changing angle.

while the only remaining symmetry breaking parameter is obtained to be, *cf.* eq (2.17)

$$\gamma = \frac{32\pi}{3}(x-1) \int dr \left\{ \delta' r^2 (1 - \cos F) - \beta' \cos F (F'^2 r^2 + 2 \sin^2 F) \right\}. \quad (2.44)$$

Although the direct influence of the β' type symmetry breaker is small its impact on γ is very important because it accounts for $f_K \neq f_\pi$. As a consequence $\delta'(x-1) \propto f_K^2 m_K^2 - f_\pi^2 m_\pi^2 \approx 1.5 f_\pi^2 m_K^2$ and the symmetry breaker γ is significantly increased as compared to the case when the β' term is omitted [47].

Unfortunately the strange moment of inertia is not as straightforwardly obtained from the *ansatz* (2.28) [65]. As already remarked the Wess–Zumino term (2.23) is linear in the time derivatives. As a consequence static kaon fluctuations, which are represented in the form of a two–component isospinor $K(\mathbf{r})$,

$$U(\mathbf{r}, t) = A^\dagger(t) e^{iZ(\mathbf{r})} U_0 e^{iZ(\mathbf{r})} A(t), \quad Z(\mathbf{r}) = \begin{pmatrix} 0 & | & K(\mathbf{r}) \\ \hline - & & - \\ K^\dagger(\mathbf{r}) & | & 0 \end{pmatrix}, \quad (2.45)$$

appear in the action with a linear coupling to the time derivative of the rigidly rotating hedgehog (2.25). Stated otherwise, the Wess–Zumino term provides the source for induced kaon fields $K(\mathbf{r})$. As this source is linear in the angular velocities $\Omega_4, \dots, \Omega_7$ the induced kaon fields are as well. Hence a suitable *ansatz*, which also takes care of the pseudo–scalar nature of the kaon fields is [65, 47]

$$K(\mathbf{r}) = W(r) \boldsymbol{\tau} \cdot \hat{\mathbf{r}} \Omega_K, \quad \Omega_K = \begin{pmatrix} \Omega_4 - i\Omega_5 \\ \Omega_6 - i\Omega_7 \end{pmatrix}. \quad (2.46)$$

Expanding the Lagrangian up to quadratic order in Ω_α yields additional contributions for the strange moment of inertia β^2 which then is a functional of the radial function $W(r)$. The explicit form of this functional is displayed in appendix B, eqs (B.10, B.11). In principle $W(r)$ is complex, however, it turns out that only the real part becomes excited by the Wess–Zumino term. The radial dependence of $W(r)$ is finally determined by extremizing β^2 . Although this completes the calculation of the collective Lagrangian a note should be added concerning possible double counting of kaonic fields. Denoting those kaon fields which are already contained in the original *ansatz* (2.25) by K_0 it turns out that the overlap

$$\langle K_0 | K \rangle \propto \int_0^\infty r^2 dr W(r) \sin \frac{F}{2} \quad (2.47)$$

indeed is non–zero. Although an overall normalization of the overlap is missing it turns out that (2.47) decreases rapidly when increasing the parameter representing the kaon mass m_K . In ref [47] one order of magnitude of decrease was obtained for (2.47) by changing m_k from 200 MeV to the physical value of 495 MeV. This behavior indicates that for physically relevant parameters the overlap is actually negligible^h. It is worthwhile to mention that at least in principle also the symmetry breaking will induce kaon fields [40]. At present, however, these have not been considered.

Except for the Skyrme parameter e all parameters are determined in the meson sector (2.21). Choosing $e = 4.0$ finally providesⁱ

$$\begin{aligned} E &= 1.744 \text{ GeV}, & \gamma &= 1.374 \text{ GeV}, \\ \alpha^2 &= 6.04 \text{ GeV}^{-1}, & \beta^2 &= 4.53 \text{ GeV}^{-1}, \end{aligned} \quad (2.48)$$

^hA more elaborate metric in (2.47) might alter this conclusion [66].

ⁱIn the main part of ref [47] a simplified version of \mathcal{L}_{SB} was employed to compute β^2 , which yielded a somewhat larger value, see however appendix C of that reference.

Table 2.1: The mass differences, which are obtained by exact diagonalization of the collective Hamiltonian (2.36), of the neighboring $\frac{1}{2}^+$ and $\frac{3}{2}^+$ in the pseudo-scalar model for $e=4.0$ are compared to the experimental data. Also the mass differences with respect to the nucleon are listed. The values in parentheses are obtained with a Lagrange multiplier included to guarantee a vanishing overlap (2.47) of the induced kaon components with the would-be zero mode of the hedgehog configuration. In that case the Skyrme parameter has slightly been readjusted to $e=3.9$. All data are in MeV.

Baryons	Model	Expt.	Baryons	Model	Expt.
$\Lambda - N$	154 (163)	177	$\Lambda - N$	154 (163)	177
$\Sigma - \Lambda$	88 (101)	77	$\Sigma - N$	242 (264)	254
$\Xi - \Sigma$	124 (122)	125	$\Xi - N$	366 (388)	379
$\Delta - \Xi$	-88 (-120)	-86	$\Delta - N$	278 (268)	293
$\Sigma^* - \Delta$	132 (138)	153	$\Sigma^* - N$	410 (406)	446
$\Xi^* - \Sigma^*$	134 (139)	145	$\Xi^* - N$	544 (545)	591
$\Omega - \Xi^*$	133 (135)	142	$\Omega - N$	677 (680)	733

while all other parameters in the collective Hamiltonian (2.36) vanish. Although the strange moment of inertia β^2 is dominated by the hedgehog contribution the share due to the induced components (2.45) is about 35%. One might be tempted to enforce a vanishing matrix element (2.47) by including an appropriate Lagrange multiplier. This reduces β^2 somewhat to 3.52GeV^{-1} . Although such a treatment would be mandatory if one wanted to construct $W(r)$ in the flavor symmetric case, there is no apparent need to do so when this symmetry is broken because then the homogeneous part of the differential equation does not possess a regular solution. In other words, the constraint represents the driving term in the equation of motion only when flavor symmetry breaking is small. We will therefore stick to the value in eq (2.48). In any event, the appearance of the induced components are an indication that the collective treatment is merely an approximation to the physical case when flavor symmetry is broken. This is especially reflected by the fact that the radial function $W(r)$ decays like $\exp(-m_K r)$ in contrast to the hedgehog configuration rotated into strange direction according to (2.28). The latter behaves like $\exp(-m_\pi r)$ at large r . Furthermore the inclusion of induced kaon fields is mandatory to obtain the proper divergence of the axial current. This proof is indicated in appendix C.

This value $e = 4.0$ has been chosen since it leads to a reasonable description of the baryon mass differences as can be seen from table 2.1. A major reason for this result is the fact that γ is significantly enlarged by including the effects associated with $f_K \neq f_\pi$. These effects were omitted in the original studies [58, 67, 68, 62] yielding far too low mass splittings between baryons of different strangeness for physically motivated parameters of the effective Lagrangian^j. It is also apparent from table 2.1 that the inclusion of a constraint to ensure a vanishing overlap (2.47) can be compensated by a small variation of the Skyrme parameter, e . This indicates that double counting effects play only a subleading role. It is interesting to remark that the mass differences for the $\frac{1}{2}^+$ baryons deviate strongly from the prediction in leading order of the flavor symmetry breaking. This can easily be observed from the ratios

$$(M_\Lambda - M_N) : (M_\Sigma - M_\Lambda) : (M_\Xi - M_\Sigma) = 1 : 0.52 : 0.85 \quad (2.49)$$

^jMany of these authors used to consider f_π as a free parameter fitted to the absolute values of the baryon masses. Without the β' term this yielded f_π as low as 25MeV [67].

which are in much better agreement with the experimental data (1:0.43:0.69) than the leading order result (1:1:0.5) of eq (2.39). Obviously the higher order contributions are important. This also indicates that the baryon wave-functions contain sizable admixtures of higher dimensional $SU(3)$ representations, *cf.* eq (2.40). Nevertheless the deviation from the Gell–Mann–Okubo relations (2.37) is only moderate, in particular the equal spacing among the $\frac{3}{2}^+$ baryons is well reproduced.

The value for the Skyrme parameter $e = 4.0$ obtained from this best fit to the baryon mass differences is then employed to evaluate static properties of baryons within this model. In order to do so one first constructs the Noether currents associated with the symmetry transformation (2.2). A convenient method is to extend these global symmetries to local ones by introducing external gauge fields (*e.g.* the gauge fields of the electroweak interactions) into the action (2.24). The Noether currents are then read off as the expressions which couple linearly to these gauge fields. This procedure is especially appropriate for the Wess–Zumino term (2.23) because this non–local term can only be made gauge invariant by a trial and error type procedure [50, 52]. The final form of the nonet ($a = 0, \dots, 8$) vector (V_μ^a) and axial–vector (A_μ^a) currents reads [38] (for $N_C = 3$)

$$\begin{aligned} V_\mu^a(A_\mu^a) &= -\frac{i}{2}f_\pi^2 \text{tr} \{Q^a (\alpha_\mu \mp \beta_\mu)\} - \frac{i}{8e^2} \text{tr} \{Q^a ([\alpha_\nu, [\alpha_\mu, \alpha_\nu]] \mp [\beta_\nu, [\beta_\mu, \beta_\nu]])\} \\ &\quad - \frac{1}{16\pi^2} \epsilon^{\mu\nu\rho\sigma} \text{tr} \{Q^a (\alpha_\nu \alpha_\rho \alpha_\sigma \pm \beta_\nu \beta_\rho \beta_\sigma)\} \\ &\quad - i\beta' \text{tr} \left\{ Q^a \left(\{U\mathcal{M} + \mathcal{M}U^\dagger, \alpha_\mu\} \mp \{\mathcal{M}U + U^\dagger\mathcal{M}, \beta_\mu\} \right) \right\}, \end{aligned} \quad (2.50)$$

where $Q^a = (\frac{1}{3}, \frac{\lambda^1}{2}, \dots, \frac{\lambda^8}{2})$ denote the Hermitian nonet generators. The combination

$$Q^{\text{e.m.}} = \text{diag} \left(\frac{2}{3}, -\frac{1}{3}, -\frac{1}{3} \right) = Q^3 + \frac{1}{\sqrt{3}}Q^8 \quad (2.51)$$

is of special interest because it enters the computation of the electromagnetic properties. The associated form factors of the $\frac{1}{2}^+$ baryons (B) are defined by

$$\langle B(\mathbf{p}') | V_\mu^{\text{e.m.}} | B(\mathbf{p}) \rangle = \bar{u}(\mathbf{p}') \left[\gamma_\mu F_1^B(q^2) + \frac{\sigma_{\mu\nu} q^\nu}{2M_B} F_2^B(q^2) \right] u(\mathbf{p}), \quad q_\mu = p_\mu - p'_\mu. \quad (2.52)$$

Frequently it is convenient to introduce “electric” and “magnetic” form factors

$$G_E^B(q^2) = F_1^B(q^2) - \frac{q^2}{4M_B^2} F_2^B(q^2), \quad G_M^B(q^2) = F_1^B(q^2) + F_2^B(q^2). \quad (2.53)$$

Further relevant form factors are the matrix elements of the diagonal vector currents of the individual quarks in the proton state

$$\langle P(\mathbf{p}') | \bar{q}_i \gamma_\mu q_i | P(\mathbf{p}) \rangle = \bar{u}(\mathbf{p}') \left[\gamma_\mu F_i(q^2) + \frac{\sigma_{\mu\nu} q^\nu}{2M_p} \tilde{F}_i(q^2) \right] u(\mathbf{p}), \quad i = u, d, s, \quad (2.54)$$

as well the analogous expressions for the axial–vector currents

$$\langle P(\mathbf{p}') | \bar{q}_i \gamma_\mu \gamma_5 q_i | P(\mathbf{p}) \rangle = \bar{u}(\mathbf{p}') \left[\gamma_\mu H_i(q^2) + \frac{q_\mu}{2M_p} \tilde{H}_i(q^2) \right] \gamma_5 u(\mathbf{p}). \quad (2.55)$$

The list of relevant form factors is completed by the matrix elements of strangeness changing components of the currents (2.50) between different baryon states. These form factors are relevant for the description of the semi-leptonic decays of the hyperons. Their generic form is

$$\begin{aligned}\langle B'(\mathbf{p}')|V_\mu^\alpha|B(\mathbf{p})\rangle &= \bar{u}(\mathbf{p}') \left[\gamma_\mu g_V(q^2) + \dots \right] u(\mathbf{p}) , \\ \langle B'(\mathbf{p}')|A_\mu^\alpha|B(\mathbf{p})\rangle &= \bar{u}(\mathbf{p}') \left[\gamma_\mu \gamma_5 g_A(q^2) + \dots \right] u(\mathbf{p}) .\end{aligned}\quad (2.56)$$

Here the ellipses represent contributions involving the momentum transfer q_μ , which need not be considered in the present context. To be precise, separate $g_V(q^2)$ and $g_A(q^2)$ must be introduced for each baryon pair (B', B) and flavor index $\alpha = 4, \dots, 7$.

Having collected these definitions of the form factors it is straightforward (although tedious) to compute the corresponding predictions of the $SU(3)$ Skyrme model. In the first step the parametrization (2.45) is substituted into the defining equation of the currents (2.50). This yields for the spatial components of the vector current^k

$$\begin{aligned}V_i^a &= V_1(r)\epsilon_{ijk}x_jD_{ak} + \frac{\sqrt{3}}{2}B(r)\epsilon_{ijk}\Omega_jx_kD_{a8} + V_2(r)\epsilon_{ijk}x_jd_{d\alpha\beta}D_{a\alpha}\Omega_\beta \\ &+ V_3(r)\epsilon_{ijk}x_jD_{88}D_{ak} + V_4(r)\epsilon_{ijk}x_jd_{d\alpha\beta}D_{8\alpha}D_{a\beta} + \dots ,\end{aligned}\quad (2.57)$$

where

$$B(r) = \frac{-1}{2\pi^2}F'\frac{\sin^2 F}{r^2}\quad (2.58)$$

is the baryon number density (2.9). The explicit form of the radial functions $V_1(r), \dots, V_4(r)$ is given in appendix B of ref [38]. The ellipsis in eq (2.57) represent terms, which vanish when sandwiched between baryon states. According to the quantization prescription (2.34) the angular velocities Ω_a are substituted by the right generators R_a of $SU(3)$. Taking the Fourier transform of the resulting matrix elements allows one to identify the magnetic form factor in the Breit frame [69, 70]

$$\begin{aligned}G_M^B(\mathbf{q}^2) &= -8\pi M_B \int_0^\infty r^2 dr \frac{r}{|\mathbf{q}|} j_1(r|\mathbf{q}|) \left\{ V_1(r)\langle D_{e3} \rangle_B - \frac{1}{2\alpha^2}B(r)\langle D_{e8}R_8 \rangle_B \right. \\ &\quad \left. - \frac{1}{\beta^2}V_2(r)\langle d_{3\alpha\beta}D_{e\alpha}R_\beta \rangle_B + V_3(r)\langle D_{88}D_{e3} \rangle_B + V_4(r)\langle d_{3\alpha\beta}D_{e\alpha}D_{8\beta} \rangle_B \right\} .\end{aligned}\quad (2.59)$$

Here the flavor index e refers to the ‘‘electromagnetic’’ direction (2.51). The magnetic moment corresponds to the magnetic form factor at zero momentum transfer $\mu_B = G_M^B(0)$. Similarly the electric form factor is given by Fourier transforming the time component of the electromagnetic current

$$G_E^B = 4\pi \int_0^\infty r^2 dr j_0(r|\mathbf{q}|) \left\{ \frac{\sqrt{3}}{2}B(r)\langle D_{e3} \rangle_B + \frac{1}{\alpha^2}V_7(r)\langle D_{ei}R_i \rangle_B + \frac{1}{\beta^2}V_8(r)\langle D_{e\alpha}R_\alpha \rangle_B \right\} .\quad (2.60)$$

The two new radial functions $V_7(r)$ and $V_8(r)$ are listed in appendix B of ref [38] as well. Integrating V_7 and V_8 yields the moments of inertia, α^2 and β^2 , respectively. Hence the electric charges are properly normalized. It should be remarked that the baryon matrix elements in

^kThe conventions are $i, j, k = 1, 2, 3$ and $\alpha, \beta = 4, \dots, 7$.

Table 2.2: The electromagnetic properties of the baryons compared to the experimental data. The predictions of the Skyrme model are taken from ref [38].

B	$\mu_B(\text{n.m.})$		$r_M^2(\text{fm}^2)$		$r_E^2(\text{fm}^2)$	
	$e = 4.0$	Expt.	$e = 4.0$	Expt.	$e = 4.0$	Expt.
p	2.03	2.79	0.43	0.74	0.59	0.74
n	-1.58	-1.91	0.46	0.77	-0.22	-0.12
Λ	-0.71	-0.61	0.36	—	-0.08	—
Σ^+	1.99	2.42	0.45	—	0.59	—
Σ^0	0.60	—	0.36	—	-0.02	—
Σ^-	-0.79	-1.16	0.58	—	-0.63	—
Ξ^0	-1.55	-1.25	0.38	—	-0.15	—
Ξ^-	-0.64	-0.69	0.43	—	-0.49	—
$\Sigma^0 \rightarrow \Lambda$	-1.39	-1.61	0.48	—	—	—

the space of the collective coordinates are computed using the exact eigenstates (A.8) of (2.42) and adopting the representations (A.7) for the $SU(3)$ generators. The results for the magnetic moments and the radii

$$r_M^2 = -\frac{6}{\mu_B} \left. \frac{dG_M^B(\mathbf{q}^2)}{d\mathbf{q}^2} \right|_{\mathbf{q}^2=0}, \quad r_E^2 = -6 \left. \frac{dG_E^B(\mathbf{q}^2)}{d\mathbf{q}^2} \right|_{\mathbf{q}^2=0}. \quad (2.61)$$

are shown in table 2.2. As in the two flavor model [10] the isovector part of the magnetic moments is underestimated while the isoscalar part is reasonably well reproduced. Despite the fact that the flavor symmetry breaking is large for the baryon wave-functions, the predicted magnetic moments do not strongly deviate from the $SU(3)$ relations [71]

$$\begin{aligned} \mu_{\Sigma^+} &= \mu_p, \quad \mu_{\Sigma^0} = \frac{1}{2}(\mu_{\Sigma^+} + \mu_{\Sigma^-}), \quad \mu_{\Sigma^-} = \mu_{\Xi^-}, \\ 2\mu_{\Lambda} &= -(\mu_{\Sigma^+} + \mu_{\Sigma^-}) = -2\mu_{\Sigma^0} = \mu_n = \mu_{\Xi^0} = \frac{2}{\sqrt{3}}\mu_{\Sigma^0\Lambda}. \end{aligned} \quad (2.62)$$

Later it will become clear that an even more elaborate treatment of the flavor symmetry breaking is necessary in order to accommodate for the experimental breaking of the U -spin symmetry which *e.g.* causes the approximate identity $\mu_{\Sigma^+} \approx \mu_p$. The moderate difference between the various magnetic radii r_M^2 is a further hint that symmetry breaking effects are mitigated. The comparison with the available empirical data for the radii shows that the predictions turn out too small in magnitude (except of the neutron electric radius). This is a strong indication that essential ingredients are still missing in the model. In chapter 4 it will be explained that the effects, which are associated with vector meson dominance (VMD), will account for this deficiency. Nevertheless the overall picture gained for the electromagnetic properties of the $\frac{1}{2}^+$ and $\frac{3}{2}^+$ can at least be characterized as satisfactory, especially in view of the fact that the only free parameter of the model has been fixed beforehand. As a side remark it should be mentioned that the direct contribution of the induced fields (2.45) to the magnetic moments is as small as 5–10%. For example, when supplementing the model by a Lagrange multiplier such that the overlap (2.47) vanishes, the proton and neutron magnetic moments are changed to 1.88 and -1.49, respectively. The results displayed in table 2.2 might

be regained by a minor change of the Skyrme parameter, e . The relevance of these fields appears merely to be of formal nature.

From here it is straightforward to compute the strange vector form factors $F_s(q^2)$ and $\tilde{F}_s(q^2)$, which are defined in eq (2.54). Up to now no precise measurement of the associated form factors has been performed. As already indicated in section 1.3, these form factors are currently under intensive experimental investigation, *cf.* refs [34, 35]. These form factors have been estimated in various models. They range from vector–meson–pole fits [36] of dispersion relations [37] through vector meson dominance approaches [38] and kaon–loop calculations with [34] and without [72] vector meson dominance contributions to soliton model calculations [38, 40, 41]. The numerical results for the strange magnetic moment $\mu_S = \tilde{F}_s(0) \approx -0.31 \pm 0.09 \dots 0.25$ are quite diverse. The predictions for the strange charge radius $r_S^2 = -6dF_s(q^2)/dq^2|_{q=0}$ are almost equally scattered $r_S^2 \approx -0.20 \dots 0.14\text{fm}^2$. See table 4.3 for a comprehensive list of predictions on μ_S and r_S^2 . In order to evaluate these objects in the three flavor Skyrme model one requires the matrix elements of the “strange” combination

$$Q^s = \frac{1}{3}\mathbf{1} - \frac{1}{\sqrt{3}}\lambda_8 = Q^0 - \frac{2}{\sqrt{3}}Q^8 \quad (2.63)$$

between proton states rather than the electromagnetic ones (2.51). Using the above established value $e = 4.0$ yields

$$\mu_S = -0.13 , \quad r_S^2 = -0.10\text{fm}^2 . \quad (2.64)$$

As usual, magnetic moments are in units of nuclear magnetons. It should be stressed that these results are obtained within the Yabu–Ando approach, *i.e.* the proton wave–function contains sizable admixtures of higher dimensional representations. If a pure octet wave–function were employed to compute the matrix elements of the collective operators the strange magnetic moment would have been $\mu_S = -0.33$. The proper inclusion of symmetry breaking into the nucleon wave–function apparently reduces the effect of the strange degrees of freedom in the nucleon. This is also intuitively clear, since for a flavor symmetric wave–function virtual $\bar{s}s$ pairs are as probable as virtual $\bar{u}u$ or $\bar{d}d$ pairs. However, as the strange quarks within the nucleon become more massive (effect of symmetry breaking) their excitation is less likely.

Before discussing the predictions of the three flavor Skyrme model on the axial properties of the $\frac{1}{2}^+$ baryons it is illuminating to discuss a few general aspects of the so–called proton spin puzzle. The purpose of these studies is to disentangle the three form factors $H_i(q^2 = 0)$ of the proton matrix element (2.55). Assuming isospin invariance the analysis of the neutron–beta decay provides the linear combination

$$H_u(0) - H_d(0) = g_A = 1.257 . \quad (2.65)$$

More recently extensive measurements have been carried out to gain data for the combination

$$\frac{1}{9}H_u(0) \left(C_{ns}(q^2) + C_s(q^2) \right) - \frac{1}{18} \left(H_d(0) + H_s(0) \right) \left(C_{ns}(q^2) + 2C_s(q^2) \right) = \Gamma_1^p(q^2) . \quad (2.66)$$

The momentum dependent coefficients C_s , C_{ns} are computed in perturbative QCD and may *e.g.* be taken from ref [73]. The combined analysis of the EMC [21], SLAC [74] and SMC [75] data may be summarized as $\Gamma_1^p(q^2 = (10.7\text{GeV})^2) = 0.129 \pm 0.010$. Defining R as the linear combination, which corresponds to the eighth component of the axial–vector current matrix element

$$H_u(0) + H_d(0) - 2H_s(0) = R , \quad (2.67)$$

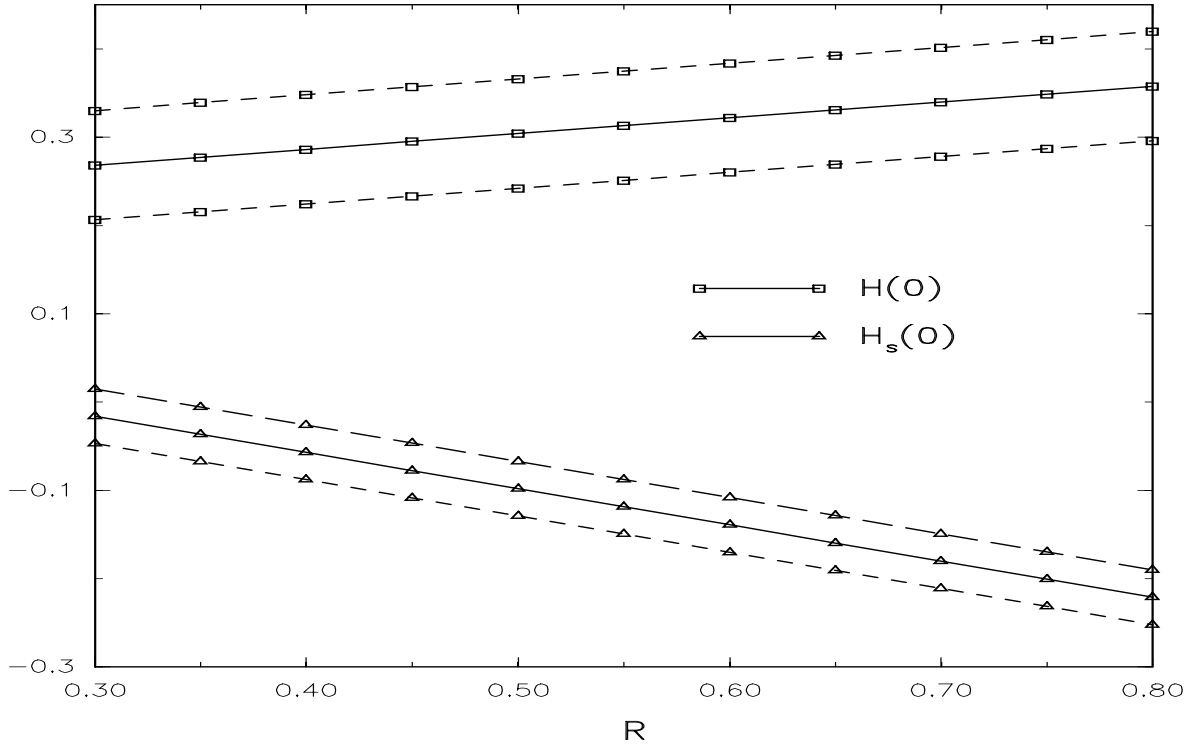


Figure 2.2: The dependence of the matrix elements of the singlet axial current $H(0)$ and the strange contribution $H_s(0)$ on flavor symmetry breaking. The flavor symmetric case corresponds to $R=0.575\pm 0.016$. The dashed lines indicate errors caused by the uncertainty of Γ_1^P . See also refs [25] and [29].

flavor symmetry may provide the final ingredient to extract all three $H_i(0)$. Taking this symmetry for granted allows one to relate R to the data obtained from the semi-leptonic hyperon decays such as $\Lambda \rightarrow pe^-\bar{\nu}_e$ yielding $R = 0.575 \pm 0.016$ [23, 76, 27, 77]. For the time being let us, however, treat R as an independent parameter. The dependences of $H_s(0)$ as well as of the singlet combination

$$H(q^2) = H_u(q^2) + H_d(q^2) + H_s(q^2) \quad (2.68)$$

at $q^2 = 0$ on R are shown in figure 2.2. One observes that $H(0) \approx 0.3 \pm 0.1$ within a wide range of R . The issue of $H(0)$ being considerably smaller than unity has become known as the proton spin puzzle (or crisis) because in a quark parton model interpretation this quantity is identical to twice the quarks' contribution to the proton spin. The puzzle is caused by the fact that $H(0)$ is unity in a naïve quark model. On the other hand the strange quark contribution varies strongly with symmetry breaking. For the flavor symmetric value of R one finds $H_s(0) \approx -0.11 \pm 0.05$. Originally this sizable value caused an additional point of confusion because it implies the unexpectedly large ratio $|H_s(0)/H_d(0)| \approx 0.3$. However, as the role of symmetry breaking became clearer it was soon recognized that a smaller $H_s(0)$ may well be in agreement with the experimental data.

Simultaneously with the publication of the first data on Γ_1^P [21], the three flavor Skyrme model was observed to be an excellent candidate to explain the smallness of $H(0)$ [20]. From eq (2.50) the axial singlet current ($Q^0 = 1/3$) is found to be

$$A_\mu^0 = -\frac{i}{3} f_\pi^2 \text{tr} \left(\partial_\mu U U^\dagger \right) - 4i\beta' \partial_\mu \text{tr} \left(\mathcal{M} \left[U - U^\dagger \right] \right) . \quad (2.69)$$

Separating the singlet piece of the nonet matrix U by introducing the unitary-unimodular

matrix $\tilde{U} = e^{-i\chi U}$ leads to

$$A_\mu^0 = f_\pi^2 \partial_\mu \chi - 4i\beta' \partial_\mu \text{tr} \left(\mathcal{M} \left[U - U^\dagger \right] \right) \quad (2.70)$$

which obviously is a total derivative [78]. Hence only the induced form factor $\tilde{H}(q^2) = \tilde{H}_u(q^2) + \tilde{H}_d(q^2) + \tilde{H}_s(q^2)$ in eq (2.55) acquires a non-zero value. This implies that in the Skyrme model which contains only pseudo-scalar fields

$$H(q^2) \equiv 0, \quad (2.71)$$

even in the presence of flavor symmetry breaking terms. This is in contrast to the original estimates [20] of the effect of symmetry breaking on $H(q^2)$. Later it will be argued that short range effects are responsible for a non-vanishing (although small) value for $H(0)$. There have been several attempts to obtain a non-vanishing $H(0)$ in the pseudo-scalar Skyrme model. Adding the symmetric fourth order term $\text{tr}(\alpha_\mu \alpha^\mu \alpha_\nu \alpha^\nu)$ gives a contribution to axial the singlet current [79]

$$\delta A_\mu^0 = ic \text{tr} (\alpha_\nu \alpha_\mu \alpha^\nu), \quad (2.72)$$

where c is an arbitrary constant. This expression contains terms which are quadratic in the angular velocities Ω_a causing ordering ambiguities when applying the quantization prescription (2.34). Although originally a non-vanishing contribution to $H(0)$ was obtained [79] it has recently been shown that this result was almost completely due to those ordering ambiguities. In the two flavor case one can easily demand the proper behavior under the particle conjugation transformation. This requires one to choose an ordering such that $H(0)$, associated with (2.72), vanishes. In the three flavor model, however, the proper ordering of the collective coordinates might give $H(0) \neq 0$ [80]. From a physical point of view it is, nevertheless, more appealing to find already a non-vanishing $H(0)$ in the two flavor version of the model under consideration. Another way to achieve $H(0) \neq 0$ is to augment the Lagrangian by

$$\delta \mathcal{L} = \tilde{c} \epsilon_{\mu\nu\rho\sigma} \partial^\mu (\ln \det U) B^\nu \partial^\rho B^\sigma, \quad (2.73)$$

which is motivated by the local approximation to vector mesons [81] and indeed leads to a non-trivial contribution to the axial singlet current [82]

$$\delta A_\mu^0 = 3\tilde{c} \epsilon_{\mu\nu\rho\sigma} B^\nu \partial^\rho B^\sigma. \quad (2.74)$$

However, as (2.73) does not constitute a single trace, this type of singlet current will suffer additional suppression from the quark line (or OZI [83]) rule. Therefore the explicit consideration of vector meson seems to be more appropriate (see chapter 4). Aiming towards completeness (without possibly gaining it) on this subject, it should be mentioned that there are other studies of the axial singlet matrix elements in related models. These are *e.g.* a linear chiral model with quark and gluon confinement [84] or a hybrid chiral bag model [85]. It is interesting to note that in this bag model the axial singlet matrix element is quite sensitive to the bag radius^l, R , in contrast to g_A [87]. The authors of ref [85] have employed this sensitivity to constrain the radius $R \lesssim 0.5\text{fm}$ from the data on the axial singlet matrix element.

Due to the vanishing singlet matrix element in the Skyrme model of pseudo-scalars it is more appropriate to discuss the general behavior of matrix elements of the axial current under

^lSee ref [86] for a review on bag models and the *Cheshire Cat* principle.

symmetry breaking rather than the detailed results for these quantities. The leading order term (in $1/N_C$) of the spatial components of the axial current is straightforwardly obtained to be

$$\int d^3r A_i^a = \mathcal{C} D_{ai}(A) . \quad (2.75)$$

The constant \mathcal{C} denotes an integral over the chiral angle. However, since its actual value will be of no importance for the following discussions we refer the interested reader to refs [88, 38] for the explicit expression. The semi-leptonic decays of the hyperons^m are described by the ratios g_A/g_V defined in eq (2.56). The numerator can easily be obtained from (2.75)

$$g_A^a(B', B) = \mathcal{C} \langle B' | D_{a3} | B \rangle . \quad (2.76)$$

The flavor index a has to be chosen according to whether strangeness conserving ($a = 1, 2, 3, 8$) or strangeness changing ($a = 4, \dots, 7$) processes are considered. Although for the current studies the actual value of \mathcal{C} is not important, it should be admitted that the corresponding result for the axial charge of the nucleon $g_A = g_A^{1+i2}(n, p)$, as measured in neutron-beta decay, is predicted too low in many soliton modelsⁿ. This problem is already encountered in the two flavor model and gets worse in $SU(3)$ as the Clebsch-Gordon coefficient associated with $D_{1+i2} \mathbf{3}$ changes by a factor of 7/10. As symmetry breaking is included the $SU(3)$ prediction for g_A becomes larger [24]

$$g_A(SU(3)) = \frac{7}{10} [1 + 0.0514\gamma\beta^2 + \dots] g_A(SU(2)) . \quad (2.77)$$

Actually the exact treatment shows that with increasing symmetry breaking the two flavor result is approached, although only slowly. Taking everything together, including subleading terms in (2.76), finally gives $g_A = 0.98$ for $e = 4.0$ [38] which is about 4/5 of the experimental value $g_A(\text{expt.}) = 1.26$.

Returning to the more general studies it should first be remarked that flavor symmetry relates the matrix elements between various baryons. Most conveniently they are expressed in terms of two unknown constants F and D . One has to use models to determine these constants. In the flavor symmetric Skyrme model one finds [71] $D/F = 9/5$ and $D + F = 7\mathcal{C}/15 = g_A$. In table 2.3 the flavor symmetric dependencies of the matrix elements on F and D are displayed. In addition one finds $R = 3F - D$. As one departs from the flavor symmetric case the baryon wave-functions acquire admixtures from higher dimensional $SU(3)$ representations making the notion of F and D obsolete.

In addition to the expansion (2.40) one *e.g.* finds for the Λ hyperon

$$|\Lambda\rangle = |\Lambda, \mathbf{8}\rangle + \frac{3}{50}\gamma\beta^2|\Lambda, \mathbf{27}\rangle + \dots . \quad (2.78)$$

Such expansions may be used to evaluate the behavior of the matrix elements entering the Cabibbo scheme [91] for the semi-leptonic hyperon decays. Noting that the D -functions mix the $SU(3)$ representations, a typical example is

$$\langle p \uparrow | D_{K-3} | \Lambda \uparrow \rangle = \frac{2}{5\sqrt{3}} - \frac{7\sqrt{3}}{1125}\gamma\beta^2 + \dots , \quad D_{K-3} = \frac{1}{\sqrt{2}} (D_{43} - iD_{53}) . \quad (2.79)$$

^mIn ref [89] non-leptonic decays have been studied using flavor symmetric wave-functions.

ⁿNote, however, that in the chiral quark model g_A is somewhat overestimated [90].

Table 2.3: The matrix elements of the axial–vector current 2.76 between different baryon states in the flavor symmetric limit. Displayed are both the strangeness conserving (a) and strangeness changing (b) processes. The first column gives the relevant flavor component of the axial current.

A^{π^-}	$n \rightarrow p$ $F + D$	$\Sigma^- \rightarrow \Lambda$ $\frac{2}{\sqrt{6}}D$	(a) $\Sigma^- \rightarrow \Sigma^0$ $\sqrt{2}F$	$\Xi^- \rightarrow \Xi^0$ $D - F$
A^{K^-}	$\Lambda \rightarrow p$ $\frac{1}{\sqrt{6}}(3F + D)$	$\Sigma^- \rightarrow n$ $D - F$	(b) $\Xi^- \rightarrow \Lambda$ $\frac{1}{\sqrt{6}}(3F - D)$	$\Xi^- \rightarrow \Sigma^0$ $\frac{1}{\sqrt{2}}(F + D)$

Of course, this expansion just provides a first approximation to the symmetry breaking dependence of the Cabibbo matrix elements. Using the exact treatment initiated by Yabu and Ando [62] this dependence can be computed numerically as shown in figure 2.3 for the processes of interest. Those results are normalized to the $SU(3)$ symmetric values (2.3) to illuminate that these matrix elements vary in a completely different way with symmetry breaking. In this figure also the variation of the strange quarks' contribution to the nucleon matrix element of the axial singlet current $H_3(0) = \langle N | \bar{s} \gamma_3 \gamma_5 s | N \rangle$ is displayed. Obviously $H_3(0)$ decreases very rapidly with increasing symmetry breaking. On the contrary the Cabibbo matrix elements exhibit only a moderate dependence on $\gamma\beta^2$. It is this different behavior of the matrix elements that makes the application of flavor symmetry to the analyses of the EMC–SLAC–SMC experiments suspicious [92]. Stated otherwise, the strange quark contribution to the proton spin may be decreased significantly as a consequence of symmetry breaking without contradicting the successful Cabibbo scheme for the semi–leptonic decays of the hyperons.

As the ratio g_A/g_V enters the description of the hyperon decays one may worry whether the dependence of g_V on the symmetry breaking changes this conclusion. The dominating contribution is given by the matrix elements of the flavor generators

$$g_V^a(B', B) = \langle B' | L_a | B \rangle . \quad (2.80)$$

From a general point of view it is important to remark that these matrix elements are protected by the Ademollo–Gatto theorem [93]. This theorem states that the leading term in the difference of $g_V^a(B', B)$ from its symmetric value must be at least quadratic in symmetry breaking. In the framework of the Skyrme model this can easily be understood because the matrix elements of the generators L_a vanish between different $SU(3)$ representations. Using the Yabu–Ando scheme this has numerically been confirmed [88] resulting in, at most, 10% deviation from the symmetric values, even for large symmetry breaking, *e.g.* $\gamma\beta^2 \approx 7$.

A reduction of the strangeness in the nucleon is also observed for the scalar strange content fraction of the proton

$$X_s = \frac{\langle p | \bar{s}s | p \rangle - \langle 0 | \bar{s}s | 0 \rangle}{\langle p | \bar{u}u + \bar{d}d + \bar{s}s | p \rangle - \langle 0 | \bar{u}u + \bar{d}d + \bar{s}s | 0 \rangle} . \quad (2.81)$$

Here the state $|0\rangle$ refers to the soliton being absent. As will become apparent from NJL–model studies (*cf.* chapter 6) X_S is related to

$$X_s = \frac{1}{3} \langle p | 1 - D_{88} | p \rangle \approx \frac{7}{30} - \frac{43}{2250} \gamma\beta^2 + \dots . \quad (2.82)$$

$$\langle B' | A^a_3 | B \rangle$$

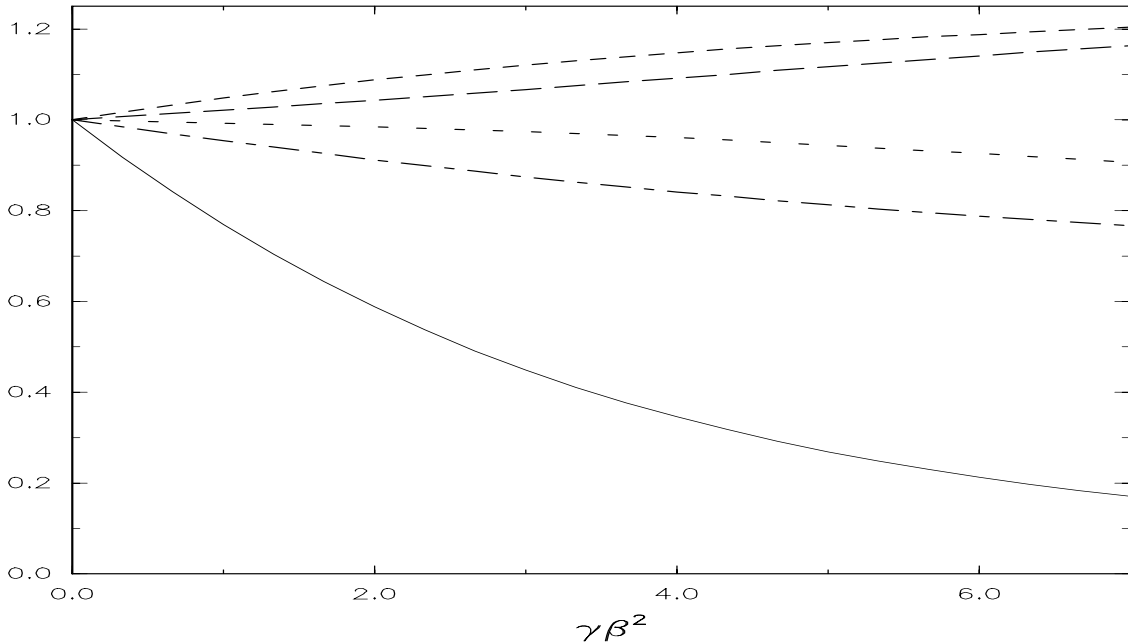


Figure 2.3: The variation of the matrix elements describing the semi-leptonic hyperon decays with the effective symmetry breaking parameter $\gamma\beta^2$. Full line: $\langle p|\bar{s}\gamma_3\gamma_5s|p\rangle$; dashed dotted line: $\langle p|\bar{u}\gamma_3\gamma_5s|\Lambda\rangle$; dotted line: $\langle n|\bar{u}\gamma_3\gamma_5s|\Sigma^-\rangle$; long dashed line: $\langle\Lambda|\bar{u}\gamma_3\gamma_5s|\Xi^-\rangle$; dashed line: $\langle p|\bar{u}\gamma_3\gamma_5d|n\rangle$; These matrix elements, which are taken from refs [78] and [88], are normalized to the flavor symmetric values.

In this case, however, the deviation from the flavor symmetric result [94] ($X_s = 7/30$) is considerably mitigated [95] as compared to the variation of H_s . The symmetry breaking has to be as large as $\gamma\beta^2 \approx 4.5$ to obtain a reduction of the order of 50%. In the case of H_s this was already achieved for $\gamma\beta^2 \approx 2.5$. In any event, the additional quark-antiquark excitations in the nucleon, which are parametrized by the admixtures of higher dimensional $SU(3)$ representations (2.40), apparently tend to cancel the virtual strange quarks of the octet nucleon.

To summarize this section on baryon spectroscopy and form factors it should be mentioned that the effects of higher orders in the flavor symmetry breaking are important. Furthermore the soliton approach provides a unique framework to demonstrate that flavor symmetry breaking may effect various physical quantities in a completely different manner. Also the conjecture [96] is confirmed that some operators see a fairly large amount of strangeness in the nucleon while others do not. In this section we have concentrated on general aspects of flavor symmetry breaking of baryon properties in the soliton approach rather than gathering numerical results of the model. The reason is that the Skyrme model, which contains only pseudo-scalar degrees of freedom, lacks important short range effects. Therefore more reliable predictions are expected in extensions of the model containing meson fields whose profile functions have their major support at small distances, say $r \leq 0.5fm$. An excellent candidate is the vector meson model to be described in chapter 4.

In ref [97] the use of an alternative Skyrme term

$$\mathcal{L}_{Sk}^{\text{alt.}} = \frac{1}{16e^2} \left[\text{tr}(\alpha_\mu\alpha_\nu) \text{tr}(\alpha^\mu\alpha^\nu) - (\text{tr}(\alpha_\mu\alpha^\mu))^2 \right] \quad (2.83)$$

has been considered together with the meson configuration (2.28). Although the resulting Lagrange function is identical to (2.7) in the two flavor reduction its contribution to the moment of inertia β^2 is four times as large. According to eqs (2.39) and (2.40) the effect of symmetry breaking is increased yielding a slightly improved pattern for the baryon spectrum. However, the predictions for the static properties of the baryons exhibit almost no variation as compared to the ordinary Skyrme term. The effects of the induced components (2.46) have not been investigated in the context of (2.83).

2.5 Further Developments

In this section studies will briefly be discussed, which do not directly effect static properties of the strange baryons but are special beyond the two flavor model and should be mentioned to achieve a higher level of completeness.

By adding a term to the Lagrangian which represents the $U_A(1)$ anomaly of QCD [98]

$$\mathcal{L}_A = \frac{\kappa}{48} \left[\ln \left(\det U - \det U^\dagger \right) \right]^2 \quad (2.84)$$

and extending the symmetry breaking matrix (2.16)

$$\mathcal{M} \rightarrow \mathcal{M} + i \frac{\lambda_\Theta}{4f_\pi^2}, \quad (2.85)$$

it is possible to imitate the effects of the QCD Θ angle [99] since a non-zero Θ is equivalent to \mathcal{M} having a non-vanishing phase [100]. The constant κ can be determined from the mass of the η' meson, *cf.* section 4.4. Substituting the experimental values one obtains [101] $\lambda_\Theta = 9 \times 10^{-3} \Theta \text{GeV}^2$. This extended Lagrangian contains a strong CP violating term

$$\delta\mathcal{L}_{CP} \approx \frac{\lambda_\Theta}{\sqrt{3}} f_\pi (1 - \cos F) (\phi^8 + \sqrt{2}\phi_0) \quad (2.86)$$

where ϕ_8 and ϕ_0 denote the flavor octet and singlet components (2.12) of the η -fields, respectively. Including the contribution of $\delta\mathcal{L}_{CP}$ to the Euler Lagrange equations causes non-trivial profiles for ϕ_8 and ϕ_0 . As a consequence the expression for the neutron electric dipole moment

$$D_n = \langle n | \int d^3r r J_0^{\text{e.m.}} | n \rangle, \quad (2.87)$$

which is linear in these η fields, allows one to relate the neutron electric dipole moment to the QCD Θ -angle. In ref [101] the numerical result $D_n = 2 \times 10^{-6} \Theta e \text{cm}$ was obtained which is somewhat smaller than the current algebra result ($3.6 \times 10^{-6} \Theta e \text{cm}$) of ref [102]. Future experiments on the neutron electric dipole moment will provide a means to estimate QCD Θ -angle.

A prominent issue to be discussed within the $SU(3)$ Skyrme model is the question of whether or not the H -dibaryon is bound. Originally the H -dibaryon was considered as a six quark state, which has strangeness -2, in the MIT bag model [103]. It was found to be bound by about 80MeV against a decay into two Λ hyperons. For the Skyrme model calculation a corresponding *ansatz* for a soliton configuration

$$V_H(\mathbf{r}) = e^{i\Psi(r)} + i\mathbf{A} \cdot \hat{\mathbf{r}} \sin\chi(r) + (\mathbf{A} \cdot \hat{\mathbf{r}})^2 e^{-i\Psi(r)/2} \cos\chi(r) e^{i\Psi(r)} \quad (2.88)$$

was proposed by Balachandran *et al.* [104, 105]. Here $\Lambda_1 = \lambda^7$, $\Lambda_2 = -\lambda^5$ and $\Lambda_3 = \lambda^2$ denote the generators of an $SO(3)$ subgroup of $SU(3)$. Minimizing the static energy by variation of the radial functions $\Psi(r)$ and $\chi(r)$ and subsequent canonical quantization yielded a binding energy of about 130MeV [105]. More recently the order N_C^0 corrections to the mass of the H -dibaryon were estimated [106]. These estimates are based on the observation that zero mode channels provide the dominant contribution to the Casimir energy of the soliton [107, 13]

$$E_{\text{Cas}} = -\frac{1}{4} \text{tr} \left[\frac{(H - H_0)^2}{H_0} \right] \leq -\frac{1}{4} \sum_{k,a,\zeta} \omega(k) |\langle \mathbf{k}, a | \zeta \rangle|^2 . \quad (2.89)$$

Here H and H_0 denote the Hamilton operator for the meson fields in the background and absence of the soliton, respectively. $|\mathbf{k}, a\rangle$ is a plane wave state of momentum \mathbf{k} and flavor a , while ζ refers to the zero modes of the soliton. Including these corrections it is found [106] that $E[V_H] \approx 3E_{B=1}$, where $E_{B=1}$ is the hedgehog energy with the associated Casimir energy included. Obviously the quantum corrections, which the configuration V_H suffers, are significantly lower than twice the corrections of the hedgehog. This is intuitively clear from eq (2.89) because the number of zero modes does not depend on the baryon number but rather on the symmetries of the model and *ansätze*. As the $1/N_C$ -rotational corrections are included a slightly bound H -dibaryon is found. However, as (2.89) just represents a bound for the quantum corrections, the authors of ref [106] conjecture that the H -dibaryon is most likely unbound.

In ref [108] further dibaryon configurations have been considered by generalizing the product *ansatz* [109] to flavor $SU(3)$

$$U(\mathbf{r}) = AU_0 \left(x, y, z - \frac{R}{2} \right) CU_0 \left(x, y, z + \frac{R}{2} \right) C^\dagger A . \quad (2.90)$$

Here A and $C = A^\dagger B$ denote constant flavor rotations which are defined such that A and B describe the individual flavor orientations of the single $SU(3)$ Skyrmions (2.25). Furthermore R measures the distance between the two Skyrmions. Substitution of (2.90) into the action gives the typical interaction term [108]

$$V(R; A, B) \xrightarrow{R \rightarrow \infty} 4\pi f_\pi^2 \partial_i \partial_j \left\{ D_{ki}(A) D_{kj} \frac{e^{-m_\pi R}}{R} + \dots \right\} . \quad (2.91)$$

This permits one to extract the potential for the baryon-baryon interaction in certain spin and flavor channels^o since, according to the Wigner-Eckart theorem, $D_{ab} \sim L_a R_b$ when taking matrix elements. In this case bound dibaryon states were found for the channels $N - N(I = 1/2, J = 1)$, $N - \Sigma(I = 1/2, J = 1)$, $N - \Xi(I =, J = 0)$, $\Lambda - \Lambda(I = 0, J = 0)$, $\Sigma - \Sigma(I = 2, J = 2)$ and $\Xi - \Xi(I = 0, J = 1)$. These results are in agreement with the general expectations from boson exchange models. See ref [111] for a review on these models and a compilation of references.

It is also interesting to note that the collective treatment of section 2.3 can be generalized to flavor $SU(N_f)$ [112], with N_f being the number of flavor degrees of freedom. As a generalization of the *ansatz* (2.25) the hedgehog is embedded in the isospin subgroup and collective rotations are parametrized by the $SU(N_f)$ matrix A as in eq (2.28). Here the case of $N_f = 4$ will briefly be discussed. Then, eq (2.29) defines 15 angular velocities Ω_a . Further in analogy

^oThe $SU(3)$ -central potential has also been studied in ref [110].

to the quantization prescription, (2.34), 15 right generators R_a are introduced. The flavor symmetric part of the collective Hamiltonian is similar to the symmetric part in the three flavor case (2.36)

$$H_{\text{sym.}} = E + \frac{1}{2\alpha^2} \sum_{i=1}^3 R_i^2 + \frac{1}{2\beta^2} \left(\sum_{\alpha=4}^7 R_\alpha^2 + \sum_{m=9}^{12} R_m^2 \right). \quad (2.92)$$

The moments of inertia are identical to the three flavor expressions. First class constraints [113] are obtained for all generators associated with those λ matrices of the group $SU(N_f)$ which commute with the static hedgehog configuration

$$R_8 = \frac{N_C B}{2\sqrt{3}}, \quad R_{13} = R_{14} = 0, \quad R_{15} = \frac{N_C B}{2\sqrt{6}}. \quad (2.93)$$

The first one, which again requires half-integer spin for the allowed eigenstates, is the same as in $SU(3)$, *cf.* eq (2.34). Also the last one stems from the Wess–Zumino term (2.23). These constraints uniquely select (for $N_C = 3$ and $B = 1$) the ground state representations of $SU(4)$

$$\mathbf{20}, \quad J = \frac{1}{2} \quad \text{and} \quad \mathbf{20}', \quad J = \frac{3}{2}. \quad (2.94)$$

A diagrammatic representation of these multiplets is *e.g.* given in figure 30.2 of ref [33]. In the same way the isospin multiplets are subsets of the $SU(3)$ multiplets in figure 1.1, the $SU(3)$ multiplets are subsets of the $SU(4)$ multiplets (2.94). The energy difference between the lowest lying states in these multiplets (nucleon and Δ) is found to be independent of N_f : $M_\Delta - M_N = 3/2\alpha^2$. Adding symmetry breaking terms to account for different meson masses $m_D = 1.9\text{GeV}$ and decay constants $f_D \approx 1.7f_\pi$ shows that the relevant symmetry breaking parameters in the baryon sector are about an order of magnitude larger than in the case of flavor $SU(3)$ in reasonable agreement with the experimental data. Unfortunately the complete symmetry breaking pattern for the $SU(4)$ effective Lagrangian is still unknown. Furthermore, due to the lack of a comprehensive set of $SU(4)$ Clebsch–Gordon coefficients, the important expansion in symmetry breaking, as in eq (2.39), has not been carried out. Due to the large symmetry breaking in the charm sector, the consideration of the D -meson as a “would-be” Goldstone boson and hence the application of the collective approach is doubtful. Nevertheless it is interesting that this approach yields the same ground states as the quark model. As in the three flavor model this is caused by the constraints originating from Wess–Zumino term (2.23), which represents the anomaly structure of QCD.

Another generalization of the Skyrme model wave-functions is to consider an arbitrary, odd number of colors, N_C , in particular the limit $N_C \rightarrow \infty$ is of interest. This has been studied for the three flavor symmetric model [57]. The main result is that for $N_C \rightarrow \infty$ the matrix elements of collective space operators are (up to an overall factor) identical to their analogous matrix elements obtained in the non-relativistic quark model in the same limit [114]. In the three flavor description the generalization to arbitrary N_C is more involved as in the two flavor case because the tensor structure of the baryon wave-functions is more complicated [115, 116].

In what comes we are exclusively interested in the predictions of the soliton picture for physical observables. Henceforth we will only consider the case $N_C = 3$ in three flavor models.

3 Symmetry Breaking and the Size of the Skyrmion

Up to now non-vanishing strange fields have been constructed simply by rigidly rotating the hedgehog configuration, which is embedded in the isospin subgroup, into strange directions (2.28). Except for the induced components (2.45) the effect of symmetry breaking on the meson configuration has completely been ignored. In this chapter two approaches will be presented, which go beyond this approximation by allowing the radial dependence of the chiral angle $F(r)$ to depend on the flavor orientation. This approach is intuitive because for the kaon fields one expects the asymptotic behavior $\exp(-m_K r)$ rather than $\exp(-m_\pi r)$ as is implied by the configuration (2.28). This change in the profile will also cause favorable deviations from the $SU(3)$ relations (2.62) which could not be achieved by any form of the Yabu-Ando method, meaning *e.g.* that whatever complicated structure of the symmetry breaking is assumed for the collective Hamiltonian (2.36), the ratio μ_{Σ^+}/μ_p stays close to unity rather than 0.85 as demanded by the experimental data.

3.1 The “Slow-Rotator” Approach

Let us, for the moment, ignore the time dependence of the collective rotations. Then the angles describing the spatial and isospin orientations of the hedgehog may be absorbed by symmetry transformations. This, however, is not the case for the whole flavor space due to $SU(3)$ symmetry breaking. Denoting the angle which describes the strangeness changing orientation by $\nu = 0 \dots \pi/2$ a suitable parametrization for (2.28) is therefore given by (see also appendix A)

$$U(\mathbf{r}, \nu) = e^{-i\nu\lambda_4} U_0(\mathbf{r}) e^{i\nu\lambda_4} . \quad (3.1)$$

Substituting this *ansatz* into the action (2.24) yields an energy functional which is not only a functional of the chiral angle F , but also a function of the strangeness changing angle ν [117]

$$E(\nu)[F] = \int d^3r \left[\frac{f_\pi^2}{2} (F'^2 + 2 \frac{\sin^2 F}{r^2}) + \frac{\sin^2 F}{e^2 r^2} (F'^2 + \frac{\sin^2 F}{2r^2}) + \epsilon_6^2 \frac{F'^2 \sin^4 F}{8\pi^4 r^4} + m_\pi^2 f_\pi^2 (1 - \cos F) + \sin^2 \nu \left(\frac{1}{2} (f_K^2 - f_\pi^2) (F'^2 + \frac{2\sin^2 F}{r^2}) \cos F + (m_K^2 f_K^2 - m_\pi^2 f_\pi^2) (1 - \cos F) \right) \right] . \quad (3.2)$$

Here the relations (2.20) have been employed to make the dependence on the physical parameters more transparent. Also an additional parameter, ϵ_6 , has been introduced via the sixth order term

$$\mathcal{L}_6 = -\frac{\epsilon_6^2}{2} B_\mu B^\mu , \quad (3.3)$$

with the baryon number current being defined in eq (2.9). Since this term may be considered as the approximation to the exchange of an infinitely heavy ω -meson [109] one obtains at least an estimate $\epsilon_6 \approx 0.015 \text{MeV}^{-1}$ [118]. Nevertheless, ϵ_6 has been considered to be an adjustable parameter in ref [117].

For a given value of $\nu \in [0, \pi/2]$ the minimum of the energy functional (3.2) is obtained. Hence the chiral angle is not only a function of the radial distance but also of the $SU(3)$ “Euler angle” ν : $F = F(r, \nu)$. The philosophy is that the rotation (2.28) proceeds slowly enough that F can adjust itself to the momentary orientation in flavor space. This causes the notion of “slow rotator” in contrast to the “rigid rotator” which is characterized by the chiral

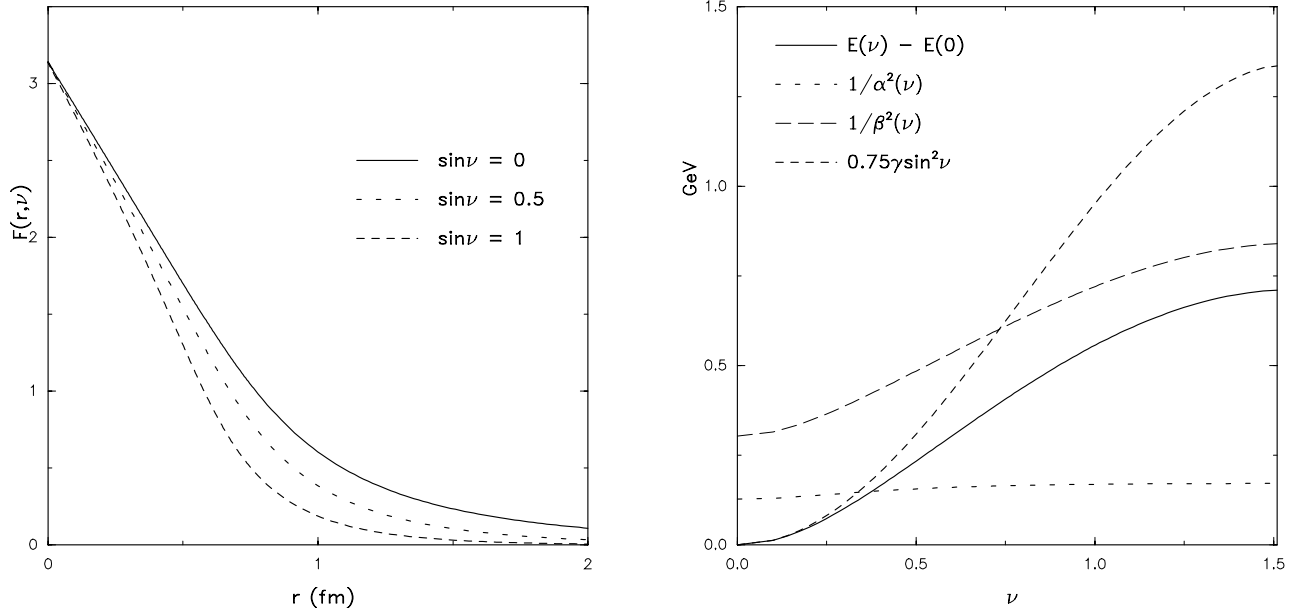


Figure 3.1: Left panel: The chiral angle as functions of the radial distance r and the $SU(3)$ angle ν . Right panel: The quantities in the eigenvalue problem (3.5) as functions of the strangeness changing angle ν . For comparison also the behavior of the symmetry breaker in the “rigid rotator” approach is shown. The results correspond to the model with the sixth order term (3.3) included.

angle confined to two-flavor reduction as discussed in the preceding chapter. From (3.2) it is furthermore transparent that the symmetry breaking forces yield $F(r, \pi/2) \rightarrow \exp(-m_K r)$ for $r \rightarrow \infty$, *i.e.* the kaon field has the proper long-distance behavior. This is indicated in the left part of figure 3.1. In the next step the time-independence of the flavor rotations is waived. This yields kinetic terms in the collective Lagrangian as in eq (2.32)

$$L = -E(\nu) + \frac{1}{2}\alpha^2(\nu) \sum_{i=1}^3 \Omega_i^2 + \frac{1}{2}\beta^2(\nu) \sum_{\alpha=4}^7 \Omega_\alpha^2 - \frac{N_C}{2\sqrt{3}}\Omega_8 + \dot{\nu}^2 \Delta(\nu) . \quad (3.4)$$

Since the moments of inertia α^2 and β^2 are functionals of the chiral angle (*cf.* eq (2.43)) these quantities parametrically depend on the strangeness changing angle ν . For the expressions of $\alpha^2(\nu)$ and $\beta^2(\nu)$ the reader may consult ref [117]. The static part $E(\nu)$ not only has an explicit dependence on ν via $1 - D_{88}$, but also an implicit one implied by the chiral angle. The ν -dependencies of these quantities is shown in the right part of figure 3.1. Obviously the symmetry breaking exhibited by $E(\nu)$ is much more moderate than in the case of the “rigid rotator”. The positivity of $E(\nu) - E(0)$ also verifies the earlier statement that the hedgehog in the isospin subgroup indeed minimizes the classical energy functional in the presence of flavor symmetry breaking. The implicit time-dependence of the chiral angle causes the appearance of the additional term $\dot{\nu}^2 \Delta(\nu)$ in eq (3.4). It has been argued [117] that its influence on baryon properties is only moderate and may easily be compensated by a slight change of the model parameters. Due to the ν -dependence of the moment of inertia for rotations into strange directions, β^2 , the quantization is plagued by ordering ambiguities. The most straightforward procedure to obtain an Hermitian Hamiltonian is to substitute the expression $(1/\beta^2)C_2$ by the anti-commutator which leads to the collective Hamiltonian

$$H = E(\nu) + \left(\frac{1}{2\alpha^2(\nu)} - \frac{1}{2\beta^2(\nu)} \right) \mathbf{J}^2 + \frac{1}{2} \left\{ \frac{1}{2\beta^2(\nu)}, C_2[SU(3)] \right\} - \frac{3}{8\beta^2(\nu)} . \quad (3.5)$$

Table 3.1: The mass differences of the low-lying $\frac{1}{2}^+$ and $\frac{3}{2}^+$ with respect to the nucleon in the “slow-rotator” approach. The models SK4 and SK46 are explained in the text. All data (from refs [120, 117]) are in MeV.

Baryons	SK4	SK46	Expt.
Λ	177	180	177
Σ	285	299	254
Ξ	381	400	379
Δ	298	296	293
Σ^*	477	457	446
Ξ^*	619	590	591
Ω	731	699	733

From figure 3.1 it is observed that $1/\beta^2$ depends on ν only moderately. Hence a different ordering of the collective operators, as *e.g.* suggested by the Pauli-prescription [119], does not cause substantial changes. The eigenvalues and eigenstates of (3.5) are constructed in analogy to the Yabu-Ando approach [62] by separating the ν -dependence of the baryon wave-functions and writing the quadratic Casimir operator C_2 as a differential operator with respect to the $SU(3)$ “Euler angles”. The details of this treatment may be extracted from appendix A.

In table 3.1 the resulting mass differences are listed for two sets of parameters

$$\begin{array}{ll}
 SK4 & SK46 \\
 e = 3.46 & e = 5.61 \\
 \epsilon_6 = 0 & \epsilon_6 = 0.0118\text{MeV}^{-1} \\
 f_K = 118\text{MeV} & f_K = 108\text{MeV} .
 \end{array} \tag{3.6}$$

In the presence of the repulsive sixth order term (3.3) the coefficient of the Skyrme term may be decreased without strongly effecting the soliton profile. The predictions of both models favorably agree with the experimental data. Although f_K has been fine-tuned to better reproduce the baryon mass differences it is only a little different from the experimental value (113MeV).

Having established the slow-rotator approach from the baryon mass differences it is, of course, suggestive to apply this treatment for a study of the static properties of the baryons. This investigation proceeds analogously to those for the rigid rotator by calculating the form factors defined in section 2.4. Although an extensive study of static properties of baryons has been carried out [117, 121] we will focus on the magnetic moments. Here care has to be taken of the fact that the radial functions, V_i , defined in (2.57) not only depend on the radial coordinate r , but also on the strangeness changing angle ν as a consequence of the implicit dependence of the chiral angle. Hence we write $V_i = V_i(r, \nu)$. A typical term contributing to the magnetic moments is then given by

$$G_M^B(\mathbf{q}^2) = -8\pi M_B \left\langle \int_0^\infty r^2 dr \frac{r}{|\mathbf{q}|} j_1(r|\mathbf{q}|) \left\{ V_1(r, \nu) D_{e3} + \dots \right\} \right\rangle_B . \tag{3.7}$$

Numerically these matrix elements may be evaluated with the techniques explained at the end of appendix A. The results are displayed in the lower part of table 3.2. As already mentioned in the previous chapter the rigid rotator approach is not capable of reproducing the experimentally observed deviations from the $SU(3)$ predictions (2.62). Actually these

Table 3.2: The U–spin symmetry for the magnetic moments (in units of the proton magnetic moment) compared to the experimental data. The $\frac{1}{2}^+$ baryons are arranged as in figure 1.1. The rigid rotator results correspond to table 2.2 while the data for the non–relativistic quark model are taken from ref [122]. The lower part gives the predictions of the slow–rotator approach [117].

-0.68	1.0			b	1.0
	-0.22				-b/2
-0.42	?	0.87		c	b/2
	-0.25	-0.45		c	b
	Experiment			U-spin symmetric case	
-0.78	1.0			-0.60	1.0
	-0.35				-0.20
-0.39	0.30	0.98		-0.41	0.29
	-0.31	-0.76		-0.24	-0.46
	rigid rotator			nr quark model	
-0.83	1.0			-0.79	1.0
	-0.25				-0.29
-0.40	0.23	0.85		-0.40	0.27
	-0.20	-0.54		-0.24	-0.63
	Sk4			Sk46	

relations just reflect the U–spin symmetry of the magnetic moments in the flavor octet, which is also indicated in table 3.2. This feature occurs in the rigid rotator approach although the U–spin operation does not relate various eigenstates of the collective Hamiltonian (2.36) since these eigenstates represent are no pure octet states; *cf* eq (2.40). Amusingly, the non–relativistic quark model, which commonly is celebrated for its successful determination of the baryon magnetic moments, does not depart from this symmetry either, especially for the ratio μ_{Σ^+}/μ_p [122]. One immediately observes that for the pattern of the magnetic moments the slow rotator approach gives the desired improvement compared to the rigid rotator. Stated otherwise, the influence of flavor symmetry breaking on the soliton profile is responsible for breaking the U–spin symmetry. Obviously this effect is stronger when the soliton is stabilized by the Skyrme term than in the case when also a sixth order term is present. It should, however, be admitted that the absolute values for the magnetic moments are predicted to be too small for both sets of parameters (3.6)

$$\text{SK4} : \mu_p = 1.78 \quad \text{SK46} : \mu_p = 1.90 . \quad (3.8)$$

Also in ref [117] the magnetic moments of the $\frac{3}{2}^+$ baryons and the electric radii have been calculated. Since experimentally little is known about these quantities we will not go into further detail but only mention that again sizable deviations from the flavor symmetric predictions were observed. Again these turned out to be larger for SK4 than SK46. In

addition the strangeness matrix elements of the (axial)vector currents, which are relevant for the description of the semi-leptonic hyperon decays were studied. Apart from the too small result for $g_a \approx 1$, reasonable agreement with the experimentally known data was obtained despite of the large deviation of the wave-functions from their flavor symmetric forms. In particular the strange quark contribution to the nucleon matrix element of the axial current was found to be reduced to about a quarter of the flavor symmetric value in the model SK4. For SK46 the reduction is mitigated to 40%.

In the framework of the the slow rotator approach the electric quadrupole moments of the $\frac{3}{2}^+$ baryons have been studied in ref [121]. In particular the influence of flavor symmetry breaking has been explored. Various strengths of symmetry breaking are parametrized by a different value of the quark mass ration x (2.17). As a change in x gives different results for X_s (2.81,2.82) these strengths can be translated into the strangeness content of the proton. As already explained a large strangeness content $X_s = 0.23$ is found in the flavor symmetric case while X_s vanishes for infinite symmetry breaking. It turns out that the electric quadrupole moments are rather sensitive to the assumed symmetry breaking. While the use of flavor symmetric wave-functions causes the electric quadrupole moments to be proportional to the charge Q of the considered baryon, an infinite symmetry breaking only yields a proportionality to the isospin projection I_3 (the constant of proportionality depends on the isospin multiplet under consideration). These two cases are very interesting from a conceptual point of view. In a quenched lattice gauge calculation [123] a proportionality to the charges was obtained. This is in contrast to the recent chiral perturbation calculation of ref [124] which found the quadrupole moments to be proportional to the isospin. In the sense that symmetry breaking may be considered an adjustable quantity measured by the strangeness content of the proton, the three flavor soliton models permit a smooth interpolation between the limiting cases. However, some care has to be taken since we have already observed that X_s decreases only slowly as x increases. Other quantities like H_s exhibit a stronger dependence on x . For the above established model SK4, a charge dominated pattern for the quadrupole moments is actually found. For example, the quadrupole moment of the Ω^- is obtained as 0.024efm^2 , while that of the Ξ^{*0} almost vanishes (-0.007efm^2). This pattern agrees with the lattice result, although it is an order of magnitude larger [123].

Summarizing the slow rotator approach, it has to be concluded that the force exerted by symmetry breaking on the soliton configuration has significant effects which, in particular, provide the proper deviation from the U-spin symmetric relations.

3.2 Radial Excitations

In section 2.3 the admixtures of higher dimensional $SU(3)$ representations to the standard octet and decuplet wave-functions have been shown to account for a proper description of the flavor symmetry breaking pattern in the spectrum of the low-lying baryons. Naturally the question arises as to what extent the states in these representations are related to experimentally observed baryons. Ignoring symmetry breaking the mass difference between the state with nucleon quantum numbers in the $\overline{\mathbf{10}}$ and the nucleon itself is given by

$$M_{N(\overline{\mathbf{10}})} - M_{N(\mathbf{8})} = \frac{1}{2\beta^2} \{C_2(\overline{\mathbf{10}}) - C_2(\mathbf{8})\} \approx 350\text{MeV} \quad (3.9)$$

for typical values of β^2 (2.480). Since this is not too different from the position of the Δ resonance the physical significance of such states needs to be explored. As long as $\beta^2 < \alpha^2$,

to which no exception has been obtained in any known soliton model, this state lies above the Δ resonance. The quantum numbers of the $N(\overline{\mathbf{10}})$ state suggest its identification as the Roper resonance (1440). As has been mentioned earlier, the admixture of higher dimensional $SU(3)$ representations can be interpreted as additional quark–antiquark excitations. Hence the identification of the $N(\overline{\mathbf{10}})$ state as the Roper resonance would imply that the Roper represents a quark–antiquark rather than a radial excitation of the nucleon. In general one, however, expects a complicated interplay between states of $SU(3)$ representations and radial excitations. In order to study such questions the field configuration

$$U(\mathbf{r},t) = A(t)U(\mu(t)\mathbf{r},t)A^\dagger(t) \quad (3.10)$$

has been considered in refs [125, 126]. While $A(t)$ again describes the flavor orientation of the hedgehog, the collective coordinate $\mu(t)$ is introduced to describe radial excitations [127]. Commonly this degree of freedom it is referred to as the breathing mode. As will be explained shortly the resulting baryon spectrum exhibits too strong a flavor symmetry breaking. For that reason a model has been considered in ref [126] which contains an additional isoscalar scalar meson field σ . This degree of freedom is incorporated as an order parameter for the gluon condensate to imitate the QCD trace anomaly [128]. For the details of this effective meson Lagrangian the reader may consult ref [129]. Here it suffices to display the flavor symmetry breaking part

$$\mathcal{L}_{SB} = \text{tr} \left\{ \mathcal{M} \left[-\beta' e^{2\sigma} \left(\partial_\mu U \partial^\mu U^\dagger U + U^\dagger \partial_\mu U \partial^\mu U^\dagger \right) + \delta' e^{3\sigma} \left(U + U^\dagger \right) \right] \right\} . \quad (3.11)$$

As a further change of the Lagrangian the non–linear σ term (2.3) acquires a factor $e^{2\sigma}$. There are also kinetic and mass terms for the σ –field. These involve an additional parameter which can be determined from the empirical value of the gluon condensate [129]. Since the profile $\sigma(r) \leq 0$, it is obvious that the extension by this scalar fields mitigates the effects of flavor symmetry breaking. Only configurations, which correspond to shallow bags, *e.g.* $\sigma(r=0)$ being close to zero, have been considered in ref [126].

Substitution of the parametrization (3.10) into the mesonic action (2.24,3.11) yields a Lagrangian for the collective coordinates $A(t)$ as well as $x(t) = [\mu(t)]^{-3/2}$

$$\begin{aligned} L(x, \dot{x}, A, \dot{A}) &= \frac{4}{9} \left(a_1 + a_2 x^{-\frac{4}{3}} \right) \dot{x}^2 - \left(b_1 x^{\frac{2}{3}} + b_2 x^{-\frac{2}{3}} + b_3 x^2 \right) + \frac{1}{2} \left(\alpha_1 x^2 + \alpha_2 x^{\frac{2}{3}} \right) \sum_{a=1}^3 \Omega_a^2 \\ &+ \frac{1}{2} \left(\beta_1 x^2 + \beta_2 x^{\frac{2}{3}} \right) \sum_{a=4}^7 \Omega_a^2 + \frac{\sqrt{3}}{2} \Omega_8 - \left(s_1 x^2 + s_2 x^{\frac{2}{3}} + \frac{4}{9} s_3 \dot{x}^2 \right) (1 - D_{88}) . \end{aligned} \quad (3.12)$$

A term linear in \dot{x} , which would originate from flavor symmetry breaking terms, has been omitted because the matrix elements of the associated $SU(3)$ operators vanishes when properly accounting for Hermiticity in the process of quantization [38]. The expressions for the constants a_1, \dots, s_3 as functionals of the chiral angle as well as numerical values may be extracted from refs [125, 126].

The baryon states corresponding to the Lagrangian (3.12) are obtained in a two–step procedure. For convenience one defines

$$m = m(x) = \frac{8}{9} (a_1 + a_2 x^2) , \alpha = \alpha(x) = \alpha_1 x^2 + \alpha_2 x^{\frac{2}{3}} , \dots , s = s(x) = s_1 x^2 + s x^{\frac{2}{3}} . \quad (3.13)$$

Then the flavor symmetric part of the collective Hamiltonian

$$H = -\frac{1}{2\sqrt{m\alpha^2\beta^4}}\frac{\partial}{\partial x}\sqrt{\frac{\alpha^3\beta^4}{m}}\frac{\partial}{\partial x} + b + \left(\frac{1}{2\alpha} - \frac{1}{2\beta}\right)J(J+1) + \frac{1}{2\beta}C_2(\mu) - \frac{3}{8\beta} + s, \quad (3.14)$$

is diagonalized for a definite $SU(3)$ representation μ . Denote the eigenvalues by \mathcal{E}_{μ,n_μ} and the corresponding eigenstates by $|\mu, n_\mu\rangle$, where n_μ labels the radial excitations. Actually the eigenstates factorize $|\mu, n_\mu\rangle = |\mu\rangle|n_\mu\rangle$. In this language the nucleon corresponds to $|\mathbf{8}, 1\rangle$ while the first excited state, which commonly is identified with the Roper (1440) resonance, would be $|\mathbf{8}, 2\rangle$. Of course, we are interested in the role of states like $|\overline{\mathbf{10}}, n_{\overline{\mathbf{10}}}\rangle$. In order to answer this question the symmetry breaking part has to be taken into account as well. This is done by employing the states $|\mu, n_\mu\rangle$ as a basis to diagonalize the complete Hamiltonian matrix

$$H_{\mu,n_\mu;\mu',n'_{\mu'}} = \mathcal{E}_{\mu,n_\mu}\delta_{\mu,\mu'} - \langle\mu|D_{88}|\mu'\rangle\langle n_\mu|s(x)|n'_{\mu'}\rangle. \quad (3.15)$$

The flavor part of these matrix elements is computed using $SU(3)$ Clebsch–Gordon coefficients while the radial part is calculated using the appropriate eigenstates of (3.14). Of course, this can be done for each isospin multiplet separately, *i.e.* flavor quantum numbers are not mixed. The physical baryon states $|B, m\rangle$ are finally expressed as linear combinations of the eigenstates of the symmetric part

$$|B, m\rangle = \sum_{\mu,n_\mu} C_{\mu,n_\mu}^{(B,m)}|\mu, n_\mu\rangle. \quad (3.16)$$

The corresponding eigen energies are denoted by $E_{B,m}$. The nucleon $|N, 1\rangle$ is then identified as the lowest energy solution with the associated quantum numbers, while the Roper is defined as the next state ($|N, 2\rangle$) in the same spin – isospin channel. Turning to the quantum numbers of the Λ provides not only the energy $E_{\Lambda,1}$ and wave–function $|\Lambda, 1\rangle$ of this hyperon but also the analogous quantities for the radially excited Λ 's: $E_{\Lambda,n}$ and $|\Lambda, n\rangle$ with $n \geq 2$. These calculations are repeated for the other spin – isospin channels yielding the spectrum not only of the ground state $\frac{1}{2}^+$ and $\frac{3}{2}^+$ baryons but also their radial excitations. For both models (with and without scalar field) the predicted eigen energies of the Hamiltonian (3.15) are compared to those of the experimentally observed baryons in figure 3.2. As remarked previously this treatment of the pure Skyrme model yields mass differences of the hyperons which are considerably larger than the empirical data. Including, however, the scalar field according to eq (3.11) provides an excellent agreement for the mass differences for the ground states of each spin–isospin channel. The inclusion of the scalar field also leads to an improved prediction for the Roper resonance although its position is still underestimated by about 80MeV. Nevertheless, the overall picture obtained for the mass differences suggests that the model gives quite reliable information about the structure of the baryon wave–functions. This structure is parametrized by the coefficients $C_{\mu,n_\mu}^{(B,m)}$ defined in eq (3.16). For the lowest energy states with nucleon quantum numbers these are displayed in figure 3.3. As expected the nucleon state $|N, 1\rangle$ is dominated by the lowest octet excitation. In addition to the admixtures of the higher dimensional $SU(3)$ representations, which are expected from the expansion (2.40), the second octet excitation has a sizable amplitude. More surprisingly, the structure of the Roper resonance is very complicated. Although the assumption that this state is dominated by $|\mathbf{8}, 2\rangle$ is confirmed in so far that this component has the largest amplitude, other components (especially $|\mathbf{8}, 1\rangle$) are equally important. The picture of the Roper being a radial excited nucleon is partially verified because it is always the second radial state, which dominates in

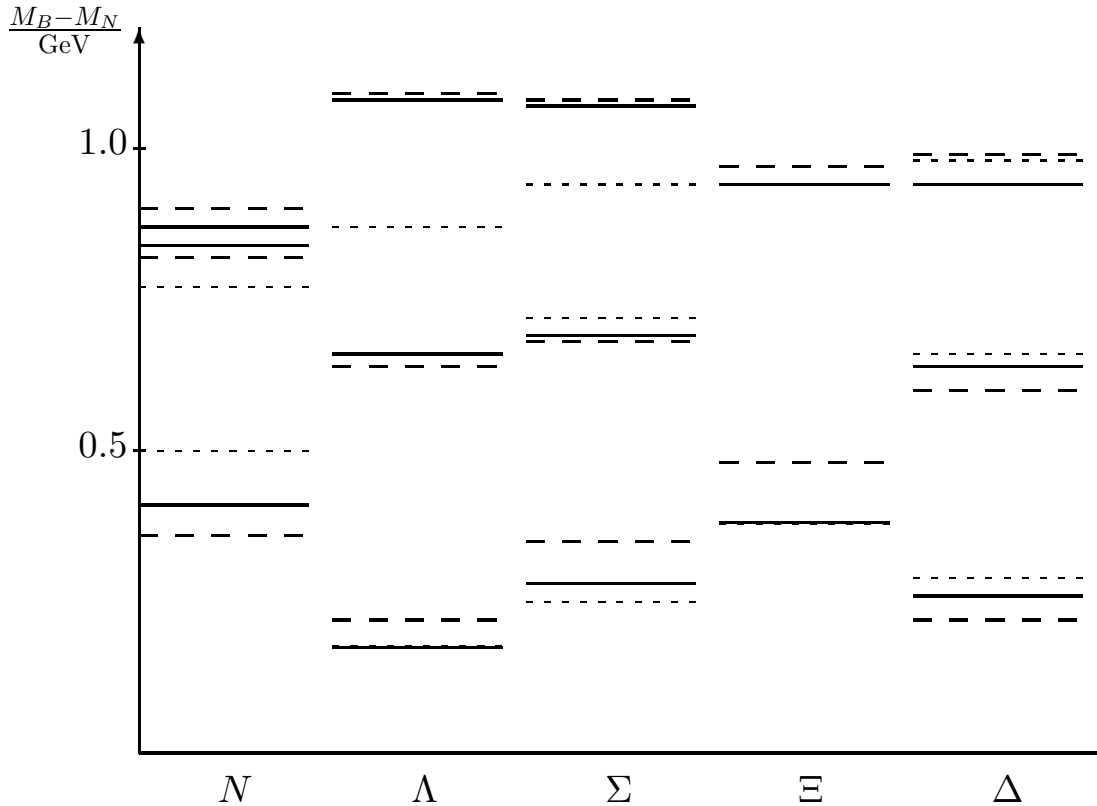


Figure 3.2: The mass differences of the predicted baryons in the breathing mode treatment of the three flavor Skyrme model with $\epsilon=5.0$. Full lines: scalar field included [126]; dashed lines: pure Skyrme model [125]; dotted lines: experimentally observed states [33]. In this presentation the ground states of the Λ and Ξ channels in the model with the scalar field and the experimentally observed counterparts are (almost) indistinguishable.

the higher dimensional $SU(3)$ representations. In the case of the pure Skyrme model one actually finds $|C_{\mathbf{8},1}^{\text{Roper}}| > |C_{\mathbf{8},2}^{\text{Roper}}|$ [125]. Amusingly the $|\mathbf{8}, 1\rangle$ component is completely absent in the wave-function of the next state above the Roper with nucleon quantum numbers. This state should be identified with the $P_{11}(1710)$ resonance. The analogous studies for the Λ , Σ and Ξ channels are presented in ref [125] for the case of the pure Skyrme model.

In the framework of the scaling treatment various static properties of the low-lying baryons have been computed [125, 126]. As an example the predicted magnetic moments of the $\frac{1}{2}^+$ baryons are shown in table 3.3.

As for the mass differences in the pure Skyrme model, the scaling treatment over-estimates the symmetry breaking: The deviation from the $SU(3)$ relations (2.62) is larger than experimentally found. On the other hand the additional scalar field mitigates the flavor symmetry breaking effects properly. Again the experimentally observed deviation from the U-spin relations (*cf.* table 3.2) is reproduced, comparable to the slow rotator approach. It is especially this result for the magnetic moments which indicates that the scaling and slow rotator approaches are quite similar. As a matter of fact both treatments attempt to incorporate the effects of flavor symmetry breaking on the soliton profile. While the slow rotator does this on a classical level, the admixture of radially excited states may be regarded as a quantum description of the same problem.

For completeness it should also be remarked that the axial properties of the hyperons have also been studied in the scaling treatment. As in the rigid and slow rotator approaches,

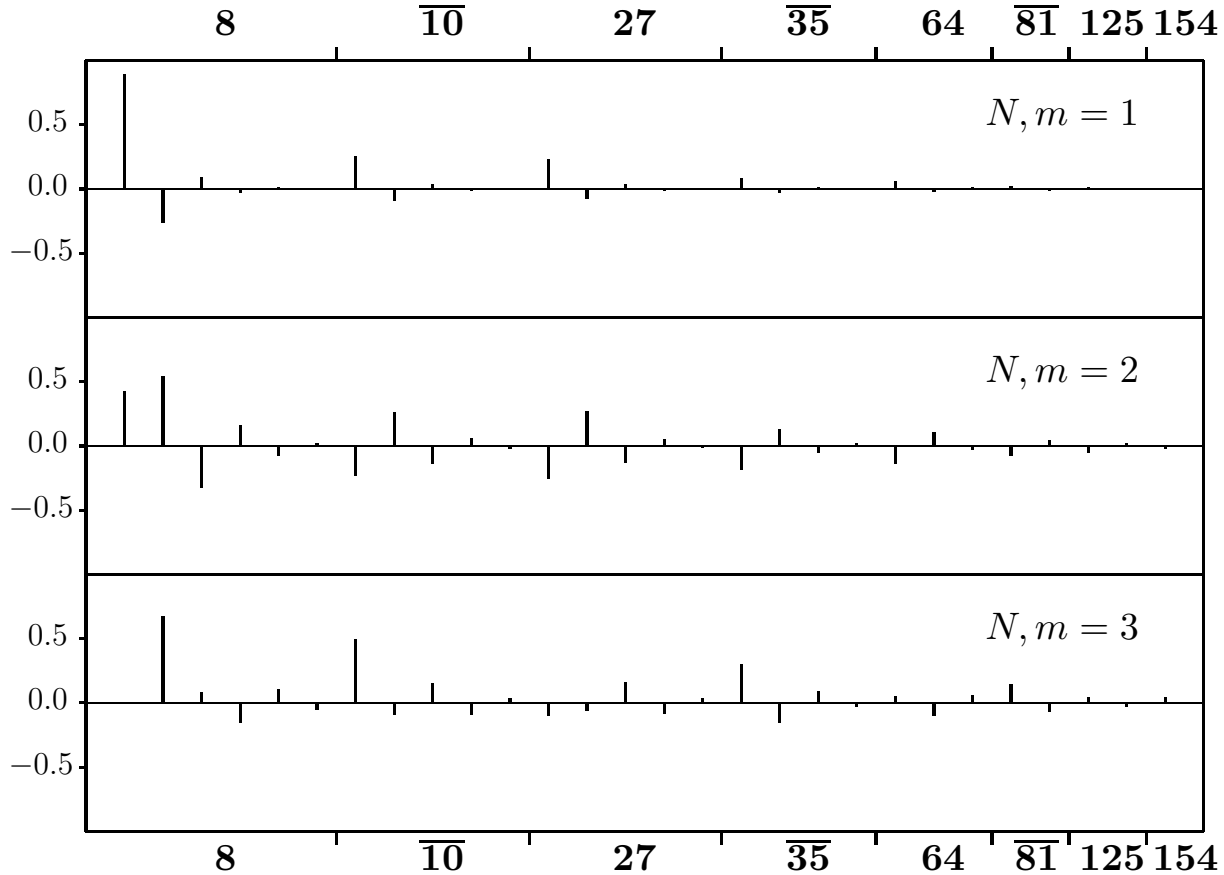


Figure 3.3: The amplitudes $C_{\mu, n\mu}^{(N, m)}$ of the three lowest states with nucleon quantum numbers. The intervals indicated along the abscissa refer to the radially excited states within an $SU(3)$ representation μ . Here the model including the scalar field has been used with $e=5.0$.

consistency with the Cabibbo model [91] was obtained together with a strong reduction of strange quark contribution to the axial current of the nucleon. This appears to be a common feature of models, which incorporate flavor symmetry breaking in the baryon wave-function. To be specific, the matrix element of the eighth component of the axialvector current between nucleon states (see eq (2.67)) is only one third of its flavor symmetric value while the predictions for the matrix elements characterizing the semi-leptonic hyperons decays agree with the experimental values within 10% after normalizing with respect to the axial charge of the nucleon.

In order to summarize the studies compiled in this chapter it is important to remark that one has to go beyond the rigid rotator treatment in order to reproduce the detailed structure of the baryon properties. In particular, this has become obvious for the magnetic moments of the $\frac{1}{2}^+$ baryons. As will be discussed in chapter 5 the bound state approach to include strange degrees of freedom [130, 131] can be compared to the rigid rotator in the limit of very large flavor symmetry breaking. Hence the bound state approach result $\mu_{\Sigma^+}/\mu_p \approx 1.1$ [132, 133] (see also table 5.2) has to be considered as an additional support of the above statement that the rigid rotator is too crude an approximation for a detailed prescription of baryon properties.

Unfortunately the two treatments introduced in the present chapter cannot straightforwardly be applied to more complicated but also more realistic effective meson Lagrangians. This is also the case for the vector meson model to be discussed next. The reason being that the time components of the vector meson fields commonly have to satisfy special constraints

Table 3.3: The magnetic moments in the scaling treatment of the Skyrme model (I). Model (II) contains the additional scalar field (3.11). Results are given in nucleon magnetons as well as ratios of the proton magnetic moment.

Baryon	I		II		Expt.	
	μ_B	μ_B/μ_p	μ_B	μ_B/μ_p	μ_B	μ_B/μ_p
p	2.58	1.00	2.21	1.00	2.79	1.00
n	-2.26	-0.86	-1.84	-0.83	-1.91	-0.68
Λ	-0.50	-0.20	-0.52	-0.24	-0.61	-0.22
Σ^+	2.01	0.78	1.82	0.82	2.42	0.87
Σ^0	0.40	0.16	0.44	0.20	—	—
Σ^-	-1.21	-0.47	-0.94	-0.43	-1.16	-0.42
Ξ^0	-1.06	-0.41	-1.06	-0.48	-1.25	-0.45
Ξ^-	-0.37	-0.14	-0.41	-0.19	-0.69	-0.25
$\Sigma^0 \rightarrow \Lambda$	-1.55	-0.60	-1.37	-0.62	-1.61	-0.58

which are fulfilled by the classical soliton configuration. However, the introduction of additional time dependence (either via the strangeness changing angle $\nu(t)$ as in section 3.1 or the breathing mode coordinate $\mu(t)$ as in section 3.2) would spoil these constraints making impossible the quantum prescription.

Furthermore, all the above described modifications of the rigid rotator treatment predict $\mu_{\Xi^-}/\mu_{\Lambda} < 1$ in contrast to the experimental observation. This indicates that further refinements are necessary.

4 Inclusion of Vector Mesons

As already mentioned earlier, short range effects are missing within the pseudo–scalar Skyrme model. Such effects may elegantly be incorporated by extending the model to contain vector meson fields. The associated profile functions have their major support in the vicinity of the origin. From the studies of two nucleon reactions in meson exchange models [134] it is well known that these fields play an important role in the description of low energy processes. Also the phenomenologically successful concept of vector meson dominance (VMD) [135] supports the explicit consideration of these fields. The VMD hypothesis states that a photon does not interact directly with the nucleon but rather it switches to a heavy vector meson, which then couples to the nucleon. On the other hand it has already been remarked in the preceding chapters that the stabilizing terms (2.7) and (3.3) can be motivated within the infinite mass limit of the interaction of the pions with the ρ and ω vector mesons, respectively. In that limit the Skyrme parameter is identical to the coupling constant of the ρ meson to two pions, $g_{\rho\pi\pi}$ while ϵ_6 is proportional to $g_{\omega\pi\pi\pi}$, the coupling of the ω meson to three pions. Of course, it is more appealing to keep these mesons explicitly in the effective meson Lagrangian rather than to assume the infinite mass approximation. The explicit incorporation of these fields yields important improvements for the description of baryon properties. Some of them were already encountered soon after the soliton picture for baryons had become popular. Before going into the details of the vector meson model for three flavors, it is illuminating to briefly comment on a few of these improvements. The presence of a finite mass ω meson provides an increase of the isoscalar radius [70]

$$\langle r^2 \rangle_{I=0} \approx \langle r^2 \rangle_B + \frac{6}{m_V^2} , \quad (4.1)$$

where $\langle r^2 \rangle_B$ is the radius associated with baryon number current (2.9). The additional piece in eq (4.1) is a consequence of (approximate) VMD, which indeed is observed when including the vector mesons in a chirally invariant manner. As can be seen from table 2.2 this increase of about 0.35fm^2 will significantly improve the prediction for the radii. Another interesting feature of finite mass vector mesons concerns the πN scattering amplitudes. In this context it was soon realized [136] that keeping the mass, m_V , of the vector mesons finite solves the problem of the ever–rising phase shifts observed in the Skyrme model description of πN scattering [137]. Actually, this effect is similar to the transition from the Fermi model for weak interactions to the standard model. It just implies a reduction of the contact interaction at large momentum

$$g_{\rho\pi\pi}^2 \longrightarrow \frac{g_{\rho\pi\pi}^2 m_V^2}{m_V^2 - q^2} . \quad (4.2)$$

Other interesting features of the vector mesons are that these fields are mandatory to obtain a finite matrix element of the singlet axial current [25] as well as a non–vanishing prediction for the strong interaction piece of the neutron proton mass difference [46]. As a matter of fact, these two issues are strongly related as will be discussed in section 4.4.

4.1 The Vector Meson Lagrangian

In this section a realistic effective Lagrangian, which contains vector meson degrees of freedom as well as the pseudo–scalar fields, will be constructed. Here the language of the

massive Yang–Mills approach will be used although the resulting Lagrangian is identical to the one obtained in the hidden symmetry approach [138] when terms, which do not transform properly under charge conjugation, are omitted [139].

In order to avoid the appearance of explicit axial–vector fields without violating global chiral symmetry it is helpful to introduce auxiliary “gauge fields” A_μ^L and A_μ^R [52]. Under a local chiral transformation (2.2) these fields are assumed to behave like

$$A_\mu^L \rightarrow L \left(A_\mu^L + \frac{i}{g} \partial_\mu \right) L^\dagger \quad \text{and} \quad A_\mu^R \rightarrow R \left(A_\mu^R + \frac{i}{g} \partial_\mu \right) R^\dagger. \quad (4.3)$$

The physical relevance of the gauge coupling constant g will be explained shortly. Under parity one demands $A_\mu^L \leftrightarrow A_\mu^R$. The axial–vector content of A_μ^L and A_μ^R is then eliminated by imposing the condition

$$A_\mu^L = U \left(A_\mu^R + \frac{i}{g} \partial_\mu \right) U^\dagger \quad (4.4)$$

on these auxiliary fields. Here U denotes the chiral field (2.13) which transforms according to (2.2). Since the *RHS* of eq (4.4) transforms like a “left gauge field” chiral invariance is not violated when replacing A_μ^L accordingly. A convenient realization of the condition (4.4) is given by

$$A_\mu^L = \xi \left(\rho_\mu + \frac{i}{g} \partial_\mu \right) \xi^\dagger \quad \text{and} \quad A_\mu^R = \xi^\dagger \left(\rho_\mu + \frac{i}{g} \partial_\mu \right) \xi, \quad (4.5)$$

where the root of the chiral field has been introduced, $\xi = U^{1/2}$. Since under parity $\xi \leftrightarrow \xi^\dagger$ it is easy to verify that ρ_μ contains vector meson degrees of freedom only. This field is therefore identified with the physical vector meson nonet

$$\rho = \sum_{a=1}^8 \frac{\rho^a}{2} \lambda^a = \begin{pmatrix} \frac{1}{2} \rho^0 + \frac{1}{2} \omega & \frac{1}{\sqrt{2}} \rho^+ & \frac{1}{\sqrt{2}} K^{*+} \\ \frac{1}{\sqrt{2}} \rho^- & -\frac{1}{2} \rho^0 + \frac{1}{2} \omega & \frac{1}{\sqrt{2}} K^{*0} \\ \frac{1}{\sqrt{2}} K^{*-} & \frac{1}{\sqrt{2}} \bar{K}^{*0} & \frac{1}{\sqrt{2}} \varphi \end{pmatrix}, \quad (4.6)$$

where the Lorentz indices have been suppressed. Under the chiral transformation this vector field also behaves like a gauge field [140]

$$\rho_\mu \rightarrow K \left(\rho_\mu + \frac{i}{g} \partial_\mu \right) K^\dagger \quad \text{and} \quad \xi \rightarrow L \xi K^\dagger = K \xi R^\dagger. \quad (4.7)$$

For vector transformations the last equation, which defines the matrix K , is trivially solved by $L = R = K$ while for axial transformations, $L = R^\dagger$, the matrix K depends on the meson field configuration ξ .

The effective vector meson pseudo–scalar Lagrangian is developed in two steps. First a chirally invariant Lagrangian is constructed in terms of the auxiliary fields $A_\mu^{L,R}$. Subsequently the axial–vector degrees of freedom are eliminated by the realization (4.5). As this realization merely is a gauge transformation for the fields $A_\mu^{L,R}$, the kinetic part for the vector mesons is uniquely given by

$$-\frac{1}{2} \text{tr} [F_{\mu\nu}(\rho) F^{\mu\nu}(\rho)], \quad (4.8)$$

where $F_{\mu\nu}(\rho) = \partial_\mu\rho_\nu - \partial_\nu\rho_\mu - ig[\rho_\mu, \rho_\nu]$ refers to the field strength tensor of the ρ meson. This field acquires a mass by adding terms quadratic in $A_\mu^{L,R}$ which are invariant under global chiral transformations only

$$\frac{m_0^2}{2}\text{tr} \left[A_\mu^L A^{L\mu} + A_\mu^R A^{R\mu} \right] - \frac{B}{2}\text{tr} \left[A_\mu^L U A^{R\mu} U^\dagger \right]. \quad (4.9)$$

The identical coefficients of the first two terms are demanded by parity invariance. Employing the realization (4.5) one observes that the expression (4.9) not only contains the vector meson mass term but also the non-linear σ model when identifying $4m_0^2 - 2B = m_V^2$ and $4m_0^2 + 2B = g^2 \tilde{f}_\pi^2$. Here m_V denotes an average mass of the vector meson nonet (4.6). Next, one has to account for the mass splittings of the vector mesons. To leading order in the symmetry breaking, an appropriate term which properly behaves under chiral transformations, can be constructed from the last expression in (4.9)

$$-\alpha'\text{tr} \left[\mathcal{M} \left(A_\mu^L U A^{R\mu} + A_\mu^R U^\dagger A^{L\mu} \right) \right]. \quad (4.10)$$

The reader may consult ref [141] for a very recent and elaborate study of symmetry breaking in the meson sector. Introducing, for convenience

$$\begin{aligned} p_\mu &= \partial_\mu \xi \xi^\dagger + \xi^\dagger \partial_\mu \xi, & R_\mu &= \rho_\mu - \frac{i}{2g} \left(\partial_\mu \xi \xi^\dagger + \xi^\dagger \partial_\mu \xi \right) \\ T^\pm &= \xi T \xi \pm \xi^\dagger T \xi^\dagger, & S^\pm &= \xi S \xi \pm \xi^\dagger S \xi^\dagger \end{aligned} \quad (4.11)$$

(see eq (2.16) for the relevant definitions) the explicit form of the Lagrangian may compactly be written as

$$\begin{aligned} \mathcal{L}_{\text{non-an}} &= \text{tr} \left[-\frac{1}{4} \tilde{f}_\pi^2 p_\mu p^\mu - \frac{1}{2} F_{\mu\nu}(\rho) F^{\mu\nu}(\rho) + m_V^2 R_\mu R^\mu \right. \\ &\quad - 2\alpha' R_\mu R^\mu (T^+ + xS^+) - \frac{i}{g} [R_\mu, p^\mu] (T^- + xS^-) \\ &\quad \left. + \left(\beta' - \frac{\alpha'}{2g^2} \right) p_\mu p^\mu (T^+ + xS^+) + \delta' (T^+ - 2T + x(S^+ - 2S)) \right], \end{aligned} \quad (4.12)$$

where the index indicates that the anomalous terms (involving the anti-symmetric tensor $\epsilon_{\mu\nu\rho\sigma}$) have not yet been included. Expanding this Lagrangian up to quadratic order in the meson fields allows one to express the parameters of the model in terms of the physical decay constants and masses. Typical examples are (see also eq (2.20))

$$f_\pi^2 = \tilde{f}_\pi^2 + \alpha' - 8\beta', \quad m_{K^*}^2 = m_V^2 - 2\alpha'(1+x). \quad (4.13)$$

The complete set of equations may be found in ref [46]. The third term in eq (4.12) contains the $\rho\pi\pi$ vertex

$$m_V^2 \text{tr} [R_\mu R^\mu] = \frac{m_V^2}{2} \left\{ \rho_\mu^a \rho^{\mu a} + \frac{1}{g \tilde{f}_\pi^2} \boldsymbol{\rho}_\mu \cdot (\boldsymbol{\pi} \times \partial^\mu \boldsymbol{\pi}) + \dots \right\}. \quad (4.14)$$

Utilizing the experimental data ($f_\pi = 93\text{MeV}$, $g_{\rho\pi\pi} = m_V^2/\sqrt{2}g\tilde{f}_\pi^2 = 8.66^a$) yields the parameters [40]

$$\begin{aligned} \tilde{f}_\pi &\approx 0.092\text{GeV} , & m_V &\approx 0.766\text{GeV} , & g &\approx 5.57 , & x &\approx 36 , \\ \alpha' &\approx -2.8 \times 10^{-3}\text{GeV}^2 , & \beta' &\approx -7.14 \times 10^{-5}\text{GeV}^2 , & \delta' &\approx 4.15 \times 10^{-5}\text{GeV}^2 . \end{aligned} \quad (4.15)$$

Due to the presence of the α' type symmetry breaker the values of β' and x are slightly changed compared to the pure pseudo-scalar model (2.21). One might want to include a symmetry breaker for the kinetic part of the vector meson fields [46]. As it is the goal to describe the baryons with a minimal set of terms in the effective meson Lagrangian, such a term is omitted unless some fine-tuning of the model is required.

In order to complete the vector meson model Lagrangian the anomalous terms have to be added. For their presentation it is most useful to introduce the notation of differential forms: $A^R = A_\mu^R dx^\mu$, $d = \partial_\mu dx^\mu$, etc. . Since the left and right ‘‘gauge fields’’ are related via the chiral constraint (4.4) the number of linear independent terms, which transform properly under the chiral transformation as well as parity and charge conjugation, is quite limited [52, 139]:

$$A^L \alpha^3 , \quad dA^L \alpha A^L - A^L \alpha dA^L + A^L \alpha A^L \alpha , \quad 2 \left(A^L \right)^3 \alpha + \frac{i}{g} A^L \alpha A^L \alpha . \quad (4.16)$$

Of course, including these terms in the model Lagrangian will introduce three more parameters: γ_1, γ_2 and γ_3 . Noting that $\alpha = \xi p \xi^\dagger$ a suitable presentation of the anomalous part of the action is given in terms of the quantities defined in eq (4.11)

$$\begin{aligned} \Gamma_{\text{an}} &= \frac{iN_C}{240\pi^2} \int_{M_5} \text{tr} \left(p^5 \right) \\ &+ \int_{M_4} \text{tr} \left(\frac{1}{6} \left[\gamma_1 + \frac{3}{2} \gamma_2 \right] R p^3 - \frac{i}{4} g \gamma_2 F(\rho) [pR - Rp] - g^2 [\gamma_2 + 2\gamma_3] R^3 p \right) , \end{aligned} \quad (4.17)$$

where also the Wess–Zumino term (2.23) is included. In ref [139] two of the three unknown constants, $\gamma_{1,2,3}$ were determined from purely strong interaction processes like $\omega \rightarrow 3\pi$. Defining $\tilde{h} = -2\sqrt{2}\gamma_1/3$, $\tilde{g}_{VV\phi} = g\gamma_2$ and $\kappa = \gamma_3/\gamma_2$ the central values $\tilde{h} = \pm 0.4$ and $\tilde{g}_{VV\phi} = \pm 1.9$ were found. Within experimental uncertainties (stemming from the errors in the $\omega - \phi$ mixing angle) these may vary in the range $\tilde{h} = -0.15, \dots, 0.7$ and $\tilde{g}_{VV\phi} = 1.3, \dots, 2.2$ subject to the condition $|\tilde{g}_{VV\phi} - \tilde{h}| \approx 1.5$. The third parameter, κ could not be fixed in the meson sector. From studies [142] of nucleon properties in the two flavor model it was argued that $\kappa \approx 1$ represents a reasonable choice. These studies also allowed one to fix the overall signs of the parameters $\gamma_{1,2,3}$ (which cannot be determined in the meson sector) to be $\tilde{g}_{VV\phi} \approx +1.9$ when $F(0) = +\pi$. The model can equivalently be formulated for $F(0) = -\pi$. Then the signs of the coefficients $\gamma_{1,2,3}$ as well as that of the Wess–Zumino term (2.23) have to be changed.

4.2 Baryon Masses

In order to compute the spectrum of the low-lying baryons in the vector meson model the coefficients in the collective Hamiltonian (2.36) have to be evaluated from the action

$$\Gamma = \int d^4x \mathcal{L}_{\text{non-an}} + \Gamma_{\text{an}} . \quad (4.18)$$

^aThe coupling constant $g_{\rho\pi\pi}$ is computed from the width $\Gamma_{\rho\pi\pi} = 151\text{MeV}$ [33].

The generalization of the hedgehog *ansatz* (2.10) to the vector meson model requires the time component of the ω field and the space components of the ρ field to be different from zero. All static fields are embedded in the isospin subgroup of $SU(3)$. Parity and grand spin symmetry allow for three radial functions

$$\xi_\pi = \exp\left(\frac{i}{2}\hat{\mathbf{r}} \cdot \boldsymbol{\tau} F(r)\right), \quad \omega_0 = \frac{\omega(r)}{2g}, \quad \rho_i^a = \frac{G(r)}{gr} \epsilon_{ija} \hat{r}_j. \quad (4.19)$$

Substituting these *ansätze* into the action (4.18) yields the classical mass E . Its functional form is displayed in eq (B.1). Application of the variational principle to this functional leads to second order coupled non-linear differential equations for the radial functions $F(r)$, $\omega(r)$ and $G(r)$. The boundary conditions for the chiral angle $F(r) = \pi$ and $F(\infty) = 0$, which correspond to a unit baryon number, also determine the boundary conditions of the vector meson profiles via the differential equations, *e.g.* $G(0) = -2$. A typical set of resulting profile functions is shown in figure 4.1a. These radial functions are subsequently employed to evaluate the symmetry breaking parameters γ , α_1 and β_1 , *cf.* eqs (B.8) and (B.9).

The computation of the moments of inertias α^2 and β^2 is more involved due to the appearance of induced components. In contrast to the pure pseudo-scalar model also (mainly vector meson) fields are also excited by the collective rotation in coordinate space. In the context of the collective approach to the three flavor model the collectively rotating vector meson fields are parametrized as

$$\rho_\mu(\mathbf{r}, t) = A(t) \begin{pmatrix} \boldsymbol{\rho}_\mu \cdot \boldsymbol{\tau} + \omega_\mu & K_\mu^* \\ K_\mu^{*\dagger} & 0 \end{pmatrix} A^\dagger(t), \quad (4.20)$$

where $A(t)$ again is an $SU(3)$ matrix. In addition to the static vector meson profiles $\rho(\mathbf{r})$ and $\omega(r)$ (4.19) three radial fields are induced by the spatial rotation [70]

$$\boldsymbol{\rho}_0 = \frac{1}{2g} [\xi_1(r)\boldsymbol{\Omega} + \xi_2(r)(\hat{\mathbf{r}} \cdot \boldsymbol{\Omega})\hat{\mathbf{r}}], \quad \omega_i = \frac{\Phi(r)}{2g} \epsilon_{ijk} \Omega_j \hat{r}_k. \quad (4.21)$$

Suitable *ansätze* for the vector meson fields^b which are excited by the flavor rotation into the direction of strangeness are given by [144]

$$K_0^* = \frac{S(r)}{g} \Omega_K, \quad K_i^* = \frac{1}{2g} \left[iE(r)\hat{r}_i + \frac{D(r)}{r} \epsilon_{ijk} \hat{r}_j \tau_k \right] \Omega_K. \quad (4.22)$$

Again the flavor decomposition of the angular velocity matrix $\sum_{a=1}^8 \Omega_a \lambda^a$, as in eqs (2.29) and (2.46), has been employed. The parametrization (2.45) for the pseudo-scalar fields has to be augmented by an η field component

$$Z(\mathbf{r}) = \begin{pmatrix} \eta_T(\mathbf{r}) & | & K(\mathbf{r}) \\ -\frac{\eta_T(\mathbf{r})}{K^\dagger(\mathbf{r})} & | & 0 \end{pmatrix}. \quad (4.23)$$

The pseudo-scalar nature of the η meson requires the *ansatz* $\eta_T = \eta(r)\hat{\mathbf{r}} \cdot \boldsymbol{\Omega}/f_\pi$. The kaon field is again given by (2.45). As explained in the context of the pseudo-scalar model (section

^bIn ref [143] a simplified treatment has been considered where the time component of the vector field, $S(r)$ represents the only non-trivial excitation due to the rotation into the direction of strangeness.

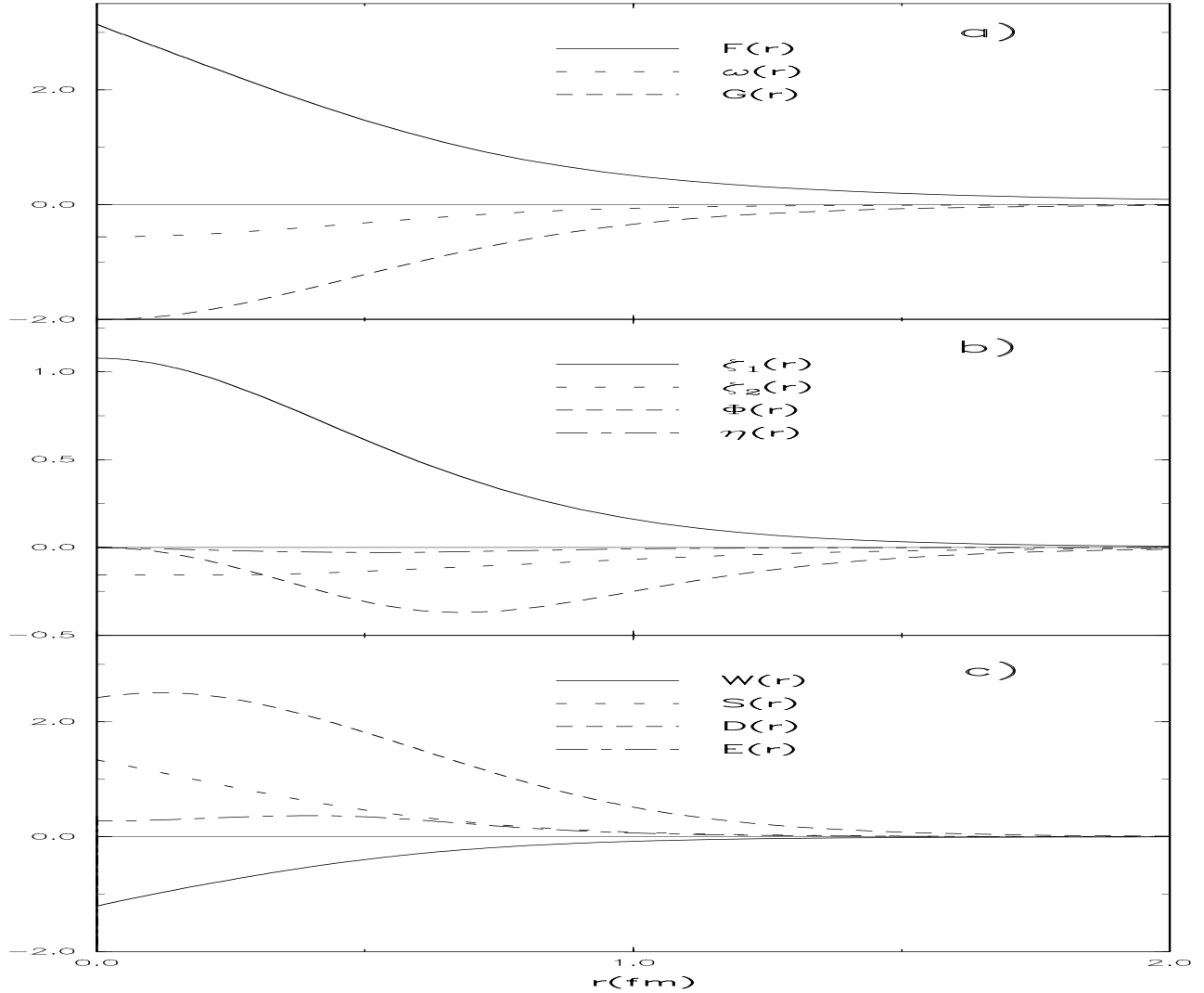


Figure 4.1: The radial dependencies of the profile functions in the vector meson model. a) classical fields minimizing the static energy M , b) induced fields for the moment of inertia α^2 , c) induced fields for the moment of inertia β^2 . ω is in GeV, ϕ, W and D are in GeV^{-1} while all other fields are dimensionless. The profile functions correspond to the parameter set (4.15) and (4.24).

2.3) those terms in the effective action, which are linear in the time derivative, provide the sources for these induced radial functions. These sources are functions of the classical fields (4.19). The variational treatment of the spatial moment of inertia, α^2 then yields the radial functions ξ_1, ξ_2, Φ and η , which are displayed in figure 4.1b. Similarly the radial functions S, E, D and W drawn in figure 4.1c, are obtained from the strange moment of inertia, β^2 . In an attempt to frighten the reader, the explicit expressions for these moments of inertia are presented in appendix B.

The remaining coefficients γ_S, γ_T and γ_{TS} of the collective Hamiltonian (2.36) vanish for the action (4.18).

For a given set of parameters of the effective action the coefficients of the collective Hamiltonian (2.36) may now be evaluated. Subsequently its eigenvalues, which are identified as the baryon masses, are computed using the exact diagonalization procedure described in section 2.3 and appendix A. The remaining freedom in choosing the parameters $\tilde{h}, \tilde{g}_{V\phi}$ and κ is used

Table 4.1: The predictions for the mass differences of various baryons with respect to the nucleon in the vector meson model (VM) compared to the experimental data (all in MeV).

	Λ	Σ	Ξ	Δ	Σ^*	Ξ^*	Ω
VM	159	270	398	311	448	592	718
Expt.	177	254	379	293	446	591	733

to optimize the predictions for the baryon mass differences. This yields

$$\tilde{h} = 0.3, \quad \tilde{g}_{VV\phi} = 1.3, \quad \kappa = 1.2, \quad (4.24)$$

which actually is close to the central values discussed above. These parameters together with (4.15) result in

$$\begin{aligned} E &= 1.628 \text{GeV}, \quad \alpha^2 = 5.144 \text{GeV}^{-1}, \quad \beta^2 = 4.302 \text{GeV}^{-1}, \\ \gamma &= 1.755 \text{GeV}, \quad \alpha_1 = 2\beta_1 = 0.454 \end{aligned} \quad (4.25)$$

for the non-vanishing coefficients of the collective Hamiltonian (2.36). The induced meson fields η, \dots, D actually cause the moments of inertia to decrease compared to the case when these fields are omitted. While the contribution of the induced components to the spatial moment of inertia α^2 is sizable, it is almost negligible [144] for the strange moment of inertia β^2 .

In table 4.1 the mass differences obtained for the set (4.25) are compared with the experimental data. Obviously a reasonable agreement with experimental data can be gained. These mass differences certainly represent an improvement over the pseudo-scalar model (see table 2.1). In particular, the $\frac{3}{2}^+$ baryons lie higher in energy (relative to the nucleon) than in the pseudo-scalar model. This is caused by the decrease of the spatial moment of inertia α^2 , which is due to quite an extended soliton, see figure 4.1. As will be discussed in the proceeding section such large extension of the soliton is also reflected in the predictions for the baryon radii. Simultaneously the larger soliton leads to a sizable symmetry breaking coefficient γ . Nevertheless the ratios (2.49) of the mass differences are closer (1:0.70:0.81) to the leading order (in symmetry breaking) prediction than in the pseudo-scalar model. The reason being that the additional coefficients α_1 and β_1 mitigate the effect of symmetry breaking. In case α_1 and β_1 had turned out to have the opposite sign, the effects of the symmetry breaking terms would have added coherently to γ .

Up to now isospin breaking effects have been ignored, *i.e.* $y = 0$ in eq (2.17). Substituting the above described meson field configurations into the relevant pieces of the action yields

$$\mathcal{L}_{\Delta I} = \left(\frac{2y\delta'}{3f_\pi} \eta \sin F + \dots \right) D_{3i} \Omega_i - D_{38} \left(\frac{2y\delta'}{\sqrt{3}} (1 - \cos F) + \dots \right), \quad (4.26)$$

where only typical two and three flavor expression involving respectively the collective expressions $D_{3i} \Omega_i$ and D_{38} are shown^c. For the nucleon the matrix elements of D_{38} and D_{83} only differ in sign. From figure 2.3 one therefore deduces that $\langle N | D_{38} | N \rangle$ suffers a large reduction for actual amount of symmetry breaking. Hence the proper description of the neutron

^cObviously $\mathcal{L}_{\Delta I}$ yields the strong interaction parts to the mass differences within an isospin multiplet when first computing the integrals over the radial functions and subsequently evaluating the matrix elements of the collective operators.

proton mass difference Δ_N requires the major contribution from the two flavor piece. This, of course, is expected because this mass difference is nothing but a consequence of different current up and down quark masses and should therefore already be present at the two flavor level. However, in a purely pseudo-scalar model one finds $\eta(r) \equiv 0$. Hence there is no two flavor contribution to Δ_N in purely pseudo-scalar models. This conclusion also holds for the terms not explicitly shown in eq (4.26). The η meson is only induced in the presence of vector mesons. Hence a two flavor contribution to Δ_N only occurs when the pseudo-scalar model is augmented by short range effects, which are imitated by the vector mesons, The actual calculation [46] in the vector meson model gives about 1.3MeV for the two flavor contribution to Δ_N . Three flavor effects may account for additional 0.5MeV. Hence the sum (1.8MeV) favorably agrees with the experimental value (1.3MeV) when the effects of the electromagnetic interaction [48], $\Delta_N^{\text{e.m.}} = -0.76 \pm 0.30\text{MeV}$ are taken into account. In section 4.4 we will see that fine-tuning Δ_N provides a handle to disentangle the matter and glue contributions to the axial singlet matrix element of the nucleon.

4.3 Static Properties

The appropriate definitions of the observables and form factors have already been provided in section 2.4. The covariant expression for the currents associated with the action is presented in eq (2.12) of ref [40]. Rather than going into detail it is interesting to consider the expansion of the vector current in terms of the meson fields (2.13,4.11)

$$V_\mu^a = \frac{m_V^2}{g} \text{tr} \left\{ Q^a \left[2\rho_\mu - i \left(\frac{2g^2 f_\pi^2}{m_V^2} - 1 \right) \Phi \partial_\mu \Phi \right] \right\} + \dots \quad (4.27)$$

The first term in this expression reflects exact VMD while the second one approximately vanishes^d for the parameters (4.15). Hence the model contains the VMD concept, at least approximately [146].

When substituting the parametrizations (4.19,4.21,4.22), the formal structure of the currents remains unaltered compared to that of the pseudo-scalar model. Here, however, the radial functions $V_1(r)$, etc. in eq (2.57) are given in terms of the profiles $F(r)$, $\omega(r)$, $G(r)$, $\xi_1(r), \dots, D(r)$, whose computation has been described in the preceding section. The explicit expressions, which are quite awkward, are given in appendix B of ref [40]. Only for the case of the axial singlet current (which in the pseudo-scalar model is a total derivative (2.70)) conceptually important changes will appear. This will be considered at the pertinent occasion.

The numerical results for electromagnetic observables obtained in the vector meson model, which are computed in analogy to the pseudo-scalar model, are presented in table 4.2. Like in the case of the mass differences an improvement over the pseudo-scalar model is obtained. Most apparently, the absolute values of the magnetic moments have increased significantly as a consequence of the more extended soliton. Accept for the hyperon Ξ^0 this represents a desired result. The prediction is about 40% off the experimental value in this special case. This is again linked to the fact that only minor deviations from the $SU(3)$ relations (2.62) occur. It has already been discussed in chapter 3 that the rigid rotator approach, which has been applied here, cannot accommodate the experimentally observed deviations. However, the vector meson model correctly describes the ratio μ_{Ξ^-}/μ_Λ , which was not possible with the pseudo-scalar model, even when the rigid rotator approach was modified. Statements on

^dIt vanishes identically when parameters satisfying the KSRF relation [145] are used.

Table 4.2: The electromagnetic properties of the baryons compared to the experimental data. The predictions of the vector meson model are taken from ref [40] and correspond to the parameter set (4.15) and (4.24).

B	$\mu_B(\text{n.m.})$		$r_M^2(\text{fm}^2)$		$r_E^2(\text{fm}^2)$	
	VM	Expt.	VM	Expt.	VM	Expt.
p	2.36	2.79	0.94	0.74	1.20	0.74
n	-1.87	-1.91	0.94	0.77	-0.15	-0.12
Λ	-0.60	-0.61	0.78	—	-0.06	—
Σ^+	2.41	2.42	0.96	—	1.20	—
Σ^0	0.66	—	0.86	—	-0.01	—
Σ^-	-1.10	-1.16	1.07	—	-1.21	—
Ξ^0	-1.96	-1.25	0.90	—	-0.10	—
Ξ^-	-0.84	-0.69	0.84	—	-1.21	—
$\Sigma^0 \rightarrow \Lambda$	-1.74	-1.61	0.97	—	—	—

this ratio are apparently model dependent, in particular because the $SU(3)$ relations (2.62) give no information. One further recognizes much larger magnetic and isoscalar electric radii than in the pseudo–scalar model. Of course, this is partially due to the bigger soliton but mainly this result reflects the effects of VMD as discussed in the introduction to this chapter, see eq (4.1). In the case of the electric radius of the proton these effects are too strong and some improvement appears to be needed. This can also be observed from the full momentum dependence of the proton electric form factor (see *e.g.* figure 3a of ref [40]), which drops off more rapidly than the dipole fit, $(1 + Q^2/0.71\text{GeV}^2)^{-2}$. On the other hand the momentum dependence of the neutron electric form factor agrees reasonably well with the empirical data.

When adopting the suitable generator (2.63) the vector currents, which have provided the electromagnetic properties, may also be employed to compute the strangeness form factors in the nucleon. The vector meson model predicts [40]

$$\mu_S = -0.05 , \quad r_S^2 = 0.05\text{fm}^2 . \quad (4.28)$$

The absolute value of the strange magnetic moment μ_S is even smaller than in the pseudo–scalar model (2.64), which already represented quite a reduction from Jaffe’s result (-0.31 ± 0.09) [36]. The latter was obtained by using a three pole vector meson fit to dispersion relations suggested by Höhler et al. [37]. In ref [40] this has been explained as a consequence of flavor symmetry breaking because the use of an $SU(3)$ symmetric nucleon wave–function (A.11) resulted in $\mu_S \approx -0.54$. Amusingly, the prediction for the squared strange radius r_S^2 has the opposite sign as the one in the pseudo–scalar model (2.64). It has been conjectured that the positiveness of r_s^2 is linked to VMD. The argument is that a one pole VMD approach, together with $\omega - \phi$ mixing, leads to $r_s^2 = 0.01\text{fm}^2$ [38]; which, however, is much smaller in magnitude. Also Jaffe [36] obtained a positive value $r_s^2 = 0.16 \pm 0.06\text{fm}^2$. In table 4.3 the predictions of various models for μ_S and r_s^2 are summarized. Obviously these predictions are quite diverse and precision experiments should soon provide some resolution.

When substituting the meson configurations of section 4.2 into the covariant expression for the axial current, one obtains for the octet part ($a = 1, \dots, 8$) the general structure

$$\begin{aligned} A_i^a = & \mathcal{A}_{ik}^{(1)} D_{ak} + \mathcal{A}_{ik}^{(2)} d_{k\alpha\beta} D_{a\alpha} \Omega_\beta + \mathcal{A}_{ik}^{(3)} D_{ak} \Omega_k \\ & + \mathcal{A}_{ik}^{(4)} D_{ak} (D_{88} - 1) + \mathcal{A}_{ik}^{(5)} d_{k\alpha\beta} D_{a\alpha} D_{8\beta} , \end{aligned} \quad (4.29)$$

Table 4.3: Predictions for the strange magnetic moment μ_S and the strangeness radius r_S^2 : a. pole fit [36], b. $SU(3)$ symmetric treatment of kaon loops [34], c. kaon loop calculation [39], d. single pole VMD [38], e. VMD combined with kaon loops [39], f. pseudo-scalar Skyrme model (2.64), g. vector meson Skyrme model (4.28), h. NJL soliton model [41].

	a.	b.	c.	d.	e.	f.	g.	h.
$\mu_S(\text{n.m.})$	-0.22...-0.40	-0.30...-0.40	-0.24...-0.32	-0.003	-0.24...-0.32	-0.13	-0.05	-0.05...0.25
$r_S^2(\text{fm}^2)$	0.07...0.21	-0.03	-0.02...-0.03	0.01	-0.04...-0.05	-0.10	0.05	-0.15...-0.25

with $\mathcal{A}_{ik}^{(l)} = A^{(l)}(r)\delta_{ik} + B^{(l)}(r)\hat{r}_i\hat{r}_j$. The radial functions $A^{(l)}$ and $B^{(l)}$ may be extracted from appendix B of ref [40]. It is important to remark that $\mathcal{A}_{ik}^{(3)}$ is solely due to the anomalous part of the action (4.17) and would vanish identically if no vector meson fields were present. This also causes the axial singlet current to be different from a total derivative

$$A_i^0 = 2\sqrt{3}f_\pi\partial_i\eta^0 + \tilde{A}_i^0 \quad \text{with} \quad \tilde{A}_i^0 = \frac{2}{\sqrt{3}}\mathcal{A}_{ik}^{(3)}\Omega_k . \quad (4.30)$$

Here η^0 refers to the singlet component of the pseudo-scalar field Φ in the decomposition $U = \exp(i(\Phi + \eta^0/\sqrt{3}f_\pi))$, with $\text{tr}\Phi = 0$. Now a non-trivial result may be obtained for the axial singlet matrix element $H(q^2)$ defined in eq (2.68). Obviously, the vector mesons provide a conceptual difference over pure pseudo-scalar models. Actually the anomaly equation $-\partial_i A_i^0 = f_\eta m_\eta^2 \eta$ is identical to the equation of motion for the profile function $\eta(r)$ obtained from varying the spatial moment of inertia α^2 . This is another manifestation of the fact that the η field is only excited when vector meson fields (more generally short range effects) are incorporated because $\mathcal{A}^{(3)}$ is the source term. Apparently, the non-trivial result for $H(q^2)$ is subject to the semi-classical treatment (4.21), while $H(q^2)$ vanishes for the static configuration (4.19). A similar feature was already encountered when studying the neutron proton mass difference. This strongly supports the above conjecture that the issue of the proton spin puzzle is closely connected to this mass difference.

Due to isospin invariance the Fourier transforms of the components $2A_3^3$, $2\sqrt{3}A_3^8$ and $3\tilde{A}_3^0$ respectively provide the form factors $G_A(q^2)$, $R(Q^2)$ and $H(q^2)$, of the nucleon after computing the matrix elements of the collective operators between the nucleon eigenstate of the collective Hamiltonian. These form factors are related to the individual quark contributions defined in eq (2.55) via

$$\begin{aligned} G_A(q^2) &= H_u(q^2) - H_d(q^2) , \\ R(q^2) &= H_u(q^2) + H_d(q^2) - 2H_s(q^2) , \\ H(q^2) &= H_u(q^2) + H_d(q^2) + H_s(q^2) . \end{aligned} \quad (4.31)$$

The predicted momentum dependencies^e of these form factors as well as the strange quark contribution to the axial current matrix element of the proton, $H_s(q^2)$ are shown in figure 4.2. It is a long-standing problem of mesonic soliton models that the axial charge of the nucleon $g_A = G_A(q^2 = 0)$ is underestimated when parameters are adopted which are suitable for the description of the baryon spectrum (see, however, ref [90]). It is hence not surprising that for the set (4.24) g_A is predicted too small by about 30%

$$g_A = 0.93 , \quad R(0) = 0.38 , \quad H(0) = 0.29 . \quad (4.32)$$

^eSimilar studies for the two flavor reduction of this models are presented in ref [147].

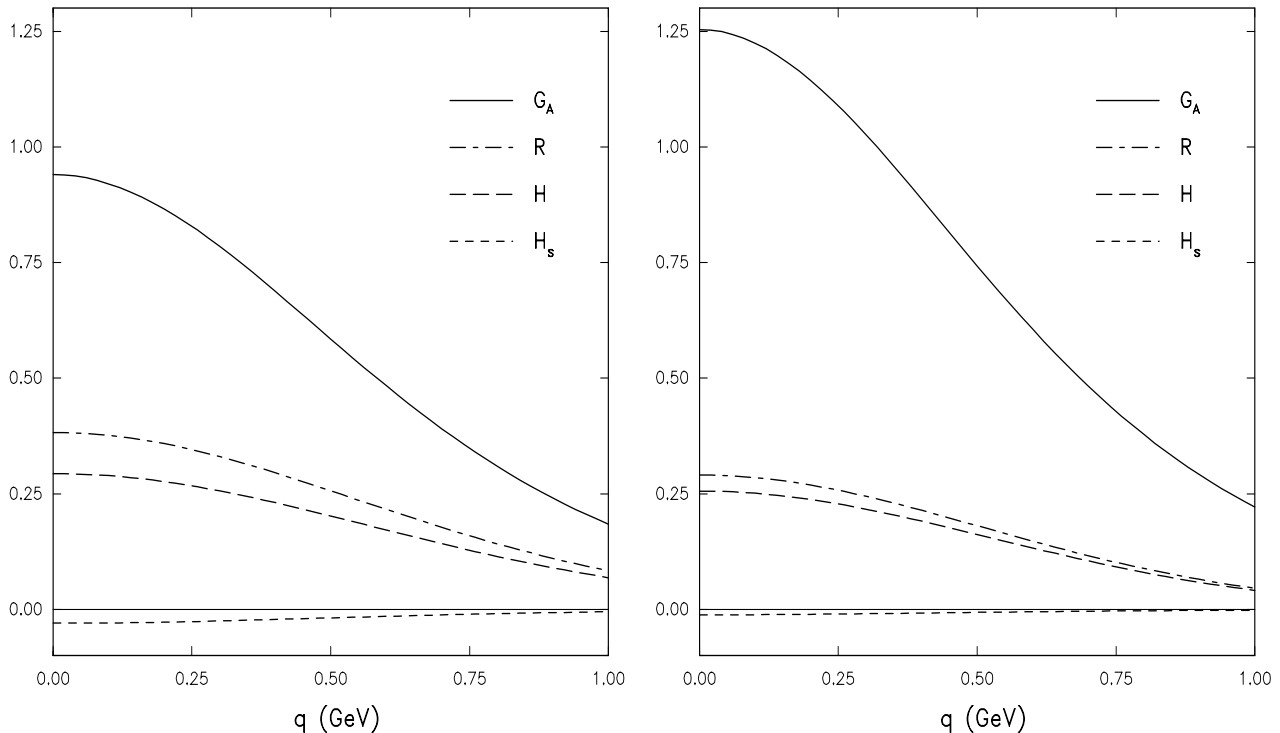


Figure 4.2: The momentum dependence of the nucleon matrix elements of the axial–vector current, which are associated with the strangeness conserving components. For the definition of the displayed quantities see eqs (2.55) and (4.31). Left panel (4.24), right panel (4.33). In both cases the parameters of the non–anomalous part of the action are given by (4.15).

Amusingly these results approximately satisfy the $SU(3)$ relation $R(0) = 3g_A/7$. However, it is important to establish that the isosinglet form factors $R(0)$ and $H(0)$ show almost no variation within the allowed parameter space of $\tilde{h} =, \tilde{g}_{VV\phi}$ and κ [25], while g_A exhibits quite a strong parameter dependence. Stated otherwise, the above given values for $R(0)$ and $H(0)$ represent firm predictions of the vector meson model. Furthermore these form factors are dominated by the contribution of the $\mathcal{A}_{ik}^{(3)}$ in eq (4.29) in contrast to G_A , which is dominated by $\mathcal{A}_{ik}^{(1)}$. Hence the above quoted $SU(3)$ relation between $R(0)$ and g_A is purely accidental for the parameters (4.24). The reason actually is the too small prediction for g_A . The correlations between $R(0)$ and $H(0)$ furthermore cause the strange contribution to axial current of the nucleon, $H_s(q^2)$ always to be tiny as can also be seen from figure 4.2. In order to confirm these statements a parameter set

$$\tilde{h} = -0.1, \quad \tilde{g}_{VV\phi} = 1.4, \quad \kappa = 1.0, \quad (4.33)$$

which properly reproduces g_A has been considered. This set is neither in the allowed parameter space nor does it reasonably describe the baryon spectrum. Nevertheless it is helpful for the discussion of axial properties of the nucleon. As can be observed from the right panel in figure 4.2 the isoscalar form factors are indeed strongly correlated and neither of them scales with G_A . For this set of parameters a significant deviation from the $SU(3)$ relation between g_A and $R(0)$ is obtained, namely $R(0) = 0.23g_A$.

Of course, it is very interesting to put these results into perspective with the EMC, SLAC and SMC measurements [21, 74, 75] of the axial form factors of the nucleon. Although the (firm) prediction $H(0) \approx 0.29$ favorably agrees with the value extracted from these experiments (0.24 ± 0.09 [96]) neither $R(0)$ nor $H(0)$ are suited to carry out this comparison because the

present model is formulated to incorporate flavor symmetry breaking effects but no independent information on $H_s(0)$ is currently available. Rather the vector meson model prediction for the structure function $\Gamma_1^p(q^2)$ (2.66), which depends on the individual quark pieces $H_{u,d,s}(0)$, should be compared with the “world average” 0.129 ± 0.010 at $q^2 = (10.7\text{GeV})^2$. Using the q^2 -dependent coefficients $C_{ns}(q^2)$ and $C_s(q^2)$ as given in ref [73] yields^f

$$\Gamma_1^p(q^2 = 10.7\text{GeV}^2) = \begin{cases} 0.11 & \text{set (4.24)} \\ 0.13 & \text{set (4.33)} \end{cases}. \quad (4.34)$$

Obviously, the vector meson model excellently explains what commonly is quoted as the proton spin puzzle. Once the model parameters are adjusted to give the correct value for g_A , the integral of the polarized structure function is exactly reproduced. The naïvely expected matrix element of the axial singlet current, $H(0)=1$, together with $g_A = 1.25$ and the assumption of flavor symmetry yields 0.22, which is much bigger.

In ref [40] the matrix elements describing the semi-leptonic hyperon decays have also been computed. As in the pseudo-scalar model these matrix elements are found to be consistent with the empirical data of the Cabibbo scheme after accounting for the too small value of the nucleon axial charge g_A . The deviation of these strangeness changing matrix elements from the $SU(3)$ symmetry relations is very moderate compared to the change which may be observed for the matrix element of strangeness conserving component R .

This section can be summarized by stating that for many aspects the vector meson model represents an improvement over the pseudo-scalar model, at least for the treatment within the rigid rotator approach. The explicit appearance of the vector mesons incorporates short range effects, which are not present in the pseudo-scalar model. As a consequence the two flavor contribution to the neutron proton mass difference as well as the axial singlet current matrix element are different from zero. Especially, since the model nicely describes the measurements on polarized lepton-nucleon scattering [21, 74, 75] one wonders whether more information on the proton spin structure can be extracted from this model. Related studies will be the major issue of the following section.

4.4 Two Component Approach to the Proton Spin Puzzle

Soon after the advent of the proton spin puzzle, explanations [148] for the smallness of $H(0)$ were attempted via the axial anomaly of QCD

$$\partial^\mu A_\mu^0 = 2i \sum_{i=u,d,s} m_i \bar{q}_i \gamma_5 q_i + \partial^\mu K_\mu, \quad (4.35)$$

where

$$K_\mu = -\frac{3ig_{QCD}^2}{4\pi^2} \epsilon_{\mu\nu\rho\sigma} \text{tr} \left\{ A^\nu \partial^\rho A^\sigma - \frac{2ig_{QCD}}{3} A^\nu A^\rho A^\sigma \right\} \quad (4.36)$$

is the Chern-Simons current of QCD. Here A_μ refers to the gauge fields of QCD. It has been suggested to associate the matrix element of $A_\mu^0 - K_\mu$ as the ordinary “matter” contribution to the axial singlet current. Hence one would suspect $\langle A_3^0 - K_3 \rangle \approx 1$. Essentially it is assumed that quark spin is cancelled by the gluonic contribution leading to a small $H(0)$. However,

^fThe variation of $\Gamma_1^p(q^2)$ with the scale q^2 is quite moderate as can be seen from table 1 of ref [96].

this treatment is suspicious because the matrix element of K_μ is not gauge invariant [149], in contrast to $\partial^\mu K_\mu$. To nevertheless firmly disentangle the “matter” and “glue” contributions to $H(0)$, it has been suggested to take the matrix elements of eq (4.35) and use pole saturation [150, 151] for the evaluation of the *RHS*

$$\begin{aligned}\langle P(\mathbf{p})|\partial^\mu A_\mu^0|P(\mathbf{p})\rangle &= 2i\langle P(\mathbf{p})|\sum_{i=u,d,s} m_i\bar{q}_i\gamma_5q_i|P(\mathbf{p})\rangle + \langle P(\mathbf{p})|\partial^\mu K_\mu|P(\mathbf{p})\rangle \\ &= 2M_N H(0)\bar{u}(\mathbf{p})\gamma_5u(\mathbf{p})\end{aligned}\quad (4.37)$$

The “matter” and “glue” components of $H(q^2)$ are obtained by identifying the appropriate terms on the *RHS*. The “matter” and “glue” pieces correspond to coupling constants $g_{\eta'NN}$ of the singlet pseudo-scalar field η' and g_{GNN} of an effective gluon field $G = \partial_\mu K^\mu$ to the nucleon. In this section the Skyrme model analogue [152] to this investigation, which is known as the two component approach to the proton spin⁹, will be described. For this analysis it is important to note the effects of the η mesons on baryon properties are commonly very moderate [142]. There seems to be only one exception, the strong interaction part of the neutron proton mass difference Δ_N [46].

As a first step the anomaly (4.35) has to be incorporated into the effective Lagrangian [98]

$$\mathcal{L}_{ax-an} = \frac{1}{\kappa}G^2 + \frac{i}{12}G\left(\ln\det U - \ln\det U^\dagger\right) + \dots\quad (4.38)$$

where the ellipses indicate flavor symmetry breaking terms associated with G . These terms are not specified here. The interested reader may consult ref [45] for details. In the context of effective meson Lagrangians the pseudo-scalar gluon field G is the equivalent of the scalar glueball field $\exp(\sigma)$, which was introduced in section 3.2 to imitate the scale anomaly of QCD. Since there is no kinetic term for G , it may be eliminated by its equation of motion. This gives rise to η meson masses

$$m_{\eta,\eta'}^2 = \frac{1}{4f_\pi^2}\left\{8\delta'(1+x) + \frac{\kappa}{6} \pm \sqrt{\left(8\delta'(1-x) + \frac{\kappa}{18}\right)^2 + \frac{4}{9}\kappa^2}\right\} + \dots,\quad (4.39)$$

thereby relating the constant κ to physical quantities. The coupling of the pseudo-scalar glueball field to the nucleon has to be put in explicitly [150, 151, 154]. In the soliton picture this is achieved by adding the chirally invariant term

$$\mathcal{L}_{GNN} = \frac{2t}{m_{\eta'}^4}\tilde{A}_\mu^0\partial^\mu G\quad (4.40)$$

to the effective Lagrangian. Finally one may consider a deviation from the nonet structure of the pseudo-scalar and vector meson fields by introducing the additional parameter s into eq (4.30)

$$A_i^0 = 2\sqrt{3}f_\pi\partial_i\eta^0 + s\tilde{A}_i^0.\quad (4.41)$$

This alters the prediction for the singlet matrix element

$$H(0) = (0.30 \pm 0.03)s,\quad (4.42)$$

⁹Ref. [153] provides a brief review and a list of references on the gauge invariant two component decomposition to the proton spin.

wherein an estimate for the “theoretical uncertainty” was made.

Sandwiching the anomaly equation, which essentially is the equation of motion of the η' field

$$\left(\partial_\mu\partial^\mu + m_{\eta'}^2\right)\eta' = \frac{s-t}{2\sqrt{3}f_\pi}\partial^\mu\tilde{A}_\mu^0 + \dots \quad (4.43)$$

between nucleon states, gives the Goldberg–Treiman relation for the axial singlet current [150]

$$g_{\eta'NN} = \frac{s-t}{s}\frac{M_p}{\sqrt{3}f_\pi}H(0) . \quad (4.44)$$

From eq (4.40) the gluon coupling constant is extracted to be

$$g_{GNN} = \frac{4tM_N}{sm_{\eta'}^4}H(0) = \frac{t}{t-s}\frac{2\sqrt{3}F_\pi}{m_{\eta'}^4}g_{\eta'NN} . \quad (4.45)$$

Solving these two equations for $H(0)$ finally gives the “matter”+“glue” decomposition of the axial singlet matrix element

$$H(0) = \frac{\sqrt{3}F_\pi}{2M_p}\left(g_{\eta'NN} - \frac{m_{\eta'}^4}{2\sqrt{3}F_\pi}g_{GNN}\right) = \text{“matter”} + \text{“glue”} . \quad (4.46)$$

The incorporation of the axial anomaly of QCD into the effective meson theory and abandoning the nonet structure has introduced two dimensionless parameters, s and t . For a given value of $H(0)$ the model determines the “fudge factor” s , while the strong interaction piece of the neutron proton mass difference, $\Delta_N \approx 2\text{MeV}$ can be employed to fix t . In order to explain the latter point it is illustrative to once again consider a typical contribution to Δ_N , which has already been indicated in eq (4.26),

$$\Delta_N = \frac{2y\delta'}{3\alpha^2}\int d^3r \sin F(r)\eta_T(r) + \dots, \quad (4.47)$$

where $\eta_T(r)$ refers to profile function of the non–strange combination of the η fields, $\eta_T = \eta_T(r)\hat{\mathbf{r}} \cdot \mathbf{\Omega}$. In ref [45] a detailed analysis of isospin breaking in the meson sector has been performed yielding $y \approx 0.42$. This analysis also includes second order symmetry breaking terms like $\text{tr}(\mathcal{M}U^\dagger\mathcal{M}^\dagger U)$, which in the soliton sectors give rise to non–vanishing coefficients Γ_T , Γ_S and Γ_{TS} in (2.36). From the equation of motion (4.43) it is apparent that the radial function $\eta_T(r)$, which is obtained by extremizing the spatial moment of inertia α^2 , strongly depends on the parameters s and t . It is then obvious that for a given value of $H(0)$ the parameters s and t can be determined from eq (4.42) and reproducing the strong interaction part of the neutron proton mass difference. For s of the order unity, t varies in the range $-0.5 \dots -1.5$, the uncertainty being caused by the one in $\Delta_N = (2.0 \pm 0.3)\text{MeV}$ [48]. In any event, $g_{\eta'NN}$ and g_{GNN} have opposite signs. For two sets of parameters^{*h*} the resulting two component decomposition is given in table 4.4. The important message to be extracted from these investigations is that soliton models for baryons indeed indicate that the smallness of the singlet matrix element is due to a cancellation mechanism between quark and gluon

^{*h*}The detailed analysis [45] of the symmetry breaking leads to minor changes in the parameters (4.15). A more recent investigation including electroweak interactions favors a smaller value $x \approx 25$ [141].

Table 4.4: The decomposition of the axial singlet matrix element $H(0)$ into “matter” and “glue” contributions for two parameter sets. I: $\tilde{h}=0.36$, $\tilde{g}_{VV\Phi}=1.88$, $\kappa=1.0$ and $x=28$. II: $\tilde{h}=0.4$, $\tilde{g}_{VV\Phi}=1.9$, $\kappa=1.0$ and $x=31.5$. Results are taken from refs [45, 155].

$H(0)$	Set I		Set II	
	“matter”	“glue”	“matter”	“glue”
0.0	0.54 ± 0.26	-0.54 ± 0.26	0.32 ± 0.26	-0.32 ± 0.26
0.1	0.57 ± 0.30	-0.47 ± 0.30	0.31 ± 0.30	-0.21 ± 0.27
0.2	0.58 ± 0.30	-0.38 ± 0.30	0.31 ± 0.26	-0.11 ± 0.28
0.3	0.58 ± 0.30	-0.28 ± 0.30	0.31 ± 0.30	-0.01 ± 0.28
0.4	0.58 ± 0.28	-0.18 ± 0.28	0.32 ± 0.27	0.08 ± 0.27

contribution. However, the pure matter component of $H(0)$ is still significantly smaller than unity, in contrast to the original speculation. Unfortunately, the predictions for the individual components of $H(0)$ possess uncertainties, which are quite large. Their accuracy could be improved if a more accurate value of the photon exchange contribution to $M_n - M_p$ were available.

Let us finish this chapter by mentioning that a similar analysis of Δ_N can be used to study the Gottfried sum rule

$$S_G = \frac{1}{3} \int_0^1 dx \{u(x) + \bar{u}(x) - d(x) - \bar{d}(x)\} \quad (4.48)$$

in soliton models. Here $u(x)$ denotes the up-quark distribution function in the nucleon, $\bar{u}(x)$ that of the anti up-quark, etc.. Assuming that all antiquarks are equally distributed predicts, $S_G = 1/3$ [156]. The evaluation based on the recent NMC data, however, gives a smaller value $S_G = 0.240 \pm 0.016$ [157]. Sandwiching the symmetry breaking term (2.15) between nucleon states and assuming isospin invariance yields

$$S_G = \frac{\Delta_N}{3(m_d - m_u)} \quad (4.49)$$

to leading order symmetry breaking. In ref [158] the effects of higher order corrections to this relation have been estimated to be negligibly small in Skyrme type models. As all available data on the difference $m_d - m_u$ are larger than Δ_N (see *e.g.* ref [33]), the soliton models provide an interesting explanation of the unexpected smallness of S_G .

5 The Bound State Approach

In the previous chapters several treatments of the three flavor soliton have been discussed. These have been based on the assumption that the time-dependent solution to the Euler-Lagrange equations is reasonably approximated by elevating the coordinates, which parametrize the flavor orientation, to time dependent quantities. Of course, such treatments are motivated by considering the flavor symmetry to be approximately realized, allowing for large amplitude fluctuations in the direction of symmetry breaking. Subsequently the symmetry breaking effects are treated within the space of these collective coordinates. The exact diagonalization of the resulting collective Hamiltonian is possible according to the Yabu-Ando approach [62] and

yields the baryon masses and wave-functions. Adopting, however, the opposite point of view that only small amplitude fluctuations are permitted, implying that the restoring forces exerted by the symmetry breaking are sizable, leads to the treatment, which has become known as the bound state approach. The reason for this notion is that hyperons are constructed out of the soliton and a kaon mode, which is bound in the background field of the soliton. This treatment has been initiated by Callan and Klebanov [130] and later been employed in many aspects as will be pointed out in the present chapter. Actually this approach is comparable to the old compound hypothesis, where hyperons are considered as molecules consisting of a nucleon and a kaon [159].

5.1 Small Fluctuations off the Soliton and the Kaon Bound State

The time dependent, small amplitude fluctuations are conveniently described by adopting the parametrization [130, 133]

$$U(\mathbf{r}, t) = \xi_\pi(\mathbf{r})U_K(\mathbf{r}, t)\xi_\pi(\mathbf{r}) , \quad U_K(\mathbf{r}, t) = \exp \left\{ \frac{i\sqrt{2}}{f_K} \begin{pmatrix} 0 & | & K(\mathbf{r}, t) \\ \hline K^\dagger(\mathbf{r}, t) & | & 0 \end{pmatrix} \right\} , \quad (5.1)$$

where ξ_π represents the hedgehog configuration (4.19). The general decomposition of the kaon field reads

$$K(\mathbf{r}, t) = \int \frac{d\omega}{2\pi} \sum_{GML} e^{-i\omega t} k_{GL}(r, \omega) \mathcal{Y}_{GML}(\hat{\mathbf{r}}) , \quad (5.2)$$

where \mathcal{Y}_{GML} are spinor spherical harmonics. These arise by coupling the orbital angular momentum \mathbf{L} together with isospin $t = 1/2$ to the grand spin, G . Since the soliton background, ξ_π has vanishing grand spin the radial functions k_{GL} are independent of the grand spin projection M and channels with different grand spins, G and G' decouple.

Although the general case (5.2) is of physical relevance (*cf.* section 5.2) the distinct channel $L = 1, G = 1/2$ is of special interest for examining the spectrum and static properties of the low-lying baryons. This channel contains a bound state, evolving from the zero-mode, which, in the flavor symmetric case, is associated with the rotation into the strange flavor direction. *I.e.* this bound state is the “would-be” Goldstone boson of the flavor transformations. A suitable *ansatz* for this P -wave mode reads

$$K_P(\mathbf{r}, t) = \int \frac{d\omega}{2\pi} e^{-i\omega t} k_P(r, \omega) \hat{\mathbf{r}} \cdot \boldsymbol{\tau} \begin{pmatrix} a_1(\omega) \\ a_2(\omega) \end{pmatrix} . \quad (5.3)$$

The spectral functions $a_i(\omega)$ become creation and annihilation operators in the process of quantization.

Expanding the Skyrme model action up to quadratic order in the fluctuating kaon field, K yields the Lagrangian explicitly given in eq (D.1). From this Lagrangian a differential equation for $k_P(r, \omega)$ is obtained, which can be cast in the generic form [131]

$$\left\{ -\frac{1}{r^2} \frac{d}{dr} \left(r^2 h(r) \frac{d}{dr} \right) + m_K^2 + V_P(r) - f(r)\omega^2 - 2\lambda(r)\omega \right\} k_P(r, \omega) = 0 . \quad (5.4)$$

The explicit expressions of the radial functions h, V_P, f and λ are also summarized in appendix D. The term linear in the frequency ω originates from the Wess-Zumino action (2.23) and

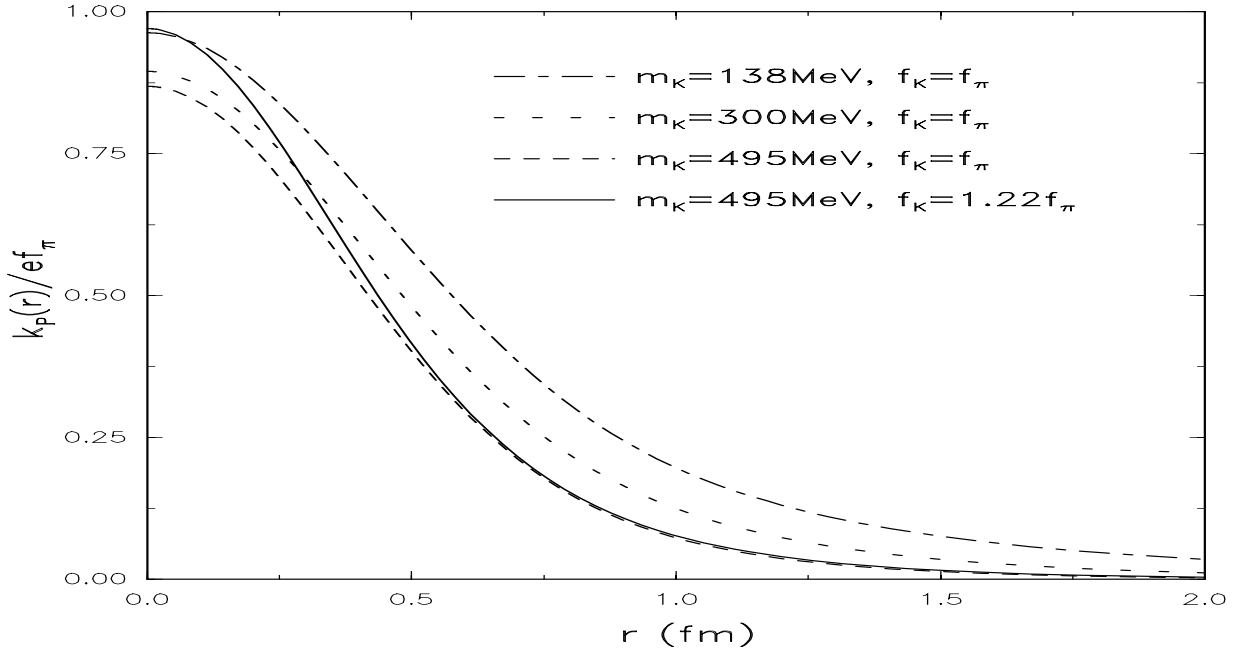


Figure 5.1: The radial dependence of the bound state wave function. The normalization is according to eq (5.5). The parameters in the non-strange sector are $f_\pi=93\text{MeV}$, $e=4.25$ and $m_\pi=138\text{MeV}$.

removes the degeneracy between solutions of positive and negative ω . From the orthogonality condition associated with the above differential equation the normalization [131]

$$2 \int dr r^2 k_P(r, \omega) (f(r)\omega + \lambda(r)) k_P(r, \omega) = \text{sgn}(\omega) \quad (5.5)$$

is derived. The above normalized solutions to the bound state equation (5.4) are drawn in figure 5.1. In particular, it is illustrated how the bound state wave-function evolves from the zero mode, which is proportional to $\sin(F/2)$, when the parameters are tuned from those describing the flavor symmetric case to physical ones. It can also be observed from figure 5.1 that the effect of $f_K \neq f_\pi$ is mainly a change in the profile at small r . This can be traced back to the bound state equation (5.4) because this inequality only shows up in the Skyrme term, which describes the short range behavior, as can be seen from eqs (D.2–D.5). The bound state energy computed with the physical parameters ($m_K = 495\text{MeV}$, $f_K = 1.22f_\pi$) is $\omega_P = 252\text{MeV}$ for the Skyrme parameter $e = 4.25$. Note that the asymptotic form of the bound state wave-function is $\exp(-\sqrt{m_K^2 - \omega_P^2}r)$ rather than $\exp(-m_K r)$ as one would expect for a kaon field.

The infinitesimal symmetry transformation for the variation of strangeness^a may be parametrized as $K(\mathbf{r}, t) \rightarrow K(\mathbf{r}, t) - i\epsilon$. It is then straightforward to obtain the strangeness charge from the associated Noether current [131]

$$S = \int \frac{d\omega}{2\pi} s(\omega), \quad s(\omega) = -\text{sgn}(\omega) \left(a_1^\dagger(\omega) a_1(\omega) + a_2^\dagger(\omega) a_2(\omega) \right), \quad (5.6)$$

where the condition (5.5) has been imposed. Obviously the $a_i(\omega)$ annihilate modes of strangeness -1 and $+1$ for positive and negative ω , respectively. Furthermore the bound state con-

^aThe generator for strangeness is defined to be $\text{diag}(0, 0, -1)$.

structed above, carries strangeness $S = -1$ suitable for the description of physical hyperons. The energy operator in a Fock space based on these operators is $\int (d\omega/2\pi) |\omega s(\omega)|$. Hence each occupation of the bound state not only lowers the strangeness by one unit but also increases the energy by ω . The mass of the Λ hyperon may then be identified with the sum $E + \omega$, where E refers to the soliton mass (2.11).

At present only the degeneracy of the baryons with respect to strangeness has been removed. In order to generate states corresponding to physical baryons and to obtain the mass differences of baryons with identical strangeness but different spin and/or isospin, collective coordinates are introduced into the field configuration (5.1) [130]

$$U(\mathbf{r}, t) = \begin{pmatrix} A(t) & | & 0 \\ \hline & & \\ 0 & | & 1 \end{pmatrix} \xi_\pi(\mathbf{r}) U_K(\mathbf{r}, t) \xi_\pi(\mathbf{r}) \begin{pmatrix} A^\dagger(t) & | & 0 \\ \hline & & \\ 0 & | & 1 \end{pmatrix} \quad (5.7)$$

where $A(t)$ is an $SU(2)$ matrix. Substituting this *ansatz* into the action augments the collective Lagrangian by terms involving the time derivative $A^\dagger \dot{A} = (i/2) \boldsymbol{\tau} \cdot \boldsymbol{\Omega}$, cf. eq (2.29)

$$L_{\boldsymbol{\Omega}} = \frac{1}{2} \alpha^2 \boldsymbol{\Omega}^2 - \frac{1}{2} \int \frac{d\omega}{2\pi} c(\omega) \boldsymbol{\Omega} \cdot \left(\sum_{i,j=1}^2 a_i^\dagger(\omega) \boldsymbol{\tau}_{ij} a_j(\omega) \right). \quad (5.8)$$

For the P-wave channel the explicit form of the spectral function $c(\omega)$ is given in eq (D.6). An infinitesimal isospin transformation of the meson configuration (5.7) may be related to its time derivative

$$\left[\frac{i}{2} \boldsymbol{\tau}_i, U \right] = -D_{ij} \frac{\partial \dot{U}}{\partial \Omega_j}, \quad (5.9)$$

where D_{ij} denotes the adjoint representation of the two flavor rotation A , cf. eq (2.30). As a consequence the total isospin is completely carried by the collective coordinates

$$I_i = -D_{ij} \frac{\partial L_{\boldsymbol{\Omega}}}{\partial \Omega_j}. \quad (5.10)$$

This identity motivates the decomposition of the total spin \mathbf{J} into soliton and bound state pieces, \mathbf{J}^F and \mathbf{J}^K , respectively. The former is defined as

$$\mathbf{J}^F = \frac{\partial L_{\boldsymbol{\Omega}}}{\partial \boldsymbol{\Omega}} = \alpha^2 \boldsymbol{\Omega} - \frac{1}{2} \int \frac{d\omega}{2\pi} c(\omega) \left(\sum_{i,j=1}^2 a_i^\dagger(\omega) \boldsymbol{\tau}_{ij} a_j(\omega) \right). \quad (5.11)$$

By construction this piece satisfies the relation $(\mathbf{J}^F)^2 = \mathbf{I}^2$. The remainder of the total spin can be cast into the form

$$\mathbf{J}^K = -\frac{1}{2} \int \frac{d\omega}{2\pi} d(\omega) \left(\sum_{i,j=1}^2 a_i^\dagger(\omega) \boldsymbol{\tau}_{ij} a_j(\omega) \right). \quad (5.12)$$

In the Skyrme model the spectral function $d(\omega)$ turns out to be unity when the fluctuating fields are normalized according to eq (5.5). This, however, is not necessarily the case (see

e.g. section 6.3). The above described decomposition, $\mathbf{J} = \mathbf{J}^F + \mathbf{J}^K$, is further motivated by re-arranging [130] the collective rotation (5.7)

$$\xi_\pi(\mathbf{r}, t) = A(t)\xi_\pi(\mathbf{r})A^\dagger(t), \quad K_P(\mathbf{r}, t) = A(t) \int \frac{d\omega}{2\pi} k_P(r, \omega) \hat{\mathbf{r}} \cdot \boldsymbol{\tau} \begin{pmatrix} a_1(\omega) \\ a_2(\omega) \end{pmatrix}. \quad (5.13)$$

Due to the hedgehog structure a spatial rotation can be re-phrased as a right multiplication of $A(t)$ and an isospin rotation of the isospinor $(a_1(\omega), a_2(\omega))$. The former leads to \mathbf{J}^F , while \mathbf{J}^K is the Noether charge associated with the latter. It is thus clear that \mathbf{J}^K formally is the isospin associated with the isospinor $(a_1(\omega), a_2(\omega))$.

In what follows, only the kaon bound state with $S = -1$ is supposed to be occupied. This projects out

$$c_P = c(\omega_P), \quad d_P = d(\omega_P) \quad (5.14)$$

from the spectral integrals. With this restriction to the kaon bound state, the collective Hamiltonian associated with L_Ω becomes

$$H_\Omega = \frac{1}{2\alpha^2} \left(\mathbf{J}^F + \frac{c_P}{2} \sum_{i,j=1}^2 a_i^\dagger \boldsymbol{\tau}_{ij} a_j \right)^2 = \frac{1}{2\alpha^2} (\mathbf{J}^F + \chi \mathbf{J}^K)^2, \quad (5.15)$$

where the parameter $\chi = -c_P/d_P$ has been introduced. It is then straightforward to obtain the baryon mass formula [131]

$$M_B = E + |S\omega_P| + \frac{1}{2\alpha^2} (\chi J(J+1) + (1-\chi)I(I+1)). \quad (5.16)$$

It should be remarked that the contribution^b, $c_P(c_P+1)/4S(S-2)$ [160], which is quartic in the kaon field, has been omitted because this order has not consistently been treated.

This approach to quantize the kaon bound state may be phrased in terms of slow (Ω) and fast (ω) moving degrees of freedom. The former is of the order $1/N_C$ while the latter are $\mathcal{O}(N_C^0)$. This distinction allows one to introduce the notion of Berry phases. For the kaon bound state this idea has extensively been discussed in ref [161].

Substituting the bound state solution of the differential equation (5.4) into (D.6) provides the mass differences displayed in table 5.1. In these computations the physical values for the masses and decay constants of the pseudo-scalar mesons have been adopted, $m_\pi = 138\text{MeV}$, $m_K = 495\text{MeV}$, $f_\pi = 93\text{MeV}$ and $f_K = 113\text{MeV}$. It was common, however, in previous calculations to employ parameters, which in the two flavor model reproduce the nucleon and Δ masses

$$\begin{aligned} f_\pi &= 64.5\text{MeV}, \quad e = 5.45, \quad m_\pi = 0 \quad [10]; \\ f_\pi &= 54.0\text{MeV}, \quad e = 4.84, \quad m_\pi = 138\text{MeV} \quad [162]. \end{aligned} \quad (5.17)$$

These parameter sets have much smaller decay constants. In the meantime it has, however, become clear that the absolute mass of the soliton is strongly reduced by quantum corrections [12, 13]. Then the absolute masses are reasonably reproduced using the physical decay constants. It is therefore more appealing to use the physical decay constants and rather consider mass differences than absolute masses (This point of view has also been assumed in the previous chapters). Then the Skyrme parameter e is the only one which is not determined in

Table 5.1: The parameters of the mass formula (5.16) and the predictions for the mass differences (in MeV) of the low-lying baryons with respect to the nucleon in the bound state approach. Various values of the Skyrme parameter e are used. The data in parenthesis include the quartic term. For completeness also the results corresponding to the reduced decay constants (5.17) are included with $m_K=495$ MeV and $f_K=1.22f_\pi$ [163].

	$e = 4.00$	$e = 4.25$	$e = 4.50$	Expt.	[10]	[162]
$\alpha^2(\text{GeV}^{-1})$	6.013	5.115	4.389	—	5.050	5.133
$\omega_P(\text{MeV})$	265	253	240	—	221	209
χ	0.261	0.332	0.401	—	0.500	0.394
Λ	218(207)	205(187)	189(168)	177	183(165)	165(147)
Σ	342(330)	334(318)	325(305)	254	283(264)	283(265)
Ξ	530(498)	505(462)	479(424)	379	442(392)	418(371)
Δ	249(249)	293(293)	342(342)	293	293(293)	292(292)
Σ^*	407(394)	431(415)	462(442)	446	432(413)	398(380)
Ξ^*	595(563)	602(559)	616(562)	591	591(541)	533(486)
Ω	814(754)	805(724)	805(702)	733	774(681)	697(610)

the meson sector. It may, *e.g.* be fixed by demanding the experimental Δ -nucleon splitting leading to $e = 4.25$. From table 5.1 we see that the resulting bound state energy is somewhat larger than the empirical value $\omega_{\text{emp}} = (M_\Xi - M_N)/2 \approx 189\text{MeV}$ causing the flavor symmetry breaking in the baryon spectrum to be overestimated. This is in particular the case for the $\frac{1}{2}^+$ baryons. The inclusion of the (presumably inconsistent) quartic term provides a slight improvement. Except for the Ω baryon, which has $S = -3$, this term has, however, only minor influence. Similarly, an empirical value for the hyperfine parameter χ can be extracted from the mass formula (5.16) $3\chi/2(1 - \chi) = (M_{\Sigma^*} - M_\Sigma)/(M_\Sigma - M_\Lambda)$, *i.e.* $\chi \approx 0.62$, which is larger than the model prediction. In case the parameters (5.17) are used together with $m_K = 495$ MeV and $f_K = 1.22f_\pi$, the agreement with the experimental mass difference is significantly improved. This is not surprising because the energy scale is reduced. However, there is no deeper reason to take the experimental ratio between the decay constant once f_π is moved away from 93MeV. Originally, the bound state approach was assumed to underestimate the flavor symmetry breaking in the baryon spectrum [131, 164, 165]. A better agreement with experiment was claimed [163] to be due to the kinetic type symmetry breakers in eq (2.19), *cf.* the discussion in the paragraph after eq (2.44). When taking the physical values for the decay constants we are confronted with the situation that the bound state approach actually overestimates the flavor symmetry breaking in the baryon spectrum. One wonders whether kinematical corrections change this conclusion. As a very crude estimate one might replace the kaon mass by the reduced mass of the kaon-soliton system into the bound state equation (5.4). For $e = 4.25$ the bound state energy decreases to 191MeV, which, of course, improves on the baryon mass differences.

Alternative parametrizations of the fluctuating kaon fields essentially reach similar results for the mass differences when identical parameters are used, see *e.g.* ref [165].

The bound state approach corresponds to filling up levels of a quantum system, without taking into account the correlations between the fluctuating meson fields. Two heavy meson correlations [166], as they could appear in the case of the Ξ baryon, might alter the description.

^bNote that $\left(\sum_{i,j=1}^2 a_i^\dagger \tau_{ij} a_j\right)^2 = S(S-2)$, when canonical commutation relations are assumed for the a_i .

In order to make statements about baryon properties in the bound state approach, the appropriate wave functions have to be constructed. These baryon states are products of eigenstates associated with the collective coordinates and elements of the Fock space built from the kaon bound state. The former are $SU(2)$ D–functions, while the latter are not only eigenstates of the strangeness operator (5.6) but also of $(\mathbf{J}^K)^2 = S(S-2)/4$ and the associated projection \mathbf{J}_3^K , defined in eq (5.12). These states are coupled to good total spin, (\mathbf{J}) , isospin, (\mathbf{I}) and hypercharge, $Y = S + 1$

$$|J, J_3; I = J_F, I_3; Y\rangle = \mathcal{N} C_{IJ_3^F, J^K J_3^K}^{JJ_3} D_{I_3, -J_3^F}^{I=J^F}(A) |S; J^K = |S|/2, J_3^K\rangle . \quad (5.18)$$

The identity, $I = J^F$ results from eq (5.10). Furthermore C refers to a Clebsch–Gordon coefficient and \mathcal{N} is a normalization constant. An extensive list of explicit baryon wave–functions is provided in table 2 of ref [133]. Apparently the collective coordinates, A , have to be quantized like a fermion if the occupation number of the kaon bound state is odd and like a boson if it is even [130].

The meson configuration (5.7) is then substituted into the covariant expression for the vector current V_μ^a (2.50) and the matrix elements between the baryon states (5.18) are computed. The magnetic moment operator is related to the spatial components of the electromagnetic combination (2.51),

$$\mu = \frac{M_N}{2} \int d^3r \epsilon_{3ij} x_i V_j^{\text{e.m.}} = \mu_{S,0} J_3^K + \mu_{S,1} J_3^K + \frac{2I_3 J_3^F}{I(I+1)} (\mu_{V,0} + \mu_{V,1} |S|) . \quad (5.19)$$

where the angular velocities have been eliminated according to the quantization prescription (5.11). The isovector part arises from matrix elements of $D_{33} = D_{00}^1(A)$ in the space of the collective coordinates, A . The coefficients $\mu_{S,V;0,1}$ (taken from ref [133]) are summarized in eq (D.7) of appendix D. The expressions not involving the fluctuating kaon field ($\mu_{S,V;0}$) are identical to their two flavor counterparts [10]. Hence the effects of virtual strange quark excitations in the nucleon are ignored. Substituting the bound state wave–function and computing the matrix elements of the operators in eq (5.19) between the baryon states (5.18) then provides the baryon magnetic moments in the bound state approach. For $e = 4.25$ these are listed in table 5.2. Although the physical value $f_\pi = 93\text{MeV}$ has been used, these results do not differ significantly from those obtained with the sets (5.17) [132, 133]. As in the collective approach (chapter 2) the absolute values of the magnetic moments come out too small. The only exception is the transition matrix element for $\Sigma^0 \rightarrow \Lambda$. Considering the bound state results for the magnetic moments in the light of the U–spin relations (table 3.2), sizable deviations from these relations are observed. However, these deviations are either in the wrong direction (μ_{Σ^+}/μ_p) or are too strong ($\mu_{\Sigma^-}/\mu_{\Xi^-}$) when compared with the experimental situation. Also the prediction for the ratio $\mu_\Lambda/\mu_{\Xi^-} \approx 1.7$ is in drastic disagreement with the physical value (~ 0.9). Obviously ample space for improvement for predictions of magnetic moments is left within the bound state description of baryons.

Generalizing the operator (5.19) to depend on the momentum transfer (analogous to eq (2.59)) allows one to compute the magnetic dipole ($M1$) transitions for the electromagnetic decay of $\frac{3}{2}^+$ baryons to $\frac{1}{2}^+$. Similarly the orbital angular momentum $l = 2$ component of the electric charge operator may be employed to compute the quadrupole transition ($E2$). The calculated [167] decay widths exhibit the same pattern as in the non–relativistic quark model [168] and the bag model [169]; *i.e.* the transitions $\Sigma^{*0} \rightarrow \Lambda\gamma$, $\Xi^{*0} \rightarrow \Xi^0\gamma$ and $\Sigma^{*+} \rightarrow \Sigma^+\gamma$ have large widths (100–200keV), while all others are about an order of magnitude smaller. In

Table 5.2: The magnetic moments in the bound state (BS) approach to the Skyrme model. Results are given in nucleon magnetons as well as ratios of the proton magnetic moment.

Baryon	BS		Expt.	
	μ_B	μ_B/μ_p	μ_B	μ_B/μ_p
p	1.78	1.00	2.79	1.00
n	-1.42	-0.80	-1.91	-0.68
Λ	-0.56	-0.31	-0.61	-0.22
Σ^+	1.97	1.10	2.42	0.87
Σ^0	0.43	0.24	—	—
Σ^-	-1.07	-0.60	-1.16	-0.42
Ξ^0	-1.31	-0.74	-1.25	-0.45
Ξ^-	-0.33	-0.18	-0.69	-0.25
$\Sigma^0 \rightarrow \Lambda$	-1.54	-0.86	-1.61	-0.58

particular the width of the reaction $\Sigma^{*-} \rightarrow \Sigma^- \gamma$ is predicted to be almost zero. All ratios $E2/M1$ for the transition matrix elements are predicted to be negative. As a consequence of delicate cancellations these ratios are largest for $\Sigma^{*-} \rightarrow \Sigma^- \gamma$ and $\Xi^{*0} \rightarrow \Xi^0 \gamma$ (about -0.5 and -0.2, respectively) [167]. For the other transitions the ratios are again down by an order of magnitude. The $E2$ contribution to the reaction $\Sigma^{*0} \rightarrow \Sigma^0 \gamma$ even vanishes identically.

For all decay widths and most of the $E2/M1$ -ratios similar results are obtained in the collective model [170]. For the reactions $\Sigma^{*-} \rightarrow \Sigma^- \gamma$ and $\Xi^{*0} \rightarrow \Xi^0 \gamma$ the collective approach predicts much smaller (~ -0.05) $E2/M1$ -ratios. In any event, the widths of these decays are very tiny. Hence the corresponding $E2/M1$ -ratios are subject to delicate cancellations. In the collective approach the symmetry breaking parameter can continuously be varied. This feature has been employed to verify the U -spin selection rule within the Skyrme model [170]. This rule states that the transition matrix elements associated with the decays of the negatively charged $\frac{3}{2}^+$ baryons vanish in the flavor symmetric case [171].

It has been indicated above that in the bound state approach the nucleon wave-function is identical to the one of the two flavor model. Hence one expects the strangeness content fraction X_s (2.81) to vanish. However, this is not the case. The non-trivial strangeness in the nucleon is caused by the fact that the Fock space built from the solutions to the bound state equation (5.4) is different from the one based on free kaon modes, *i.e.* in the absence of the soliton [172]. In particular, the nucleon state is annihilated by the operator $a(\omega)$ of the Fock space in the presence of the soliton. The creation and annihilation operators $\tilde{a}^{(\dagger)}(\omega)$ in the Fock space of free kaons are related to those (5.3) for the bound state problem

$$\begin{pmatrix} \tilde{a}(\omega) \\ \tilde{a}^\dagger(\omega) \end{pmatrix} = \int \frac{d\omega'}{2\pi} \begin{pmatrix} \mathcal{A}_{++}(\omega, \omega') & \mathcal{A}_{-+}(\omega, \omega') \\ \mathcal{A}_{+-}(\omega, \omega') & \mathcal{A}_{--}(\omega, \omega') \end{pmatrix} \begin{pmatrix} a(\omega) \\ a^\dagger(\omega) \end{pmatrix}, \quad (5.20)$$

where the transformation matrix \mathcal{A} is computed from the overlaps between the solutions of the bound state equation (5.4) and free kaon modes in a spherical wave decomposition [172, 173]. As a consequence of the mixing between the operators in the two distinct Fock spaces the nucleon state is not annihilated by $\tilde{a}(\omega)$. The calculations based on the transformation (5.20) are essentially equivalent to a treatment within the random phase approximation (RPA [174]), introducing correlations between the different vacua. Hence the nucleon matrix element of the

“free” strangeness charge

$$S_{\text{free}} = - \int \frac{d\omega}{2\pi} \text{sgn}(\omega) \tilde{a}^\dagger(\omega) \tilde{a}(\omega) \quad (5.21)$$

is different from zero. This causes a non-vanishing strangeness content fraction X_s , which can be computed from the momentum space integrals of the off-diagonal elements of \mathcal{A} . This yields $X_s \approx 3\%$ [172, 173], which is significantly lower than the corresponding result in the collective approach, *cf.* section 2.4. It should, however, be noted that in general these RPA-type integrals diverge; X_s represents one of the few exceptions. Thus, in principle, a regularization scheme would be required, which might also alter the prediction for X_s .

We would like to finish this section by remarking that in addition to the P-wave bound state discussed above, the equation (5.4) contains a solution of orbital angular momentum $l = 0$

$$K_S(\mathbf{r}, t) = \int \frac{d\omega}{2\pi} e^{-i\omega t} k_S(r, \omega) \begin{pmatrix} a_1(\omega) \\ a_2(\omega) \end{pmatrix}, \quad (5.22)$$

with $|\omega| < m_K$ [131]. The appearance of the bound state is completely due to dynamics exposed by the background soliton. This is in contrast to the P-wave bound state, which arises from the existence of a zero-mode in the flavor symmetric case. The S-wave bound state is well suited to describe the odd parity $\Lambda(1405)$. For the *ansatz* (5.22) a right transformation of the collective coordinates A (which represents the spatial rotation of the soliton) can also be rephrased as an isospin transformation of the isospinor $(a_1(\omega), a_2(\omega))$. Hence the quantization is identical to the one for the P-wave. For the parameters established above ($f_\pi = 93\text{MeV}$, $e = 4.25$, etc.) the mass difference of the odd parity Λ to the nucleon is predicted to be 450MeV, about 40MeV over the experimental value. Not surprisingly a deficit compared to the experimental mass difference of about 100MeV is obtained when the smaller energy scale (5.17) is used. In ref [175] the magnetic moment of this hyperon has been calculated to be about 10% of the magnetic moment of the proton.

5.2 Remarks on Meson Baryon Scattering

Shortly after the rediscovery of the Skyrme model by Adkins, Nappi and Witten [10] the model was employed to compute the amplitudes of meson baryon scattering. For an extensive list of references the reader is referred to the review article [6]. Similar to the bound state approach (section 5.1) such calculations involve time-dependent meson fluctuations $\eta_a(\mathbf{r}, t)$ off the soliton. A possible parametrization in the flavor rotating frame is given by

$$U(\mathbf{r}, t) = e^{i\lambda^a \eta_a(\mathbf{r}, t)} U_0(\mathbf{r}) e^{i\lambda^a \eta_a(\mathbf{r}, t)}, \quad (5.23)$$

where the static configuration $U_0(\mathbf{r})$ is defined in eq (2.25). In the next step the action is expanded up to quadratic order in η_a in the background of the static soliton. From the solutions to the corresponding equations of motions the T -matrix elements, $\tau_{K'l'l}^{IY}$ for meson-soliton scattering may be extracted [176, 177]. The T -matrix is diagonal in the intrinsic isospin (I), hypercharge (Y) and grand spin (K) (the latter represents the vector sum of total spin and isospin). Furthermore l and l' denote the orbital angular momentum of the in- and outgoing meson, respectively. For example, $\tau_{1/2\ 1\ 1}^{1/2\ 1}$ represents the T -matrix in the bound state channel discussed in section 5.1. Assuming adiabaticity of the collective rotation and ignoring

symmetry breaking effects, the T -matrix for physical channels may be obtained within the geometrical coupling scheme [178, 177]

$$T_{\text{phys}} = (-1)^{s'-s} \frac{\dim R \dim R'}{\dim R^{\text{tot}}} \sum_{IY} \sum_i \sum_K (2i+1)(2K+1) \left\{ \begin{matrix} K & i & J \\ s' & l' & I \end{matrix} \right\} \left\{ \begin{matrix} K & i & J \\ s & l & I \end{matrix} \right\} \\ \left[\begin{array}{cc|cc} R_{\text{tot}} & \gamma' & R' & \mathbf{8} \\ i & Y+1 & s'1 & IY \end{array} \right] \left[\begin{array}{cc|cc} R & \mathbf{8} & R_{\text{tot}} & \gamma \\ s1 & IY & i & Y+1Y \end{array} \right] \tau_{K'l'}^{IY}. \quad (5.24)$$

The objects in curly and squared brackets are $6-j$ symbols and $SU(3)$ isoscalar factors [61], respectively. Furthermore s and R refer to spin and $SU(3)$ representations *e.g.* $s = \frac{1}{2}$ and $R = \mathbf{8}$ for the nucleon. The index *tot* finally denotes the total $SU(3)$ representation of the meson baryon system. For further details we refer to the original article by Karliner and Mattis [177]. It should be stressed that this coupling scheme is purely geometrical, and dynamic contributions from the collective rotations have completely been ignored. The so-obtained physical T -matrix allows to reasonably describe a huge number of scattering processes from $\pi N \rightarrow \pi N$ to $\bar{K}N \rightarrow \pi\Sigma^*$. The authors of ref [177] characterize the agreement with experiment to be good in the case that the initial states are πN , mixed for $\bar{K}N$ but poor for KN .

Although appealing, this approach suffers from the shortcoming that flavor symmetry breaking effects are not accounted for. Dominantly this concerns the thresholds, which should account for different baryon masses. Furthermore the baryon wave-functions have been assumed to be members of a certain $SU(3)$ representation R , which is also reflected in the appearance of the isoscalar factors in eq (5.24). These problems have recently been studied [179] by parametrizing the time-dependent chiral field

$$U(\mathbf{r}, t) = A(t) (U_0(\mathbf{r}))^{\frac{1}{2}} A^\dagger(t) \exp(i\lambda^a \phi^a(\mathbf{r}, t)) A(t) (U_0(\mathbf{r}))^{\frac{1}{2}} A^\dagger(t). \quad (5.25)$$

Obviously the ϕ_a are the meson fluctuations in the laboratory frame *i.e.* they are defined in the background of the collectively rotating hedgehog. Separating the radial dependence of the meson fluctuations allows one to define target wave-functions

$$\phi_{ss_3, i_3, Y}^{(t_a y_a)}(\mathbf{r}, \omega) = \sum_{l, m} C_{t_a \tau_\alpha, m_a \mu_\alpha}^{ii_3} C_{lm, j_\alpha \nu_\alpha}^{ss_3} \phi_{t_a y_a}^{l \tau_\alpha j_\alpha}(r, \omega) \Psi(\tau_\alpha, \mu_\alpha y_\alpha; j_\alpha, \nu_\alpha, 1) Y_{lm}(\hat{\mathbf{r}}), \quad (5.26)$$

where a Fourier transformation with respect to the time coordinate has been performed. Furthermore, Ψ represents the solution to the Yabu-Ando eigenvalue problem (A.8). By varying the strength of the symmetry breaking parameters, it is possible to interpolate between the flavor symmetric approach described above and the two flavor computations for πN scattering [178]. Furthermore the adiabatic approximation has been abandoned, *i.e.* time derivatives of the collective coordinates are (at least approximately) included, in this approach. This dominantly effects the P -wave channels. Finally the scattering amplitudes are extracted from the solutions of the differential equations for the radial fields $\phi_{t_a y_a}^{l \tau_\alpha j_\alpha}(r)$. It should be stressed that these calculations are rather tedious, in particular because the differential equations also contain the flavor orientation, A , of the hedgehog. As can be seen from the Argand diagrams displayed in ref [179] the agreement with experimental data is impressive for the long wavelength behavior of the scattering amplitudes, in particular for the number and approximate positions of the main decay channels of baryon resonances. Hence this extensive study of meson baryon scattering represents another interesting application of the collective treatment of

Table 5.3: Comparison of the collective and the bound state approaches to strangeness.

Collective approach (YA)	Bound state approach (CK)
Symmetry breaking small (light strange quark)	Symmetry breaking large (heavy strange quark)
↓	↓
Strange components as collective coordinates (analogous to zero modes)	Restoring force for strange fluctuations ("harmonic" potential)
↓	↓
Collective Hamiltonian in flavor SU(3) including symmetry breaking	Bound State Energy and Wave Function
↓	↓
Exact diagonalization	Collective quantization of spin and isospin
↓	↓
<i>HYPERONS</i>	<i>HYPERONS</i>

symmetry breaking. As a side product also the bound state equation of Callan and Klebanov is obtained.

An examination of scattering processes in the bound state approach appears to be technically unfeasible. Considering for example for the description of a reaction like $KN \rightarrow \pi\Sigma$, the action has to be expanded up to third order in the meson fluctuations because the scattering meson fields (K, π) as well as the hyperon (Σ) are constructed as small amplitude fluctuations in the background of the soliton.

5.3 Comparison: Collective Approach versus Bound State Approach

In this section the interesting question will be addressed as to how far the collective and bound state approaches to flavor symmetry breaking can be related. In the case of the collective treatment this discussion will be restricted to the rigid rotator. To further simplify this comparison, the symmetry breaking operator proportional to γ will be assumed to be the only one contained in the collective Hamiltonian (2.36). Although the conceptual ideas of these approaches have already been discussed earlier they are compactly summarized and compared in table 5.3.

The numerical results for the strangeness content fraction, X_s , discussed in the previous section as well as those obtained in the context of the rigid rotator suggest that the two approaches have a common limit for large symmetry breaking. For this purpose, Yabu and Ando [62] have expanded the eigenvalue problem (see appendix A for the relevant definitions)

$$\left\{ C_2(SU(3)) + \omega^2 \sin^2 \nu \right\} \Psi(A) = \epsilon_{SB} \Psi(A) , \quad \omega^2 = \frac{3}{2} \gamma \beta^2 \quad (5.27)$$

in inverse powers of the effective symmetry breaking parameter, *i.e.*, $1/\omega \rightarrow 0$. According to the discussion of chapter 2, the isoscalar functions $f_{M_L, M_R}(\nu)$ contained in the collective space wave-function $\Psi(A)$ (A.8) are strongly pronounced at $\nu = 0$ in the limit of large symmetry

breaking. The trigonometrical functions appearing in the differential equation (5.27,A.9) may thus be linearized in the limit $1/\omega \rightarrow 0$. Introducing the scaled ‘‘Euler angle’’

$$\xi = \sqrt{\omega}\nu \quad (5.28)$$

then makes possible the above mentioned expansion [62] in $1/\omega$

$$\left\{ \frac{-1}{4\xi^2} \frac{d}{d\xi} \left(\xi^3 \frac{d}{d\xi} \right) + \xi^2 + \left(\frac{1}{\xi^2} - \frac{1}{6} \right) \mathbf{T}^2 + \frac{1}{4} (Y^2 + Y_R^2 + Y Y_R) + \frac{1}{2} (\mathbf{J}^2 + \mathbf{I}^2) \right\}_{M_L, M_L'}^{M_R, M_R'} f_{M_L, M_L'}(\nu) - \frac{1}{\omega} \left[-\frac{1}{2} \xi \frac{d}{d\xi} + \frac{1}{3} \xi^4 \right] f_{M_L, M_R}(\nu) = \frac{1}{\omega} \epsilon_{\text{SB}} f_{M_L, M_R}(\nu) + \mathcal{O} \left(\frac{1}{\omega^2} \right). \quad (5.29)$$

In this expression the projection of the quadratic Casimir operator onto different components (M_L, M_R) of the intrinsic isospin and spin has been indicated. The only operator in eq (5.29), which is non-diagonal in these indices, is the ‘‘intrinsic grand spin’’ $\mathbf{T} = \tilde{\mathbf{J}} - \tilde{\mathbf{I}}$, where $\tilde{\mathbf{J}}$ and $\tilde{\mathbf{I}}$ are the intrinsic spin and isospin operators which act on the indices M_L and M_R respectively. Hence the combinations

$$F(L, M)(\nu) = \sum_{M_L, M_R} C_{I-M_L, J M_R}^{LM} f_{M_L, M_R}(\nu) \quad (5.30)$$

diagonalize \mathbf{T}^2 . The eigenvalues are $L(L+1)$ with [62]

$$\max(|I - J|, |S|/2) \leq L \leq I + J, \quad (5.31)$$

where the *LHS* is due to the constraint $S = Y - Y_R = 2(M_L - M_R)$. For the baryons we are interested in ($N, \Lambda, \dots, \Omega$), the value $L = |S|/2$ is always permitted. Obviously, the ‘‘intrinsic grand spin’’ plays the role of the kaon spin operator \mathbf{J}^K in the bound state approach. This can also be argued from the decomposition (5.13) because in the intrinsic frame ($A = 1$) the grand spin of ξ_π vanishes, while the grand spin of K is nothing but the isospin of the kaon. In leading order of the $1/\omega$ expansion, the eigenvalue problem for $F(L, M)(\nu)$ can be formulated as that of a four dimensional harmonic oscillator. Hence the eigenvalues may readily be evaluated. The state of lowest energy corresponds to the case when the wave-function $F(L, M)(\nu)$ does not possess a node. The associated contribution to the mass formula (2.41) is [62]

$$\frac{1}{2\beta^2} \epsilon_{\text{SB}} = \frac{\omega}{2\beta^2} |S| + \frac{1}{4\beta^2} [I(I+1) + J(J+1)] + \frac{1}{8\beta^2} \left[3S - 2|S| + \frac{1}{2} S^2 \right] + \mathcal{O} \left(\frac{1}{\omega} \right), \quad (5.32)$$

where a constant contribution has been ignored because we are only interested in mass differences. Comparison with the mass formula of the bound state approach (5.16) suggests the identifications

$$\omega_P = \frac{1}{2\beta^2} \sqrt{\frac{3}{2} \beta^2 \gamma} \approx 337 \text{MeV}, \quad \chi = 1 - \frac{\alpha^2}{2\beta^2} \approx 0.33. \quad (5.33)$$

These data are obtained from eq (2.48), which have been computed for $e = 4.0$. Although the analytical identifications (5.33) have been obtained in the large symmetry breaking limit, the numerical values reasonably agree with the exact results in the bound state approach even for the physical case (see table 5.1). It should be remarked that the inclusion of induced

components (2.45) is important to arrive at this result. Otherwise it can generally be shown that $2\beta^2 < \alpha^2$ [62] causing the estimate for χ to be negative.

Another way to establish the correspondence between the two approaches in the large symmetry breaking limit, is to expand [160, 180] the Lagrangian (2.32) in powers of the strange components contained in the three flavor collective matrix $A(t)$ (2.25). This procedure provides approximations for the parameters in the mass formula (5.16). Unfortunately, this approximation overestimates the bound state energy ω_P , while the hyperfine parameter χ comes out too small.

In the flavor symmetric case one has $\omega_P = 0$ and $\chi = 1$ due to the appearance of the zero mode. Hence the bound state mass formula reproduces the degeneracy of the baryons within a given $SU(3)$ multiplet. One may therefore ask the question whether or not the two approaches can be related in the small symmetry breaking limit as well. However, it can easily be shown that this is not the case. In the first non-trivial order of flavor symmetry breaking the Gell–Mann–Okubo mass formula (2.38) is not recovered in the bound state approach. That is,

$$2(M_N + M_\Xi) - M_\Sigma - 3M_\Lambda = \frac{1}{2\alpha^2} \left(1 - \chi + \frac{3}{4}\chi(\chi - 1) \right), \quad (5.34)$$

which is of the order of 50MeV. The second term is due to the quartic term which has been omitted in eq (5.16). Hence the equivalence between the bound state and collective approaches can only be established in the large symmetry breaking limit. This statement is further supported by comparing the recent computations of the electric quadrupole moments of the $\frac{3}{2}^+$ baryons. In the bound state approach all these moments are found to be proportional to the baryon isospin [181]. In the collective approach this proportionality only appears in the large symmetry breaking limit, while for small breaking the quadrupole moments happen to be linked to the baryon charge [121], see also section 3.1. In any event, comparing the results displayed in tables 2.1 and 5.1 unambiguously shows that the collective approach provides better agreement with the experimental mass differences than the bound state approach when the parameters of the Skyrme model are determined from meson data.

5.4 Baryons with a Heavy Quark

In this section a brief remark on an additional application of the bound state approach will be given. This application concerns the description of baryons containing one (very) heavy quark like charm or bottom. For a more detailed survey article the reader may consult ref [182]. Although these investigations are outside the three flavor regime they are worth mentioning here because they are based on the bound state approach described in section 5.1.

The heavy baryons are constructed from a D or B meson bound in the background field of the soliton. The straightforward generalization of this treatment consists of substituting the masses and decay constants of such heavy mesons into the bound state equation (5.4) [183]. However, this treatment does not incorporate the heavy quark symmetry [184, 185] which (among other features) states that pseudo-scalar and vector mesons containing one heavy quark are degenerate. Hence an effective meson Lagrangian suitable for the soliton picture of heavy baryons should contain heavy vector meson fields (Q_μ) in addition to the heavy pseudo-scalar fields (P). The interaction among the light degrees of freedom should be described in accordance to chiral symmetry. Since the heavy mesons are composed of a heavy quark (c, b) and a light (anti)quark (up, down or strange) this concept describes the interaction of the heavy and light mesons. The latter fields support the soliton.

When constructing the part of the action, which describes the interaction of the heavy and light mesons, one minimally extends the chirally and heavy quark symmetric action to finite masses, M , of the heavy meson [186]

$$\begin{aligned} \mathcal{L}_H = & D_\mu P (D^\mu P)^\dagger - \frac{1}{2} Q_{\mu\nu} (Q^{\mu\nu})^\dagger - M^2 P P^\dagger + M^{*2} Q_\mu Q^{\mu\dagger} \\ & + 2iMd \left(P p_\mu Q^{\mu\dagger} - Q_\mu p^\mu P^\dagger \right) - \frac{d}{2} \epsilon^{\alpha\beta\mu\nu} \left[Q_{\nu\alpha} p_\mu Q_\beta^\dagger + Q_\beta p_\mu (Q_{\nu\alpha})^\dagger \right] \\ & - \frac{2\sqrt{2}icM}{m_V} \left\{ 2Q_\mu F^{\mu\nu}(\rho) Q_\nu^\dagger + \frac{i}{M} \epsilon^{\alpha\beta\mu\nu} \left[D_\beta P F_{\mu\nu}(\rho) Q_\alpha^\dagger + Q_\alpha F_{\mu\nu}(\rho) (D_\beta P)^\dagger \right] \right\}. \end{aligned} \quad (5.35)$$

Here the mass M of the heavy pseudo-scalar meson P is allowed to differ from the mass M^* of the heavy vector meson, Q_μ . Note that the heavy mesons are conventionally defined as *row* vectors in isospace. When light vector mesons are included, the covariant derivative introduces the additional parameter α :

$$D_\mu P^\dagger = \left\{ \partial_\mu - i\alpha g \rho_\mu + \frac{1-\alpha}{2} \left(\xi \partial_\mu \xi^\dagger + \xi^\dagger \partial_\mu \xi \right) \right\} P^\dagger. \quad (5.36)$$

The covariant field tensor of the heavy vector meson is defined as

$$(Q_{\mu\nu})^\dagger = D_\mu Q_\nu^\dagger - D_\nu Q_\mu^\dagger. \quad (5.37)$$

The parameters d , c and α have still not been very accurately determined. Commonly $d \approx 0.53$ and $c \approx 1.60$ are used [186]. The assumption of vector meson dominance for the electromagnetic form factors of the heavy mesons suggests $\alpha \approx 1$ [187], although other values are allowed as well.

Suitable *ansätze* for the P-wave heavy mesons are

$$\begin{aligned} P^\dagger &= \frac{\Phi(r)}{\sqrt{4\pi}} \hat{\mathbf{r}} \cdot \boldsymbol{\tau} \chi e^{i\omega t}, & Q_0^\dagger &= \frac{\Psi_0(r)}{\sqrt{4\pi}} \chi e^{i\omega t}, \\ Q_i^\dagger &= \frac{1}{\sqrt{4\pi}} \left[i\Psi_1(r) \hat{r}_i + \frac{1}{2} \Psi_2(r) \epsilon_{ijk} \hat{r}_j \tau_k \right] \chi e^{i\omega t} \end{aligned} \quad (5.38)$$

which actually are motivated by the form of the induced fields for the collective rotation into the strange flavor direction (4.22). The isospinor χ contains spectral functions as in eq (5.3). The bound state solutions for the heavy mesons have been constructed for the cases that the light soliton only contains the pseudo-scalar fields (*i.e.* the Skyrmion) [188, 189] as well as the inclusion of the light vector mesons in the soliton configuration as in eq (4.19) [189]. A consistent description of both the light and heavy baryon masses can only be obtained when the light vector mesons were included. This improvement is due to the additional freedom in choosing the parameter α . For $\alpha \approx 0$ the binding energy $\epsilon_b = 780\text{MeV}$ of the heavy baryon Λ_b is reproduced for the experimental masses $M = 5.28\text{GeV}$, $M^* = 5.33\text{GeV}$. Using $M = 1.87\text{GeV}$, $M^* = 2.01\text{GeV}$ in the charm sector then predicts $\epsilon_c = 536\text{MeV}$ for the binding of Λ_c , which reasonably agrees with the experimental value of 630MeV . The associated heavy meson wave-functions are displayed in figure 5.2

Here just a brief introduction has been provided to the description of heavy quark baryons as composite systems of solitons and heavy mesons in order to demonstrate that the bound state approach can suitably be extended. Many aspects of this approach have not been addressed here. In particular the issue of kinematical corrections has been ignored [190]. These corrections are supposedly sizable as a consequence of the large meson masses involved.

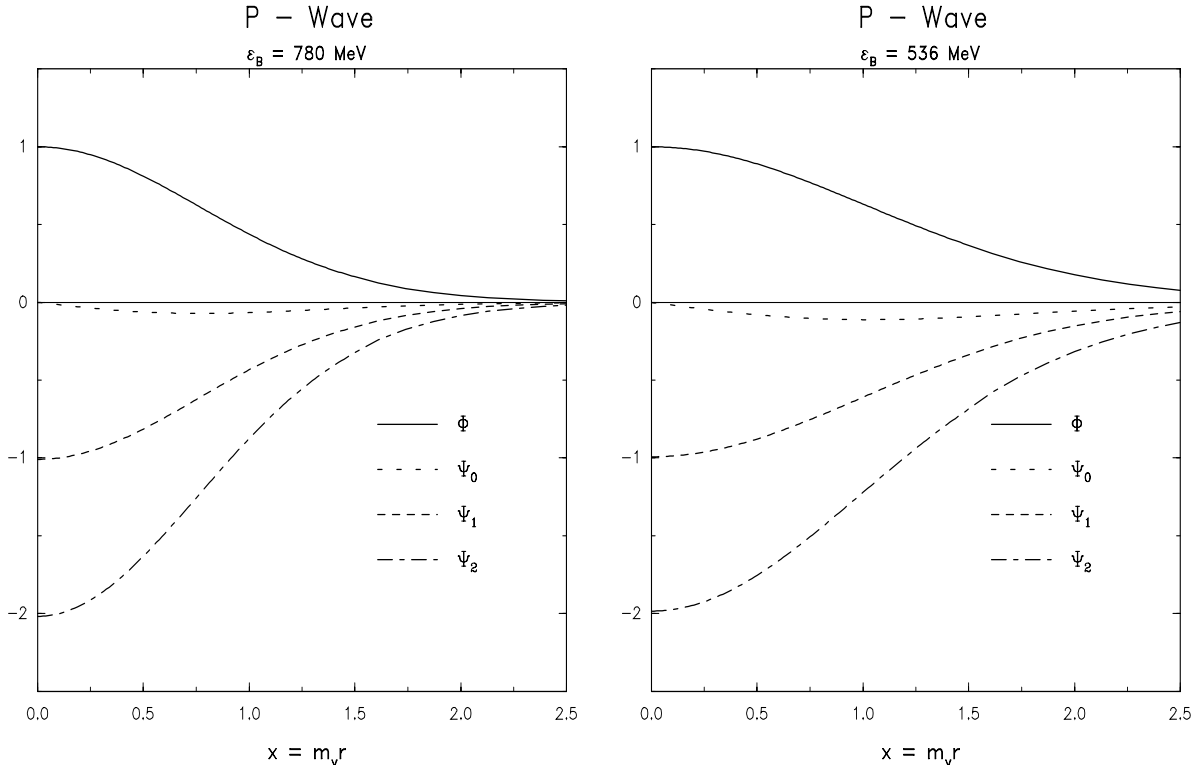


Figure 5.2: The radial dependence of the heavy meson bound state wave functions in both the bottom (left) and charm (right) sectors. Here m_V is the light vector meson mass (4.15). This figure is taken from ref [189].

6 Explicit Quark Degrees of Freedom: The NJL Model

The meson [191, 192] as well as the soliton [193] sectors of the Nambu–Jona–Lasinio [17] (NJL) model have already been reviewed elsewhere. It is therefore beyond the scope of the present article to describe this model in detail. Nevertheless a short discussion on the general aspects of the model is in order to put the NJL model in perspective. The main interest in the NJL model is due to the fact that it constitutes a simple, chirally symmetric theory of the quark flavor dynamics while the flavor symmetry breaking is completely located in the current quark mass terms. This feature is analogous to QCD. Otherwise the NJL model is much simpler in structure making possible the derivation of the effective meson theory, which is equivalent to the NJL Lagrangian. The derivation of this meson theory is commonly referred to as bosonization. The main issue of the present chapter will be to demonstrate that the previously discussed aspects of soliton models for three flavors can be obtained not only in purely mesonic models, but also from such a microscopic theory of the quark flavor dynamics. For the sake of argument the NJL model will be employed although similar studies have been performed in bag models [194].

6.1 The NJL Soliton

In the NJL model the free Dirac Lagrangian is supplemented by a chirally symmetric four quark contact interaction [17]

$$\mathcal{L}_{\text{NJL}} = \bar{q}(i\cancel{\partial} - \hat{m}^0)q + 2G_{\text{NJL}} \sum_{a=0}^8 \left((\bar{q}Q^a q)^2 + (\bar{q}Q^a i\gamma_5 q)^2 \right). \quad (6.1)$$

Here q denotes the quark field, which represents a vector in flavor space

$$q = \begin{pmatrix} u \\ d \\ s \end{pmatrix}, \quad (6.2)$$

with each entry being a Dirac spinor. In the following isospin symmetry is assumed, *i.e.* the current quark mass matrix is taken to be $\hat{m}^0 = \text{diag}(m^0, m^0, m_s^0)$. The flavor matrices $Q^a = (\frac{1}{3}, \frac{\lambda^1}{2}, \dots, \frac{\lambda^8}{2})$ are identical to those employed in the preceding chapters. The dimensionful coupling constant, G_{NJL} will shortly be determined from meson properties. Except for the quark mass term this Lagrangian is invariant under the chiral transformation

$$q_L \rightarrow Lq_L, \quad q_R \rightarrow Rq_R, \quad q_{R,L} = \frac{1}{2}(1 \pm \gamma_5)q, \quad (6.3)$$

which has already been considered earlier (2.18).

Using functional integral bosonization techniques the quark fields can be integrated out from the model Lagrangian (6.1) in favor of composite meson fields [18, 19]. The resulting effective action is the sum, $\mathcal{A}_{\text{NJL}} = \mathcal{A}_F + \mathcal{A}_m$, of a fermion determinant

$$\mathcal{A}_F = \text{Tr} \log(i\mathcal{D}) = \text{Tr} \log_{\Lambda} \left\{ i\cancel{\partial} - \frac{1}{2} \left[(1 + \gamma_5)M + (1 - \gamma_5)M^\dagger \right] \right\} \quad (6.4)$$

and a purely mesonic part

$$\mathcal{A}_m = \int d^4x \left\{ -\frac{1}{4G_{\text{NJL}}} \text{tr} \left(M^\dagger M - \hat{m}^0(M + M^\dagger) + (\hat{m}^0)^2 \right) \right\}. \quad (6.5)$$

The complex matrix $M = S + iP$ parametrizes the scalar and pseudo-scalar meson fields. From eq (6.4) it can be deduced that the meson fields behave like

$$M \rightarrow LMR^\dagger \quad (6.6)$$

under the chiral transformation (6.3). Employing the polar decomposition, $M = U\Phi$, the transformation property (2.2) of the chiral field becomes apparent. As the quark coupling constant is dimensionful, the functional trace (6.4) is not renormalizable and requires regularization. This is indicated by the cut-off Λ , which apparently acquires a physical meaning. As in the original study [195] of the NJL soliton, this cut-off will be introduced via the $O(4)$ invariant proper time regularization [196], which is applied to the fermion determinant in Euclidean space. After Wick-rotating ($t = -ix_4 = -i\tau$) to Euclidean space, the fermion determinant in general is a complex quantity, $\mathcal{A}_F = \mathcal{A}_R + \mathcal{A}_I$. The proper time regularization scheme consists of replacing the real part, \mathcal{A}_R by a parameter integral with the short distance contribution cut off

$$\mathcal{A}_R = \frac{1}{2} \text{Tr} \log_{\Lambda} \left(\cancel{\mathcal{D}}_E^\dagger \cancel{\mathcal{D}}_E \right) = -\frac{1}{2} \int_{1/\Lambda^2}^{\infty} \frac{ds}{s} \text{Tr} \exp \left(-s \cancel{\mathcal{D}}_E^\dagger \cancel{\mathcal{D}}_E \right). \quad (6.7)$$

Although the imaginary part

$$\mathcal{A}_I = \frac{1}{2} \text{Tr} \log \left((\cancel{\mathcal{D}}_E^\dagger)^{-1} \cancel{\mathcal{D}}_E \right) \quad (6.8)$$

is finite it will be regularized^a as well.

Although the starting point (6.1) has been a quark theory, the bosonization procedure has led to an action ($\mathcal{A}_R + \mathcal{A}_I$), which essentially is a functional of the meson configuration M . Expanding this action in derivatives of M yields Lagrangians which are similar to one of the Skyrme model [19]. However, models obtained in this fashion may not necessarily support soliton solutions. Therefore the complete fermion determinant will be retained and exactly be computed for a given configuration M . In doing so, it will be recognized that the notion of quarks cannot be abandoned completely.

In order to determine the parameters of the model, the real part \mathcal{A}_R is expanded up to quadratic order in the meson fields and subsequently continued back to Minkowski space. In this context a convenient parametrization for the scalar and pseudo-scalar fields is [199]

$$M = \xi_0 \xi_f \Sigma \xi_f \xi_0. \quad (6.9)$$

The matrix Σ is Hermitian whereas the matrices ξ_0 and ξ_f are unitary. The space-time dependent pseudo-scalar meson fluctuations $\eta_a(x)$ are contained in $\xi_f(x) = \exp(i \sum_{a=0}^8 \eta_a(x) Q^a)$, while the quantity ξ_0 has been introduced to simplify the inclusion of the soliton. In the baryon number zero sector ξ_0 is replaced by the unit matrix. Varying the action with respect to Σ yields the Schwinger–Dyson or gap equation, which determines the vacuum expectation value $\langle \Sigma \rangle = \text{diag}(m, m, m_s)$

$$m_i = m_i^0 + m_i^3 \frac{N_C G_{\text{NJL}}}{2\pi^2} \Gamma \left(-1, \left(\frac{m_i}{\Lambda} \right)^2 \right) = m_i^0 - 2G_{\text{NJL}} \langle \bar{q}q \rangle_i. \quad (6.10)$$

Here $m_i = m, m_s$ denote the constituent masses of non-strange and strange quarks, respectively. The appearance of a non-vanishing quark condensate $\langle \bar{q}q \rangle_i$ is the outstanding feature of the spontaneous breaking of chiral symmetry [200]. Henceforth the scalar fields will be approximated by their vacuum expectation values, $\Sigma = \langle \Sigma \rangle$. By expanding the action in the pseudo-scalar fields η^a their inverse propagator can be extracted [63, 201]. The on-shell condition requires this meson propagator to possess a pole at the physical meson masses, m_{phys} ,

$$\frac{(m_i^0 + m_j^0)(m_i + m_j)}{2G_{\text{NJL}}} + \Pi_{ij}(m_{\text{phys}}^2) = 0. \quad (6.11)$$

Here the polarization operator

$$\Pi_{ij}(q^2) = -2q^2 f_{ij}^2(q^2) + 2(m_i - m_j)^2 f_{ij}^2(q^2) - \frac{1}{2}(m_i^2 - m_j^2) \left(\frac{\langle \bar{q}q \rangle_i}{m_i} - \frac{\langle \bar{q}q \rangle_j}{m_j} \right) \quad (6.12)$$

is given in terms of the quark condensates, $\langle \bar{q}q \rangle_i$ and the off-shell meson decay constants

$$f_{ij}^2(q^2) = \frac{1}{4}(m_i + m_j)^2 \frac{N_c}{4\pi^2} \int_0^1 dx \Gamma \left(0, [(1-x)m_i^2 + xm_j^2 - x(1-x)q^2]/\Lambda^2 \right). \quad (6.13)$$

The Feynman parameter integral reflects the quark loop contained in the bosonized form (6.4) of the NJL model action. From eq (6.13) the on-shell meson decay constants can be read off

$$f_\pi^2 = m^2 \frac{N_c}{4\pi^2} \int_0^1 dx \Gamma \left(0, [m^2 - x(1-x)m_\pi^2]/\Lambda^2 \right) \quad (6.14)$$

$$f_K^2 = \frac{1}{4}(m + m_s)^2 \frac{N_c}{4\pi^2} \int_0^1 dx \Gamma \left(0, [xm^2 + (1-x)m_s^2 - x(1-x)m_K^2]/\Lambda^2 \right). \quad (6.15)$$

^aRegularization of the imaginary part is supposed to incorrectly reproduce the anomalous decay $\pi^0 \rightarrow \gamma\gamma$ [197]. More recently it has been speculated [198] that this short-coming may be cured by higher order contributions to the ABJ triangle anomaly [53] when the cut-off is finite.

Table 6.1: The up and strange constituent and current masses, the cutoff as well the pion and kaon decay constants in the NJL model. These results are taken from [203].

m (MeV)	m_s (MeV)	m_s^0/m_u^0	Λ (MeV)	f_π (MeV)	f_K (MeV)
350	577	23.5	641	93.0	104.4
400	613	22.8	631	93.0	100.3
450	650	22.4	633	93.0	97.4
500	687	22.3	642	93.0	95.5
350	575	24.3	698	99.3	113.0
400	610	23.9	707	103.0	113.0
450	647	23.6	719	105.7	113.0
500	685	23.4	734	107.9	113.0

Substituting in eq (6.12) the coupling constant, G_{NJL} by the quark condensate $\langle \bar{q}q \rangle$ via the gap-equation (6.10), immediately leads to the Gell-Mann–Oakes–Renner (GMOR) relations, $f_\pi^2 m_\pi^2 = m^0 \langle \bar{u}u + \bar{d}d \rangle$, and similarly for f_K [202].

The above eqs (6.10)–(6.15) relate the parameters of the NJL model, G_{NJL} , Λ , m^0 and m_s^0 , to the physical masses and decay constants. Using $m_\pi = 135\text{MeV}$, $m_K = 495\text{MeV}$ and fixing the pion decay constant $f_\pi = 93\text{MeV}$ yields too small a value for the kaon decay constant^b, see table 6.1. On the other hand, requiring $f_K = 113\text{MeV}$ gives too large a value for f_π . In view of the discussion after eq (2.44) the too small prediction for the ratio f_K/f_π gives rise to the suspicion that the NJL model will underestimate the baryon mass differences.

For the discussion of static soliton configurations it is appropriate to introduce the Dirac Hamiltonian h

$$i\beta\mathcal{D}_E = -\partial_\tau - h, \quad (6.16)$$

which is time independent, *i.e.* $[\partial_\tau, h] = 0$. Furthermore it will be assumed that h is Hermitian. Denoting the eigenvalues of h by ϵ_ν , the action \mathcal{A}_F (6.4) is found [204, 205, 206] to be decomposable into a vacuum part

$$\mathcal{A}_0 = \frac{1}{2}T \sum_\nu |\epsilon_\nu| \quad (6.17)$$

and valence (anti-)quark parts

$$\mathcal{A}_V^{\{\eta_\nu\}} = -T \sum_\nu \eta_\nu |\epsilon_\nu| = -TE_V^{\{\eta_\nu\}}. \quad (6.18)$$

Here T denotes the Euclidean time interval under consideration. The total action involves all possible sets of occupation numbers, $\eta_\nu = 0, 1$, *i.e.* $\mathcal{A}_F = \mathcal{A}_0 + \log \sum_{\{\eta_\nu\}} \mathcal{A}_V^{\{\eta_\nu\}}$. These occupation numbers furthermore specify the baryon number

$$B = \sum_\nu \left(\eta_\nu - \frac{1}{2} \right) \text{sgn}(\epsilon_\nu). \quad (6.19)$$

The soliton configuration uniquely determines the eigenvalues ϵ_ν . Hence these occupation numbers functionally depend on the field configuration as well once the baryon number is

^bDetermining f_π or f_K fixes the ratio Λ/m . This leaves one adjustable parameter, which for convenience is chosen to be the up constituent mass, m .

fixed. The vacuum contribution, \mathcal{A}_0 is obviously divergent. The standard recipe to extract the vacuum part from the regularized determinant^c (6.7) is to consider the limit $T \rightarrow \infty$. In that limit the eigenvalues of the differential operator ∂_τ lie densely and the sum over these eigenvalues is replaced by an integral

$$\mathcal{A}_0 = -\frac{T}{2} \sum_\nu \int_{-\infty}^{\infty} \frac{dz}{2\pi} \int_{1/\Lambda^2}^{\infty} \frac{ds}{s} \exp \left\{ -s \left(z^2 + \epsilon_\nu^2 \right) \right\} . \quad (6.20)$$

This expression allows one to read off the vacuum part of the energy, E_0 , in the proper time regularization scheme because $A_0 \rightarrow -TE_0$ when $T \rightarrow \infty$.

As in the purely mesonic models, the soliton configuration in the baryon number one sector is assumed to be of hedgehog structure

$$\xi_0(\mathbf{r}) = \exp \left\{ \frac{i}{2} \boldsymbol{\tau} \cdot \hat{\mathbf{r}} F(r) \right\} , \quad (6.21)$$

(for the moment, the time dependent fluctuations are ignored ($\xi_f = 1$)). Then the Dirac Hamiltonian becomes

$$h = \boldsymbol{\alpha} \cdot \mathbf{p} + \begin{pmatrix} m \exp(i\gamma_5 \boldsymbol{\tau} \cdot \hat{\mathbf{r}} F(r)) & | & 0 \\ \hline 0 & | & m_s \end{pmatrix} . \quad (6.22)$$

As in the meson models the static soliton configuration does not effect the strange degrees of freedom. In order to compute $E_V^{(\eta_\nu)}$ the occupation numbers have to be determined from eq (6.19) for a given profile function $F(r)$. In the case of $B = 1$ the vacuum contribution $-(1/2) \sum_\nu \text{sgn}(\epsilon_\nu)$, is either zero or one. Hence at most one of the η_ν can be different from zero. Minimization of the total energy enforces this to be the one with the lowest absolute value of the energy eigenvalue, $|\epsilon_\nu|$. This level is referred to as the valence quark state. The only non-vanishing occupation therefore is $\eta_{\text{val}} = [1 + \text{sgn}(\epsilon_{\text{val}})]$. The total energy functional is finally given by

$$E_{\text{tot}}[F] = E_0[F] - E_0[F \equiv 0] + \frac{N_C}{2} \eta_{\text{val}} \epsilon_{\text{val}} + E_m , \quad (6.23)$$

$$E_0[F] = \frac{N_C}{2} \int_{1/\Lambda^2}^{\infty} \frac{ds}{\sqrt{4\pi s^3}} \sum_\nu \exp(-s\epsilon_\nu^2) , \quad E_m = m_\pi^2 f_\pi^2 \int d^3r (1 - \cos F(r)) , \quad (6.24)$$

where the dependence on the number of colors has been made explicit and a constant contribution, which is associated with the energy of the trivial meson configuration, has been subtracted. The mesonic part of the energy, E_m originates from A_m (6.5) after substituting $G_{\text{NJL}} = m^0 m / m_\pi^2 f_\pi^2$ [19], see also eqs (6.12) and (6.11).

Soliton configurations, which minimize the functional $E[F]$, indeed exist for $m \geq 350\text{MeV}$ [195]. These solitons are constructed by iteration, *i.e.* the Hamiltonian h (6.22) is diagonalized for a test profile $F(r)$. The resulting eigenvalues and eigenvectors are substituted into the equation of motion $\delta E / \delta F(r) = 0$ to update the profile function. This procedure is repeated until convergence is achieved^d. This procedure, of course, provides the eigenvalues and eigenstates of the Dirac Hamiltonian, ϵ_ν and $|\nu\rangle$, respectively. The resulting profile function,

^cThe imaginary part vanishes as long as h is Hermitian and time independent.

^dSee ref [207] for a detailed prescription of the numerical treatment. A parametrical solution to the minimization problem was considered in ref [208].

Table 6.2: The soliton energy E_{tot} and its various contributions according to the sum (6.23) as functions of the constituent quark mass m . All numbers are in MeV.

m	350	400	500	600	700	800
E_{tot}	1236	1239	1221	1193	1161	1130
E_V	745	633	460	293	121	-55
E_0	459	571	728	869	1012	1103
E_m	31	34	33	31	28	26

$F(r)$ is similar to the one displayed in figure 2.1, however, for $B = 1$ the equation of motion only allows a solution with the reversed sign, $F(0) = -\pi$. This is in contrast to the purely mesonic models discussed in the previous chapters. The reason being that the quarks fields are maintained. This fixes the sign of the (anomalous) baryon current unambiguously whereas the sign of the Wess–Zumino (2.23) term could not be determined from meson properties. For the self-consistent soliton of the NJL model the various contributions to the energy are displayed in table 6.2. By expanding the action in arbitrary fluctuations off the hedgehog configuration it can furthermore be shown, that the term linear in these fluctuations vanishes when $\delta E/\delta F(r) = 0$ is satisfied [199]. Hence the hedgehog configuration represents a true solution to the full Euler–Lagrange equations. Obviously the total energy is quite insensitive to variations of the constituent quark mass.

A major difference between the soliton in the NJL model and the soliton solutions considered in the previous chapters is the non-topological character of the NJL model soliton. As a consequence, this soliton does not necessarily represent the global minimum in the $B = 1$ sector. Indeed, the soliton energy is larger than the three quark threshold as long as $m \lesssim 420\text{MeV}$ and a continuous deformation can be constructed of the soliton to the configuration of three non-interacting quarks. Furthermore, the valence quark energy stays positive for a large range in the parameter space implying that the baryon number is carried by the explicit occupation of this orbit, *i.e.* $\eta_{\text{val}} = 1$. This illustrates the above mentioned feature that the notion of quarks cannot be abandoned completely despite the model being a functional of meson fields. At this point it should be mentioned that this situation changes drastically when (axial)vector meson fields are added to the NJL model Lagrangian. For the corresponding self-consistent soliton the valence quark is strongly bound and the baryon number is actually carried by the polarized vacuum, *i.e.* $\eta_{\text{val}} = 0$ [209, 210]. This feature has been taken as a strong support for Witten’s conjecture [50] that in effective meson theories the baryon number current is identical to the topological current, B_μ , defined in eq (2.9). The argument goes as follows [209]: The leading term in the gradient expansion of the baryon number current in the NJL model is indeed the topological current [211]. However, the gradient expansion exclusively takes into account the vacuum part of the action, while explicitly occupied levels are ignored. Hence for these currents to be equivalent, the baryon number must be carried by the vacuum. This, apparently, is the case for the self-consistent soliton in the NJL model with (axial)vector meson fields. These results of the (axial)vector meson NJL model may furthermore be interpreted as an indication that explicit valence quark and (axial)vector meson fields should not simultaneously be contained in a model. This conclusion that keeping both may cause double counting effects has also been reached from phenomenological studies on baryon properties in soliton models [46, 25]

6.2 The Collective Approach to the NJL Model

In this section the parameters in the collective Hamiltonian (2.36) will be derived within the context of the pseudo–scalar NJL model, which is defined in eq (6.1). For this purpose the flavor rotating field configuration is parametrized as

$$M(\mathbf{r}, t) = A(t)\xi_0(\mathbf{r})A^\dagger(t)\langle\Sigma\rangle A(t)\xi_0(\mathbf{r})A^\dagger(t) \quad A(t) \in SU(3) , \quad (6.25)$$

which represents the NJL model equivalent to eq (2.28). Obviously, only the pseudo–scalar fields rotate in flavor space while the scalar fields are kept at their vacuum expectation values. In order to evaluate the fermion determinant (6.4) for this field configuration, it is appropriate to transform the quark fields to the flavor rotating frame [206]: $q = Rq'$. This transformation eliminates the “outer” rotations in (6.25) at the expense of an induced rotational part

$$h_{rot} = \sum_{a=1}^8 Q^a \Omega_a , \quad (6.26)$$

with the angular velocities defined as in eq (2.29). In the rotating frame the Dirac operator reads

$$i\beta\mathcal{D}' = i\partial_t - h - h_{rot} - h_{SB} , \quad (6.27)$$

where h is the static one–particle Hamiltonian (6.22). The symmetry breaking part of the Dirac operator is compactly displayed by introducing $\mathcal{T} = (\xi_0^\dagger + \xi_0)/2 + \gamma_5(\xi_0^\dagger - \xi_0)/2$

$$\begin{aligned} h_{SB} &= \mathcal{T}\beta \left(A^\dagger \langle \Sigma \rangle A - \langle \Sigma \rangle \right) \mathcal{T}^\dagger \\ &= \frac{2(m - m_s)}{\sqrt{3}} \mathcal{T}\beta \left(\sum_{i=1}^3 D_{8i} Q^i + \sum_{\alpha=4}^7 D_{8\alpha} Q^\alpha + (D_{88} - 1)Q^8 \right) \mathcal{T}^\dagger. \end{aligned} \quad (6.28)$$

The $SU(3)$ D–functions are those of eq (2.30), the argument being the collective rotation A . The $SU(2)$ invariant pieces have also been indicated. The computation proceeds by expanding the regularized action in powers of h_{rot} and h_{SB} , which are approximated to be time independent. Furthermore, only expansions up to quadratic order have been considered in the literature [212, 63, 213, 64]. As in the case of the classical energy, the action separates into valence quark and vacuum pieces. The valence quark piece is analyzed by treating the extended Dirac equation for the valence quark state

$$(h + h_{rot} + h_{SB}) \Psi_{val} = \epsilon_{val} \Psi_{val} \quad (6.29)$$

in stationary perturbation theory. The expansion of the vacuum part is more involved. Since regularization is mandatory, the detour over Euclidean space is unavoidable. In Euclidean space h_{rot} is an anti–Hermitian quantity since it is linear in the time derivative. Stated otherwise, $\Omega_a^{(E)} = i\Omega_a$ is considered to be a real quantity. Then the real and imaginary parts of the action are

$$\mathcal{A}_R = -\frac{1}{2} \int_{1/\Lambda^2}^{\infty} \frac{ds}{s} \text{Tr} \exp \left\{ -s \left[-\partial_\tau^2 + h^2 + \{h, h_{SB}\} + h_{SB}^2 + [h, h_{rot}] - h_{rot}^2 \right] \right\} , \quad (6.30)$$

$$\mathcal{A}_I = \frac{1}{2} \text{Tr} \left\{ [(\partial_\tau - h - h_{SB})(-\partial_\tau - h - h_{SB})]^{-1} \{h_{rot}, h + h_{SB}\} \right\} + \dots \quad (6.31)$$

$$\rightarrow \frac{1}{2} \int_{1/\Lambda^2}^{\infty} ds \text{Tr} \{h_{rot}, h + h_{SB}\} \exp \left\{ -s \left[-\partial_\tau^2 + h^2 + \{h, h_{SB}\} + [h, h_{rot}] \right] \right\} + \dots \quad (6.32)$$

Here the imaginary part has been regularized in a way consistent with the introduction of the cut-off, Λ in eq (6.30). Note also that the expression (6.30) is still exact, while eq (6.31) already represents an expansion in h_{rot} and h_{SB} . Abbreviating the arguments of the exponentials by A_i , where the subscript labels the order of the perturbation, these expressions are analyzed using the general formula for an expansion up to quadratic order

$$e^{A_0+A_1+A_2} = e^{A_0} + \int_0^1 d\zeta e^{\zeta A_0} (A_1 + A_2) e^{(1-\zeta)A_0} + \int_0^1 d\zeta \int_0^{1-\zeta} d\eta e^{\eta A_0} A_1 e^{(1-\zeta-\eta)A_0} A_1 e^{\zeta A_0} + \dots, \quad (6.33)$$

which introduces Feynman parameter integrals. Since the perturbation is taken to be static the temporal part of the functional trace is straightforwardly converted into Gaussian type integrals as in eq (6.20). The remainder of the trace is evaluated using the eigenstates, $|\mu\rangle$ of the Dirac Hamiltonian in the background of the chiral soliton (6.22). Having obtained the expanded Euclidean action, the coefficients of the collective Hamiltonian (2.36) are extracted after continuing back to Minkowski space ($\Omega_a^{(E)} \rightarrow \Omega_a = -i\Omega_a^{(E)}$). These coefficients are listed in appendix D of ref [193] and do not need to be repeated here. For illustration, however, the matrix Θ_{ab} , which defines the term of the collective Lagrangian bilinear in the angular velocities, $L = (1/2)\Theta_{ab}\Omega_a\Omega_b + \dots$ is shown because it contains the moments of inertia. According to the above mentioned decomposition of the action, Θ_{ab} is the sum

$$\Theta_{ab} = \eta_{\text{val}}\Theta_{ab}^{\text{val}} + \Theta_{ab}^{\text{vac}}. \quad (6.34)$$

The valence quark piece is given by

$$\Theta_{ab}^{\text{val}} = 2N_C \sum_{\mu \neq \text{val}} \frac{\langle \text{val} | Q^a | \mu \rangle \langle \mu | Q^b | \text{val} \rangle}{\epsilon_\mu - \epsilon_{\text{val}}}. \quad (6.35)$$

In contrast to the purely mesonic models the cranking type structure [54, 174] of the inertial parameters is apparent. The vacuum contribution to the moment of inertia is obtained to be [206, 63]

$$\Theta_{ab}^{\text{vac}} = 2N_C \sum_{\mu\nu} f_\Lambda(\epsilon_\mu, \epsilon_\nu) \langle \mu | Q^a | \nu \rangle \langle \nu | Q^b | \mu \rangle \quad (6.36)$$

where the cut-off function

$$f_\Lambda(\epsilon_\mu, \epsilon_\nu) = \frac{\Lambda}{\sqrt{\pi}} \frac{e^{-(\epsilon_\mu/\Lambda)^2} - e^{-(\epsilon_\nu/\Lambda)^2}}{\epsilon_\nu^2 - \epsilon_\mu^2} - \frac{\text{sgn}(\epsilon_\nu)\text{erfc}\left(\left|\frac{\epsilon_\nu}{\Lambda}\right|\right) - \text{sgn}(\epsilon_\mu)\text{erfc}\left(\left|\frac{\epsilon_\mu}{\Lambda}\right|\right)}{2(\epsilon_\mu - \epsilon_\nu)} \quad (6.37)$$

has the interesting property that it vanishes in the case $\epsilon_\mu = \epsilon_\nu$ [206]. This causes Θ_{ab} to vanish when the soliton is absent because the quark matrix elements of the flavor matrices Q^a are diagonal for $F \equiv 0$, *i.e.* $\langle \nu | Q^a | \mu \rangle \propto \delta_{\mu\nu}$. This feature just reflects rotational invariance, which is violated in the presence of the soliton^e. The moments of inertia for rotations into different directions correspond to certain choices of flavor matrices, *e.g.* $\alpha^2 = \Theta_{33}$. For the strange moment of inertia, β^2 the contribution (β_I) of the induced components (2.45) has

^eSpecial care has to be taken when choosing the boundary conditions for the eigenstates diagonalizing h . Such boundary conditions may violate rotational invariance resulting in $\Theta_{ab} \neq 0$ even for $F \equiv 0$. Nevertheless a proper choice is possible, see appendix B of ref [63].

Table 6.3: The mass differences of the low-lying $\frac{1}{2}^+$ and $\frac{3}{2}^+$ baryons with respect to the nucleon as obtained in the collective approach to the NJL model. The up-quark constituent mass m is chosen such that the experimental Δ -nucleon mass difference is reproduced. The last column refers to the case when the symmetry breaker γ is scaled by $(f_K^{\text{expt.}}/f_K^{\text{pred.}})^2$. All data (from ref [214]) are in MeV.

	f_π fixed	f_K fixed	Expt.	$f_K^{\text{corr.}}$
Λ	105	109	177	175
Σ	148	151	254	248
Ξ	236	243	379	396
Δ	293	293	293	291
Σ^*	387	391	446	449
Ξ^*	482	489	591	608
Ω	576	586	733	765

been estimated in the gradient expansion, hence $\beta^2 = \Theta_{44} + \beta_I$. These formulas for the moments of inertia have been obtained by expanding the action in h_{rot} . The expansion in $h_{rot} \times h_{SB}$ yields α_1 and β_1 . The distinction between these coefficients originates from the $SU(2)$ decomposition in eq (6.28). Similarly, the expansion in h_{SB} gives the contribution of the fermion determinant to γ , γ_T , γ_S and γ_{TS} , which acquire additional contributions by substituting the field configuration (6.25) into the mesonic part of the action \mathcal{A}_m (6.5). After eliminating the coupling constant via $G_{\text{NJL}} = m^0 m / m_\pi^2 f_\pi^2$, the strange current quark mass, m_s^0 only appears in form of the ratio m_s^0 / m^0 . Since this ratio is known to be insensitive on the regularization prescription [192] the above described expansion scheme avoids uncertainties stemming from the choice of the regularization prescription. On the contrary, the absolute values of the current quark masses are subject to major changes when the regularization scheme is altered.

The extraction of the coefficients of collective Hamiltonian from the NJL model action is now completed and numerical results for the baryon mass differences will be discussed. Of course, these mass differences, which are displayed in table 6.3, are obtained within the generalized Yabu-Ando approach, *i.e.* by exact diagonalization of the collective Hamiltonian according to the prescription outlined in appendix A. As already speculated earlier, the mass differences are underestimated in the collective approach to the NJL model. That this shortcoming is due to the too small prediction for the ratio f_K/f_π is also illustrated in table 6.3 by choosing two different set of parameters. First, $f_\pi = 93\text{MeV}$ is kept at its empirical value and $m = 407\text{MeV}$ is chosen to reproduce the experimental Δ -nucleon mass difference yielding $f_K = 99.8\text{MeV} = 1.07f_\pi$. In the second set of parameters the cut-off Λ is tuned to correctly give $f_K = 114\text{MeV}$. Again $m = 433\text{MeV}$ is determined from the experimental Δ -nucleon mass difference. Then $f_\pi = 104.9\text{MeV}$ is increased considerably, however, the ratio $f_K/f_\pi = 1.09$ remains almost unaltered. Apparently the change in the mass differences for the two sets is not larger than the change for the ratio f_K/f_π . The sensitivity of the symmetry breaking parameters on f_K has been traced in the gradient expansion [63]

$$\begin{aligned} \gamma_{\text{grad. exp.}} = & \frac{4}{3} \int d^3r \left\{ (m_K^2 f_K^2 - m_\pi^2 f_\pi^2)(1 - \cos F) \right. \\ & \left. + \frac{f_K^2 - f_\pi^2}{2} \cos F \left(F'^2 + \frac{2\sin^2 F}{r^2} \right) + \dots \right\}. \end{aligned} \quad (6.38)$$

The dominating term in this expansion is the one involving $m_K^2 f_K^2$. It is therefore intuitive to scale the vacuum contribution to γ by $(f_K^{\text{expt.}}/f_K^{\text{pred.}})^2 \approx (114/100)^2$ and re-evaluate the baryon spectrum. The resulting mass differences are in perfect agreement with the experimental data as can be observed from the last column of table 6.3. Hence the problem of underestimating the mass differences in the collective approach is completely inherited from the meson sector of the model, which is unable to properly reproduce the ratio f_K/f_π .

The expansion scheme employed above is somewhat different from the one used in refs [213, 64]. In the first place the meson fields differ by a constant but flavor symmetry breaking amount, $M \rightarrow M + \hat{m}^0$. Then the mesonic part, \mathcal{A}_m vanishes and the current quark mass matrix is contained in the fermion determinant, \mathcal{A}_F . Of course, this re-parametrization does not make any difference when the Euler–Lagrange equations are solved exactly. However, in the collective approach the time dependent solutions are approximated by the rigidly rotation field configuration (6.25). Whence it is not obvious whether or not these parametrizations are equivalent. For simplicity the constituent quark masses have been set equal, *i.e.* $m = m_s$ in refs [213, 64]. This also implies the approximation $f_K = f_\pi$. In that treatment the remaining symmetry breaking term is of the structure (6.28) too, but with the constituent masses replaced by the current masses. Furthermore a different regularization scheme has been used, which brings into the game one additional parameter. Nevertheless similar results for the baryon mass differences have been observed, in particular the symmetry breaking is underestimated when empirical values ($m^0 \approx 6\text{MeV}$, $m_s^0 \approx 150\text{MeV}$ [33]) are used. A mass splitting pattern similar to the one in the last column of table 6.3 was obtained when increasing m_s^0 by about 20%. This is not surprising because the relation between m_K and m_s^0 is almost linear as a consequence of the GMOR relations [202]. Thus the increase in m_s^0 is equivalent to a corresponding scaling of the symmetry breaking coefficient γ , *cf.* eq (6.38).

Baryon properties can be computed similarly to the meson models. First, the symmetry currents have to be obtained. The straightforward procedure is to extend the action by introducing external gauge fields, $a_\mu^a(x)$, $i\partial_\mu \rightarrow i\partial_\mu + a_\mu^a(x)\gamma^\mu\Gamma^a$, with Γ^a being the generator of the symmetry under consideration. For example, $\Gamma^a \sim \boldsymbol{\tau}$ for the isovector vector current. The expressions linear in $a_\mu^a(x)$ are identified as the currents. These currents are again decomposed into a valence quark and vacuum piece

$$j_\mu^a = N_C \left\{ \eta_{\text{val}} j_{\text{val } \mu}^a + j_{\text{vac } \mu}^a \right\} . \quad (6.39)$$

Denoting $\Psi_\mu(x)$ with the spatial representation of the eigenstates $|\mu\rangle$, a compact notation for the currents is possible

$$j_{\text{val } \mu}^a = \bar{\Psi}_{\text{val}}(x) A^\dagger \gamma_\mu \Gamma^a A \Psi_{\text{val}}(x) + \sum_{\mu \neq \text{val}} \left\{ \Omega_a, \frac{\langle \text{val} | Q^a | \mu \rangle}{\epsilon_\mu - \epsilon_{\text{val}}} \bar{\Psi}_\mu(x) A^\dagger \gamma_\mu \Gamma^a A \Psi_{\text{val}}(x) \right\} , \quad (6.40)$$

$$j_{\text{vac } \mu}^a = -\frac{1}{2} \left[\sum_\mu \text{sgn}(\epsilon_\mu) \text{erfc} \left(\left| \frac{\epsilon_\mu}{\Lambda} \right| \right) \bar{\Psi}_\mu(x) A^\dagger \gamma_\mu \Gamma^a A \Psi_\mu(x) \right. \\ \left. - \sum_{\mu\nu} f_\Lambda(\epsilon_\mu, \epsilon_\nu) \left\{ \Omega_a, \langle \nu | Q^a | \mu \rangle \bar{\Psi}_\mu(x) A^\dagger \gamma_\mu \Gamma^a A \Psi_\nu(x) \right\} \right] . \quad (6.41)$$

In order to obtain the vacuum part the detour over Euclidean space has to be taken again in order to be consistent with the proper time regularization scheme. The anti-commutators are understood between the collective coordinates, A , and the $SU(3)$ generators, R_a . The latter are related to the angular velocities, Ω_a via the quantization rule (2.34). The appearance

Table 6.4: The baryon magnetic moments in the NJL model. These results are taken from ref [215] for the constituent quark mass $m=420\text{MeV}$. Data are given in nucleon magnetons as well as ratios of the proton magnetic moment.

Baryon	NJL		Expt.	
	μ_B	μ_B/μ_p	μ_B	μ_B/μ_p
p	2.30	1.00	2.79	1.00
n	-1.66	-0.72	-1.91	-0.68
Λ	-0.76	-0.33	-0.61	-0.22
Σ^+	2.34	1.02	2.42	0.87
Σ^0	0.74	0.33	—	—
Σ^-	-0.85	-0.37	-1.16	-0.42
Ξ^0	-1.59	-0.69	-1.25	-0.45
Ξ^-	-0.67	-0.29	-0.69	-0.25
$\Sigma^0 \rightarrow \Lambda$	-1.44	-0.62	-1.61	-0.58

of the regulator function, $f_\Lambda(\epsilon_\mu, \epsilon_\mu)$ is not accidental but rather guarantees the proper normalization of the baryon charges. From the above expressions the radial functions like $V_i(r)$ in eq (2.57) may be extracted when considering $\Gamma^a = Q^a$. Then the computation of static baryon properties proceeds along the lines outlined in section 2.4. This procedure has recently been employed [215] to compute the magnetic moments of the $\frac{1}{2}^+$ baryons in the NJL model. These results are summarized in table 6.4. As for all other treatments within the rigid rotator approach, the deviation from the $SU(3)$ symmetry relations (2.62) is only moderate. The predictions compare with those obtained in the vector meson model, *cf.* table 4.2. However, a word of caution has to be added to the results obtained in ref [215]. These contain $1/N_C$ corrections (not included in eqs (6.39–6.41)), which rely on a special ordering prescription for the collective operators [216]. Although this description is in agreement with the generally expected form of the magnetic moment operator [116] it is not unambiguous either. In particular, the application of this description to the axial current violates the PCAC relation by about 30% [207]. That is, this ordering does not respect one of the fundamental symmetries imposed in constructing the model Lagrangian. Moreover, the $1/N_C$ corrections constitute the major contribution to the magnetic moments leading to the suspicion that the series has not yet converged. As a matter of fact the leading order (in $1/N_C$) contribution to the isovector magnetic moment, $\mu_V = \mu_p - \mu_n$ is predicted to be about two [217, 215], which is almost a factor three off the experimental value, which is $\mu_V = 4.70$.

Substituting the generator $\Gamma^a = Q^0 - 2Q^8/\sqrt{3}$ into eqs (6.40) and (6.41) gives the strange vector current in the NJL soliton model. The resulting predictions [41] on the nucleon matrix element of the strange vector current have already been presented in table 4.3.

Employing the generators $\Gamma^a = \gamma_5 Q^a$ leads to the axial–vector currents. In analogy to the discussion before eq (4.31), the components $a = 3, 8$ and 0 may be used to extract the individual quark contributions $H_{u,d,s}$ to the axial–vector matrix element of the nucleon (2.55). For the constituent quark mass $m = 420$ these are obtained to be [218]^f

$$H_u(0) = 0.64(0.90) \quad H_d(0) = -0.24(-0.48) \quad H_s(0) = -0.02(-0.05) , \quad (6.42)$$

^fIn these calculations the effective symmetry breaking has artificially been increased by tuning m_s^0 , *cf.* the discussion after eq (6.38).

where the data in parentheses include the above mentioned PCAC violating $1/N_C$ corrections. In any event, the singlet contribution $H(0) = 0.38$ is not effected by these corrections and turns out to be somewhat large. This presumably has to be interpreted as reminiscent of the quark model character of the NJL model. This statement is also supported by the fact that the valence contribution (6.40) to $H(0)$ absolutely dominates the vacuum part (6.41). Nevertheless the prediction for the polarized nucleon structure function (2.66) $\Gamma_1(q^2 = (10.7\text{GeV})^2) = 0.12(0.16)$ is well within experimental data (0.129 ± 0.010) , at least when the $1/N_C$ corrections are ignored.

As a side remark the relation for the strangeness content fraction (2.82) will be explained to emerge from the NJL model. The strangeness content is defined as the expectation value of the associated bilinear

$$\begin{aligned} \langle \bar{s}s \rangle &= \int D\bar{q}Dq \int d^4x \bar{s}(x)s(x) \exp(i\mathcal{A}_{\text{NJL}}) \\ &= \left. \frac{\partial}{\partial \zeta} \int D\bar{q}Dq \exp\left(i\mathcal{A}_{\text{NJL}} + \zeta \int d^4x \bar{s}(x)s(x)\right) \right|_{\zeta=0}, \end{aligned} \quad (6.43)$$

where $\mathcal{A}_{\text{NJL}} = \int d^4x \mathcal{L}_{\text{NJL}}$ denotes the action associated with the NJL Lagrangian (6.1). Including the additional source term in the bosonization process and shifting the corresponding component of the meson fields, $M_{33} \rightarrow M_{33} - \zeta \bar{s}s$, moves the source into the mesonic part of the action. It is then straightforward to compute the derivative with respect to ζ . Next the rotating hedgehog (6.25) is substituted and the baryon number zero contribution is subtracted. When normalizing with respect to the sum $\langle \bar{u}u + \bar{d}d + \bar{s}s \rangle$ the expression (2.82) is obtained.

In this section it has been shown that the rigid rotator approach to describe hyperons in the framework of chiral solitons can be applied to a microscopic theory of the quark flavor dynamics. The deficiencies of the numerical results are linked to an immanent problem of the NJL model, namely the too small prediction for the kaon decay constant. A further shortcoming of this model, which has not been addressed here, is the presence of quark–antiquark thresholds, *i.e.* the model is not confining. This makes difficult the extension of the rigid rotator treatment to more sophisticated considerations like *e.g.* the scaling approach of section 3.2. As a consequence of non–confinement, the potential associated with the scaling variable (μ in eq (3.10)) possesses additional (unphysical) minima [219], which makes a diagonalization as in section 3.2 unfeasible.

6.3 Baryon Masses in the Bound State Approach

In the present section the derivation of the parameters in the mass formula (5.16) within the NJL soliton model will be described. According to the investigations in section 5.3, which concluded that the collective treatment gives smaller symmetry breaking in the baryon spectrum than the bound state approach, the predictions of the NJL model on the baryon mass differences within the latter approach are expected to better agree with the experimental data.

Similarly to the Skyrme model, the bound state approach to the NJL model is set up by substituting a P–wave *ansatz* with kaon quantum numbers for the fluctuating field $\xi_f = \exp(i \sum_a \eta_a(x) Q^a)$ in eq (6.9), see also eq (5.3)

$$\eta_a(x) Q^a = \int \frac{d\omega}{2\pi} e^{-i\omega t} \begin{pmatrix} 0 & K(\mathbf{r}, \omega) \\ K^\dagger(\mathbf{r}, -\omega) & 0 \end{pmatrix}, \quad K(\mathbf{r}, \omega) = k_P(r, \omega) \hat{\mathbf{r}} \cdot \boldsymbol{\tau} \begin{pmatrix} a_1(\omega) \\ a_2(\omega) \end{pmatrix}. \quad (6.44)$$

Here the Fourier transformation of the kaon isospinor, K has been written explicitly. One proceeds along the standard path and expands the NJL model action up to quadratic order in $k_P(r, \omega)$ in the background field of the chiral soliton, $\xi_0 = \exp(i\boldsymbol{\tau} \cdot \hat{\mathbf{r}}F(r)/2)$. In contrast to the collective approach the Dirac operator contains perturbative parts (h_1 and h_2)

$$i\beta\mathcal{D} = i\partial_t - h - h_1 - h_2 \quad (6.45)$$

which are not time independent but rather

$$h_1 = -\frac{m + m_s}{2} \int \frac{d\omega}{2\pi} e^{-i\omega t} \begin{pmatrix} 0 & u_0(\mathbf{r})\Omega(\omega) \\ \Omega^\dagger(-\omega)u_0(\mathbf{r}) & 0 \end{pmatrix}, \quad (6.46)$$

$$h_2 = \frac{m + m_s}{4} \int \frac{d\omega}{2\pi} \frac{d\omega'}{2\pi} e^{-i(\omega+\omega')t} \begin{pmatrix} u_0(\mathbf{r})\beta\Omega(\omega)\Omega^\dagger(-\omega')u_0(\mathbf{r}) & 0 \\ 0 & -\beta\Omega^\dagger(-\omega)\Omega(\omega') \end{pmatrix}. \quad (6.47)$$

For simplicity the unitary, self-adjoint matrix

$$u_0(\mathbf{r}) = \beta \left(\sin \frac{\Theta}{2} - i\gamma_5 \hat{\mathbf{r}} \cdot \boldsymbol{\tau} \cos \frac{\Theta}{2} \right) \quad (6.48)$$

has been introduced and the spatial arguments of the isospinor

$$\Omega(\omega) = k_P(r, \omega) \begin{pmatrix} a_1(\omega) \\ a_2(\omega) \end{pmatrix} \quad (6.49)$$

have been omitted. By again taking the detour via Euclidean space to establish the proper time regularization, the expansion is performed with the formalism made available in eq (6.33). The final expression is comprised in terms of local and bilocal kernels $\Phi_1(r)$ and $\Phi_2(\omega; r, r')$, respectively [199, 203]

$$\mathcal{A}^{(2)}[\Omega] = \int_{-\infty}^{+\infty} \frac{d\omega}{2\pi} \left\{ \int dr r^2 \int dr' r'^2 \Phi_2(\omega; r, r') \Omega^\dagger(r, \omega) \Omega(r', \omega) + \int dr r^2 \Phi_1(r) \Omega^\dagger(r, \omega) \Omega(r, \omega) \right\}. \quad (6.50)$$

The explicit expressions of these kernels are summed up in appendix D. As a consequence of isospin invariance they are diagonal in the associated indices. As can be observed from eqs (D.8)–(D.10) the kernels contain both, even and odd terms in the frequency ω . The former stem from the real part of the Euclidean action, \mathcal{A}_R , while the latter are due to imaginary part, \mathcal{A}_I . Comparison with the bound state approach to the Skyrme model (section 5.1) indicates that the imaginary part takes over the part of the Wess–Zumino term, Γ_{WZ} (2.23). Of course, this is expected rather than surprising because \mathcal{A}_I is found to coincide with Γ_{WZ} in leading order of the gradient expansion [19].

The NJL model analogue of the bound state equation (5.4) apparently is an integral equation rather than a differential equation

$$r^2 \left\{ \int dr' r'^2 \Phi_2(\omega; r, r') k_P(r', \omega) + \Phi_1(r) k_P(r, \omega) \right\} = 0, \quad (6.51)$$

which actually may be interpreted as the Bethe–Salpeter equation for the kaon field in the soliton background. In this equation, the frequency ω has to be adjusted to the bound state

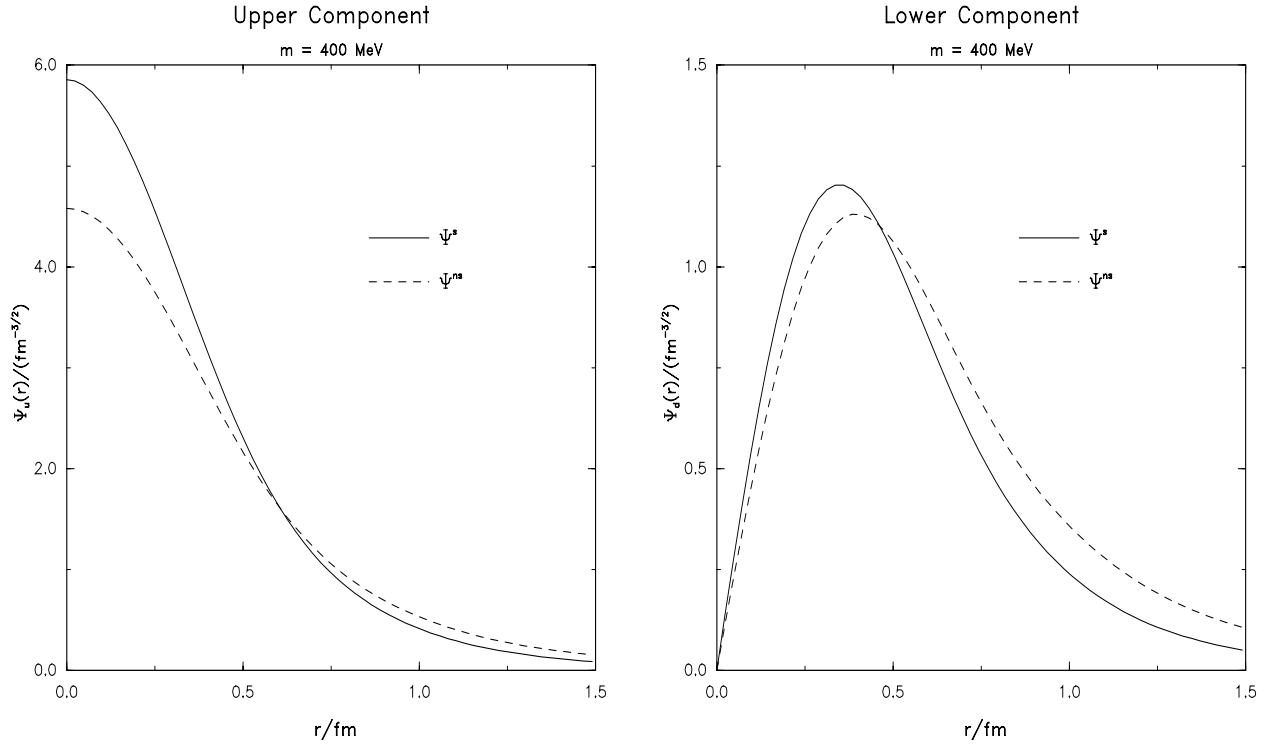


Figure 6.1: Comparison of the radial dependencies of the induced strange valence quark (s) and the non-strange valence quark (ns) levels.

energy, ω_P such that a non-trivial solution, $k_P \neq 0$ is obtained^g. The resulting radial function is identified as the bound state wave-function. The explicit expressions (6.46–6.49) for the perturbative parts of the Dirac Hamiltonian clearly illustrate that for small radii, r the P-wave *ansatz* (6.44) is transmuted to an S-wave fluctuation as a consequence of the soliton background. Hence there is not centrifugal barrier for the bound state and therefore $k_P(r = 0, \omega_P) \neq 0$ is allowed. This, of course, is in no way different from the Skyrme model as can be inferred from figure 5.1. In the NJL model this bound state induces a strange (s) valence quark field

$$\Psi_{\text{val}}^s(\omega_P) = -\frac{m + m_s}{2} (\epsilon_{\text{val}} - \omega_P - h)^{-1} \Omega^\dagger(r, \omega_P) \left(\sin \frac{F}{2} - i\gamma_5 \hat{\mathbf{r}} \cdot \boldsymbol{\tau} \cos \frac{F}{2} \right) \Psi_{\text{val}}^{ns}, \quad (6.52)$$

where $\Omega^\dagger(r, \omega_P)$ contains the bound state wave-function $k_P(r, \omega_P)$. This expression also illustrates how the isospin components of the up-down (ns) valence quark spinor are saturated. In figure 6.1 the radial dependence of this induced strange valence quark is compared to that of the non-strange valence quark level. As for the kaon profile (*cf.* figure 5.1) one observes that the strange quark field is more strongly concentrated at the origin than the “hedgehog” spinor. This shows that the strange degrees of freedom are bound by the soliton. The fact that the upper component of the wave-function $\Psi_{\text{val}}^s(\omega_P)$ is significantly larger than the lower one, indicates that the induced strange quark is of quark rather than antiquark character. Upon explicit computation it has been verified [203] that the strangeness charge associated with this bound state indeed is negative. A bound state carrying positive strangeness was not detected. The occupation of such a state would corresponded to an exotic baryon with baryon number and strangeness both being +1. In the quark model language it would have the structure $qqq\bar{s}q$, a so-called pentaquark [221].

^gSee ref [220] for a description of the numerical treatment of eq (6.51).

In the next step the degeneracy between states of identical strangeness but different spin and isospin has to be removed. Again collective coordinates are introduced for these symmetries

$$M = A(t)\xi_0\xi_f\langle\Sigma\rangle\xi_f\xi_0A^\dagger(t) \quad \text{with} \quad A(t) \in SU(2). \quad (6.53)$$

This parametrization can be formulated as in eq (5.13) for the pion and kaon fields. Hence all the relations between spin and isospin, which were discussed in section 5.1, are recovered. Nevertheless, it is interesting to consider the spin expectation value

$$\langle\mathbf{J}\rangle = \int D\bar{q}Dq \int d^3r q^\dagger \mathbf{J}q \exp(i\mathcal{A}_{\text{NJL}}) \quad (6.54)$$

on the microscopic level. Here \mathbf{J} is the spin operator for a Dirac spinor and $\mathcal{A}_{\text{NJL}} = \int d^4x \mathcal{L}_{\text{NJL}}$ denotes the action associated with the NJL Lagrangian (6.1). Since the spin operator commutes with the iso-rotations $A(t)$ the transformation to the rotating frame $q = Aq'$ is trivial

$$\langle\mathbf{J}\rangle = \int D\bar{q}'Dq' \int d^3r q'^\dagger \mathbf{J}q' \exp(i\mathcal{A}'_{\text{NJL}}). \quad (6.55)$$

$\mathcal{A}'_{\text{NJL}}$ represents the NJL action in the rotating frame, which also contains the Coriolis term

$$\mathcal{A}'_{\text{NJL}} = \int d^4x \left(\mathcal{L}_{\text{NJL}} - \frac{1}{2}q'^\dagger \boldsymbol{\tau} \cdot \boldsymbol{\Omega}q' \right). \quad (6.56)$$

Substituting the definition of the grand spin (\mathbf{G}) into eq (6.55) yields

$$\langle\mathbf{J}\rangle = \int D\bar{q}'Dq' \int d^3r q'^\dagger \left(\mathbf{G} - \frac{\boldsymbol{\tau}}{2} \right) q' \exp(i\mathcal{A}'_{\text{NJL}}). \quad (6.57)$$

The soliton contribution to the spin, \mathbf{J}^F is identified by differentiating $\mathcal{A}'_{\text{NJL}}$ with respect to the angular velocity $\boldsymbol{\Omega}$

$$\langle\mathbf{J}\rangle = \langle\mathbf{G}\rangle + \int D\bar{q}'Dq' \frac{1}{T} \frac{\partial \mathcal{A}'_{\text{NJL}}}{\partial \boldsymbol{\Omega}} \exp(i\mathcal{A}'_{\text{NJL}}) = \langle\mathbf{G}\rangle + \mathbf{J}^F. \quad (6.58)$$

This immediately shows that the spin, \mathbf{J}^K (5.12) associated with kaon bound state is identical to the grand spin in the flavor rotating frame. This could straightforwardly be shown on the microscopic level, while an elaborate chain of arguments (or tedious calculation) was needed to establish this relation for the Skyrme model, see *e.g.* the discussion after eq (5.31). The identity $\mathbf{J}^K = \langle\mathbf{G}\rangle$ considerably simplifies the computation of the spectral function $d(\omega)$ defined in eq (5.12) because the eigenstates, $|\mu\rangle$ of the one particle Hamiltonian (6.22) also diagonalize the grand spin projection, *i.e.* $G_3|\mu\rangle = M_\mu|\mu\rangle$. Hence, to extract the spectral function $d(\omega)$ one only has to repeat the expansion leading to eq (6.50), with the projection quantum number, M_μ , included when taking matrix elements. To compute the other spectral function, $c(\omega)$ (5.8) one first expands the action with respect to the angular velocity $\boldsymbol{\Omega}$

$$\mathcal{A}_F = \mathcal{A}_F(\boldsymbol{\Omega} = 0) + \sum_{a=1}^3 \Omega_a \left. \frac{\partial \mathcal{A}_F}{\partial \Omega_a} \right|_{\boldsymbol{\Omega}=0} + \mathcal{O}(\boldsymbol{\Omega}^2) = \mathcal{A}_F^{(0)} + \mathcal{A}_F^{(1)} + \mathcal{O}(\boldsymbol{\Omega}^2), \quad (6.59)$$

where the contributions of order $\boldsymbol{\Omega}^2$ yield the spatial moment of inertia, $\alpha^2 = \Theta_{33}$ (6.34). In the second step the linear term $\mathcal{A}_F^{(1)}$ is expanded up to quadratic order in the kaon fluctuations.

Table 6.5: The mass differences of the low-lying $\frac{1}{2}^+$ and $\frac{3}{2}^+$ baryons with respect to the nucleon in the bound state approach to the NJL model. The up-quark constituent mass, m is chosen such that the Δ -nucleon mass difference is reproduced. All data (from ref.[203]) are in MeV.

	f_π fixed	f_K fixed	Expt.
Λ	132	137	177
Σ	234	247	254
Ξ	341	357	379
Δ	293	293	293
Σ^*	374	375	446
Ξ^*	481	485	591
Ω	613	622	733

This painful exercise has been carried out in ref [203] where the explicit expressions and numerical results for $c(\omega)$ and $d(\omega)$ may be traced. The numerical results for ω_P reflect that the kaon decay constant is underestimated in the NJL model. In case the cut-off, Λ is fixed from f_π , $|\omega_P|$ decreases from about 200MeV to 150MeV when the constituent quark mass is varied from 350MeV to 500MeV. These frequencies are smaller than the Skyrme model analogue (*cf.* table 5.1) reflecting the fact that the kaon decay constant is underestimated in the NJL model. It turns out that d_P is slightly smaller than unity. This difference with respect to the Skyrme model has been interpreted [203] as the polarization of the vacuum caused by the kaon bound state. Despite the denominator of $\chi = -c_P/d_P$ being smaller than in the Skyrme model, the numerical results for this ratio turn out to be similar. The baryon mass differences, which are obtained from eq (5.16), are exhibited in table 6.5. The parameters of the model are again obtained by first determining the ratio Λ/m from either f_π or f_K . Next the constituent quark mass is fitted to the Δ -nucleon splitting. Then the remaining six mass differences are predicted as shown in table 6.3. Comparing the results in table 6.5 with those in table 6.3 the prejudice from the beginning of this section is confirmed, that the bound state approach gives better agreement with the experimental mass differences. In particular this is the case for the $\frac{1}{2}^+$ baryons. Despite of this improvement the flavor symmetry breaking in the baryon spectrum remains underestimated in the NJL model.

Finally this chapter will be concluded by also remarking that S-wave fluctuations off the NJL soliton have been investigated [222]. As in the Skyrme model, the bound state in this channel is suited to describe the odd parity hyperon $\Lambda(1405)$. Here, however, the non-confining character of the NJL raises some problems since for small constituent quark masses the threshold for scattering the valence quark into the strange continuum is as small as the expected frequency of the bound state in the S-wave channel. Hence a bound state is only found when the constituent mass, m , of the up-quark (on which m_s depends) exceeds a critical value. This value has been obtained to be ~ 425 MeV when the cut-off is linked to the experimental value of the pion decay constant. When m is further increased the mass difference between the lowest odd parity hyperon and the nucleon shows almost no variation and is predicted to be about 415MeV. This is somewhat lower than the empirical value of 465MeV.

7 Concluding Remarks

In this article the incorporation of strange degrees of freedom in the soliton description of baryons has been surveyed. The models considered reach from the simple Skyrme model, which contains pseudo-scalar degrees of freedom only, to extended Skyrme type models containing vector meson degrees of freedom and finally to a microscopic theory of the quark flavor dynamics. The latter has been specified to be the Nambu–Jona–Lasinio (NJL) model. All these models are treated in a similar fashion. A chirally invariant Lagrangian is supplemented by appropriate flavor symmetry breaking terms with the model parameters being determined from meson properties as much as possible. Subsequently the soliton solutions corresponding to a unit baryon number are obtained. These (static) field configurations, which commonly are of hedgehog structure, do not possess the quantum numbers of physical baryons. In order to generate states with good spin and flavor quantum numbers approximations to the time-dependent solutions of the Euler–Lagrange equations are considered. In general these approximations introduce time-dependent coordinates or fields, which in turn are quantized canonically. Here two seemingly opposite procedures to gain hyperon wave-functions has been reflected about: (i) the introduction of collective coordinates in the whole $SU(3)$ flavor space and (ii) the construction of hyperon states such as a kaon cloud bound by the soliton background field. In the former approach strange degrees of freedom are considered as large amplitude fluctuations off the soliton, while in the latter the strange fields are limited to the harmonic approximation. Although these two treatments seem to coincide in the large symmetry breaking limit, they apparently do not in the case that flavor symmetry breaking is small. This has been argued from the simple fact that the bound state approach does not reproduce the Gell–Mann Okubo mass relation. For model parameters, which are adjusted to the meson properties, the Skyrme model examinations have revealed that the bound state approach overestimates the flavor symmetry breaking in the baryon spectrum. The collective treatment appears to be superior in this respect.

Despite of the progress achieved so far, one should acknowledge that the collective treatment has not yet been brought to complete fruition. For example, the treatment of the induced strange fields, which are mandatory to maintain the proper divergence of the currents, may undergo some changes when double counting effects are accounted for. As argued, these changes are supposedly small, in particular for the baryon properties. Also fields induced by the symmetry breaking have not yet been considered in meson models. The studies in the NJL model, however, indicate that these effects are negligible. This may be argued from the fact that those contributions to the baryon masses are small, which are quadratic in the symmetry breaking part of the Dirac Hamiltonian. These terms essentially correspond to the inclusion of quark excitations due to symmetry breaking.

The collective approach has been employed to extensively study the static properties of the low-lying $\frac{1}{2}^+$ baryons. In particular, the role of virtual strange quark–antiquark excitations in the nucleon has been examined. It has been established that the inclusion of symmetry breaking effects in the nucleon wave-functions significantly reduces the predictions on the amount of strangeness in the nucleon. Furthermore, it has been explained how the nucleon matrix elements of various operators, which are bilinear in the strange quark spinors, evolve differently with symmetry breaking when the collective Hamiltonian (including flavor symmetry breaking terms) is diagonalized exactly. These effects go together with strong deviations from flavor covariant baryon wave-functions. Nevertheless a reasonable agreement with the Cabibbo scheme of the semi-leptonic hyperon decays is achieved.

The investigation of the baryon magnetic moments demonstrates that even the exact diagonalization within rigid rotator approach apparently contains symmetries which are not reflected in nature. This feature not only indicates the demand for refined quantization pro-

cedures, it even effects the classical soliton configuration because the strange fields do not acquire the asymptotic form expected for a kaon wave–function. This happens to be the case in both, the rigid rotator as well as the bound state approach. Hence one is tempted to ask the question whether flavor symmetry breaking could cause deviations from the hedgehog shape of the classical field configuration. For related studies, space dependent kaon fields need to be considered. The harmonic expansion of the bound state approach will certainly not be sufficient.

The soliton description of baryons has proven especially successful in explaining the data for polarized muon scattering. In all models the polarized structure function $\Gamma_1^p(q^2 = (10.7\text{GeV})^2)$ was predicted to be only slightly above 0.1, which compares favorably with the experimental value, 0.129 ± 0.010 . As a reminder it should be noted that the naïvely expected matrix element of the axial singlet current, $H(0)=1$, together with $g_A = 1.25$ and the assumption of flavor symmetry yields 0.22. As verified in the case of the NJL model, chiral solitons not only exist in effective meson theories but they may also occur in microscopic models of the quark flavor dynamics. These quark model solitons similarly explain the smallness of Γ_1^p , even for configurations which are dominated by the valence contribution. Thus, one is tempted to consider the smallness of Γ_1^p as manifestation for the soliton structure of the baryons. However, as has been indicated, in order to account for the detailed structure of the baryons the pure pseudo–scalar solitons need to be extended; *e.g.* by vector mesons or explicit quark fields.

Acknowledgements

The author is indebted to J. Schechter, B. Schwesinger, N. W. Park, A. Subbaraman, R. Alkofer and H. Reinhardt for many helpful contributions and to L. Gamberg for carefully reading the manuscript. Furthermore numerous illuminating discussions on the subjects covered in this article with G. Holzwarth, H. Walliser, Ulf.–G. Meißner, P. Jain, U. Zückert and A. Abada are gratefully acknowledged.

Appendix A

In this appendix the explicit forms of the right $SU(3)$ generators R_a ($a = 1, \dots, 8$) are displayed in terms of differential operators with respect to $SU(3)$ “Euler angles” [62]. An appropriate definition of these angles is given by parametrizing the collective flavor rotations (2.28) via

$$A = e^{-i(\alpha/2)\lambda_3} e^{-i(\beta/2)\lambda_2} e^{-i(\gamma/2)\lambda_3} e^{-i\nu\lambda_4} e^{-i(\alpha'/2)\lambda_3} e^{-i(\beta'/2)\lambda_2} e^{-i(\gamma'/2)\lambda_3} e^{-i(\rho/\sqrt{3})\lambda_8} . \quad (\text{A.1})$$

The group manifold is completely covered by varying the angles $\alpha, \beta, \dots, \rho$ according to

$$0 \leq \alpha, \gamma, \alpha', \gamma' < 2\pi, \quad 0 \leq \beta, \beta' < \pi, \quad 0 \leq \nu < \pi/2, \quad 0 \leq \rho < 3\pi. \quad (\text{A.2})$$

Since the $SU(3)$ generators are linear operators they may in general be written as linear combinations of differential operators [223]

$$R_a = id_{ba}(\boldsymbol{\alpha}) \frac{\partial}{\partial \alpha_b}, \quad (\text{A.3})$$

where $\boldsymbol{\alpha} = (\alpha_1, \alpha_2, \dots, \alpha_8) = (\alpha, \beta, \dots, \rho)$ compactly refers to the eight ‘‘Euler angles’’. The coefficient functions $d_{ab}(\boldsymbol{\alpha})$ are extracted from the defining equation of the $SU(3)$ algebra

$$AR_a A^\dagger = \frac{1}{2} A \lambda_a A^\dagger = \frac{1}{2} \lambda_b D_{ba}(\boldsymbol{\alpha}), \quad (\text{A.4})$$

where D_{ab} denotes the adjoint representation of the rotation matrix A , see eq (2.30). Explicit computation of the *LHS* of eq (A.4) provides the quantities M_{ab} , which are defined by

$$AR_a A^\dagger = \lambda_b M_{bc}(\boldsymbol{\alpha}) d_{ca}(\boldsymbol{\alpha}). \quad (\text{A.5})$$

From this one may read off

$$d_{ab}(\boldsymbol{\alpha}) = \left(M^{-1}(\boldsymbol{\alpha}) \right)_{ac} D_{cb}(\boldsymbol{\alpha}). \quad (\text{A.6})$$

The explicit expressions are

$$\begin{aligned} R_1 &= i \frac{\cos \gamma'}{\sin \beta'} \frac{\partial}{\partial \alpha'} - i \sin \gamma' \frac{\partial}{\partial \beta'} - i \cos \gamma' \cot \beta' \frac{\partial}{\partial \gamma'}, \\ R_2 &= -i \frac{\sin \gamma'}{\sin \beta'} \frac{\partial}{\partial \alpha'} - i \cos \gamma' \frac{\partial}{\partial \beta'} + i \sin \gamma' \cot \beta' \frac{\partial}{\partial \gamma'}, \\ R_3 &= -i \frac{\partial}{\partial \gamma'}, \\ R_4 &= -i \sin \left(\gamma - \rho + \frac{\alpha' - \gamma'}{2} \right) \frac{\sin \frac{\beta'}{2}}{\sin \beta \sin \nu} \frac{\partial}{\partial \alpha} - i \cos \left(\gamma - \rho + \frac{\alpha' - \gamma'}{2} \right) \frac{\sin \frac{\beta'}{2}}{\sin \nu} \frac{\partial}{\partial \beta} \\ &\quad - i \left[2 \sin \left(\rho + \frac{\alpha' + \gamma'}{2} \right) \frac{\cos \frac{\beta'}{2}}{\sin 2\nu} - \sin \left(\gamma - \rho + \frac{\alpha' - \gamma'}{2} \right) \cot \beta \frac{\sin \frac{\beta'}{2}}{\sin \nu} \right] \frac{\partial}{\partial \gamma} \\ &\quad - \frac{i}{2} \cos \left(\rho + \frac{\alpha' + \gamma'}{2} \right) \cos \frac{\beta'}{2} \frac{\partial}{\partial \nu} - \frac{3i}{4} \sin \left(\rho + \frac{\alpha' + \gamma'}{2} \right) \tan \nu \cos \frac{\beta'}{2} \frac{\partial}{\partial \rho} \\ &\quad + \frac{i}{2} \sin \left(\rho + \frac{\alpha' + \gamma'}{2} \right) \left[\cos \frac{\beta'}{2} \tan \nu + \frac{\cot \nu}{\cos \frac{\beta'}{2}} \right] \frac{\partial}{\partial \alpha'} \\ &\quad + i \cos \left(\rho + \frac{\alpha' + \gamma'}{2} \right) \cot \nu \sin \frac{\beta'}{2} \frac{\partial}{\partial \beta'} + \frac{i}{2} \sin \left(\rho + \frac{\alpha' + \gamma'}{2} \right) \frac{\cot \nu}{\cos \frac{\beta'}{2}} \frac{\partial}{\partial \gamma'}, \\ R_5 &= i \cos \left(\gamma - \rho + \frac{\alpha' - \gamma'}{2} \right) \frac{\sin \frac{\beta'}{2}}{\sin \beta \sin \nu} \frac{\partial}{\partial \alpha} - i \sin \left(\gamma - \rho + \frac{\alpha' - \gamma'}{2} \right) \frac{\sin \frac{\beta'}{2}}{\sin \nu} \frac{\partial}{\partial \beta} \\ &\quad - i \left[2 \cos \left(\rho + \frac{\alpha' + \gamma'}{2} \right) \frac{\cos \frac{\beta'}{2}}{\sin 2\nu} + \cos \left(\gamma - \rho + \frac{\alpha' - \gamma'}{2} \right) \cot \beta \frac{\sin \frac{\beta'}{2}}{\sin \nu} \right] \frac{\partial}{\partial \gamma} \\ &\quad + \frac{i}{2} \sin \left(\rho + \frac{\alpha' + \gamma'}{2} \right) \cos \frac{\beta'}{2} \frac{\partial}{\partial \nu} - \frac{3i}{4} \cos \left(\rho + \frac{\alpha' + \gamma'}{2} \right) \tan \nu \cos \frac{\beta'}{2} \frac{\partial}{\partial \rho} \end{aligned}$$

$$\begin{aligned}
& +\frac{i}{2}\cos\left(\rho+\frac{\alpha'+\gamma'}{2}\right)\left[\cos\frac{\beta'}{2}\tan\nu+\frac{\cot\nu}{\cos\frac{\beta'}{2}}\right]\frac{\partial}{\partial\alpha'} \\
& -i\sin\left(\rho+\frac{\alpha'+\gamma'}{2}\right)\cot\nu\sin\frac{\beta'}{2}\frac{\partial}{\partial\beta'}+\frac{i}{2}\cos\left(\rho+\frac{\alpha'+\gamma'}{2}\right)\frac{\cot\nu}{\cos\frac{\beta'}{2}}\frac{\partial}{\partial\gamma'}\ , \\
R_6 = & -i\sin\left(\gamma-\rho+\frac{\alpha'+\gamma'}{2}\right)\frac{\cos\frac{\beta'}{2}}{\sin\beta\sin\nu}\frac{\partial}{\partial\alpha}-i\cos\left(\gamma-\rho+\frac{\alpha'+\gamma'}{2}\right)\frac{\cos\frac{\beta'}{2}}{\sin\nu}\frac{\partial}{\partial\beta} \\
& +i\left[2\sin\left(\rho+\frac{\alpha'-\gamma'}{2}\right)\frac{\sin\frac{\beta'}{2}}{\sin 2\nu}+\sin\left(\gamma-\rho+\frac{\alpha'+\gamma'}{2}\right)\cot\beta\frac{\cos\frac{\beta'}{2}}{\sin\nu}\right]\frac{\partial}{\partial\gamma} \\
& +\frac{i}{2}\cos\left(\rho+\frac{\alpha'-\gamma'}{2}\right)\sin\frac{\beta'}{2}\frac{\partial}{\partial\nu}+\frac{3i}{4}\sin\left(\rho+\frac{\alpha'-\gamma'}{2}\right)\tan\nu\sin\frac{\beta'}{2}\frac{\partial}{\partial\rho} \\
& -\frac{i}{2}\sin\left(\rho+\frac{\alpha'-\gamma'}{2}\right)\left[\sin\frac{\beta'}{2}\tan\nu+\frac{\cot\nu}{\sin\frac{\beta'}{2}}\right]\frac{\partial}{\partial\alpha'} \\
& +i\cos\left(\rho+\frac{\alpha'-\gamma'}{2}\right)\cot\nu\cos\frac{\beta'}{2}\frac{\partial}{\partial\beta'}+\frac{i}{2}\sin\left(\rho+\frac{\alpha'-\gamma'}{2}\right)\frac{\cot\nu}{\sin\frac{\beta'}{2}}\frac{\partial}{\partial\gamma'}\ , \\
R_7 = & i\cos\left(\gamma-\rho+\frac{\alpha'+\gamma'}{2}\right)\frac{\cos\frac{\beta'}{2}}{\sin\beta\sin\nu}\frac{\partial}{\partial\alpha}-i\sin\left(\gamma-\rho+\frac{\alpha'+\gamma'}{2}\right)\frac{\cos\frac{\beta'}{2}}{\sin\nu}\frac{\partial}{\partial\beta} \\
& +i\left[2\cos\left(\rho+\frac{\alpha'-\gamma'}{2}\right)\frac{\sin\frac{\beta'}{2}}{\sin 2\nu}-\cos\left(\gamma-\rho+\frac{\alpha'+\gamma'}{2}\right)\cot\beta\frac{\cos\frac{\beta'}{2}}{\sin\nu}\right]\frac{\partial}{\partial\gamma} \\
& -\frac{i}{2}\sin\left(\rho+\frac{\alpha'-\gamma'}{2}\right)\sin\frac{\beta'}{2}\frac{\partial}{\partial\nu}+\frac{3i}{4}\cos\left(\rho+\frac{\alpha'-\gamma'}{2}\right)\tan\nu\sin\frac{\beta'}{2}\frac{\partial}{\partial\rho} \\
& -\frac{i}{2}\cos\left(\rho+\frac{\alpha'-\gamma'}{2}\right)\left[\sin\frac{\beta'}{2}\tan\nu+\frac{\cot\nu}{\sin\frac{\beta'}{2}}\right]\frac{\partial}{\partial\alpha'} \\
& -i\sin\left(\rho+\frac{\alpha'-\gamma'}{2}\right)\cot\nu\cos\frac{\beta'}{2}\frac{\partial}{\partial\beta'}+\frac{i}{2}\cos\left(\rho+\frac{\alpha'-\gamma'}{2}\right)\frac{\cot\nu}{\sin\frac{\beta'}{2}}\frac{\partial}{\partial\gamma'}\ , \\
R_8 = & -\frac{i\sqrt{3}}{2}\frac{\partial}{\partial\rho}\ .
\end{aligned} \tag{A.7}$$

Here we also want to outline how the eigenvalue problem for the collective Hamiltonian (2.36) reduces to coupled differential equations for functions, which only depend on the strangeness changing angle ν . Up to the normalization a suitable decomposition of the baryon wave-functions is given by [62]

$$\Psi(I, I_3, Y; J, J_3, Y_R) = \sum_{M_L, M_R} D_{I_3, M_L}^{(I)*}(\alpha, \beta, \gamma) f_{M_L, M_R}^{(I, Y; J, Y_R)}(\nu) e^{iY_R \rho} D_{M_R, -J_3}^{(J)*}(\alpha', \beta', \gamma')\ . \tag{A.8}$$

The D -functions refer to $SU(2)$ Wigner functions. It is important to note that the sums over the intrinsic spins ($M_R = -J, -J+1, \dots, J$) and isospins ($M_L = -I, -I+1, \dots, I$) are subject to the constraint $M_L - M_R = (Y - Y_R)/2$. Using the explicit forms for the $SU(3)$ generators (A.7) the action of the quadratic Casimir operator $C_2 = \sum_{a=1}^8 R_a^2$ on the baryon wave-function (A.8) is found to be

$$C_2 \Psi(I, I_3, Y; J, J_3, Y_R) = \sum_{M_L, M_R} D_{I_3, M_L}^{(I)*}(\alpha, \beta, \gamma) e^{iY_R \rho} D_{J_3, M_R}^{(J)*}(\alpha', \beta', \gamma')$$

$$\begin{aligned}
& \times \left\{ -\frac{1}{4} \left[\frac{d^2}{d\nu^2} + (3\cot\nu - \tan\nu) \frac{d}{d\nu} \right] + \frac{I^2 + J^2}{\sin^2\nu} + \frac{M_L^2}{\cos^2\nu} + \frac{M_R^2}{4} \left(3 + \frac{1}{\cos^2\nu} \right) \right. \\
& - \frac{1 + \cos^2\nu}{\sin^2\nu \cos^2\nu} M_L M_R + \frac{3Y_R M_L}{2\cos^2\nu} - 3 \frac{1 + \cos^2\nu}{4\cos^2\nu} Y_R M_R + \left(\frac{3}{4} + \frac{9}{16} \tan^2\nu \right) \left. \right\} f_{M_L, M_R}^{(I, Y; J, Y_R)}(\nu) \\
& - \frac{\cos\nu}{\sin^2\nu} \sqrt{(I + M_L + 1)(I - M_L)(J + M_R + 1)(J - M_R)} f_{M_L+1, M_R+1}^{(I, Y; J, Y_R)}(\nu) \\
& - \frac{\cos\nu}{\sin^2\nu} \sqrt{(I - M_L + 1)(I + M_L)(J - M_R + 1)(J + M_R)} f_{M_L-1, M_R-1}^{(I, Y; J, Y_R)}(\nu). \tag{A.9}
\end{aligned}$$

Obviously the dependence on the angles other than ν can be factorized leaving a set of coupled ordinary differential equations in the variable ν . This becomes even more transparent by displaying the ν dependence of the dominating symmetry breaking term in the collective Hamiltonian (2.36)

$$1 - D_{88} = \frac{3}{2} \sin^2\nu. \tag{A.10}$$

Eq. (A.9) also illustrates how the intrinsic functions $f_{M_L, M_R}^{(I, Y; J, Y_R)}(\nu)$ depend on the spin and isospin quantum numbers.

The eigenvalue equation $C_2\Psi = \mu\Psi$ yields the flavor symmetric $SU(3)$ D-functions, which correspond to irreducible representations. As an example we display the non-vanishing intrinsic functions for the baryon octet. The constraint $M_L - M_R = (Y - 1)/2$ has to be taken into consideration.

$$\begin{aligned}
N & : f_{\frac{1}{2}, \frac{1}{2}}^{\frac{1}{2}, 1; \frac{1}{2}, 1}(\nu) = \cos^2\nu, f_{-\frac{1}{2}, -\frac{1}{2}}^{\frac{1}{2}, 1; \frac{1}{2}, 1}(\nu) = \cos\nu; & \Lambda & : f_{0, \frac{1}{2}}^{0, 0; \frac{1}{2}, 1}(\nu) = \sin\nu \cos\nu; \\
\Sigma & : f_{0, \frac{1}{2}}^{1, 0; \frac{1}{2}, 1}(\nu) = \frac{1}{\sqrt{2}} \cos\nu \sin\nu, f_{-1, -\frac{1}{2}}^{1, 0; \frac{1}{2}, 1}(\nu) = \sin\nu; & \Xi & : f_{-\frac{1}{2}, \frac{1}{2}}^{\frac{1}{2}, -1; \frac{1}{2}, 1}(\nu) = \sin^2\nu. \tag{A.11}
\end{aligned}$$

Obviously non of these wave-functions vanishes except at the boundaries $\nu = 0, \pi/2$. This is, of course, a special feature of the ground states, which reside in the $\mathbf{8}$ representation. The isoscalar wave-functions associated with baryons in higher dimensional representations, which carry the same physical quantum numbers (I, J, Y) , may well develop nodes.

When the eigenvalue problem is augmented by symmetry breaking terms the intrinsic function deviate from (A.11) such that they get more pronounced at small ν , *i.e.* rotations into the direction of strangeness are suppressed. This can also be deduced from figure A.1 where the dependencies of the nucleon isoscalar functions $f_{\pm\frac{1}{2}, \pm\frac{1}{2}}^{\frac{1}{2}, 1; \frac{1}{2}, 1}(\nu)$ are displayed for the symmetric case, $\gamma\beta^2 = 0$ as well as for large symmetry breaking $\gamma\beta^2 = 9$. All other symmetry breakers have been ignored.

It should be noted that this procedure to compute the eigenvalues of the collective Hamiltonian (2.36) is completely equivalent to diagonalizing it in a basis built from $SU(3)$ representations. In addition to the constraint $Y_R = 1$ for the allowed representations one more condition has to be satisfied, which stems from the grand spin symmetry of the hedgehog *ansatz*. For $\nu = 0$ the wave-function must be invariant under a combined spin and isospin transformation T . Denoting the coordinate and isospin space ‘‘Euler angles’’ by $R_J = (\alpha', \beta', \gamma')$ and $R_I = (\alpha, \beta, \gamma)$, this implies

$$\begin{aligned}
& \sum_{M_L, M_R} D_{I_3, M_L}^{(I)*}(R_I T) f_{M_L, M_R}^{(I, Y; J, Y_R)}(0) D_{M_R, -J_3}^{(J)*}(T^{-1} R_J) \\
& = \sum_{M_L, M_R} D_{I_3, M_L}^{(I)*}(R_I) f_{M_L, M_R}^{(I, Y; J, Y_R)}(0) D_{M_R, -J_3}^{(J)*}(R_J) \tag{A.12}
\end{aligned}$$

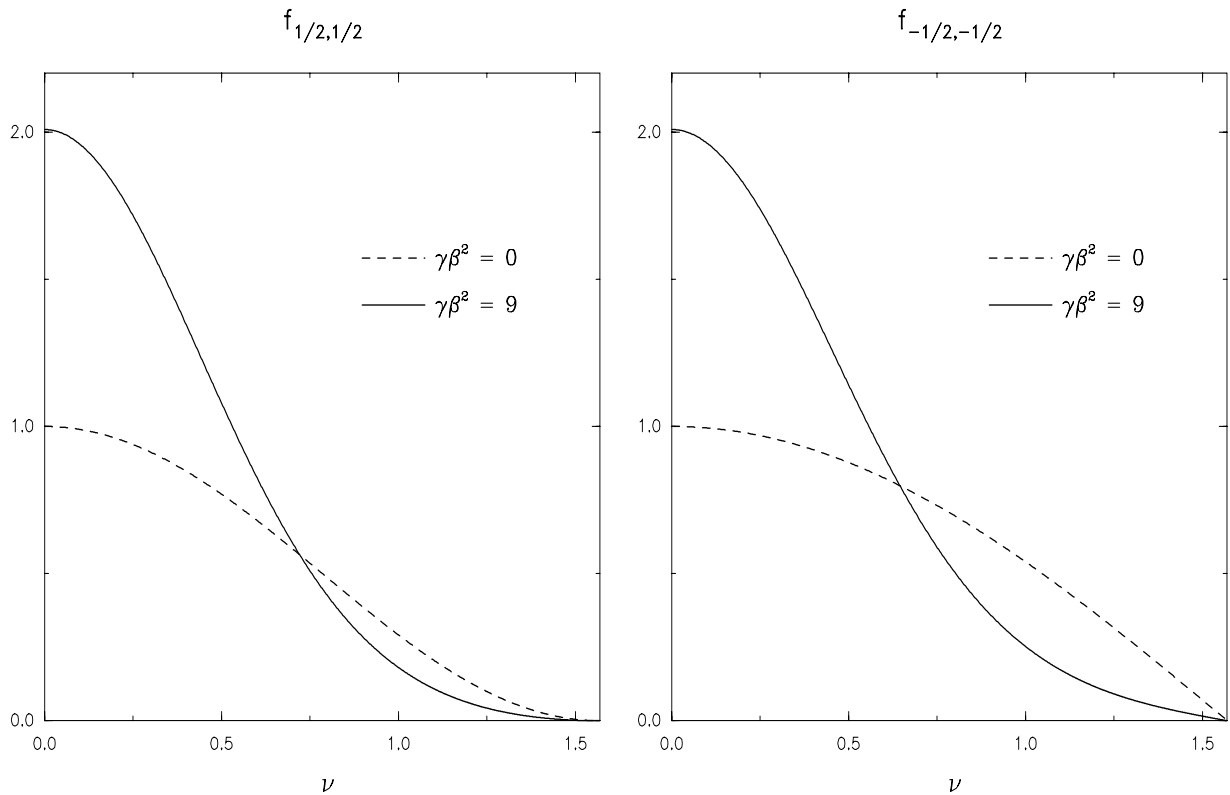


Figure A.1: The dependencies of the nucleon scalar functions on the strangeness changing angle ν for two values of the symmetry breaking. The case $\gamma\beta^2=0$ should be compared with the expressions for (N) in eq (A.11).

which can only be solved if

$$f_{M_L, M_R}^{(I, Y; J, Y_R)}(0) = \mathcal{C}(I; Y, Y_R) \delta_{M_L, M_R} \delta_{I, J}. \quad (\text{A.13})$$

Because of completeness, at least one of $\mathcal{C}(I; Y, Y_R)$ must not vanish within a specified representation. Hence in each of the $SU(3)$ representations, which constitute the basis for diagonalizing the collective Hamiltonian, a state with $I = J$ must exist [57]. Since the static field configuration (2.25) commutes with λ^8 this state must furthermore satisfy $Y = Y_R$. The fact that $\mathcal{C}(1/2; 1, 1)$ does not depend on the intrinsic projections $M_{L, R}$ can also be seen in figure A.1. In the limit of large symmetry breaking the isoscalar functions can be approximated by $f_{M_L, M_R}(\nu) \approx f_{M_L, M_R}(0) \delta(\nu)$. It is therefore obvious from eq (A.13) that this limit corresponds to the two flavor model.

Here also a few comments on the treatment of the slow rotator discussed in section 3.1 will be added. In a first step the explicit form (A.9) for the Casimir operator is used in order to express the Hamiltonian (3.5) as a second order differential equation for the isoscalar functions $f_{M_L, M_R}^{(I, Y; J, Y_R)}(\nu)$, which are defined in eq (A.8). These coupled differential equations are then integrated by standard means. In order to evaluate matrix elements like (3.7) one again employs the decomposition (A.8) to reduce these to expressions which only contain functions of the strangeness changing angle ν and $f_{M_L, M_R}^{(I, Y; J, Y_R)}(\nu)$. The final result is obtained by integrating with respect to the measure

$$\int_0^{\frac{\pi}{2}} d\nu \sin 2\nu \sin^2 \nu \{ \dots \}. \quad (\text{A.14})$$

For example, the contribution of the first term in eq (3.7) to the magnetic moment of the proton is found to be

$$\begin{aligned} \mu_p = & -\frac{8\pi}{3}M_N \int_0^{\frac{\pi}{2}} d\nu \sin 2\nu \sin^2 \nu m_1(\nu) \left\{ \frac{2}{3} \sin^2 \nu \left(\left(f_{\frac{1}{2}, \frac{1}{2}}^{\frac{1}{2}, 1; \frac{1}{2}, 1}(\nu) \right)^2 - \left(f_{-\frac{1}{2}, -\frac{1}{2}}^{\frac{1}{2}, 1; \frac{1}{2}, 1}(\nu) \right)^2 \right) \right. \\ & \left. - \frac{2}{9} \left[(1 + \cos^2 \nu) \left(\left(f_{\frac{1}{2}, \frac{1}{2}}^{\frac{1}{2}, 1; \frac{1}{2}, 1}(\nu) \right)^2 + \left(f_{-\frac{1}{2}, -\frac{1}{2}}^{\frac{1}{2}, 1; \frac{1}{2}, 1}(\nu) \right)^2 \right) + 8 \cos \nu f_{\frac{1}{2}, \frac{1}{2}}^{\frac{1}{2}, 1; \frac{1}{2}, 1}(\nu) f_{-\frac{1}{2}, -\frac{1}{2}}^{\frac{1}{2}, 1; \frac{1}{2}, 1}(\nu) \right] \right\}, \end{aligned} \quad (\text{A.15})$$

where the isoscalar functions $f(\nu)$ are obtained by constructing the eigenstates of the Hamiltonian (3.5). Their normalization is determined by the one of $\Psi(I, I_3, Y; J, J_3, Y_R)$. The ν dependence of m_1 is purely due to the implicit dependence of the chiral angle $F = F(r, \nu)$ in the slow rotator approach [117]

$$m_1(\nu) = \int_0^\infty dr r^2 \sin^2 F \left[f_\pi^2 + \frac{1}{e^2} \left(F'^2 + \frac{\sin^2 F}{r^2} \right) + \frac{\epsilon_6^2}{4\pi^4} \frac{F'^2 \sin^2 F}{r^2} + \frac{2}{3} (f_K^2 - f_\pi^2) \cos F \right]. \quad (\text{A.16})$$

A prime indicates a derivative with respect to the radial coordinate, *i.e.* $F' = \partial F(r, \nu) / \partial r$.

Appendix B

In this appendix we will present the quantities relevant for the collective Hamiltonian in the vector meson model, which is discussed in Section 4.2. Also a few typographical errors are corrected, which happened to occur in the corresponding expressions of ref [40]. For convenience the notation $\alpha'' = x\alpha'$, etc. will be introduced, where x measures the strangeness symmetry breaking (2.17).

The classical mass is given by

$$\begin{aligned} E = & 4\pi \int dr \left[\frac{f_\pi^2}{2} (F'^2 r^2 + 2 \sin^2 F) - \frac{r^2}{2g^2} (\omega'^2 + m_\rho^2 \omega^2) + \frac{1}{g^2} [G'^2 + \frac{G^2}{2r^2} (G+2)^2] \right. \\ & + \frac{m_V^2}{g^2} (1 + G - \cos F)^2 + \frac{\gamma_1}{g} F' \omega \sin^2 F - \frac{2\gamma_2}{g} G' \omega \sin F \\ & + \frac{\gamma_3}{g} F' \omega G (G+2) + \frac{1}{g} (\gamma_2 + \gamma_3) F' \omega [1 - 2(G+1) \cos F + \cos^2 F] \\ & + (1 - \cos F) \left\{ 4\delta' r^2 + 2(2\beta' - \frac{\alpha'}{g^2}) (F'^2 r^2 + 2 \sin^2 F) \right. \\ & \left. - \frac{2\alpha'}{g^2} [\omega^2 r^2 - 2(G+1 - \cos F)^2 - 4(1 + \cos F)(1 + G - \cos F)] \right\} \Big]. \end{aligned} \quad (\text{B.1})$$

For the moment of inertia for rotations in coordinate space, $\alpha^2 = \alpha_S^2 + \alpha_{SB}^2$ we get

$$\begin{aligned} \alpha_S^2 = & \frac{8\pi}{3} \int dr \left[f_\pi^2 r^2 \sin^2 F - \frac{4}{g^2} (\phi'^2 + 2 \frac{\phi^2}{r^2} + m_\rho^2 \phi^2) \right. \\ & + \frac{m_\rho^2}{2g^2} r^2 [(\xi_1 + \xi_2)^2 + 2(\xi_1 - 1 + \cos F)^2] \\ & + \frac{1}{2g^2} [(3\xi_1'^2 + 2\xi_1' \xi_2' + \xi_2'^2) r^2 + 2(G^2 + 2G + 2)\xi_2^2 + 4G^2(\xi_1^2 + \xi_1 \xi_2 - 2\xi_2 - \xi_2 + 1)] \\ & \left. + \frac{4}{g} \gamma_1 \phi F' \sin^2 F + \frac{4}{g} \gamma_3 \phi F' [(G - \xi_1)(1 - \cos F) + (1 - \cos F)^2 - G\xi_1] \right] \end{aligned}$$

$$\begin{aligned}
& + \frac{2\gamma_2}{g} \{ \phi' \sin F (G - \xi_1 + 2 - 2\cos F) + \phi \sin F (\xi_1' - G') \\
& + \phi F' [2 + 2\sin^2 F + (\xi_1 - G - 2)\cos F - 2(\xi_1 + \xi_2)] \} \\
& \quad - \frac{1}{2} [\eta'^2 r^2 + 2\eta^2 + \tilde{m}_\eta^2 r^2 \eta^2] \\
& - \frac{\gamma_1}{3g f_\pi} [\eta' (\xi_1 + \xi_2) \sin^2 F + 2\eta F' (G + \xi_1) \sin F] - \frac{3\gamma_3}{g f_\pi} \eta' (G + 1 - \cos F)^2 (\xi_1 + \xi_2) \\
& - \frac{\gamma_2}{g f_\pi} (\eta' [(G + \xi_1)G + (\xi_1 + \xi_2)[(1 - \cos F)^2 - 2G\cos F]] + \eta (G\xi_1' - G'\xi_1)) \\
& + \frac{\gamma_2 g}{2f_\pi} [\eta (\phi\omega' - \omega\phi') - \eta' \phi\omega], \tag{B.2}
\end{aligned}$$

$$\begin{aligned}
\alpha_{SB}^2 = & -\frac{4\pi}{3} \int dr \left[8(\beta' - \frac{\alpha'}{2g^2}) \left\{ 2r^2 \sin^2 F \cos F - \frac{1}{f_\pi^2} [(\eta'^2 r^2 + 2\eta^2 \right. \right. \\
& \quad \left. \left. - \frac{1}{2}(F'^2 r^2 + 2\sin^2 F)\eta^2) \cos F - 2r^2 \sin F F' \eta \eta' \right\} + \frac{\delta'}{4f_\pi^2} r^2 \cos F \eta^2 \right. \\
& + \frac{4\alpha'}{g^2} r^2 [\cos F [2(\xi_1 - 1 + \cos F)^2 + (\xi_1 + \xi_2)^2 - \frac{8}{r^2} \phi^2] + 4\sin^2 F (\xi_1 - 1 + \cos F)] \\
& \left. - \frac{2\alpha'}{g^2 f_\pi^2} [(1 + G - \cos F) \sin^2 F \eta^2 + [\omega^2 r^2 - 2(1 + G - \cos F)^2] \cos F \eta^2 \right. \\
& \quad \left. + 2f_\pi \omega \sin F \eta (\xi_1 + \xi_2) \right]. \tag{B.3}
\end{aligned}$$

The expression for the moment of inertia associated with rotations into the direction of strangeness is slightly lengthy. We therefore split it into pieces according to which part of the action they originate (flavor symmetric, anomalous and flavor symmetry breaking)

$$\beta^2 = \beta_S^2 + \beta_{an}^2 + \beta_{SB}^2 \tag{B.4}$$

and list them separately.

$$\begin{aligned}
\beta_S^2 = & \pi \int dr \left\{ 2f_\pi^2 \left[r^2 (1 - \cos F) - 2r^2 (1 + \cos \frac{F}{2})^2 W'^2 - 2r^2 \sin \frac{F}{2} F' W W' \right. \right. \\
& \quad \left. + [\sin F (3\sin F + 4\sin \frac{F}{2}) - (1 + 2\cos \frac{F}{2} + \cos F)^2 + \frac{1}{2} r^2 F'^2] W^2 \right\} \\
& + \frac{1}{g^2} \left[2G' D E + 4r^2 (S' + \frac{\omega}{4} E)^2 + 2[\frac{\omega}{2} D + G(S - 1)]^2 \right. \\
& \quad \left. - 2(D' + \frac{E}{2} G)^2 + 2r^2 \omega' E (1 - S) - \frac{2}{r^2} (G + 1)(G + 2) D^2 \right] \\
& + 2\frac{m_V^2}{g^2} \left[2r^2 \omega W \sin \frac{F}{2} - (1 + 4\cos \frac{F}{2} + 3\cos F)(1 + G - \cos F) W^2 + 2r^2 \left(S - 1 + \cos \frac{F}{2} \right)^2 \right. \\
& \quad \left. - \frac{r^2}{2} \left(E + 2\cos \frac{F}{2} W' - F' W \right)^2 - [D + 2W \sin \frac{F}{2} (1 + \cos \frac{F}{2})]^2 \right] \} \tag{B.5}
\end{aligned}$$

$$\begin{aligned}
\beta_{an}^2 = & \frac{\pi}{g} \int dr \left\{ \frac{g}{\pi^2} \left\{ F' [3\sin^2 F \sin \frac{F}{2} + 4\sin F \cos^2 \frac{F}{2} (1 + \cos \frac{F}{2})] W \right. \right. \\
& \quad \left. \left. + 2\cos \frac{F}{2} \sin^2 F (1 + \cos \frac{F}{2}) W' \right\} \right.
\end{aligned}$$

$$\begin{aligned}
& -(2\gamma_1 + 3\gamma_2) \left\{ 2F' \sin \frac{F}{2} \sin^2 FW + 2\omega \sin \frac{F}{2} \sin^2 FWW' \right. \\
& \quad - \omega F' \left(\frac{7}{2} \sin F + 4 \sin \frac{F}{2} \right) \sin FW^2 \\
& \quad - \frac{8}{3} \sin \frac{F}{2} \sin F \left(1 + \cos \frac{F}{2} \right) (1 + G - \cos F) W' \\
& \quad + \frac{1}{3} \omega \left(1 + 2 \cos \frac{F}{2} + \cos F \right) \left[F' \left(1 + 2 \cos \frac{F}{2} + \cos \frac{F}{2} \right) W^2 + 4 \sin F \left(1 + \cos \frac{F}{2} \right) WW' \right] \\
& \quad - \frac{2}{3} \sin^2 F \left[\sin \frac{F}{2} \left(E + 2 \sin \frac{F}{2} W' - F' W \right) - 2 \left(1 + \cos \frac{F}{2} \right) S W' + \left(1 - \cos F \right) W' \right] \\
& \quad + \frac{4}{3} F' \sin F \left[\left(1 + 2 \cos \frac{F}{2} + \cos F \right) \left(S - 1 + \cos \frac{F}{2} \right) W \right. \\
& \quad \quad \left. + \sin \frac{F}{2} \left(D + 2W \sin \frac{F}{2} \left(1 + \cos \frac{F}{2} \right) \right) \right] \left. \right\} \\
& + \gamma_2 \left\{ \omega' \left[\left(1 + G - \cos F \right) \left(3 \sin F + 4 \sin \frac{F}{2} \right) - \sin F \left(1 + 4 \cos \frac{F}{2} + 3 \cos F \right) \right] W^2 \right. \\
& \quad - 2 \sin F \left(1 + G - \cos F \right) \left(1 - S \right) E + 2F' G \left(G + 2 \right) \sin \frac{F}{2} W + \frac{\omega}{2} F' D^2 - \omega \sin F D E \\
& \quad + \omega G \left(G + 2 \right) \left(2 \sin \frac{F}{2} WW' - \frac{F'}{2} W^2 \right) + 4 \sin F \sin \frac{F}{2} G' W - \omega G' \left(3 \sin F + 4 \sin \frac{F}{2} \right) W^2 \\
& \quad - \omega' \left(1 + 2 \cos \frac{F}{2} + \cos F \right) \left[D + 2W \sin \frac{F}{2} \left(1 + \cos \frac{F}{2} \right) \right] W \\
& \quad + \omega \left[\left(1 + \cos \frac{F}{2} \right) \left(G + 2 \right) D W' + \left(1 + 2 \cos \frac{F}{2} + \cos F \right) \left(D' + \frac{E}{2} G \right) W \right] \\
& \quad + 2G' \sin \frac{F}{2} \left[D + 2W \sin \frac{F}{2} \left(1 + \cos \frac{F}{2} \right) \right] + 2G' \left(1 + 2 \cos \frac{F}{2} + \cos F \right) \left(S - 1 + \cos \frac{F}{2} \right) W \\
& \quad + G \left(G + 2 \right) \left[2 \left(1 + \cos \frac{F}{2} \right) \left(S - 1 + \cos \frac{F}{2} \right) W' - \sin \frac{F}{2} \left(E + 2 \sin \frac{F}{2} W' - F' W \right) \right] \\
& \quad - \left(1 + G - \cos F \right) \left[2 \left(1 + 2 \cos \frac{F}{2} + \cos F \right) \left(S' + \frac{\omega}{4} E \right) W \right. \\
& \quad \left. + \left(1 + \cos \frac{F}{2} \right) \left[\omega D + 2G \left(1 - S \right) \right] W' + 2 \sin \frac{F}{2} \left(D' + \frac{E}{2} G \right) \right] \\
& \quad + F' \left[\left[\frac{\omega}{2} D + G \left(1 - S \right) \right] \left[D + 2W \sin \frac{F}{2} \left(1 + \cos \frac{F}{2} \right) \right] + \left(G + 2 \right) \left(S - 1 + \cos \frac{F}{2} \right) D \right] \\
& \quad + 2 \sin F \left(S - 1 + \cos \frac{F}{2} \right) \left(D' + \frac{E}{2} G \right) - 2 \sin F \left[\left(S' + \frac{\omega}{4} E \right) \left[D + 2W \sin \frac{F}{2} \left(1 + \cos \frac{F}{2} \right) \right] \right. \\
& \quad \left. + \frac{1}{4} \left[\omega D + 2G \left(1 - S \right) \right] \left(E + 2 \sin \frac{F}{2} W' - F' W \right) \right] \left. \right\} \\
& - \left(\gamma_2 + 2\gamma_3 \right) \left[2 \sin \frac{F}{2} \left(1 + G - \cos F \right)^2 \left(F' + \omega W' \right) W \right. \\
& \quad + \omega F' \left[D + 2W \sin \frac{F}{2} \left(1 + \cos \frac{F}{2} \right) \right]^2 \\
& \quad + \frac{\omega}{2} F' \left(1 + G - \cos F \right) \left(1 - G + 8 \cos \frac{F}{2} + 7 \cos F \right) W^2 \\
& \quad \left. - 2 \omega \sin F \left(E + 2 \sin \frac{F}{2} W' - F' W \right) \left[D + 2W \sin \frac{F}{2} \left(1 + \cos \frac{F}{2} \right) \right] \right]
\end{aligned}$$

$$\begin{aligned}
& -2(1 + G - \cos F)^2 \left[\sin \frac{F}{2} (E + 2 \sin \frac{F}{2} W' - F'W) \right. \\
& \quad \left. - 2(1 + \cos \frac{F}{2})(S - 1 + \cos \frac{F}{2})W' \right] \\
& + 4 \sin F (1 + G - \cos F)(S - 1 + \cos \frac{F}{2})(E + 2 \sin \frac{F}{2} W' - F'W) \Big] \Big\}, \tag{B.6}
\end{aligned}$$

$$\begin{aligned}
\beta_{SB}^2 = & 4\pi \int \left\{ (2\beta' - \frac{\alpha'}{g^2}) \left[\cos F [\cos F - 1 + 2(1 + \cos \frac{F}{2})^2 (W'^2 + \frac{2}{r^2} \cos^2 \frac{F}{2} W^2) \right. \right. \\
& + 4 \sin \frac{F}{2} F' W' W - F'^2 W^2 - \frac{2}{r^2} \sin F (3 \sin F + 4 \sin \frac{F}{2}) W^2 \Big] \\
& + (F'^2 + \frac{2}{r^2} \sin^2 F)(1 + \cos \frac{F}{2})(1 - 2 \cos \frac{F}{2}) W^2 \\
& - 2(1 + \cos \frac{F}{2})(\sin F + \sin \frac{F}{2})(F' W' + \frac{2}{r^2} \sin F \cos \frac{F}{2} W) W \Big] \\
& + (2\beta'' - \frac{\alpha''}{g^2})(1 + \cos \frac{F}{2}) \left[2(\cos \frac{F}{2} - 1) + 2(1 + \cos \frac{F}{2})(W'^2 + \frac{2}{r^2} \cos^2 \frac{F}{2} W^2) \right. \\
& - 2 \sin \frac{F}{2} (F' W' W + \frac{2}{r^2} \sin F \cos \frac{F}{2} W^2) - \cos \frac{F}{2} (F'^2 + \frac{2}{r^2} \sin^2 F) W^2 \Big] \\
& - \alpha' \cos F \left[4 \omega \sin \frac{F}{2} W - \frac{2}{r^2} (1 + G - \cos F)(1 + 4 \cos \frac{F}{2} + 3 \cos F) W^2 \right] \\
& - 2(\alpha' \cos F + \alpha'') \left[(S - 1 + \cos \frac{F}{2})^2 - \frac{1}{4} (E + 2 \sin \frac{F}{2} W' - F'W)^2 \right. \\
& \quad \left. - \frac{1}{2r^2} [D + 2W \sin \frac{F}{2} (1 + \cos \frac{F}{2})]^2 \right] \\
& + (1 + \cos \frac{F}{2}) \left[\alpha' (2 \cos \frac{F}{2} - 1) + \alpha'' \cos \frac{F}{2} \right] \left[\omega^2 - \frac{2}{r^2} (1 + G - \cos F)^2 \right] W^2 \\
& + 2 \left[\alpha' (\sin F + \sin \frac{F}{2}) + \alpha'' \sin \frac{F}{2} \right] \left[\omega (S - 1 + \cos \frac{F}{2}) W \right. \\
& \quad \left. - \frac{1}{r^2} (1 + G - \cos F) [D + 2W \sin \frac{F}{2} (1 + \cos \frac{F}{2})] W \right] \\
& + 2 \left[\alpha' (\cos F + \cos \frac{F}{2}) + \alpha'' (1 + \cos \frac{F}{2}) \right] \left[r^2 \omega \sin \frac{F}{2} + \frac{r^2}{2} F' (E + 2 \sin \frac{F}{2} W' - F'W) \right. \\
& \quad \left. - \sin F [D + 2W \sin \frac{F}{2} (1 + \cos \frac{F}{2})] - (1 + 2 \cos \frac{F}{2} + \cos F)(1 + G - \cos F) W \right] W \\
& + 2 \left[2 \alpha' (\sin F + \sin \frac{F}{2}) + \alpha'' (\sin F + 2 \sin \frac{F}{2}) \right] \sin F (1 + G - \cos F) W^2 \\
& - 2 \alpha' \sin F \left[2r^2 \sin \frac{F}{2} (S - 1 + \cos \frac{F}{2}) + r^2 (1 + \cos \frac{F}{2})(E + 2 \sin \frac{F}{2} W' - F'W) W' \right. \\
& \quad \left. + (1 + 2 \cos \frac{F}{2} + \cos F) [D + 2W \sin \frac{F}{2} (1 + \cos \frac{F}{2})] W \right. \\
& \quad \left. - [(1 + G - \cos F)(3 \sin F + 4 \sin \frac{F}{2}) - \sin F (1 + 4 \cos \frac{F}{2} + 3 \cos F)] W^2 \right] \\
& \left. - [\delta' (1 + 4 \cos \frac{F}{2} + 3 \cos F) + \delta'' (3 + 4 \cos \frac{F}{2} + \cos F)] W^2 \right\}. \tag{B.7}
\end{aligned}$$

Finally the symmetry breaking parameters, γ , α_1 and β_1 are integrals over the classical profile

functions only

$$\begin{aligned} \gamma = & \frac{16\pi}{3} \int dr \left\{ 2(\delta'' - \delta')r^2(1 - \cos F) + 2(\beta' - \beta'' - \frac{\alpha' - \alpha''}{2g^2})\cos F(F'^2r^2 + 2\sin^2 F) \right. \\ & \left. + \frac{\alpha'' - \alpha'}{g^2} [\cos F[\omega^2r^2 - 2(1 + G - \cos F)^2] + 4\sin^2 F(G + 1 - \cos F)] \right\}, \end{aligned} \quad (\text{B.8})$$

$$\alpha_1 = 2\beta_1 = \frac{16\pi}{\sqrt{3}} \frac{\alpha'' - \alpha'}{g^2} \int dr r^2 \omega \cos F. \quad (\text{B.9})$$

For completeness we also display the Skyrme model expression for the moment of inertia $\beta^2 = \beta_S^2 + \beta_{SB}^2$ which enters the computations of Section 2.3. The contribution from the Wess–Zumino term is included in β_S^2 .

$$\begin{aligned} \beta_S^2 = & \pi \int dr \left\{ 2f_\pi^2 r^2 (1 - \cos F) + \frac{1}{2e^2} (1 - \cos F) (F'^2 r^2 + 2\sin^2 F) \right. \\ & - 2 \left(2f_\pi^2 r^2 + \frac{1}{e^2} \sin^2 F \right) \left(1 + \cos \frac{F}{2} \right)^2 W'^2 \\ & - 2F' \left[2f_\pi^2 r^2 \sin \frac{F}{2} + \frac{4}{e^2} \sin^2 F \sin \frac{F}{2} + \frac{6}{e^2} \sin F \cos \frac{F}{2} \left(1 + \cos \frac{F}{2} \right)^2 \right] W W' \\ & + \left[F'^2 \left(f_\pi^2 r^2 + \frac{8}{e^2} \sin^2 F + \frac{8}{e^2} \sin F \sin \frac{F}{2} \right) + \frac{2}{r^2} \sin F \left(f_\pi^2 r^2 + \frac{\sin^2 F}{e^2} \right) \left(3\sin F + 4\sin \frac{F}{2} \right) \right. \\ & \left. - \frac{1}{r^2} \left(2f_\pi^2 r^2 + \frac{1}{2e^2} F'^2 r^2 + \frac{2}{e^2} \sin^2 F \right) \left(1 + 2\cos \frac{F}{2} + \cos^2 F \right)^2 \right] W^2 \\ & \left. + \frac{F'}{\pi^2} \left[3\sin \frac{F}{2} \sin^2 F + 4\cos^2 \frac{F}{2} \sin F \left(1 + \cos \frac{F}{2} \right) \right] W + \frac{2}{\pi^2} \cos \frac{F}{2} \sin^2 F \left(1 + \cos \frac{F}{2} \right) W' \right\}, \end{aligned} \quad (\text{B.10})$$

$$\begin{aligned} \beta_{SB}^2 = & 8\pi \int dr r^2 \left\{ \beta' \left[\cos F [\cos F - 1 + 2 \left(1 + \cos \frac{F}{2} \right)^2 \left(W'^2 + \frac{2}{r^2} \cos^2 \frac{F}{2} W^2 \right) \right. \right. \\ & + 4F' \sin \frac{F}{2} W' W - F'^2 W^2 - \frac{2}{r^2} \sin F \left(3\sin F + 4\sin \frac{F}{2} \right) W^2] \\ & + \left(F'^2 + \frac{2}{r^2} \sin^2 F \right) \left(1 + \cos \frac{F}{2} \right) \left(1 - 2\cos \frac{F}{2} \right) W^2 \\ & - 2 \left(1 + \cos \frac{F}{2} \right) \left(\sin \frac{F}{2} + \sin F \right) \left(F' W' + \frac{2}{r^2} \sin F \cos \frac{F}{2} W \right) W \left. \right] \\ & + \beta'' \left(1 + \cos \frac{F}{2} \right) \left[2 \left(\cos \frac{F}{2} - 1 \right) + 2 \left(1 + \cos \frac{F}{2} \right) \left(W'^2 + \frac{2}{r^2} \cos^2 \frac{F}{2} W^2 \right) \right. \\ & \left. - \cos \frac{F}{2} \left(F'^2 + \frac{2}{r^2} \sin^2 F \right) W^2 - 2\sin \frac{F}{2} \left(F' W' + \frac{2}{r^2} \sin F \cos \frac{F}{2} W \right) \right] \\ & \left. - \frac{1}{2} \left[\delta' \left(3\cos F + 4\cos \frac{F}{2} + 1 \right) + \delta'' \left(\cos F + 4\cos \frac{F}{2} + 3 \right) \right] W^2 \right\}. \end{aligned} \quad (\text{B.11})$$

Appendix C

In this appendix a short remark on the conservation of the axial current and the role of the induced fields is added. For this illustrative purpose it suffices to only consider the non-linear

σ -model (2.3) supplemented by the Wess–Zumino term (2.23). Although no solution to the corresponding equation of motion

$$r^2 F'' + 2r F' = \sin 2F \quad (\text{C.1})$$

for the chiral angle exists, it may be used formally since the Skyrme term (2.7) is omitted for convenience only. Here we are interested in those parts of the axial–vector current, which contain the angular velocities (2.29) $\Omega_4, \dots, \Omega_7$, for the rotations into the direction of strangeness. In the notation of refs [38, 40] these parts are given by

$$A_i^a = [A_3(r)\delta_{ik} + A_4(r)\hat{r}_i\hat{r}_k] d_{k\alpha\beta} D_{a\alpha} \Omega_\beta . \quad (\text{C.2})$$

As usual the convention $i, j, k = 1, 2, 3$ and $\alpha, \beta = 4, \dots, 7$ is adopted. The contribution [224] from the Wess–Zumino term is purely due to the rotation of the classical fields (2.28)

$$\begin{aligned} A_3^{\text{WZ}} &= -\frac{1}{2\pi^2 r^2} F' \sin F \sin \frac{F}{2} , \\ A_4^{\text{WZ}} &= -A_3^{\text{WZ}} + \frac{1}{2\pi^2 r^2} \sin^2 F \sin^2 \frac{F}{2} . \end{aligned} \quad (\text{C.3})$$

A straightforward computation shows that this piece has a non–vanishing divergence

$$\partial_i A_i^a \text{WZ} = \hat{r}_a \frac{3}{4\pi^2} F' \frac{\sin^3 F}{r^2} . \quad (\text{C.4})$$

As long as the field configuration is restricted to the rotating hedgehog (2.28) there will be no other contribution to A_3 and/or A_4 . Hence the (partial) conservation of the axial current is violated. On the other hand the non–linear σ -model contributes via the induced components (2.45, 2.46)

$$\begin{aligned} A_3^{nl\sigma} &= \frac{1}{r} \cos \frac{F}{2} \left(1 + \cos \frac{F}{2} \right) \cos F W \\ A_4^{nl\sigma} &= -A_3^{nl\sigma} + \frac{1}{2} F' \sin \frac{F}{2} W + \cos \frac{F}{2} \left(1 + \cos \frac{F}{2} \right) W' \end{aligned} \quad (\text{C.5})$$

Using the truncated equation of motion (C.1) the divergence of this part of the axial current is obtained to be

$$\begin{aligned} \partial_i A_i^{nl\sigma} &= \hat{r}_a \frac{\cos \frac{F}{2}}{r} \left\{ r^2 \left(1 + \cos \frac{F}{2} \right) W'^2 - r^2 \sin \frac{F}{2} W' + 2r \left(1 + \cos \frac{F}{2} \right) W' \right. \\ &\quad \left. + W \left[\frac{r^2}{4} F'^2 - 2 \cos \frac{F}{2} \cos F \left(1 + \cos \frac{F}{2} \right) \right] \right\} . \end{aligned} \quad (\text{C.6})$$

Upon some integrations by parts and application of eq (C.1) the relevant parts of the moment of inertia for rotations into the direction of strangeness (B.10) can be cast into the form

$$\begin{aligned} \beta^2 &= \frac{1}{\pi} \int_0^\infty dr \left\{ F' \left[3 \sin^2 F \sin \frac{F}{2} + 4 \sin F \cos^2 \frac{F}{2} \left(1 + \cos \frac{F}{2} \right) \right] W \right. \\ &\quad \left. + 2 \cos \frac{F}{2} \sin^2 F \left(1 + \cos \frac{F}{2} \right) W' \right\} \\ &+ \pi \int_0^\infty dr \left\{ -2r^2 \left(1 + \cos \frac{F}{2} \right)^2 W'^2 \right. \\ &\quad \left. + \left[\frac{r^2}{2} F'^2 - 4 \cos \frac{F}{2} \cos F \left(1 + \cos \frac{F}{2} \right) \right] \left(1 + \cos \frac{F}{2} \right) W^2 \right\} + \dots , \end{aligned} \quad (\text{C.7})$$

where the ellipsis indicate terms which are neither due to the non-linear σ model nor the Wess–Zumino term. Straightforward calculation shows that the variation of β^2 yields the proper conservation of the axial current

$$\partial_i A_i^a = \hat{r}_a \frac{1}{4\pi^2 r^2} \cos \frac{F}{2} \left(1 + \cos \frac{F}{2}\right)^{-1} \frac{\delta \beta^2}{\delta W}. \quad (\text{C.8})$$

Stated otherwise, the proper divergence of the axial current can only be obtained when the induced fields are taken into account. The inclusion of a Lagrange multiplier such that the overlap (2.47) vanishes will spoil the relation (C.8) unless the radial functions A_3 and A_4 are altered accordingly. Unfortunately the equation of motion $\delta \beta^2 / \delta W$ does not have a solution in the flavor symmetric case, even when the Skyrme term is included. The reason being the existence of a zero mode, which represents a solution to the homogeneous part of the differential equation without being necessarily orthogonal to the inhomogeneity. However, this point does not give too much of a worry as for the physical situation no such zero mode exists because the flavor symmetric is broken explicitly.

Appendix D

In this appendix some formulas are summarized which are helpful for studying the bound state approach introduced in chapter 5. These expressions are taken from refs [133, 183, 132, 175, 203].

After re-expressing the parameters in the symmetry breaking parts of the Lagrangian (2.19) in terms of physical quantities, the Lagrangian for the fluctuating kaon field K defined in eq (5.1) is given by

$$\begin{aligned} \mathcal{L}_K = & (D_\mu K)^\dagger D^\mu K - m_K^2 K^\dagger K - \frac{f_\pi^2 m_\pi^2}{4f_K^2} K^\dagger \left(\xi_\pi + \xi_\pi^\dagger - 2 \right) K \\ & - \frac{1}{8} K^\dagger K \text{tr} \left(\partial_\mu \xi_\pi^\dagger \partial^\mu \xi_\pi + \frac{1}{4e^2 f_K^2} \left[\xi_\pi^\dagger \partial_\mu \xi_\pi, \xi_\pi^\dagger \partial_\nu \xi_\pi \right]^2 \right) \\ & - \frac{1}{8e^2 f_K^2} \left\{ (D_\mu K)^\dagger D_\nu K \text{tr} (p^\mu p^\nu) + (D_\mu K)^\dagger D^\mu K \text{tr} \left(\partial_\nu \xi_\pi^\dagger \partial^\nu \xi_\pi \right) \right. \\ & \left. - 3 (D_\mu K)^\dagger [p^\mu, p^\nu] D_\nu K \right\} - \frac{iN_C}{4f_K^2} B_\mu \left[K^\dagger D^\mu K - (D_\mu K)^\dagger K \right], \quad (\text{D.1}) \end{aligned}$$

where use has been made of the covariant derivative $D_\mu = \partial_\mu + (\xi_\pi^\dagger \partial_\mu \xi_\pi + \xi_\pi \partial_\mu \xi_\pi^\dagger)/2$. Furthermore $p_\mu = \partial_\mu \xi_\pi \xi_\pi^\dagger + \xi_\pi^\dagger \partial_\mu \xi_\pi$ refers to the induced axial–vector field, see also eq (4.11). Finally B_μ is the topological current (2.9). The radial functions in the differential equation (5.4) are [130, 179]

$$h(r) = 1 + \frac{1}{2e^2 f_K^2} \frac{\sin^2 F}{r^2}, \quad (\text{D.2})$$

$$f(r) = 1 + \frac{1}{4e^2 f_K^2} \left(F'^2 + 2 \frac{\sin^2 F}{r^2} \right), \quad (\text{D.3})$$

$$\lambda(r) = \frac{N_C}{8\pi^2 f_K^2} F' \frac{\sin^2 F}{r^2}, \quad (\text{D.4})$$

$$\begin{aligned}
V_P(r) = & \frac{2}{r^2} \sin^4 \frac{F}{2} \left[1 + \frac{1}{4e^2 f_K^2} \left(F'^2 + \frac{\sin^2 F}{r^2} \right) \right] - \frac{1}{4} \left(F'^2 + 2 \frac{\sin^2 F}{r^2} \right) \\
& - \frac{1}{4e^2 f_K^2} \left\{ \frac{2}{r^2} \sin^2 F \left(2F'^2 + \frac{\sin^2 F}{r^2} \right) - \frac{6}{r^2} \left(\sin^4 \frac{F}{2} \frac{\sin^2 F}{r^2} + \frac{d}{dr} F' \sin^2 F \sin^2 \frac{F}{2} \right) \right\} \\
& - \frac{1}{r^2} \left\{ \sin^2 \frac{F}{2} \left[4 + \frac{1}{e^2 f_K^2} \left(F'^2 + \frac{\sin^2 F}{r^2} \right) \right] - \frac{3}{2e^2 f_K^2} \left(\cos F \frac{\sin^2 F}{r^2} - \frac{d}{dr} F' \cos F \right) \right\} \\
& + \frac{2}{r^2} \left(F'^2 + \frac{\sin^2 F}{r^2} \right) + \frac{m_\pi^2 f_\pi^2}{2f_K^2} (\cos F - 1) \tag{D.5}
\end{aligned}$$

The spectral functions $c(\omega)$ and $d(\omega)$ may be decomposed in terms of the grand spin channels according to eq (5.2). For the present discussion the presentation of the bound state channel ($L = 1$, $G = 1/2$) suffices [131, 133]

$$\begin{aligned}
c_P(\omega) + 1 = & 2\omega \int dr k_P^*(r, \omega) \left\{ \frac{4}{3} r^2 f(r) \cos^2 \frac{F}{2} \right. \\
& \left. + \frac{1}{2e^2 f_K^2} \left[\frac{4}{3} \sin^2 F \cos^2 \frac{F}{2} - \frac{d}{dr} r^2 \sin F F' \right] \right\} k_P(r, \omega) . \tag{D.6}
\end{aligned}$$

Since one has $\omega = 0$ for the zero-mode, it is apparent that c_P is (minus) unity in the flavor symmetric case.

The coefficients in the magnetic moment operator (5.19) read [133], see also [132]

$$\begin{aligned}
\mu_{S,0} = & -\frac{2M_N}{3\pi\alpha^2} \int dr r^2 F' \sin^2 F , \quad \mu_{V,0} = \frac{1}{2} M_N \alpha^2 , \\
\mu_{S,1} = & \chi \mu_{S,0} - \frac{M_N}{3} \int dr \left\{ 4r^2 k_P^2 \cos^2 \frac{F}{2} \right. \\
& \left. + \frac{1}{e^2 f_K^2} \left[4k_P^2 \sin^2 F \cos^2 \frac{F}{2} + r^2 k_P^2 F'^2 \cos^2 \frac{F}{2} + 3r^2 k_P k_P' F' \sin F \right] \right\} , \\
\mu_{V,1} = & \frac{M_N}{3} \int dr \left\{ r^2 k_P^2 \cos^2 \frac{F}{2} \left(1 - \sin^2 \frac{F}{2} \right) + \frac{N_C M_N}{24\pi^2 f_K^2} \omega_P r^2 k_P^2 F' \sin^2 F \right. \\
& + \frac{1}{4e^2 f_K^2} \left[4k_P^2 \sin^2 F \cos^2 \frac{F}{2} \left(3 - 8\sin^2 \frac{F}{2} \right) + r^2 k_P^2 F'^2 \cos^2 \frac{F}{2} \left(1 - 18\sin^2 \frac{F}{2} \right) \right. \\
& \left. \left. + 2k_P'^2 \sin^2 F + 3k_P k_P' F' \sin F \left(3 - 4\sin^2 \frac{F}{2} \right) \right] \right\} , \tag{D.7}
\end{aligned}$$

where the arguments of the bound state wave-function $k_P = k_P(r, \omega_P)$ have been omitted.

Finally the integral kernels $\Phi_{1,2}$, which show up in the bound state equation of the NJL soliton model will be presented. The local kernel $\Phi_1(r)$ does not depend on the eigen energy ω . It acquires contributions from the meson part of the action as well as those terms involving h_1

$$\begin{aligned}
\Phi_1(r) = & -\frac{\pi}{2} m_\pi^2 f_\pi^2 \left(1 + \frac{m_s}{m} \right) \left(\cos \Theta + \frac{m_s^0}{m^0} \right) \\
& - \frac{N_C}{4} \eta_{\text{val}} (m + m_s) \int \frac{d\Omega}{4\pi} \psi_{\text{val}}^\dagger(\mathbf{r}) u_0(\mathbf{r}) \beta u_0(\mathbf{r}) \psi_{\text{val}}(\mathbf{r}) \tag{D.8}
\end{aligned}$$

$$-\frac{N_C}{4}(m+m_s)\int_{1/\Lambda^2}^{\infty}\frac{ds}{\sqrt{4\pi s}}\int\frac{d\Omega}{4\pi}\left\{\sum_{\mu=ns}\epsilon_{\mu}e^{-s\epsilon_{\mu}^2}\psi_{\mu}^{\dagger}(\mathbf{r})u_0(\mathbf{r})\beta u_0(\mathbf{r})\psi_{\mu}(\mathbf{r})\right. \\ \left.+\sum_{\rho=s}\epsilon_{\rho}e^{-s\epsilon_{\rho}^2}\psi_{\rho}^{\dagger}(\mathbf{r})\beta\psi_{\rho}(\mathbf{r})\right\}.$$

The unitary matrix u_0 has been defined in eq (6.48), while the grand spinors $\psi_{\mu}(\mathbf{r})$ denote the spatial representations of the eigenstates of the one-particle Dirac Hamiltonian (6.22). The integral $\int(d\Omega/4\pi)$ indicates that the average with regard to the internal degrees of freedom has been taken. The bilocal kernel $\Phi_2(\omega; r, r')$ originates from the terms quadratic in h_1 and is symmetric in r and r'

$$\Phi_2(\omega; r, r') = -\frac{N_C}{4}(m+m_s)^2\int\frac{d\Omega}{4\pi}\int\frac{d\Omega'}{4\pi}\left\{\eta_{\text{val}}\sum_{\rho=s}\frac{\psi_{\text{val}}^{\dagger}(\mathbf{r})u_0(\mathbf{r})\psi_{\rho}(\mathbf{r})\psi_{\rho}^{\dagger}(\mathbf{r}')u_0(\mathbf{r}')\psi_{\text{val}}(\mathbf{r}')}{\epsilon_{\text{val}}-\omega-\epsilon_{\rho}}\right. \\ \left.-\sum_{\substack{\mu=ns \\ \rho=s}}\psi_{\mu}^{\dagger}(\mathbf{r})u_0(\mathbf{r})\psi_{\rho}(\mathbf{r})\psi_{\rho}^{\dagger}(\mathbf{r}')u_0(\mathbf{r}')\psi_{\mu}(\mathbf{r}')\mathcal{R}_{\mu,\rho}(\omega)\right\}. \quad (\text{D.9})$$

The regulator function appearing eq (D.9) is obtained to be

$$\mathcal{R}_{\mu,\rho}(\omega) = \int_{1/\Lambda^2}^{\infty} ds\sqrt{\frac{s}{\pi}}\left\{\frac{e^{-s\epsilon_{\mu}^2}+e^{-s\epsilon_{\rho}^2}}{s}+[\omega^2-(\epsilon_{\mu}+\epsilon_{\rho})^2]R_0(s;\omega,\epsilon_{\mu},\epsilon_{\rho})\right. \\ \left.-2\omega\epsilon_{\rho}R_1(s;\omega,\epsilon_{\mu},\epsilon_{\rho})+2\omega\epsilon_{\mu}R_1(s;\omega,\epsilon_{\rho},\epsilon_{\mu})\right\}, \quad (\text{D.10})$$

wherein the Feynman parameter integrals

$$R_i(s;\omega,\epsilon_{\mu},\epsilon_{\nu}) = \int_0^1 x^i dx \exp\left(-s[(1-x)\epsilon_{\mu}^2+x\epsilon_{\nu}^2-x(1-x)\omega^2]\right) \quad (\text{D.11})$$

reflect the quark loops in the soliton background. The regulator function (D.11) is nothing but the analogue of the incomplete Γ -functions in eqs (6.13-6.15) when the soliton background field is present.

References

- [1] F. J. Ynduráin, *The Theory of Quark and Gluon Interactions*, Springer-Verlag, Berlin - Heidelberg - New York, 1993.
- [2] T. Muta, *Foundations of Quantum Chromodynamics*, World Scientific, Singapore, 1987.
- [3] G. Holzwarth and B. Schwesinger, Rep. Prog. Phys. **49** (1986) 825.
- [4] I. Zahed and G. E. Brown, Phys. Rep. **142** (1986) 481.
- [5] U.-G. Meißner, Phys. Rep. **161** (1988) 213.
- [6] B. Schwesinger, H. Weigel, G. Holzwarth, and A. Hayashi, Phys. Rep. **173** (1989) 173.
- [7] G. t' Hooft, Nucl. Phys. **B72** (1974) 461; **B75** (1975) 461.
- [8] E. Witten, Nucl. Phys. **B160** (1979) 57.
- [9] T. H. R. Skyrme, Proc. R. Soc. **127** (1961) 260.
- [10] G. S. Adkins, C. R. Nappi, and E. Witten, Nucl. Phys. **B228** (1983) 552.
- [11] B. Moussallam and D. Kalafatis, Phys. Lett. **B272** (1991) 196;
G. Holzwarth, Phys. Lett. **B291** (1992) 218.
- [12] B. Moussallam, Ann. Phys. (NY) **225** (1993) 264.
- [13] G. Holzwarth, Nucl. Phys. **A572** (1994) 69.
- [14] H. Weigel, R. Alkofer, and H. Reinhardt, Nucl. Phys. **A582** (1995) 484.
- [15] G. Holzwarth and H. Walliser, Nucl. Phys. **A587** (1995) 721.
- [16] J. Gasser and H. Leutwyler, Ann. Phys. (NY) **158** (1984) 142.
- [17] Y. Nambu and G. Jona-Lasinio, Phys. Rev. **122** (1961) 345; **124** (1961) 246.
- [18] T. Eguchi and H. Sugawara, Phys. Rev. **D10** (1974) 4257.
- [19] D. Ebert and H. Reinhardt, Nucl. Phys. **B271** (1986) 188.
- [20] S. Brodsky, J. Ellis, and M. Karliner, Phys. Lett. **B206** (1988) 309;
J. Ellis, and M. Karliner, Phys. Lett. **B213** (1988) 73;
- [21] J. Ashman *et al.*, Phys. Lett. **B206** (1988) 364; Nucl. Phys. **B328** (1989) 1.
- [22] J. J. J. Kokkedee, *The Quark Model*, Benjamin, New York, 1979.
- [23] M. Bourquin *et al.*, Z. Phys. **C21** (1983) 27.
- [24] N. W. Park, J. Schechter, and H. Weigel, Phys. Lett. **B224** (1989) 171.
- [25] R. Johnson, N. W. Park, J. Schechter, V. Soni, and H. Weigel, Phys. Rev. **D42** (1990) 2998.
- [26] A. Blotz, M. V. Ployakov, and K. Goeke, Phys. Lett. **B302** (1993) 151.
- [27] R. Jaffe and A. V. Manohar, Nucl. Phys. **B337** (1990) 509.
- [28] H. J. Lipkin, Phys. Lett. **B337** (1994) 157.
- [29] J. Lichtenstadt and H. J. Lipkin, Phys. Lett. **B353** (1995) 119.

- [30] T. P. Cheng and L. F. Li, *Gauge Theory of Elementary Particles*, chapter 5, Clarendon Press, 1988.
- [31] J. Gasser, H. Leutwyler, and M. E. Sanio, Phys. Lett. **253** (1991) 252, 260.
- [32] H. D. Beck, Phys. Rev. **D39** (1989) 3248.
- [33] Particle Data Group, Phys. Rev. **D50** (1994) 1171.
- [34] M. J. Musolf and T. W. Donnelly, Z. Phys. **C57** (1993) 559.
- [35] M. J. Musolf, T. W. Donnelly, J. Dubach, S. J. Pollock, S. Kowalski, and E. J. Beise, Phys. Rep. **239** (1994) 1.
- [36] R. Jaffe, Phys. Lett. **B229** (1989) 275.
- [37] G. Höhler *et al.*, Nucl. Phys. **B114** (1974) 505.
- [38] N. W. Park, J. Schechter, and H. Weigel, Phys. Rev. **D43** (1991) 869.
- [39] T. Cohen, H. Forkel, and M. Nielsen, Phys. Lett. **B316** (1993) 1.
- [40] N. W. Park and H. Weigel, Nucl. Phys. **A541** (1992) 453.
- [41] H. Weigel, A. Abada, R. Alkofer, and H. Reinhardt, Phys. Lett. **B353** (1995) 20.
- [42] G. H. Derrick, J. Math. Phys. **5** (1964) 1252.
- [43] Y. Igarashi, M. Johmura, A. Kobahashi, H. Otsu, T. Sato, and S. Sawada, Nucl. Phys. **B259** (1985) 721.
- [44] W. Pauli, *Meson Theory of Nuclear Forces*, Interscience Publishes, Inc., New York, 1946.
- [45] J. Schechter, A. Subbaraman, and H. Weigel, Phys. Rev. **D48** (1993) 339.
- [46] P. Jain, R. Johnson, N. W. Park, J. Schechter, and H. Weigel, Phys. Rev. **D40** (1989) 855.
- [47] H. Weigel, J. Schechter, N. W. Park, and Ulf-G. Meißner, Phys. Rev. **D42** (1990) 3177.
- [48] J. Gasser and H. Leutwyler, Phys. Rep. **87** (1982) 77.
- [49] D. Kaplan and A. Manohar, Phys. Rev. Lett. **56** (1986) 2004.
- [50] E. Witten, Nucl. Phys. **B233** (1983) 422, 433.
- [51] P. A. M. Dirac, Proc. R. Soc. London **A126** (1930) 360.
- [52] Ö. Kaymakçalan, S. Rajeev, and J. Schechter, Phys. Rev. **D30** (1984) 594;
Ö. Kaymakçalan and J. Schechter Phys. Rev. **D31** (1985) 1109.
- [53] S. L. Adler, Phys. Rev. **177** (1969) 2426;
J. S. Bell and R. Jackiw, Nuov. Cim. **60A** (1969) 47.
- [54] D. R. Inglis, Phys. Rev. **96** (1954) 1059.
- [55] M. Gell-Mann, Phys. Rev. **92** (1953) 833.
- [56] K. Nishijima and T. Nakano, Prog. Theor. Phys. **10** (1953) 581.
- [57] A. V. Manohar, Nucl. Phys. **B248** (1984) 19.
- [58] E. Guadagnini, Nucl. Phys. **B236** (1984) 15.
- [59] M. Gell-Mann and Y. Ne'eman, *The Eightfold Way*, Benjamin, New York, 1964.

- [60] S. Okubo, Prog. Theor. Phys. **27** (1962) 949.
- [61] J. de Swart, Rev. Mod. Phys. **35** (1963) 916.
- [62] H. Yabu and K. Ando, Nucl. Phys. **B301** (1988) 601.
- [63] H. Weigel, R. Alkofer, and H. Reinhardt, Nucl. Phys. **B397** (1992) 638.
- [64] A. Blotz, D. Diakonov, K. Goeke, N. W. Park, V. Petrov, and P. V. Pobylitsa, Nucl. Phys. **A555** (1993) 765.
- [65] J. McGovern and M. Birse, Phys. Lett. **B200** (1988) 401.
- [66] H. Walliser, *Private communication*.
- [67] M. Prasałowicz, Phys. Lett. **158B** (1983) 264.
- [68] M. Chemtob, Nucl. Phys. **B256** (1985) 600.
- [69] E. Braaten, S.-M. Tse, and C. Willcox, Phys. Rev. **D34** (1986) 1482.
- [70] Ulf-G. Meißner, N. Kaiser, and W. Weise, Nucl. Phys. **A466** (1987) 685.
- [71] G. S. Adkins and C. R. Nappi, Nucl. Phys. **B249** (1985) 507.
- [72] H. Forkel, M. Nielsen, X.-M. Jin, and T. Cohen, Phys. Rev. **C50** (1994) 3108.
- [73] S. A. Larin, Phys. Lett. **B334** (1994) 192.
- [74] P. L. Anthony *et al.*, Phys. Rev. Lett. **71** (1993) 959;
K. Abe *et al.*, Phys. Rev. Lett. **74** (1995) 1525.
- [75] D. Adams *et al.*, Phys. Lett. **B329** (1994) 399; CERN-PRE-95-097.
- [76] S. Y. Huseh *et al.*, Phys. Rev. **D38** (1988) 2056.
- [77] F. E. Close and R. G. Roberts, Phys. Lett. **B316** (1993) 165.
- [78] N. W. Park, J. Schechter, and H. Weigel, Phys. Lett. **B228** (1989) 420.
- [79] Z. Ryzak, Phys. Lett. **B217** (1989) 325, **B224** (1989) 450 (**E**).
- [80] G. Kälbermann, J. Eisenberg, and A. Schäfer, Phys. Lett. **B339** (1994) 211.
- [81] H. Walliser, An Extension of the Standard Skyrme Model, in *Baryons as Skyrme Solitons*, edited by G. Holzwarth, p. 247, World Scientific, 1994.
- [82] T. Cohen and M. Banerjee, Phys. Lett. **B230** (1989) 129.
- [83] S. Okubo, Phys. Lett. **5** (1963) 163;
J. Iizuka, Prog. Theor. Phys. Suppl. **37-8** (1966) 376;
G. Zweig, CERN report no. 8419/TH 412.
- [84] J. Stern and G. Cleément, Phys. Lett. **B231** (1989) 471.
- [85] H. Dreiner, J. Ellis, and R. A. Flores, Phys. Lett. **B221** (1989) 167.
- [86] M. Rho, Phys. Rep. **240** (1994) 1.
- [87] S. Kahana, A. D. Jackson, and G. Ripka, Nucl. Phys. **A459** (1986) 663.
- [88] N. W. Park, J. Schechter, and H. Weigel, Phys. Rev. **D41** (1990) 2836.
- [89] M. Prasałowicz and J. Trampetic, Fizika **18** (1986) 391.

- [90] P. Jain, R. Johnson, and J. Schechter, Phys. Rev. **D38** (1988) 1571.
- [91] N. Cabibbo, Phys. Rev. Lett. **10** (1963) 531.
- [92] H. L. Lipkin, Flavor Symmetry and the Spin of the Proton, in *Future Polarization Physics at Fermilab*, edited by E. Berger *et al.*, p. 261, Fermilab, Batavia, 1988.
- [93] M. Ademollo and R. Gatto, Phys. Rev. Lett. **13** (1964) 264.
- [94] J. Donoghue and C. R. Nappi, Phys. Lett. **168B** (1986) 105.
- [95] H. Yabu, Phys. Lett. **B218** (1989) 124.
- [96] J. Ellis and M. Karliner, Phys. Lett. **B313** (1993) 131.
- [97] G. Pari, B. Schwesinger, and H. Walliser, Phys. Lett. **B255** (1991) 1.
- [98] E. Witten, Nucl. Phys. **B156** (1979) 269;
P. Di Vecchia and G. Veneziano, Nucl. Phys. **B171** (1980) 253;
C. Rosenzweig, J. Schechter, and G. Trahern, Phys. Rev. **D21** (1980) 3388.
- [99] K. Huang, *Quarks, Leptons and Gauge Fields*, chapter 5.6, World Scientific, 1982.
- [100] V. Baluni, Phys. Rev. **D19** (1979) 2227.
- [101] L. Dixon, A. Angau, Y. Nir, and B. Warr, Phys. Lett. **B253** (1991) 459.
- [102] R. J. Crewther, P. Di Vecchia, G. Veneziano, and E. Witten, Phys. Lett. **88B** (1979) 123.
- [103] R. Jaffe, Phys. Rev. Lett. **38** (1977) 195.
- [104] A. P. Balachandran, A. Barducci, F. Lizzi, V. Rodgers, and A. Stern, Phys. Rev. Lett. **52** (1984) 887.
- [105] A. P. Balachandran, F. Lizzi, V. Rodgers, and A. Stern, Nucl. Phys. **B256** (1985) 525.
- [106] F. G. Scholtz, B. Schwesinger, and H. B. Geyer, Nucl. Phys. **A561** (1993) 542.
- [107] K. Cahill, A. Comtet, and R. J. Glauber, Phys. Lett. **64B** (1976) 283.
- [108] B. Schwesinger, F. G. Scholtz, and H. B. Geyer, Phys. Rev. **D51** (1995) 1228.
- [109] A. Jackson, A. D. Jackson, A. S. Goldhaber, G. E. Brown, and L. C. Castillejo, Phys. Lett. **154B** (1985) 101;
A. Jackson, A. D. Jackson, and V. Pasquier, Nucl. Phys. **A432** (1985) 567;
R. Vinh Mau, M. Lacombe, B. Loiseau, , W. N. Cottingham, and P. Lisboa, Phys. Lett. **150B** (1985) 259;
H. Yabu and K. Ando, Prog. Theor. Phys. **74** (1985) 750.
- [110] G. Kälbermann and J. Eisenberg, Phys. Rev. **D46** (1992) 446.
- [111] C. B. Dover, D. J. Milliner, and A. Gal, Phys. Rep. **184** (1989) 1.
- [112] H. Walliser, Nucl. Phys. **A548** (1992) 649.
- [113] P. A. M. Dirac, *Lectures on Quantum Mechanics*, Yeshiva University Press, 1964.
- [114] G. Karl and J. E. Paton, Phys. Rev. **D30** (1984) 238.
- [115] H. S. J. Bijnens and M. B. Wise, Can. J. Phys. **64** (1986) 1;
D. B. Kaplan and I. Klebanov, Nucl. Phys. **B335** (1990) 45.
- [116] C. R. Dashen, E. Jenkins, and A. V. Manohar, Phys. Rev. **D49** (1994) 4713.

- [117] B. Schwesinger and H. Weigel, Nucl. Phys. **A540** (1992) 461.
- [118] M. Lacombe, B. Loiseau, R. Vinh Mau, and W. N. Cottingham, Phys. Rev. Lett. **57** (1986) 170.
- [119] W. Pauli, *Handbuch der Physik, Vol. XXIV*, Springer-Verlag, Berlin, 1933.
- [120] B. Schwesinger and H. Weigel, Phys. Lett. **B267** (1991) 438.
- [121] J. Kroll and B. Schwesinger, Phys. Lett. **B334** (1994) 287.
- [122] G. Wagner, A. J. Buchmann, and A. Faessler, Phys. Lett. **B359** (1995) 288.
- [123] D. B. Leinweber, R. Draper, and R. M. Woloshyn, Phys. Rev. **D46** (1992) 3067.
- [124] M. N. Butler, M. J. Savage, and R. P. Springer, Phys. Rev. **D49** (1994) 3459.
- [125] J. Schechter and H. Weigel, Phys. Rev. **D44** (1991) 2916.
- [126] J. Schechter and H. Weigel, Phys. Lett. **B261** (1991) 235.
- [127] C. Hajduk and B. Schwesinger, Phys. Lett. **140B** (1984) 172.
- [128] N. K. Nielson, Nucl. Phys. **B120** (1977) 212.
- [129] H. Gomm, P. Jain, R. Johnson, and J. Schechter, Phys. Rev. **D33** (1986) 801,3476.
- [130] C. Callan and I. Klebanov, Nucl. Phys. **B262** (1985) 365.
- [131] C. Callan, K. Hornbostel, and I. Klebanov, Phys. Lett. **B202** (1988) 296.
- [132] J. Kunz and P. J. Mulders, Phys. Lett. **B231** (1989) 335.
- [133] Y. Oh, D. P. Min, M. Rho, and N. N. Scoccola, Nucl. Phys. **A534** (1991) 493.
- [134] M. Lacombe, B. Loiseau, J. M. Richard, R. Vinh Mau, J. Cote, P. Pires, and R. De Tournell, Phys. Rev. **C21** (1980) 861.
- [135] J. J. Sakurai, *Currents and Mesons*, University of Chicago Press, 1969.
- [136] B. Schwesinger and H. Weigel, Nucl. Phys. **A465** (1987) 733.
- [137] G. Eckart, A. Hayashi, and G. Holzwarth, Nucl. Phys. **A448** (1986) 732.
- [138] T. Tujiwara, T. Kugo, H. Terao, S. Uehara, and K. Yamawaki, Prog. Theor. Phys. **73** (1985) 926;
M. Bando, T. Kugo, and K. Yamawaki, Phys. Rep. **164** (1988) 217.
- [139] P. Jain, R. Johnson, Ulf-G. Meißner, N. W. Park, and J. Schechter, Phys. Rev. **D37** (1988) 3252.
- [140] S. Callan, S. Coleman, J. Wess, and B. Zumino, Phys. Rev. **177** (1969) 2247.
- [141] M. Harada and J. Schechter, *Effects of Symmetry breaking on the Strong and Electroweak Interactions of the Vector Nonet*, Syracuse University preprint, June 1995, hep-ph/9506473.
- [142] Ulf-G. Meißner, N. Kaiser, H. Weigel, and J. Schechter, Phys. Rev. **D39** (1989) 1956.
- [143] D. Masak and J. Kunz, Phys. Lett. **B209** (1988) 71;
D. Masak, Phys. Rev. **D39** (1989) 305.
- [144] N. W. Park and H. Weigel, Phys. Lett. **B268** (1991) 155.
- [145] K. Kawarabayashi and M. Suzuki, Phys. Rev. Lett. **16** (1966) 255;
Riazuddin and Fayyazuddin, Phys. Rev. **147** (1966) 255.

- [146] J. Schechter, Phys. Rev. **D34** (1986) 868.
- [147] V. Bernard, N. Kaiser, and Ulf-G. Meißner, Phys. Lett. **B237** (1990) 545.
- [148] G. Altarelli and G. G. Ross, Phys. Lett. **B212** (1988) 391;
R. D. Carlitz, J. C. Collins, and A. H. Mueller, Phys. Lett. **B214** (1988) 229;
A. V. Efremov, J. Soffer, and O. V. Teryaev, Nucl. Phys. **B346** (1990) 97; Phys. Rev. Lett. **64** (1990) 1495; Phys. Rev. **D44** (1991) 1369;
T. Hatsuda and I. Zahed, Phys. Lett. **B221** (1989) 173.;
M. Birse, Phys. Lett. **B249** (1990) 291.
- [149] A. V. Manohar, Phys. Rev. Lett. **66** (1991) 1663.
- [150] G. Veneziano, Mod. Phys. Lett. **A4** (1989) 1605.
- [151] J. Schechter, V. Soni, A. Subbaraman, and H. Weigel, Mod. Phys. Lett. **A5** (1990) 2543.
- [152] J. Schechter, V. Soni, A. Subbaraman, and H. Weigel, Phys. Rev. Lett. **65** (1990) 2955.
- [153] J. Schechter, V. Soni, A. Subbaraman, and H. Weigel, Mod. Phys. Lett. **A7** (1992) 1.
- [154] N. I. Kochelev, Phys. Lett. **B301** (1993) 272.
- [155] H. Weigel, The proton spin structure in Skyrme type models, in *Particles and Nuclei*, edited by A. Pascolini, p. 403, World Scientific, 1993.
- [156] K. Gottfried, Phys. Rev. Lett. **18** (1967) 1174.
- [157] P. Amaudruz et al., Phys. Rev. Lett. **66** (1991) 2712.
- [158] H. Walliser and G. Holzwarth, Phys. Lett. **B302** (1993) 377.
- [159] H. Goldhaber, Phys. Lett. **101** (1956) 433.
- [160] I. Klebanov, Strangeness in the Standard Skyrme Model, in *Hadrons and Hadronic Matter*, edited by D. Vautherin, J. Negele, and F. Lenz, p. 223, Plenum Press, 1989.
- [161] H. K. Lee, M. A. Nowak, and M. Rho, Ann. Phys. **227** (1993) 175.
- [162] G. S. Adkins and C. R. Nappi, Phys. Lett. **B233** (1984) 109.
- [163] D. O. Riska and N. N. Scoccola, Phys. Lett. **B265** (1991) 188.
- [164] N. N. Scoccola, H. Nadeau, M. A. Nowak, and M. Rho, Phys. Lett. **B201** (1988) 425;
N. N. Scoccola, D. P. Min, H. Nadeau, and M. Rho, Nucl. Phys. **A505** (1989) 497.
- [165] U. Blom, K. Dannbom, and D. O. Riska, Nucl. Phys. **A493** (1989) 384.
- [166] M. Bander and A. Subbaraman, *Tetraquarks: Mesons with two B mesons*, Irvine University preprint, March 1995, hep-ph/9503341.
- [167] C. L. Schat, N. N. Scoccola, and C. Cobbi, Phys. Lett. **B356** (1995) 1.
- [168] J. W. Darewych, M. Horbatsch, and R. Koniuk, Phys. Rev. **D28** (1993) 1125;
E. Kaxias, E. J. Moniz, and M. Soyeur, Phys. Rev. **D32** (1985) 655;
D. B. Leinweber, T. Draper, and R. M. Woloshyn, Phys. Rev. **D48** (1993) 2230.
- [169] M. N. Butler, M. J. Savage, and R. P. Springer, Nucl. Phys. **B399** (1993) 69; Phys. Lett. **B304** (1993) 353; Phys. Lett. **B314** (1993) 122 (E).
- [170] A. Abada, H. Weigel, and H. Reinhardt, *Radiative Decays of Hyperons within the Skyrme Model: E2/M1 transition Ratios*, Tübingen University preprint, September 1995, Phys. Lett. **B**, to be published.

- [171] H. J. Lipkin Phys. Rev. **D7** (1973) 846
H. J. Lipkin and M. A. Moinester Phys. Lett. **B287** (1992) 179.
- [172] J. P. Blaizot, M. Rho, and N. N. Scoccola, Phys. Lett. **B209** (1988) 27.
- [173] C. W. Wong, D. Vuong, and K. Chu, Nucl. Phys. **A515** (1990) 686.
- [174] P. Ring and P. Schuck, *The Nuclear Many Body Problem*, Springer, 1980.
- [175] C. L. Schat, N. N. Scoccola, and C. Cobbi, Nucl. Phys. **A585** (1995) 627.
- [176] H. Walliser and G. Eckart, Nucl. Phys. **A429** (1984) 514.
- [177] M. Karliner and M. P. Mattis, Phys. Rev. **D34** (1986) 1991.
- [178] A. Hayashi, G. Eckart, G. Holzwarth, and H. Walliser, Phys. Lett. **B147** (1984) 5.
- [179] B. Schwesinger, Nucl. Phys. **A537** (1992) 253.
- [180] K. M. Westerberg and I. Klebanov, Phys. Rev. **D50** (1994) 5834.
- [181] Y. Oh, Mod. Phys. Lett. **A10** (1995) 1027.
- [182] D. P. Min, Y. Oh, B. Park, and M. Rho, Int. J. Mod. Phys. **E4** (1995) 47.
- [183] M. Rho, D. O. Riska, and N. N. Scoccola, Z. Phys. **A341** (1992) 343.
- [184] E. Eichten and F. Feinberg, Phys. Rev. **D23** (1981) 2724;
M. B. Voloshin and M. A. Shifman, Yad. Fiz. **45** (1987) 463 (Sov. J. Nucl. Phys. **45** (1987) 292);
N. Isgur and M. B. Wise, Phys. Lett. **B232** (1990) 113; **B237** (1990) 527;
H. Georgi Phys. Lett. **B230** (1990) 447.
- [185] M. Neubert, Phys. Rep. **245** (1994) 259.
- [186] J. Schechter and A. Subbaraman, Phys. Rev. **D48** (1993) 332.
- [187] P. Jain, A. Momen, and J. Schechter, Int. J. Mod. Phys. **A10** (1995) 2467.
- [188] Y. Oh and B. Park, Phys. Rev. **D51** (1995) 5016.
- [189] J. Schechter, A. Subbaraman, S. Vaidya, and H. Weigel, Nucl. Phys. **A590** (1995) 655.
- [190] J. Schechter and A. Subbaraman, Phys. Rev. **D51** (1995) 2311.
- [191] U. Vogl and W. Weise, Prog. Part. Nucl. Phys. **27** (1991) 195.
- [192] T. Hatsuda and T. Kunihiro, Phys. Rep. **247** (1994) 221.
- [193] R. Alkofer, H. Reinhardt, and H. Weigel, *Baryons as Chiral Solitons in the Nambu–Jona-Lasinio Model*, Tübingen University preprint, hep-ph/9501213, Phys. Rep., to be published.
- [194] B. Y. Park, D. P. Min, and M. Rho, Nucl. Phys. **A551** (1993) 657.
- [195] H. Reinhardt and R. Wünsch, Phys. Lett. **215** (1988) 577; **B 230** (1989) 93;
T. Meißner, F. Grümmer and K. Goeke, Phys. Lett. **B 227** (1989) 296;
R. Alkofer, Phys. Lett. **B 236** (1990) 310.
- [196] J. Schwinger, Phys. Rev. **82** (1951) 664.
- [197] A. Blin, B. Hiller, and M. Schaden, Z. Phys **A331** (1988) 75.

- [198] R. Alkofer and H. Reinhardt, *The Chiral Anomaly and Electromagnetic Pion Decay in NJL-like Models*, Tübingen University preprint 1992, unpublished.
- [199] H. Weigel, H. Reinhardt, and R. Alkofer, Phys. Lett. **B313** (1993) 377.
- [200] V. A. Miransky, *Dynamical Symmetry Breaking in Quantum Field Theories*, World Scientific, 1993.
- [201] M. Jaminon, R. Mendez-Galain, G. Ripka, and P. Stassart, Nucl. Phys. **A537** (1992) 418.
- [202] M. Gell-Mann, R. J. Oakes, and B. Renner, Phys. Rev. **175** (1968) 2196.
- [203] H. Weigel, R. Alkofer, and H. Reinhardt, Nucl. Phys. **A576** (1994) 477.
- [204] R. F. Dashen, B. Hasslacher, and A. Neveu, Phys. Rev. **D12** (1975) 2443.
- [205] R. Rajaraman, *Solitons and Instantons*, North Holland, 1982.
- [206] H. Reinhardt, Nucl. Phys. **A503** (1989) 825.
- [207] R. Alkofer and H. Weigel, Comp. Phys. Comm. **82** (1994) 30.
- [208] D. Diakonov, V. Petrov, and M. Prasałowicz, Nucl. Phys. **B323** (1983) 53.
- [209] R. Alkofer, H. Reinhardt, H. Weigel, and U. Zückert, Phys. Rev. Lett. **69** (1992) 1874.
- [210] F. Döring, E. Ruiz-Arriola, and K. Goeke, Z. Phys. **A344** (1992) 159.
- [211] J. Goldstone and F. Wilczek, Phys. Rev. Lett. **47** (1981) 986.
- [212] H. Weigel, R. Alkofer, and H. Reinhardt, Phys. Lett. **B284** (1992) 296.
- [213] A. Blotz, D. Diakonov, K. Goeke, N. W. Park, V. Petrov, and P. V. Pobylitsa, Phys. Lett. **B287** (1992) 29.
- [214] H. Weigel, R. Alkofer, and H. Reinhardt, Nucl. Phys. **A576** (1994) 477.
- [215] H. Kim, M. Polyakov, A. Blotz, and K. Goeke, *Magnetic Moments of the SU(3) Octet Baryons in the semibosonized Nambu–Jona–Lasino Model*, Bochum University preprint RUB-TPII-6/95, June 1995, Phys. Rev. **D**, to be published.
- [216] C. V. Christov, A. Z. Gorski, K. Goeke, and P. V. Pobylitsa, Nucl. Phys. **A592** (1995) 513.
- [217] M. Wakamatsu and H. Yoshiki, Nucl. Phys. **A524** (1991) 561.
- [218] A. Blotz, M. Prasałowicz, and K. Goeke, *Axial Properties of the Nucleon with $1/N_C$ Corrections in the Solitonic SU(3) NJL Model*, Bochum University preprint RUB-TPII-41/93, March 1994.
- [219] A. Abada, R. Alkofer, H. Reinhardt, and H. Weigel, Nucl. Phys. **A593** (1995) 488.
- [220] H. Weigel and R. Alkofer, Comp. Phys. Comm. **82** (1994) 30.
- [221] Y. Oh, B. Y. Park, and D. P. Min, Phys. Rev. **D50** (1994) 3350.
- [222] H. Weigel, R. Alkofer, and H. Reinhardt, Phys. Rev. **D49** (1994) 5958.
- [223] D. F. Holland, J. Math. Phys **8** (1967) 857.
- [224] A. Kanazawa, Prog. Theor. Phys. **77** (1987) 1240.